ASSESSING THE PERFORMANCE OF BAMBOO STRUCTURAL COMPONENTS

by

Michael J. Richard

Bachelor of Science, Worcester Polytechnic Institute, 2008

Master of Science, Worcester Polytechnic Institute, 2009

Submitted to the Graduate Faculty of

The Swanson School of Engineering in partial fulfillment

of the requirements for the degree of

Doctor of Philosophy

University of Pittsburgh

2013

UNIVERSITY OF PITTSBURGH

SWANSON SCHOOL OF ENGINEERING

This dissertation was presented

by

Michael J. Richard

It was defended on

June 5, 2013

and approved by

Melissa Bilec, Ph.D., Assistant Professor, Civil and Environmental Engineering

John Brigham, Ph.D., Assistant Professor, Civil and Environmental Engineering

Khosrow Ghavami, Ph.D., Full Professor, Civil Engineering, PUC-Rio

C. Drew Armstrong, Ph.D., Associate Professor, Architectural Studies

Dissertation Director: Kent A. Harries, Ph.D., Associate Professor, Civil and Environmental

Engineering

ASSESSING THE PERFORMANCE OF STRUCTURAL BAMBOO COMPONENTS

Michael J. Richard, Ph.D.

University of Pittsburgh, 2013

Bamboo has been a traditional construction material in many regions for centuries. The rapid growth and maturation rate of bamboo as well as its good strength properties and global accessibility make it a promising non-conventional building material resource. However, due to limited standardization and design criteria, bamboo has often been relegated to non-engineered and marginally-engineered construction. The current study assesses the performance of full-culm structural bamboo components and appropriate standard material and member test methods. A brief overview is given to the motivation for the study of structural bamboo, placing the work in its social context, followed by background on the properties of bamboo and the structural applications of the material as well as the pathway to its further standardization and utilization. Experimental and analytical studies are conducted focusing on the tensile, flexural, buckling, and environmental sustainability performance of full-culm bamboo components. Standard bamboo tension tests are carried out to investigate the test interferences associated with the functionally graded fiber distribution across the culm wall thickness. Tension specimens oriented in both the radial and tangential directions are considered in order to isolate the effects of the fiber gradation both on test results and experimental methodology. Recognizing longitudinal splitting induced by flexure as a dominant limit state, modified standard bamboo flexural tests are performed to investigate the development of a standard test procedure for this limit state, which involves a mixed-mode longitudinal splitting failure in the flexural element. Flexural testing considers two

test configurations and three difference species of bamboo. Results of modified full-culm tests are compared with smaller clear bamboo flexural specimens taken from the culm wall as well as standard or proposed tests for pure mode I and pure mode II failure components. The experimental buckling capacity of single-culm and multiple-culm bamboo columns is studied as further understanding of column strength is critical to the construction of more robust and potentially multiple-story bamboo structures. Finally, in an effort to quantify the perceived sustainability benefits of bamboo, the environmental impacts of multiple-culm bamboo columns are compared with structurally comparable timber and steel alternatives in a comparative midpoint life cycle analysis.

TABLE OF CONTENTS

LIST OF TABLES

LIST OF FIGURES

NOMENCLATURE

2a   initial crack length for split-pint test

A   area

A_{culm} area of bamboo culm section

A_g gross area of entire cross section

b   breadth (width)

C   design equation modification factor

c   distance from the neutral axis to the extreme fiber of cross section

c_r distance from midline of the culm wall to the edge of the wall section at

                the location of rupture

d   depth

D   outer diameter of bamboo culm

E   eccentricity

E   modulus of elasticity

E_c composite moment of elasticity

E_f modulus of elasticity of bamboo fibers

E_m modulus of elasticity of lignin matrix

F   force

f_r transverse modulus of rupture (edge bearing test)

G_I	mode I strain energy release rate
h_r	distance from the culm wall midline to elastic neutral axis
I	moment of inertia
I_{culm}	moment of inertia of bamboo culm section
I_g	moment of inertia of gross cross section
K	effective length factor or spring stiffness factor
K_{eff}	experimental effective length factor
K_I	crack intensity factor
L	length
M	moment
P_{cr}	elastic buckling capacity
r	radius of gyration
R	culm radius
R_c	culm radius measured to the midwall thickness
S	span
t	thickness
V	shear force
V_f	volume fraction of bamboo fibers
w	width in tangential direction of culm
y	distance between the centroid of shear area and neutral axis
δ	out-of straightness (curvature)
ε	strain
ε_{xx}	horizontal strain

ε_{yy}	vertical strain
θ	angle
σ	stress
$\sigma\perp$	tension capacity perpendicular to the longitudinal fibers
σ_c	experimental compressive strength
σ_{cr}	critical buckling stress
σ^*	normalized critical buckling stress
τ	shear stress

ACKNOWLEDGMENTS

Prove all things; hold fast that which is good. – 1 Thessalonians 5:21

To Danielle:

for continuing to stick with me through the ups, downs, twists, and turns.

Thank you and I love you.

To Mom and Dad:

for always encouraging me to dream and for supporting me throughout.

I would like to acknowledge a few (out of many) who have helped me with this research:

Dr. Kent A. Harries for his mentorship, friendship, and the opportunity to learn from his expertise, gain confidence as an academic and engineer, and work in a full-scale structures laboratory. I look forward to future collaboration and visits to Pittsburgh.

CEE lab technician **Charles "Scooter" Hager** for all his guidance and assistance in the structures lab and his friendship

Dr. Khosrow Ghavami for not only offering his expertise and knowledge in bamboo structures but for his gracious hospitality while I studied in Rio and his continued friendship

1.0   INTRODUCTION

Used for centuries as a non-engineered construction material, bamboo has wide availability across the globe and offers a potentially more sustainable alternative to conventional engineered building practices in regions where it is readily available. With the world population estimated to reach 9 billion people by 2050 (Dickson 2002), bamboo is a much needed alternative to the global portfolio of construction materials. Structural use of bamboo offers potential advances in such areas as a) reducing homelessness rates in areas across the globe, b) mitigating damage caused by natural disasters, c) providing housing for disaster relief efforts, and d) bridging the growing socio-economic gap for growing populations. However, due to a lack of understanding, as well as a lack in engineering standardization, bamboo continues to be regarded as an inferior material by the populations that can most benefit from its use. Therefore, the objective of the current research is to extend the body of knowledge on bamboo standardization and the performance of bamboo structural components (i.e. bamboo axial and flexural members) in order to move this unique and promising material toward broad acceptance and use in the global construction field.

1.1   THE GROWING SOCIO-ECONOMIC GAP

There is a growing socio-economic gap developing between advanced and developing societies as well as between urban and rural populations (Powell 2006). Technology continues to advance in developed western nations as well as urban centers but lags in the rapidly growing populations of developing nations and remote rural regions. This is in contrast to the principle of sustainable development, especially with respect to housing and construction. Inexpensive, autonomous housing and green construction are two of the new technologies envisioned to proliferate by 2020 (Powell 2006). However, developing nations must overcome greater barriers with regard to the implementation of new technologies; structural bamboo construction offers a potential alternative.

Global development is coupled with burgeoning populations and a growing demand for improved housing. The global population is estimated to reach 9 billion people by 2050 (Dickson 2002). Construction resources are therefore being strained as conventional building resources (steel, concrete, and timber) are being sought by more people in more remote regions. Often, access to conventional building materials comes with high costs and large environmental impacts, particularly those associated with transport. However, low-cost indigenous materials like bamboo are often passed over for construction due to their perception as being 'poor man's' materials or unreliable for construction due to a lack of research and standardization. As a result, indigenous materials are typically only used in non-engineered and vernacular construction.

There is also a need for adequate housing and infrastructure in developing nations which often have large socio-economic gaps between rural and urban populations. Examples of this disparity include pervasive rural poverty (technological and economic) as compared to urban centers, and the existence of urban poverty in cities such as the *favela* of Rio de Janeiro, the

slums of Mumbai and Kolkata, and other informal settlements throughout the developing world. The latter can be considered an extension of the former since many rural people travel to the city in search of work but lack the economic resources for adequate urban housing. Additionally, developed nations are also straining conventional resources as more efficient infrastructure is needed to replace aging systems.

These trends showcase two major issues. First, the growing demand for adequate housing and infrastructure is straining conventional material resources such as concrete, timber, and steel not only in places where they are practically available but in outlying remote areas where use of these materials is not feasible. Nonetheless, they are seen as the superior or 'affluent' material choice as opposed to local indigenous materials. Second, this view is coupled with a lack of expertise in the use of conventional materials; indeed, local materials often perform better structurally. For example, bamboo houses better survived two recent seismic events as compared to conventional materials in Northeast India (Kaushik et al. 2006a, Kaushik et al. 2006b, and Murty and Sheith 2012).

1.2   HOUSING: A FUNDAMENTAL RIGHT YET GLOBAL CHALLENGE

Safe, reliable housing is recognized as a basic human need and a basic human right as "[everyone] has the right to a standard of living adequate for the health and well-being of himself and of his family, including food, clothing, housing, and medical care and necessary social services…" (UN-UDHR 1948). However, homelessness and/or inadequate housing remains a significant and growing problem across the globe as people struggle for adequate housing in both rural and urban environments. Major causes of this problem include rapid urbanization in

3

developing areas, human conflicts, natural disasters, and issues of housing affordability and availability of building resources. "Unfortunately housing affordability remains a challenge and it is worsening due to, among other factors, the economic effects of the global financial crisis and the increasing severity of disasters and conflicts, which both place an additional strain on already stretched land and housing resources" (UN-HABITAT 2011b).

Rapid urbanization is a major challenge to providing adequate housing and has led to many living in non-engineered or marginally-engineered informal settlements. UN-HABITAT estimated that as of 2011, more than 1 billion people are living in such informal settlements (often described more negatively as 'slums') and that 2 billion more people will be added to this number over the next 25 years (UN-HABITAT 2011b). Asia faces a significant challenge, as it has the fastest rate of urbanization in the world and nearly one third of households in Asia are in informal settlements: "Predictions suggest that between 2010 and 2050, the urban population in Asia will nearly double to reach 3.4 billion. Every day Asian cities will need to accommodate 120,000 new residents, which equates to a daily housing demand of at least 20,000 housing units" (UN-HABITAT 2011b). Southern Asia will see the fastest growth with its 2010 urban population of 600 million increasing to 1.4 billion by 2050 (Figure 1-1).

Figure 1-1: Example of informal settlement housing in South Asia (UN-HABITAT 2011b)

Meanwhile, Latin America and the Caribbean as well as Africa are also facing issues of homelessness and rapid urbanization. In Latin America and the Caribbean, 84.6% of the population will live in cities by 2030 (up from 75.5% in 2000). The population living in informal settlements was estimated to be 134 million in 2005; approximately one-third of the region's population (UN-HABITAT 2011a). In Africa, which is rural but quickly urbanizing, cities will need to accommodate an additional 40,000 people every day between 2011 and 2025 when nearly half (47.2%) of Africa's population will live in cities (UN-HABITAT 2011c). While North Africa and a few sub-Saharan African countries have reduced the population of dwellers living in informal settlements between the years of 2000 and 2010, the majority of African households continue to settle in informal housing due to a lack of alternatives: "Indeed, in some [African] countries slums constitute a considerable proportion of the housing stock, for example Chad (90.3%), Ethiopia (79.1%), Mozambique (80.0%), and Niger (81.9%)" (UN-HABITAT 2011c). Even in European and North American countries, homelessness is a serious problem; approximately 10% of the population lives in slums and informal settlements. Europe is estimated to have a homeless population of approximately 600,000 while 750,000 people were reported as being homeless in the United States in 2006 (UN-HABITAT 2011d).

1.3   ADEQUATE SHELTER AND NATURAL DISASTERS

Natural disasters, as well as human conflicts, pose another major challenge to providing adequate shelter to affected populations. Not only must attention be given to providing adequate temporary shelter immediately after a disaster, but also to providing long-term, sustainable, and permanent housing for populations. Relief shelter and long term housing strategies should seek

to implement housing solutions that consider and engage local resources, building skills, culture, and economy. Permanent housing must also seek to provide improved performance and hazard mitigation in order to reduce loss and casualty in future events.

The litany of available statistics from recent natural disasters illustrate the need for both better permanent shelters which can survive these events or protect their occupants so as to reduce casualties, and better shelter relief efforts and strategies immediately after an event. For example, the death totals for major earthquakes in recent years have been significant in areas with housing inadequate for the regional seismic risk. The 2003 Bam, Iran earthquake (26,300 dead), the 2005 Kashmir earthquake (80,500 dead), the 2008 Sichuan earthquake (70,000 dead), and the 2010 Haiti earthquake (230,000 dead) all resulted in significant casualty. Following such events, the number of injured persons is typically similar or greater and those displaced from their homes are often an order of magnitude greater. Similar major earthquakes in Morocco (2004) and Chile (2010) however saw much lower death totals, approximately 571 and 452 respectively (Yu et al. 2010). Additionally, more buildings remained standing in Chile than Haiti after the earthquake even though the Chilean quake was of a significantly greater magnitude (Rowell and Jackson 2010). This markedly lower death toll can be attributed to better hazard mitigation through availability and adherence to building codes; use of best practices; standardization; and guidelines for buildings. Similarly, the disparity between regions with adequate housing stock and those with more informal shelters can be also seen in the death tolls from major hurricanes and tropical cyclones. The 2008 cyclone in Myanmar and Burma resulted in approximately 135,000 deaths while Hurricane Katrina in the Southern United States in 2005 only caused 1,836 deaths.

In addition to providing better performing long-term housing, better strategies for providing temporary shelter after natural disasters are a concern. The December 2004 Indian Ocean Tsunami claimed over 250,000 lives and left millions of people homeless or displaced in the coastal areas of Indonesia, Malaysia, Southern India, Sri Lanka, Thailand, and the Maldives. Tents and shared barracks were used as temporary shelter for survivors and the need for adequate permanent housing at affordable costs remains. As of 2011 (7 years after the disaster), "it has been estimated that in [the Indonesian province of] Aceh alone, 92,000 new houses need to be built and 151,000 damaged houses rehabilitated" (UN-HABITAT 2011b). Meanwhile, the January 2010 Haitian Earthquake claimed over 300,000 lives and left 1.3 million people living in temporary shelters in the Port-au-Prince region. Another 600,000 people moved to other areas of the country seeking shelter immediately following the disaster (Government of the Republic of Haiti 2010). Approximately 105,000 homes were totally destroyed and over 208,000 were damaged. It is estimated that the housing sector alone in Haiti incurred 2.3 billion USD worth of damage (Government of the Republic of Haiti 2010). Yet, the humanitarian response was slow. Immediately after the quake, the Office of Internal Migration and its partners had only given out shelter supplies to approximately 36,000 people (Klarreich, 2010), which highlights the slow response of the relief effort in supplying shelter. By March 2010, 1.2 million people were still living in 460 spontaneously organized camps of over 25 families each; 21 of these spontaneous camps, which included some 250,000 people, presented major risks "for the well-being and safety of their inhabitants" (Government of the Republic of Haiti 2010).

Ultimately, delays in the distribution of prefabricated shelter forces many of the displaced to use salvaged and local materials. Temporary disaster relief strategies need to adjust to better facilitate affected populations. Instead of shipping outside materials, resources and prefabricated

units for shelters to the disaster site (usually from overseas), temporary shelters should instead use local materials and building expertise. This allows for a faster response time, lower costs, and a faster return to normalcy for the affected population. Use of local materials and building expertise in temporary relief shelter also transitions to their use in building of more long-term permanent structures. In Haiti, groups are working on developing and disseminating better standards and best practices to allow Haitians to use traditional and local building techniques which are more accessible for rebuilding and more robust in terms of future hazard mitigation such as wood framed structures with earthen infill walls (Rowell and Jackson 2010). The UN has recognized this and states that "transitional shelter should only require locally available tools and skill sets" and states that prefabricated shelters are not practical or appropriate based on cost and cultural perspectives (United Nations, 2004).

A new strategy for disaster relief should involve transfer of information and knowledge regarding temporary (and long term) shelter construction to complement local expertise and the development of implementation plans for relief shelter construction rather than the shipment of outside materials and resources to the site. In the ongoing effort to define solutions for disaster relief, bamboo has great potential with further standardization as it is often a local material with good structural properties and, in some areas, local inhabitants are knowledgeable in traditional methods for use in non-engineered structures.

1.4   THE STRAIN ON GLOBAL BUILDING RESOURCES

The growing demand for adequate housing across the globe is straining the resource availability of conventional building materials (steel, concrete, wood, and masonry). As the resources of these conventional materials are being sought after in more areas of the world, questions arise as to the ability to provide the supply to meet the increased demand and how to do so in a sustainable manner. The sustainability question must address the use of such materials in remote regions that lack both a native supply of conventional building materials and the expertise to build effectively with them. Figure 1-2 shows the global production of crude steel and cement between the years of 1990 and 2010. Over the last 20 years, the world has seen a significant increase in the production of both these finite material resources. According to the World Steel Association, global crude steel production has increased from 616.0 million metric tons in 1990 to 1,428.7 million metric tons in 2010, an increase of 132%. Meanwhile, concrete is the most widely used construction material in the world (Crow 2008). Global cement production has increased from 1,148.9 million metric tons in 1990 to 3,310.0 million metric tons in 2010, an increase of 188%. Much of this construction growth comes from rapidly developing countries such as Brazil, Russia, India, and China (the so-called BRIC countries). For 2010, China was the leading producer of cement accounting for 57% of total global production (van Oss 2012). This is up from a 29% share of total global production in 1994 (Solomon 1994). The next 6 producers in 2010 were India, the United States, Turkey, Brazil, Japan, and Russia (van Oss 2012). Concrete use in 2050 is also predicted to be 4 times the amount used in 1990 (Crow 2008).

While important and necessary resources for buildings, these materials are energy intensive to produce and generate a number of other negative environmental impacts. The cement industry is one of the leading industrial emitters of carbon dioxide (CO_2); it is estimated

that 0.87 to 0.92 metric tons of CO_2 emissions are produced for every metric ton of cement clinker produced (van Oss 2012). Because of the vast quantity used, concrete production contributes as much as 5% of the annual anthropogenic global CO_2 production with China alone producing 3% (Crow 2008). Efforts are being made at using recycled steel and concrete as well as looking into new admixtures and alternatives for concrete (Crow 2008). However, a broadening of the construction material resource base is still required in areas of expanding population where concrete and steel construction is a) expensive, b) not readily available and requires importation of necessary materials, and c) not viable due to a lack of expertise by the local population in using these construction techniques.
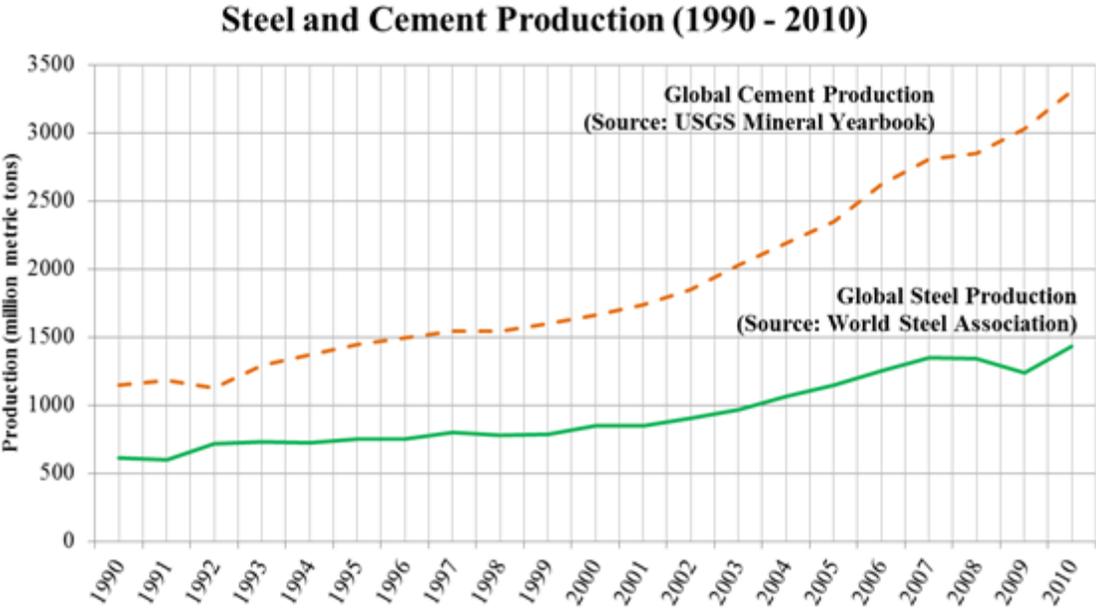
Figure 1-2: Global steel and cement production (1990-2010)

Even renewable construction material stocks such as timber are being strained by increased demand for construction as well as other demands of the growing global population such as land and agriculture. Figure 1-3 is a map of global forests indicating that 47% of global

forests have been lost over time (especially in Europe and Asia) and only 21% of forests remain as intact and untouched natural habitats.
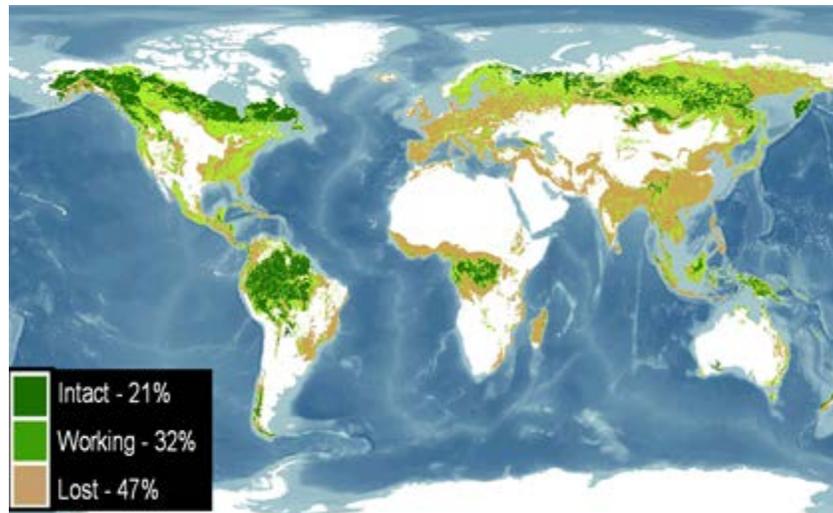
Figure 1-3: Map of global forests (World Resource Institute 2009)

While access to affordable land is the primary cause of homelessness in many areas, issues of housing affordability are also greatly affected by the high and rising cost of conventional construction materials in many areas. UN-HABITAT cites the issue of high costs for key building materials in relation to low incomes as an issue in Asia, Africa, Latin American, and the Caribbean. In Latin America, construction material costs are especially high when the materials are imported and families are often priced out of the formal housing sector and therefore seek housing through informal channels: "The prices of inputs to housing [land, materials, and persistently depressed income] can play a big part in driving up prices, making house-price-to-income ratios highly context-specific, even within a given country" (UN-HABITAT 2011a). Building materials typically represent the largest single input into the construction of housing and can "account for up to 80% of the total value of a simple domestic house" (UN-HABITAT 2011b). Put another way, "if the cost of building materials doubles in relation to average prices for other commodities, then the number of years that a household will

have to work to afford the cost of materials will likewise nearly double" (UN-HABITAT 2011b). This forces populations to seek key housing materials through less expensive informal channels, such as the supplier in Figure 1-4, to 'self-build' informal dwellings. High housing costs in relation to income is also true in Africa where construction materials costs are increasing from already high levels; in 2001 urban Africa had the highest regional housing-cost-to-income ratio globally at 12.5 or 12.5 median annual salaries required to purchase 1 median price home (UN-HABITAT 2011c). Asian Pacific countries and Arab States had a 2001 ratio of 12.5 and 11.3 respectively while Latin American countries and high income countries had ratios of 5.4 and 5.8 respectively (UN-HABITAT 2011c).

Figure 1-4: Informal material suppliers provide necessary building inputs (UN-HABITAT 2011b).

This increase in cost can be attributed in part to the adherence to using conventional building materials (steel and concrete) in the formal construction sector even when these are not the materials best suited for construction in a specific area. Many central and local governments insist on using conventional building materials and technologies through requirements in their building codes and regulations "many of which are a colonial heritage and adopted from foreign countries" (UN-HABITAT 2011b) and "prevent the use of more appropriate, readily available local building materials [and] …cost-effective and environmentally-friendly construction technologies" (UN-HABITAT 2011b). In many Asian countries, there are also issues of poor productivity and other shortcomings due to poor technology capacity in the local building

material industry which can lead to shortages and fluctuating prices. However, if countries invested resources and knowledge in low-income and affordable housing through traditional building techniques still widely used in Asia and the informal building sector, it is believed these countries could ultimately stimulate their economies: "Low income housing generates 30% more worker income than high cost housing [and] …construction in the informal sector [which is more traditional in nature and more labor intensive] creates 20% more jobs and builds six times more per dollar spent than formal sector construction" (UN-HABITAT 2011b).

Lack of appropriate standards and buildings codes and conventional building materials is also a factor in the high construction costs in sub-Saharan Africa as well as a lack of skilled labor and the high cost of importing and transporting materials. Cement, primary metals, and construction machinery are often the key building inputs that must be imported in many countries. Tariffs, foreign exchange rates, transportation, and other import costs all add to the cost of the construction material. In Kenya and Cote d'Ivoire, 37% and 35% respectively of the construction materials necessary for a median priced house are imported (UN-HABITAT 2011c). In Libya, the formal construction sector is focused primarily on concrete based buildings and technologies. However, in a desert country where water itself is a highly priced and scarce commodity, a water-based construction material can ultimately also be highly expensive in terms of initial construction costs. According to UN-HABITAT, some African countries have begun to look at revising prescriptive building codes and standards for more performance-based requirements as well as investigating non-conventional materials such as the use of stabilized soil-blocks in Sudan (UN-HABITAT 2011c).

In addition to accessing housing materials, one final issue involves addressing the durability of housing in developing areas and informal settlements. As defined in the UN-

HABITAT reports, a house is considered 'durable' if it has a permanent structure that is sufficient to protect inhabitants from climatic conditions such as precipitation, heat, cold, and humidity and the housing is located in a non-hazardous area (UN-HABITAT 2011b). However, in many cases, only the condition of the flooring material is taken into account and the number of un-durable dwellings would increase markedly if wall and roof materials and condition were also surveyed: "For example, when only the floor criterion was used in Indonesia, 84% of dwellings were considered durable as opposed to 70% when the three components were taken into account" (UN-HABITAT 2011b). Meanwhile, based on only the floor criterion, 20% of the global urban population with non-durable housing lives in sub-Saharan Africa.

Ultimately, these issues with global building material resources and high construction costs showcase a need for changing global policy with regard to providing adequate, affordable housing to populations. Rather than trying to supplant conventional building techniques and established building codes from the developed world in developing areas, work should be focused on providing the appropriate knowledge, skills, design practices, and policies to enable local populations to use appropriate and affordable local/traditional building materials and techniques for their region. Building industries which use locally sourced materials and techniques should be encouraged and strengthened. Practices that promote sustainable and environmentally conscious construction methods must be promoted. Furthermore, building codes, regulations, and standard practices should be revised and amended to pursue more 'performance-based' criteria and a broadened building material spectrum. Lastly, technical (or semi-technical) literature and design guidelines which are user-friendly and targeted toward a local population should be disseminated and proper skills training be provided to local labor in informal housing sectors (UN-HABITAT 2011b).

1.5   SUSTAINABLE DEVELOPMENT WITH BAMBOO

Ultimately, the current status quo is not promoting the principles of sustainable development which advocates balancing equity, environment, and economy (i.e. the 'triple bottom line'). Straining of conventional building materials is producing large environmental impacts through extraction, manufacturing, and transport. Furthermore, high supply costs and a lack of local expertise do not provide equity and economy, especially to rural populations, in the form of safe reliable housing. Bamboo offers an alternative to conventional building materials and practices. Found in tropical and temperate climates across the globe, this grass has the potential to be an alternative building product in areas that desperately need reliable building resources. Bamboo is currently used as a housing material in many regions and much research has been conducted on its strength properties in both its natural form and in engineered building products. Its qualitative sustainability benefits have also been highlighted. However, in much of the world, bamboo remains the 'poor man's material'. Removing the stigma and gaining greater engineering recognition and acceptance for bamboo requires formal quantification of this natural fiber material with respect to performance, standardization, and sustainability.

Research and standardization of non-conventional materials such as bamboo therefore serves both a technical and social role as these efforts can promote sustainable practices in developing regions. This ultimately leads to greater acceptance and utilization. Such acceptance, coupled with advocacy, can lead to broader social acceptance of previously marginalized vernacular construction methods. Bamboo offers a low-cost, sustainable alternative for construction in areas where conventional materials are expensive and/or difficult to obtain. Through broader utilization, adequate and reliable housing is provided to a greater population while reducing cultural, environmental, and economic impacts. In his 1981 thesis on bamboo

structures, Janssen writes that the full utilization of indigenous material is crucial to increasing the self-sufficiency of developing countries. Standardization of bamboo test methods and construction would promote greater equity with adequate housing and standards of living while also preserving culturally-important vernacular building methods. Use of local bamboo material also reduces environmental and economic impacts. With standardization of non-conventional materials like bamboo, the triple bottom line of sustainable development (Figure 1-5) is realized, especially regarding equity. Figure 1-5 highlights some of the qualitative benefits associated with using bamboo in the areas of environment, economy, and equity. The purpose of the current work is to quantify environmental impacts associated with a representative structural bamboo element and compare it to the impacts of structurally comparable steel and timber components. The hope is that this quantification and comparison will further highlight the potential of bamboo with respect to the environment and also facilitate further study of its potential in the areas of equity and economy.
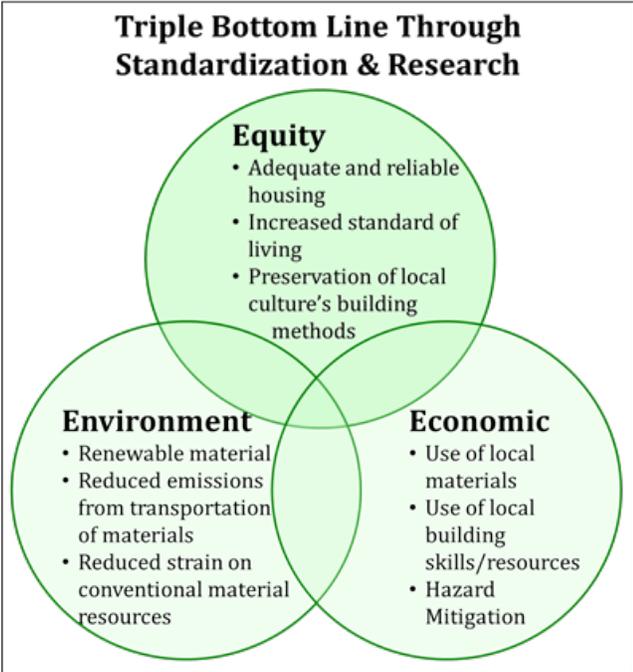
Figure 1-5: Triple bottom line through standardization and research of bamboo

1.6   SCOPE OF DOCUMENT

Bamboo offers great potential as a sustainable alternative to conventional building materials. However, its use is still often relegated to marginally or non-engineered structures due to gaps in knowledge of its performance, standardization, sustainability, and utilization. The objective of this work is to investigate the performance and methods of assessing the performance of structural bamboo components, namely axial and flexural members in an effort to further the standardization, design, and use of bamboo structures. The work also aims to quantify the sustainable benefits and environmental impacts of structural bamboo components as the qualitative benefits are often highlighted in the literature.

Chapter 2 discusses the composition of bamboo, its major material properties, and its global resources. An overview of structural applications and structural benefits of bamboo is also presented to provide an introduction to historical, current, and envisioned uses as a construction material in its natural form as well as in the form of engineered products. Chapter 2 also presents an overview of the current standardization of bamboo as a building material as well as the proposed path to further standardization in its natural form. Discussion is given to the social benefits of bamboo standardization as well as highlights recent research on developing improved standard test methods that are both laboratory and field applicable. Gaps in the understanding and standardization of full-culm bamboo properties are identified and the test methods described in subsequent chapters are placed in the context of current standard approaches.

In **Chapter 3**, often overlooked aspects of the typically-used standard tension tests for bamboo are investigated in a rigorous study. Two parameters associated with the test arrangement are considered: the orientation of specimen extraction and the degree of rotational restraint provided by the test machine. Experimental tension tests composed of full thickness

radial specimens as well as tangentially oriented specimens are conducted and monitored using a VIC-3D imaging system in an effort to capture nonlinear strain profiles. Implication of test arrangement and experimental results are discussed.

The flexural performance of bamboo beam components is discussed in **Chapter 4** specifically the study of longitudinal splitting failures and the development of a standardized test method to address this common limit state. Full scale flexural tests of un-notched and notched bamboo culm specimens are used to investigate the principle of shear flow within flexural members in order to develop an improved understanding of bamboo splitting failures. Experimental tests were conducted at both the University of Pittsburgh (Pitt) and the Pontifical Catholic University of Rio de Janeiro (PUC-Rio) in Rio de Janeiro, Brazil.

The experimental buckling behavior of bamboo columns, specifically the behavior of multiple-culm columns is presented in **Chapter 5** along with analytical results investigating the impact of initial curvature, taper, and slenderness on the column performance. Full scale experimental tests on single culm and multiple culm bamboo columns assessed the strength and buckling behavior of these components.

Chapter 6 describes a comparative midpoint life cycle analysis that was conducted to compare the environmental impacts of a representative bamboo column (studied in Chapter 5) with impacts of structurally comparable timber and steel column alternatives having similar capacity. The life cycle assessment (LCA) methodology was used to calculate environmental impacts. Structural design parameters – specifically column height and axial capacity – were used as the baseline functional units. The use of structural design parameters as functional units is envisioned to help facilitate a future framework in which sustainability considerations can be

better integrated into the structural design process through quantified relationships between sustainability metrics and properties required in the structural design process.

Finally, **Chapter 7** provides a summation of the current work, conclusions on the potential for and further acceptance of bamboo as a building material and recommendations for areas of future research.

2.0   BAMBOO AND ITS STRUCTURAL APPLICATIONS

Bamboo is found globally throughout the tropics and in some temperate regions. A member of the grass family, it is utilized throughout the world for a multitude of applications ranging from food, furniture, clothing, artistic crafts, and paper products. Yet, the primary use of bamboo continues to be for construction (Lobovikov et al. 2007); it has been used in a variety of vernacular building techniques in many regions throughout history. Today, due to the lack of engineering and materials standards, bamboo is most often associated with non-engineered construction associated with under-developed rural areas and is often superseded in these regions by conventional materials like concrete and steel. However, bamboo has also been used in major architectural works as well as for temporary structures such as scaffolding. Contemporary research is investigating the structural and sustainability benefits of bamboo; many of which stem from the material's biological composition. As a structural material, bamboo is comparable to other conventional materials in terms of most material properties. Outlining a pathway to standardization ultimately seeks to further acceptance and use of bamboo as a construction material.

2.1   BAMBOO AND ITS RESOURCES

Bamboo is a member of the larger grass family and there are hundreds of species worldwide. Species range from small diameter 'reed like' bamboo to large diameter woody bamboo that is often used in construction. A functionally graded, natural fiber-reinforced material, bamboo has evolved in nature to efficiently resist environmental loads such as wind and gravity. Bamboo has been shown to have mechanical properties comparable to those of conventional building resources. Additionally, its availability worldwide gives it great potential as a building material. Bamboo plantations of various sizes can also benefit from the advantageous growing properties of bamboo and the multitude of uses for the harvest. However, as an organic material, bamboo must be seasoned and preserved properly for intended uses, especially for exposed structures.

2.1.1   Bamboo Taxonomy and Classification

Bamboo is a member the grass family *Poaceae* or *Gramineae*. The family classification is then divided into sub-families, tribes, sub-tribes, genera, and species (Chapman and Peat 1992). The bamboo sub-family, *Bambusoideae*, is associated with the woody culm bamboo and is the "most primitive subfamily in terms of flower structure" (Chapman and Peat 1992). *Bambusoideae* is composed of 13 or 15 tribes based on the two widely used grass classifications from 1992, Clayton and Renvoize or Watson and Dallwitz respectively (Chapman 1996). The largest tribe, *Bambuseae* is the woody bamboo tribe and is divided into various sub-tribes. The sub-tribes are then divided into multiple genera such as *Arundinaria*, *Bambusa*, *Chusquea*, *Dendrocalamus*, *Gigantochloa*, *Guadua*, *Melocanna*, *Merostachys*, *Nastus*, *Phyllostachys*, *Rhipidocladum*, and *Schizostachyum* (Chapman and Peat 1992, Clark and Pohl 1996). An early 1966 estimate by

McClure classified bamboo into 63 genera and approximately 700 species (Liese 1987) but this number has grown to between 1000 and 1500 species (Grewal 2009; Laroque 2007). Common species of large diameter bamboo used in construction include *Phyllostachys heterocycla pubescens* (Moso), *Bambusa Stenostachya* (Tre Gai), *Guadua angustifolia* (Guadua), and *Dendrocalamus Giganteus* (Dendrocalamus). The experimental portion of this work includes specimens of Moso, Tre Gai and Dendrocalamus.

2.1.2 Bamboo Anatomy, Structure, and Growth

The two main anatomical features of the bamboo plant are (a) the visible culms or stalks of bamboo (Figure 2-1) which are ultimately used as the raw material for construction and (b) the underground rhizome system. Bamboo grows and matures rapidly yet only flowers once in its lifetime. Most new culm production is achieved through the expansion of the rhizome system.

Figure 2-1: Plantation of *Phyllostachys Aurea* in Bananal, Brazil

2.1.2.1 The Bamboo Culm

For most woody species, the structure of bamboo is composed of culms with solid transverse diaphragms or nodes separating hollow inter-nodal regions along its height (Figure 2-2a). Generally, depending on species, the length of internodes between diaphragms increases along most of the culm height, decreasing as it reaches the very top of the culm (Amada et al. 1996). The circular cross section is composed of unidirectional cellulosic fibers oriented parallel to the culm's longitudinal axis embedded in a lignin matrix (Figure 2-2b). Bamboo is a functionally graded material that has evolved to resist its primary loading in nature: its own self-weight and the lateral loading effects of wind. As seen in Figure 2-2b, the density of fibers increases from the culm's inner wall to the outer wall. In some species such as Tre Gai, the wall thickness of the bamboo culm will be largest at the base of the culm and decrease with height up the culm, also demonstrating a naturally efficient use of material to resist overturning due to wind while reducing gravity loads. Finally, the thin outside layer of the culm wall (approximately 0.25 mm thick) is dense and contains silica, which serves as good protection for the plant but can dull tools when bamboo is used in construction (Janssen 2000).

a) longitudinal section of culm

b) functional gradation of cellulosic fiber from inner to outer culm wall.
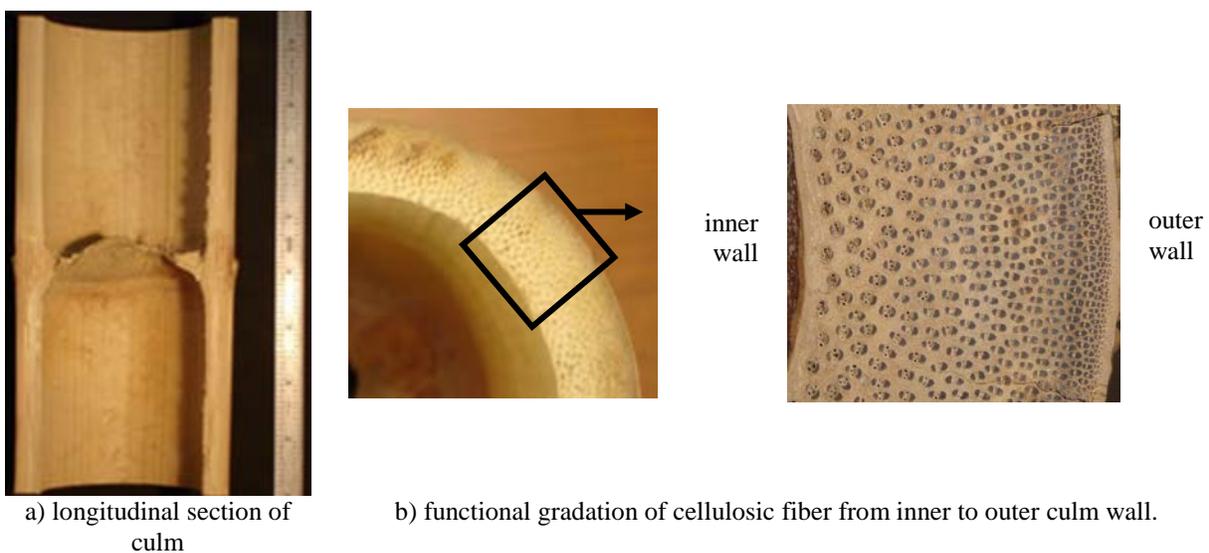
Figure 2-2: Composition of a bamboo culm

While alive, the culm is both the structural support of the bamboo and the conduit for water and sap transportation. The culm is composed of approximately 40% cellulose fibers, 10% vessels and 50% parenchyma tissue (Janssen 2000). The parenchyma tissue matrix in which fibers and vessels are embedded begins to harden or lignify over time as the culm grows. The fibers which provide the culm's strength are grouped around vessels for water and sap transport in vascular bundles as shown in Figure 2-3 or occur as isolated strands. Figure 2-3 shows that the conducting vessels are 'capped' by the bamboo fibers (darker cells) and surrounded by parenchyma. The vascular bundles are large and less densely packed near the interior wall while near the outer wall they become smaller as the vessels decrease in size and become more densely packed. The vascular bundles are also oriented such that they are 'strongest' in the radial direction of the culm. The size and quantity of vessels decrease with the height of the culm (used for nutrient transport, their volume may be reduced with increased culm height) and are replaced with bamboo fibers. This addition of fibers compensates for the loss in strength and stiffness due to reductions in diameter and wall thickness near the top of the culm (Janssen 2000). Grosser and Liese (1971) outlined four basic vascular bundle types varying in shape and size and studied how these are distributed through the cross section and vertically in various bamboo species. They used the four basic bundle types and their combinations, along with the radial order of vascular bundles in the cross section to classify species of Asian bamboo from various genera.
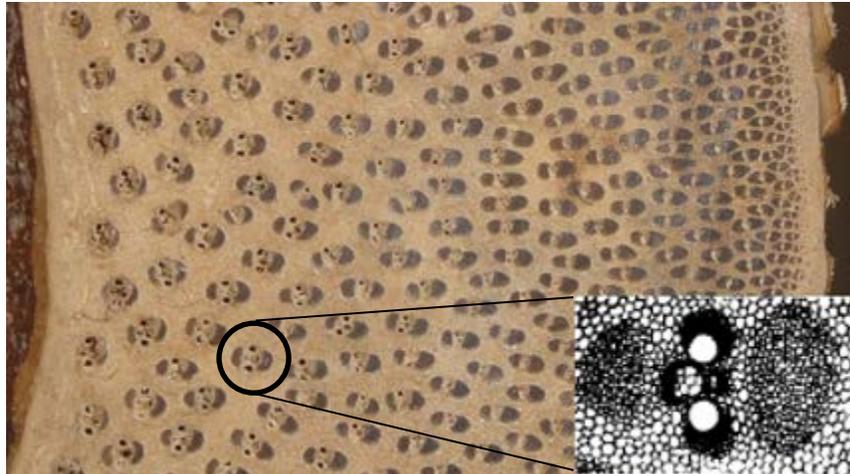
Figure 2-3: Bamboo vascular bundles (inset from Janssen 1981)

2.1.2.2 The Rhizomes

While the culm is the primary product used for construction and other applications, the underground rhizome system is equally important as it is responsible for the rapid growth and production of bamboo culm (sometimes referred to as the bamboo factory). Rhizomes are not a root but rather an underground stem having nodes and internodes that grows laterally (Clark and Pohl 1996). As shown in Figure 2-4, there are two basic forms of rhizome systems: leptomorphs and pachymorphs. A leptomorph rhizome system has larger internodes that grow or 'run' out laterally. New culms grow up and out from lateral buds at each internode perpendicular to this lateral underground stem. These species, known as running bamboo, can spread widely and are potentially invasive. The genus Phyllostachys is an example of a running bamboo (Figure 2-5a) (Clark and Pohl 1996). A pachymorph rhizome system has short and thick rhizomes that grow out and turn upwards to form new vertical culms. This causes the culms of a plant to be densely packed or 'clumped' together. These species are referred to as clumping bamboo as shown in Figure 2-5b. Some species have been found to have characteristics of both forms and are classified as amphimorph rhizomes (Clark and Pohl 1996).
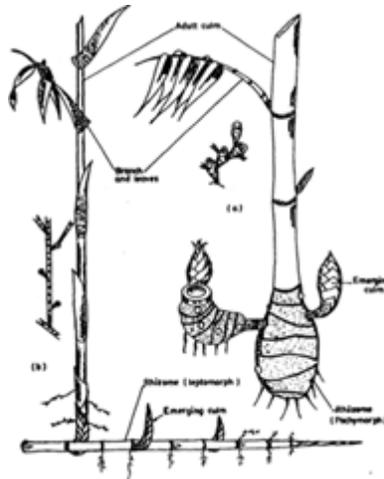
Figure 2-4: Leptomorph (left)and Pachymorph (right) rhizome systems (Banik 1995)

a) running bamboo (*P. Aurea*)   b) clumping bamboo

Figure 2-5: Running bamboo and clumping bamboo (photos courtesy of C. Thiel)

The extensive network of bamboo rhizomes effectively binds up the soil to a depth of approximately 300 mm (Chapman and Peat 1992). This makes removal of bamboo difficult although planters are investigating ways to use the rhizome material for products (Figure 2-6). The rhizome system also has potential for providing soil stabilization. Janssen (2000) writes that there have been cases of bamboo preventing riverbank erosions and therefore protecting villages. However, while the rhizomes are effective in binding up the soil, the shallowness and density of the underground system also introduces a potential weak plane between the bound shallow soil and the soil beneath the rhizomes. In the northeast hill region of India, for example, stands of

clumping bamboo are believed to be the cause of slope failures during the rainy season as the heavy clumps and attendant soil slips along the weak shallow plane beneath the rhizomes.

Figure 2-6: Pile of excavated *P. aurea* rhizomes and knife crafted from material

2.1.2.3 Bamboo Growth and Flowering

Bamboo is one of the fastest growing plants on earth and species range in size from a few centimeters to many meters tall. Large bamboo can reach their full height of 15-30 m (49-98 ft) in a period of approximately 2 to 4 months (Liese 1987). This means bamboo can have a daily growth rate as high as 20 cm to 100 cm (8-39 in). *Dendrocalamus giganteus* is the world's largest grass with a height of 30-35m (98-115 ft) (Chapman 1996). This type of growth requires a large amount of stored energy: "Taking also into account their diameter of 5-15 cm, an enormous biomass must be mobilized from the stored energy in the rhizomes within a short time; the growing culm itself hardly possesses enough leaves for producing carbohydrates by assimilation" (Liese 1987).

The primary growth method for bamboo is vegetative reproduction. Rather than regularly producing flowers and seeds, new culms are produced from the internodes (leptomorphs) or apexes (pachymorphs) of the rhizomes. This usually occurs during a certain season of the year

27

(Janssen 2000). Vegetative propagation can also be accomplished through the use of cuttings (culm, branch, or rhizome) from an existing bamboo plant (Liese 1987).

<div align="center">(Lobovikov et al. 2007)   (Janssen 2000)</div>
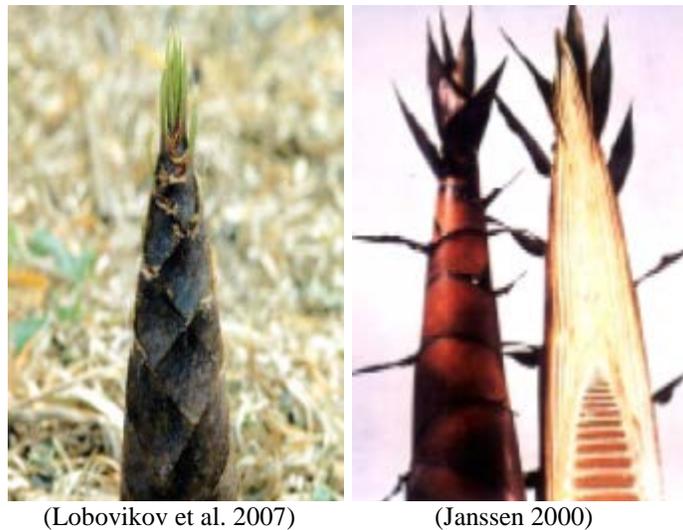
Figure 2-7: Outside view (left) and cross section (right) of a new bamboo shoot

When a new bamboo shoot emerges, it is protected by a rigid sheath of culm leaves (Figure 2-7). These leaves are shed as the culm develops and matures. The nodes and internodes (diameter and length) are already defined in the new bamboo shoot and begin to grow and expand (Liese and Weiner 1996) much like a collapsing telescope that is being stretched open. Initially the culm diameter is small. Since bamboo culms do not experience cambial growth like trees, the bamboo creates culms of larger diameter and height only through creation of new rhizomes from the first shoot. New rhizomes grow out of the base downward into the soil and then turn upwards to produce a secondary and larger culm. This process is repeated with successive rhizomes resulting in progressively larger diameter and taller culms until the system stabilizes at its final culm size (Chapman 1996).

After the initial growth period, the bamboo culm begins to mature. In comparison to timber which takes more than 10 years (softwood) or 30 years (hardwood) to mature, bamboo culms mature in only 3 to 5 years depending on species. Unlike timber which continues to

produce new tissue radially through the cambium, bamboo does not experience any secondary growth and all vessels must function through the entire life of the culm.

During this process, lignification of the parenchyma tissue and cell walls continues as more lignin accumulates. The lignin content of bamboo (20-26%) is similar in value to both North American softwoods (24−37%) and hardwoods (17−30%) (Li et al. 2007). Studies vary on how long lignification continues after bamboo reaches its full height. Some state that lignification is completed after the first year of growth while others state that the lignin content can continue to increase in fiber and parenchyma cells for one to three and even up to seven years (Li et al. 2007). Liese and Weiner (1996) saw no increase in the number of lamellae of fiber walls in specimens of *Phyllostachys viridiglaucescens* between the third and ninth year. Yet fiber wall thickness was shown to increase again between years 9 and 12.

Ultimately, the cell wall thickening of bamboo fibers within vascular bundles over time correlates to an increase in specific gravity and improved mechanical properties (Li et al. 2007, Liese and Weiner 1996). Therefore it is widely recognized that the mechanical properties of bamboo improve with age. For specimens of *Phyllostachys pubescens* grown in the southeastern United States, Li et al. (2007) showed the specific gravity increased dramatically between years one and three and only slightly thereafter in years three through five. Lignin content was shown to stabilize at year three and this was therefore deemed an appropriate time to harvest. Moisture content decreases during the maturation phase of three years and the amount of cellulose also decreases in culms after the first year. Mechanical strength also begins to decrease after five years and especially after bamboo flowering (Liese and Weiner 1996).

Bamboo flowering and seed production occur very rarely. Although some bamboos do flower and seed frequently, most species only flower once at the end of their 20 to 40 year

lifespan. The interesting aspect of bamboo flowering is that most species experience gregarious blooming where all the member of a species flower at once (Clark and Pohl 1996). This is irrespective of culm age or distribution over large areas "even over 1,000 km [621 miles]" (Liese 1987). This surge of blooming then exhausts the energy of the plant stored in the parenchyma cells of the culm and the rhizomes and the bamboo die in mass quantities. The seeds produced and any old rhizomes that survive the flowering then begin to regenerate the bamboo population (Clark and Pohl 1996). This mass flowering and die off poses a challenge to commercial applications of bamboo and the protection of bamboo habitats (and the animals that live in them).

2.1.3   Bamboo Resources

Global bamboo forests not only provide habitats for a range of birds, mammals, insects, and reptiles but are also one of the top producers of biomass. According to Janssen (2000), bamboo can produce up to 10 tons of biomass per hectare and accounts for one-quarter of the biomass in tropical regions and one-fifth in sub-tropical regions. Biomass in the form of fallen leaves helps to rejuvenate the soil while harvested culms and rhizomes are used in a variety of crafts and industries. Paired with its rapid renewability, the global availability of bamboo gives it great potential as a building material.

The world bamboo habitat, as shown in Figure 2-8, encompasses tropical and temperate climates on all continents except Europe and Antarctica; the world bamboo forest area is estimated at 62,520 square kilometers (Lobovikov et al. 2007). Most woody bamboo species grow between the latitudes of 46N and 47S (Laroque 2007). Asia has the highest percentage of bamboo forest with 65% and the leading country, with 30% of world bamboo resources, is India. About half of China's bamboo stock is *Phyllostachys edulis*, which is the principal source of

edible bamboo shoots and is also used for construction (Chapman and Peat 1992, Chapman 1996). Meanwhile, there are more than 100 species of bamboo native to India and bamboo covers about 13% of the country's total forest area (Vengala et al. 2008). Common Indian bamboo species used for construction are *Bambusa balcooa*, *Bambusa bambos*, *Bambusa tulda*, *Dendrocalamus giganteus*, *Dendrocalamus hamiltonii*, and *Dendrocalamus asper*. The species *Bambusa vulgaris* is another common bamboo found throughout the tropics.

Global Bamboo Forest Area: 62,520 km²
(Data from Lobovikov et al. 2007)

Asia: 65%

Africa: 28%

Americas: 7%

By Country:
30%   India
14%   China
5%   Indonesia
4%   Ecuador
2%   Myanmar
2%   Vietnam
43%   Others
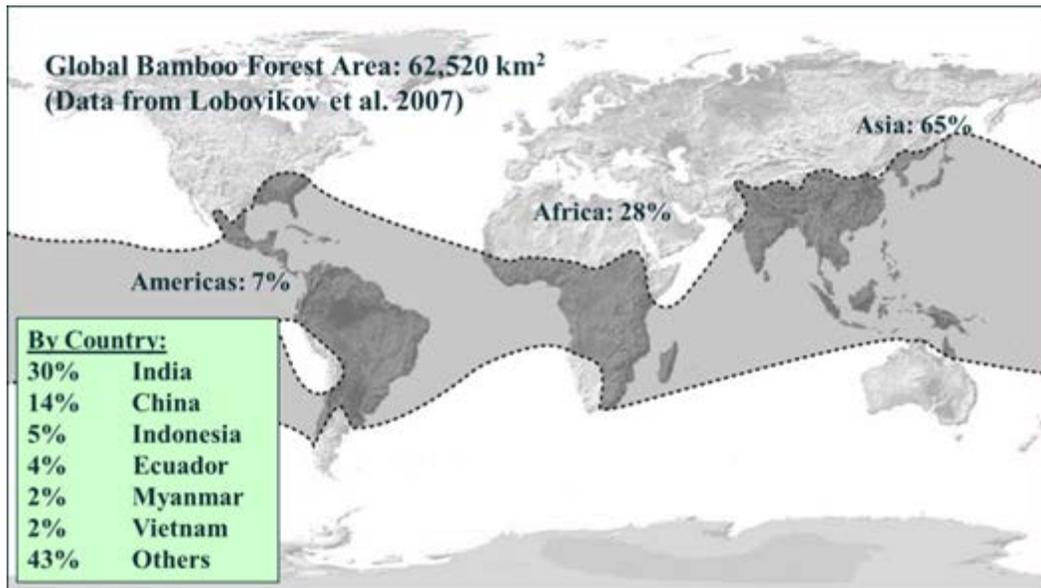
Figure 2-8: World Bamboo Habitat (adapted from Laroque 2007)

Figure 2-8 also shows the potential for bamboo in areas such as South America, Africa, and even the Southeastern United States. Ecuador has 4% of the world's bamboo forests and Colombia has approximately 520 square kilometers of native *Guadua angustifolia kunt*, one of the most widely used species for construction (Laroque 2007), growing in some regions (Correal and Lopez 2008). Brazil, despite bamboo forest only making up 2% of the country's total forest area, is said to have the greatest diversity of bamboo in Latin America with 137 species (Laroque 2007) and interest in the material is growing rapidly due to its perceived advantages. Bamboo can be grown in areas of the Southeastern United States, yet the only species native to North America is

Arundinaria gigantea, or cane, which grows along rivers and streams or in marshy areas (Clark and Pohl 1996). Bamboo can also grow outside of the tropics in temperate and even cold climates: some species of *Thamnocalamus* can survive at an elevation of 3000 meters above sea level in temperatures of -20 or -30°C for five or six months of the year in the understory of the Tibetan pine forest (Chapman 1996).

However, while bamboo species grow and can be grown throughout the world, there are concerns of depleting its resource base to meet the growing demand for bamboo products. Janssen (2000) writes that even in countries with large bamboo resources like India and China, there is a lack of material availability and that natural propagation is not enough to regenerate bamboo resources for the burgeoning industrial demand: "Active and systematic plantation programs are required if bamboo is to ever reach a utilization level that does justice to its potential" (Janssen 2000). Yet, there is also the issue of virgin natural forests being clear cut and replaced by the very bamboo plantations trying to meet this demand; effectively negating the environmental benefits espoused by the use of bamboo. Ultimately, a balance must be sought between harnessing the potential of bamboo use and limiting impacts to natural forest habitats.

2.1.4   Bamboo Harvesting and Seasoning

The harvesting of bamboo occurs through a range of methods and scales. At one end of the spectrum there is the case of local villagers cutting down bamboo culms by hand from local stands near the village as needed. On the other end of the spectrum there is the large organized plantation with industrial equipment and large outputs. The gap between is comprised of a multitude of homesteads, plantations, and co-operatives of various sizes and shapes. Yet while

the means and scale differ, the basic process of harvesting bamboo is composed of cutting, treatment, and seasoning.

2.1.4.1 Bamboo Propagation and Plantations

As a grass, harvesting of a single culm does not kill the entire bamboo plant as is the case with timber since culms continue to grow from the underground rhizome system through vegetative reproduction. Since bamboo rarely flowers over its life and natural propagation takes time, vegetative reproduction is also used to expand a plantation through the use of both horizontal and vertical cuttings (Janssen 2000). Other methods of propagation include the offset method, rhizome method, layering, macroproliferation and tissue culture (Janssen 2000). Typical vertical cuttings are 2 to 3 internodes in length and planted in the ground much like a tree sapling. Rhizomes begin to grow downward from the buried bottom node and sprouts grow from the top nodes. Horizontal cuttings involve burying a length of green culm trimmed of branches horizontally in the ground. New sprouts and rhizomes then will begin to grow at nodes where branches were cut. It is good practice to obtain cutting material from various sources to reduce the impact of gregarious blooming and die-off of the bamboo stock (Janssen 2000).

In most parts of the world, the largest stock of bamboo is still growing in natural forests (Janssen 2000). Meanwhile, privately owned homesteads are usually only for private use with little or no material being sold: "the homestead mode turns out to be less profitable only if the farmer wants to sell the bamboo on the market. The real value of homestead bamboo lies in its utility to the farmer and his family" (Janssen 2000). Plantations are owned by companies and cooperatives and the bamboo product is often sold to pulp and paper manufacturers. These companies need huge quantities of bamboo hence a large amount of land. Janssen (2000) argues that this huge allocation of land for non-food agriculture poses a major impact and advocates that

a more sustainable solution is more local bamboo plantation co-operatives. According to Liese (1987) chemical fertilization can increase yields by more than 50% and a sustained plantation yield can be estimated at amount 5-12 tons of air-dry material per hectare. Janssen (2000) estimates that a well-managed plantation yields as much as 20-30 tons (air-dry) of bamboo per hectare per year.

In June 2012, the author visited a small privately-owned bamboo plantation, Bambuparque (Bamboopark) in the Brazilian mountain town of Bananal, São Paulo State, approximately 150 kilometers from Rio de Janeiro. Owned and operated by Sr. Luis Inglês, the plantation is 2 hectares (20,000 square meters) in size and grows one commercial species *Phylloyostachus aurea*. However, the plantation also has nine other species growing on the grounds such as *Bambusa vulgaris*, *Bambusa nutenes* (native to Brazil), *Bambusa tudoides*, and *Dendrocalamus giganteus*. For the *P. aurea*, there are approximately 60,000 bamboo culms growing on the plantation and about 20% are used in a single year. Sr. Inglês (2012) does not use chemicals for pest control, fertilizer, or irrigation (although the plantation is located along a mountain stream). The growth season begins in September (Spring) with the sprouting of new bamboo shoots. No laborers are allowed in the plantation for 2 months during this first phase of growing to prevent damage to the new bamboo shoots. In 3 to 4 months, the culms reach their maximum height of 8 to 10 meters. Ultimately, the bamboo is used in furniture products as well as decorative walls and ceilings for clients in São Paulo and Rio de Janeiro. At the time of the visit, Sr. Inglês was working on developing a bamboo beach chair at a cost of approximately 120 Brazilian Reais (US$70). Three meter long cuts of bamboo culms are sold in small quantities to clients for approximately BR$6 (US$3.50) per culm. Currently, Sr. Inglês is supporting the plantation privately but has the goal of making the plantation commercially sustainable.

2.1.4.2 Bamboo Harvesting and Seasoning

Once a bamboo culm has matured 3 to 5 years, it is ready for harvest. One environmental benefit of bamboo harvesting is that there is no clear cutting of large areas. Rather the mature culms are selectively cut while remaining culms continue to grow and mature. This keeps the environment and habitat of the bamboo forest or plantation intact (Janssen 2000) and ensures a continuous supply of new culms, maturing culms, and culms ready for harvest.

Harvesting can be done manually with hand cutting tools or using mechanical equipment depending on the scale and location of the plantation. At Bambuparque, a small chainsaw is used to harvest culms of *P. aurea* (Figure 2-9a and b) and culms are cut to standard 3 meter lengths (Figure 2-9c). Culms are harvested at 5 years of age from May till September (winter) when the bamboo has the least water and starch and therefore greatest durability against insects and fungi. Culms are cut at a node to prevent water infiltration and rot in the remaining stump. Sr. Inglês also only harvests between the third quarter and new phases of the moon; a practice believed to reduce starch content yet no correlation between durability and moon phases is established (Janssen 2000). Any harvested culms of inferior quality are used as firewood. After treatment of the bamboo, the culms are stacked in an open shed to air dry (Figure 2-9d).

a and b) harvesting *P. Aurea*   c) cutting to 3m length   d) stacked for drying
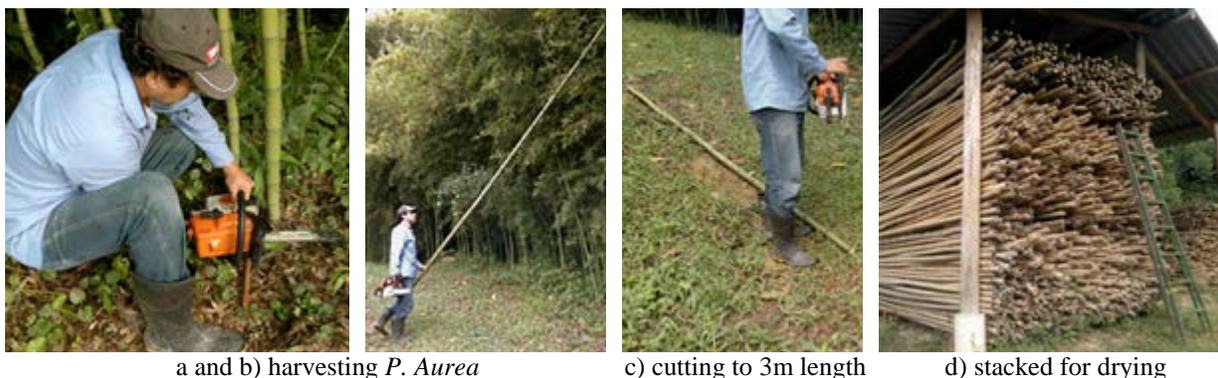
Figure 2-9: Harvesting and seasoning *P. aurea* at Bambuparque (courtesy of L. Inglês)

Air drying and kiln drying are the common methods of seasoning bamboo. Air drying typically takes 6 to 12 weeks while kiln drying in thermally insulated chambers takes 2 to 3 weeks (Laroque 2007). For air drying, the primary concern is that culms are protected from the elements (i.e. rain) with a roof or canopy and have the ability to dry quickly if exposed to moisture. Culms should also be laid horizontally with suffcent room to provide air movement and be free from soil (Janssen 2000). Bamboo often needs a longer drying period than conventional timber due to its higher moisture content (Liese 1987). With this initial high moisture content, bamboo experiences a large amount of shrinkage during seasoning; this leads to the issue of cracking and even collapse. The bamboo tissue primarily shrinks in the radial direction of the cross section (Liese 1987) with thick walled bamboo being more susceptible to cracking than a thin walled species.

2.1.4.3 Bamboo Treatment and Preservation

Untreated, the durability of bamboo varies based on the species, age, and conservation actions taken (Ghavami 2008). In the open and in contact with soil, bamboo is estimated to last 1 to 3 years; 4 to 6 years if under cover and free from soil contact (Janssen 2000, Jayanetti and Follett 2008). Only under very good storage/use conditions is untreated bamboo estimated to last 10 to 15 years.

The main culprits in bamboo degradation are water ingress, fungal attack, and infestation by insects and rodents. Fungi and insects are attracted to the starch content in the culm and animals can nest in hollow internodes. These issues are combated by the proper design and detailing of structures (Janssen 2000, Jayanetti and Follett 2008). Best practices include roof overhangs, good air circulation, drainage, the plugging of open culm ends, and ensuring no contact between a bamboo structure and soil (termite prevention). Janssen (2000) states bamboo

has less natural durability than most woods due to the absence of certain chemicals yet Li et al. (2007) states that extractive contents analogous to both trees and bamboo may help with natural decay resistance.

Ultimately, treatment processes can greatly extend the life of bamboo culms and their corresponding structures. Janssen (2000) writes that, while the price of bamboo increases approximately 30% with preservation treatment, the service life can be increased to 15 years in exterior exposure and to 25 years under cover. Preservatives range from oil based, oil soluble, water soluble, tar oil and boron-based chemicals, all of which are relatively safe options (Jayanetti and Follett 2008). Boron based chemicals such as borax and boric acid are also considered effective and inexpensive. The high silica content of the outer layer of bamboo, while providing good resistance to water and insects, also prevents infiltration of preservative. The inner layer of bamboo is also impermeable (Janssen 2000). Infiltration of preservative can only occur through the ends of the culm and the conducting vessels. These vessels close within 24 hours of harvest and therefore treatment process must occur shortly after harvest and before seasoning (Janssen 2000).

Preservation methods range in technique and complexity. Traditional methods include curing, smoking, soaking, and lime-washing of bamboo. Traditional soaking involves submerging culms in water for 6 weeks during which water soluble starch is removed from the culm. The dip diffusion method involves immersing bamboo in a chemical solution bath. In the rural village of Camburi, Brazil, culms are soaked for 2 weeks in a stone pool (Figure 2-10a) filled with a solution of water and disodium octaborate tetrahydride (Octabor). Small holes are drilled into each internode for the solution to penetrate inside the culm. The vertical soak

diffusion method involves hanging bamboo culms, which have all nodes punctured except the final node, vertically and pouring a chemical solution onto them (Adhikary 2008, Janssen 2000).

Fire treating of bamboo culms is another simple method that works for species such as *P. aurea*. At the plantation in Bananal, Brazil, the culms are washed thoroughly and then heated with a simple hand torch and propane tank (Figure 2-10b). The culm begins to sweat pyroligneous acid which is diluted with a kerosene soaked rag and spread over the culm surface. This acts as a protective varnish for the bamboo culm. The process takes approximately 15 minutes per 3 m long culm (32 culms per 8 hour day); one tank of propane, estimated to be a standard 9.1 kg (20 lb) tank, can treat approximately 200 culms.

Another common method for treating bamboo is the modified Boucherie method. This method passes a pressurized chemical solution through the conducting vessels of the culm to replace the existing sap (Adhikary 2008). Figure 2-10c shows the basic equipment needed for a field setup. A pressurized tank holds the chemical solution such as a boron compound. An airtight rubber nozzle is then attached to one end of the bamboo culm. The chemical compound is forced through the culm to replace the natural sap which seeps out the opposite open end of the culm. Once all the sap has been removed and replaced with preservative, the culm is stored for drying and seasoning. This system can be set up locally in rural communities and has been shown to treat 1200 culms per month (Adhikary 2008). A fast and effective process, the system only needs simple instruction to operate. Additionally, a range of preservative solutions can be used including cow urine or neem oil. The Boucherie method only requires that the bamboo be treated immediately after cutting and a sufficient number of culms are available to be cost effective.

a) stone submerging pool for treating with a solution of water and Octabor

b) fire treatment of P. aurea

Solution Regulator
Pressure Regulator

Pressure Gauge
Solution Outlet
Solution Input
Pressure Inlet

Splitter
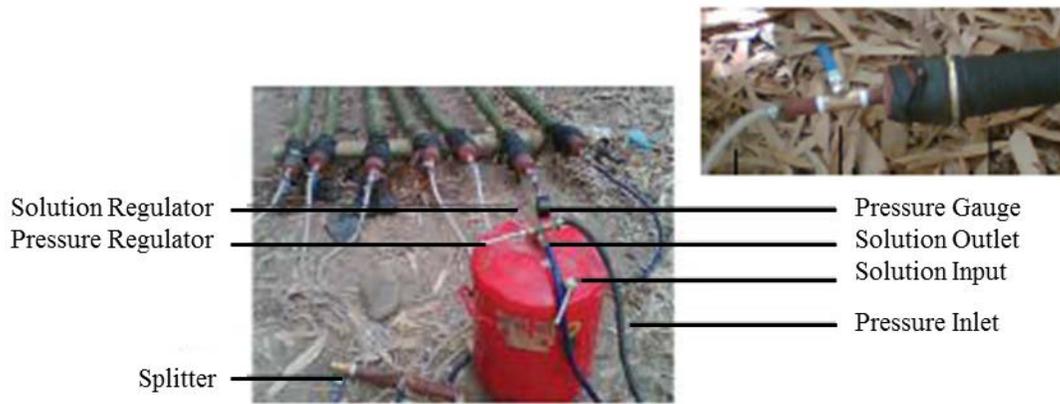
c) modified Boucherie method (Adhikary 2008)

Figure 2-10: Bamboo treatment processes

2.1.5   Mechanical Properties of Natural Bamboo

Bamboo is a promising engineered construction material because it has mechanical properties comparable to those of conventional building materials. While specifics of the mechanical properties of bamboo are discussed in detail in the pursuing chapters, these properties are highly correlated to the percentage and distribution of bamboo fibers within the culm cross section. Mechanical properties are influenced greatly by the specific gravity, which depends on fiber content, fiber diameter, and cell wall thickness (Janssen 2000). The density of

most bamboos is 700 – 800 kg/m^3 but depends on species, growing conditions, and even the position in the culm. The fibers are approximately 60 – 70% by weight of the culm tissue. The density or volume fraction of fibers is approximately 60% at the exterior face of the culm wall and 10-15% at the interior face. Density also increases along the height of a culm (Janssen 2000, Amada et al. 1996). The fiber length is longest in the middle of the culm wall section and is shorter at both the inner and outer wall faces. The shortest fibers are always at nodes. Janssen (2000) states the longitudinal modulus of elasticity is correlated to the number of vascular bundles per mm^2, while the elastic bending stress (modulus of rupture) relates to fiber length.

2.1.5.1 Modulus of Elasticity

For the modulus of elasticity, research has focused on developing equations to account for the number and gradation of the bamboo fibers which effect stiffness. Janssen (2000) states that the functional gradation of fibers in the cross section increases stiffness by 10% as compared to an even distribution of the same volume of fibers. Using an elastic modulus of 70,000 N/mm^2 for cellulose and assuming a bamboo fiber is 50% cellulose, the apparent or effective modulus is E=35,000 N/mm^2. This number is then be multiplied by the percentage of fibers in the outer and inner layers of the culm (Janssen 2000). Another technique is to determine the volume fraction of the bamboo fibers across the wall thickness. This volume fraction is then used with the rule of mixtures to determine the modulus of elasticity across the wall thickness (Amada et al. 1996, Ghavami et al. 2003, Ghavami 2008, Li and Shen 2011).

2.1.5.2 Flexural Strength

Janssen (2000) estimated the bending stress at failure for air-dry bamboo as 0.14 times the density in kg/m^3. However, in typical bending tests, the mode of failure is not fracture of the

fibers but rather longitudinal splitting of the material due to fracture of the weaker lignin bonding the fibers together. This is due to the shear in the section (i.e.: *VQ/It* shear) overcoming the capacity of the relatively weak lignin. Janssen (2000) gives a critical value of transversal strain as 0.0013 for establishing the bending capacity of bamboo. Using a Poisson's coefficient of 0.3 and a modulus of E = 17000 N/mm^2, a critical longitudinal strain of 0.00373 and an ultimate bending stress of 62 N/mm^2 are estimated, "a typical outcome" in tests (Janssen 2000).

2.1.5.3 Compression Strength

The compression strength of full-culm bamboo has been studied by multiple authors. As with bending strength, Janssen (2000) estimated the ultimate compressive stress of air-dry bamboo as 0.094 times the density in kg/m^3. During a typical compression test, the specimen often develops vertical cracks and bulges laterally (like a wooden barrel). The friction caused by contact with the loading plates holds the specimen together and can be a factor in the reported compressive strength value. Therefore, Arce-Villalobos (1993) called for the use of friction-free loading plates during testing. Arce-Villalobos (1993) also states that lignin plays a large role in bamboo failure under compression as tangential expansive forces lead to critical tangential strains.

2.1.5.4 Tensile Strength

The tensile strength of bamboo has been shown to be quite high and vary widely between species. Bamboo has been cited as having tensile strength similar to mild steel in some cases (Laroque 2007). As with Young's modulus, tensile strength is influenced primarily by the bamboo fiber volume ratio (Janssen 1981). Amada et al. (1996, 1997) studied tensile specimens from two year old *Phyllostachys edulis Riv.* (Mousou bamboo) and found that the tensile strength

of the bamboo (140-230 MPa) was greater than that of common woods such as fir, pine, and spruce (~30-50 MPa). Using the rule of mixtures, the tensile strength of the lignin matrix was estimated to be 50 MPa and that of a vascular bundle to be 610 MPa (12 times larger). The tensile modulus of elasticity was 2 GPa and 46 GPa for the matrix and bundle respectively (Amada et al. 1996, 1997). Due to their entangled fibers, bamboo nodes show more isotropic behavior and lower tensile strength (Amada et al. 1997).

While bamboo has good tensile strength in the direction of the fibers, a more critical value of bamboo strength is the tensile strength perpendicular to the unidirectional fibers. When tension is applied in the transverse direction, only the lignin matrix acts to resist the applied stress. This leads to splitting and cracking failures. Studies have shown that bamboo fails at a specific transverse strain of approximately 0.001 and that this value should be used as a limiting criterion for design (Arce-Villalobos 1993). This value can also be correlated to performance in the longitudinal direction since bamboo has a stable Poisson's ratio of approximately 0.3 (Janssen 1981).

2.1.5.5 Shear Strength

As described above, the strength of the lignin matrix is often the limiting factor for strength. Therefore, longitudinal splitting and shear strength are important characteristics for bamboo used in construction. In comparison with timber, the hollow cross section of the culm has less area to resist shear than timber although bamboo does not have defects such as knots. However, since bamboo fibers are only oriented in the longitudinal direction, there are two asymmetric shear planes in bamboo: a shear plane across the cross section of the culm and a shear plane parallel to the fibers. For a bamboo culm in flexure, Janssen (2000) estimates the critical shear stress at the neutral axis as 2.2 N/mm^2.

2.1.5.6 Commentary on Bamboo Material Properties

As can be seen in previous sections, a great deal of what is known of the material properties of bamboo consist of 'rules of thumb' or gross generalizations. Single values of limiting strain and properties estimated as a function of density – a value known to vary considerably based on many parameters – are not conducive to engineering standardization, particularly for the many bamboo species viable for construction applications. This work, along with those of Mitch (2009, 2010) and Sharma (2010), attempts to provide a framework for a better understanding and ultimately standardization of bamboo material properties and tests to determine them. The standardization philosophy is described in greater depth in Section 2.3 and Harries et al. (2012).

2.2   STRUCTURAL APPLICATIONS OF BAMBOO

The applications of bamboo material in construction are numerous. While many think of bamboo in the form of the proverbial bamboo hut, the material is used in a range of temporary and permanent structures in both natural and engineered forms. The following section focuses primarily on bamboo structures constructed with full-culm bamboo. The use of full-culm bamboo is often limited by the jointing techniques used or available and therefore a discussion of this topic is also provided. Another key aspect of the potential of bamboo structures is their ability to provide hazard mitigation and performance during extreme loading such as seismic events. Finally, mention is given to engineered bamboo products as well as the use of bamboo with other materials such as concrete and timber in the form of composites.

2.2.1 Bamboo Structures

The primary use of bamboo is in construction and its utilization encompasses a wide range of applications and forms, both temporary and permanent. For the current discussion, attention is focused on the use of natural full-culm bamboo rather than engineered bamboo products.

Bamboo scaffolding (Figure 2-11) continues to be used throughout Southeast Asia and has traditionally been used in countries like China, India, and Thailand (Janssen 2000). One of the advantages of bamboo scaffolding is its capacity and reliability in resisting hurricane force winds (Janssen 2000, Chapman 1996). Jayanetti and Follett (2008) cite non-standardized jointing techniques and lack of durability as issues hindering wider acceptance of bamboo scaffolding.

(Lobovikov et al. 2007)   Top of high rise in Hong Kong (van der Lugt et al. 2006)

Figure 2-11: Examples of bamboo scaffolding in Southeast Asia

In most cases, bamboo is used for the construction of houses and community buildings like the ones shown in Figure 2-12. Figure 2-12a showcases a bamboo schoolhouse in the village of Mungpoo, India. Composed of a bamboo frame, simple multiple-culm bolted connections are used for connections to framing members. Four-culm columns are founded on concrete plinths having reinforcing bar extending and grouted into each culm (Mitch 2010). The structure shown in Figure 2-12a is the prototype for the multiple-culm column experimental study described in

Chapter 5. Panels of woven bamboo strips are then used for the infill walls. The school is committed to sustainability and plans to construct all of its buildings using locally sourced bamboo. Figure 2-12b is a picture of the bamboo community center in the rural coastal village of Camburi in São Paulo State, Brazil. The center was constructed by the Belgium organization Bamboostic with the goal of promoting construction in the village using local stocks of bamboo (Choi et al. 2011, Ghavami 2008). Culms of *Guadua angustifolia* (Guadua) and *Phyllostachys pubescens* (Moso) were used in the construction as well as compacted earth bricks and terracotta roof tiles. Culms were treated on site in a stone pool with a chemical solution immersion bath (Fig. 2-12a). The one-story structure, which holds 3 classrooms, 2 bathrooms, an office, and a multipurpose room, is composed of four-culm bamboo columns embedded in sand within a brick plinth, bamboo beams, and bamboo roof trusses. Bolted connections are used for the bamboo components while compacted earth bricks are used to form exterior half partition infill walls. The combination of a bamboo frame and roof with masonry and plaster walls is also seen in houses in India (Fig. 2-12c) and Latin America (Fig. 2-12d).

a) St. Joseph's School in Mungpoo, India
(photo: B. Sharma)

b) village community center in Camburi, Brazil
(photo: B. Sharma)

c) bamboo house in India
(Lobovikov et al. 2007)

d) bamboo house in Latin America
(van der Lugt 2009)

Figure 2-12: Examples of bamboo housing

The construction of bamboo housing as well as community, school, and farm buildings is often related to the rural environment of the communities in which they are located: "The majority of bamboo construction relates to rural community needs in developing countries. As such, domestic housing predominates and, in accordance with their rural origins, these buildings are often simple in design and construction relying on a living tradition of local skills and methods" (Jayanetti and Follett 2008). However, bamboo has also been applied in the construction of larger architectural works. Figure 2-13a shows the large bamboo bridge at the Cross Waters Ecolodge in Quangdong Province, China. It was designed by the renowned Colombian architect Simon Velez. Velez has constructed other large exhibition structures in bamboo such as the Church without Religion in Cartagena, Colombia (Fig. 2-13b) and the ZERI

Pavilion for the 2000 World Expo in Hanover, Germany (Fig. 2-13c). Another example of bamboo architecture is the Green School in Bali, Indonesia which constructed all of its buildings with local bamboo (Fig. 2-13d).

a) bamboo bridge at the Cross Waters Ecolodge, Quangdong Province, China (Grewal 2009)

b) Church without Religion, Cartagena, Colombia (www.archleague.org/2011/02/simon-velez/)

c) ZERI Pavilion for the 2000 World Expo, Hanover, Germany (van der Lugt et al. 2006)

d) Green School, Bali, Indonesia (www.greenschool.org)

Figure 2-13: Examples of Large Architectural Bamboo Structures

In the context of bamboo housing, full–culm bamboo can be used for a range of structural components. Examples of bamboo foundations include direct contact bearing foundations (not preferred for durability considerations); bearing on stone or concrete footings (with or without dowel bars embedded into bamboo culm); bamboo embedded into concrete footings, bamboo reinforced concrete, and use of bamboo with steel shoes (Jayanetti and Follett 2008). The floor structure may consist of bamboo beams and joists with smaller culms, bamboo mats, bamboo

panels, or bamboo boards used as decking. Bamboo roofing often employs full-culm rafters or trussed systems with bamboo tiles, shingles, or mats as covering (Jayanetti and Follett 2008). Thatched roofs are also seen in bamboo structures in India and Southeast Asia (Fig. 2-13d) (Vengala et al. 2008).

Full-culm bamboo is most extensively used for wall and partition construction; often as framing paired with an infill material. This infill can take many forms: whole or halved bamboo culms, bamboo mats, split bamboo, bamboo with plaster, woven bamboo, bamboo panels, wattle, etc. (Jayanetti and Follett 2008). In northeastern and southern parts of India, housing consists of bamboo with reinforced mud walls (Vengala et al. 2008). Forms of wall construction range from traditional Bahareque and Quincha to modern grid and pre-fabricated systems (Paudel 2008). Bahareque and Quincha systems were developed in Latin American and involve a combination of bamboo laths or flattened bamboo with mud, plaster, or concrete mortar. In solid wall Bahareque, horizontal bamboo laths are attached on both sides of the bamboo framing and the interior wall cavity is filled with mud. In the hollow wall system, the horizontal bamboo laths are simply covered over with plaster or cement mortar (Paudel 2008). Modern grid and pre-fabricated systems involve a combination of wood, bamboo, plaster and mortar to create infill wall panels.

In addition to buildings, bamboo bridges (Fig. 2-13a) and space structures are two other structural forms that have garnered attention from researchers and designers. Jayanetti and Follett (2008) state that bamboo bridges are generally of trestle construction and limited span for mostly pedestrian use. However, Laroque (2007) designed and studied the use of a suspended bamboo footbridge and states that bamboo can be used in girder bridges, suspended trusses, arches, and suspension bridges. The covered bamboo arch bridges of Jörg Stamm in Colombia

can reach a span of 52 m (171 ft) and carry a 2 ton truck (Laroque 2007). Meanwhile, bamboo space structures have been studied as a solution for large span coverings (Ghavami 2008, Ghavami and Moreira 1993, Moreira and Ghavami 2009). Ultimately, bamboo was shown to be adequate for the elements of the space structure, but more research and design is needed to improve the strength and performance of connection points as experimental tests showed shear stress failure at connections.

2.2.2   Bamboo Jointing Techniques

Effective jointing in structures requires careful design, research, and practice; this is especially true for bamboo structures. Bamboo jointing techniques must not only account for the tubular form of bamboo but also the variability in size along the culm and among various culms and species (Jayanetti and Follett 2008). The splitting and crushing strengths of bamboo are specific concerns for the design of effective joints. Ultimately, the greater acceptance and utilization of bamboo in building larger, engineered, durable, and efficient structures will depend on developments, research, and improvements in bamboo jointing (Janssen 2000, Jayanetti and Follett 2008).

Janssen (1981, 2000) classified bamboo jointing techniques into eight categories based on how forces were transmitted between the bamboo culm and the joint. The five most common categories are illustrated in Figure 2-14. Category 1 involves engaging the entire bamboo culm cross section in contact through bearing (Fig. 2-14a) while category 2 (Fig. 2-14b) is composed of joints which transfer load from the inside hollow of the culm to a parallel element through a fill material (e.g. wood or cement mortar). Category 4 (Fig. 2-14c) uses parallel elements to transfer loads from the cross section (often attached by pins) while category 5 uses pins or bolt

elements perpendicular to the culm to transfer load from the cross section (Fig. 2-14d). Category 6 involves using parallel elements that transfer load between the outside of the culm and the joint (Fig. 2-14e). Categories 3, transfer from inside the culm to a perpendicular element, and 7, transfer from outside to an element perpendicular, are not often seen according to Janssen (2000) while category 8 is reserved for split bamboo connections.

a) Category 1 example: lashed bearing connection

b) Category 2 examples: plug (top) and grouted dowel (bottom) connections

c) Category 4 example: taper-wedged fishmouth connection

d) Category 5 examples: pinned or bolted connections

e) Category 6 example: 'swaged' connection
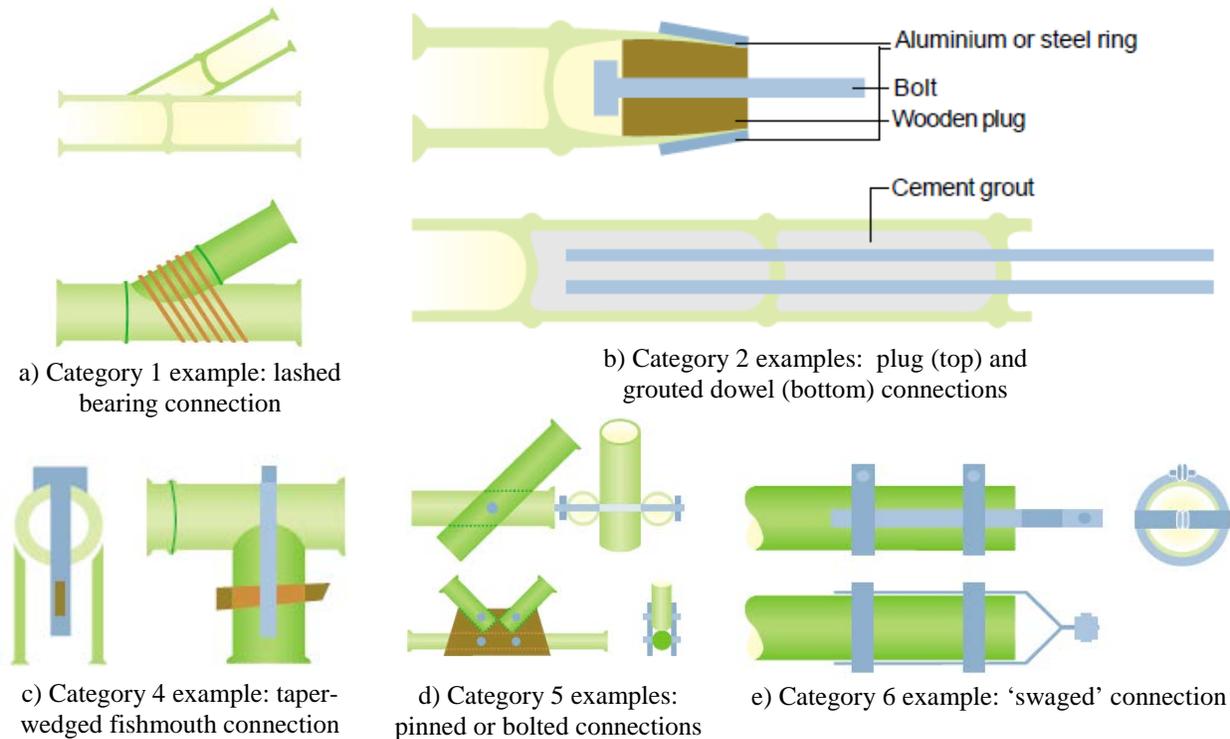
Figure 2-14: Categories of typical joints as drawn by Janssen (2000, 1981).

Ultimately, each category of joint may be comprised of either traditional jointing methods or more modern innovative alternatives. Traditional joints are often in the form of bearing connections or connections using lashing. Lashing is still one of the most widely used methods for joining bamboo as it can be fast, inexpensive, and easy to fabricate (Jayanetti and Follett 2008). This technique is often used in the tall temporary scaffolding structures seen in Southeast Asia (Arce-Villalobos1993). The lashing is often traditionally made from organic fibers like bamboo, rattan, coconut or palm; however, plastic or steel wires are also being used to

lash bamboo components. With organic lashing, the fibers are soaked before application and tighten around the bamboo as they shrink during the drying process.

However, is many cases, lashing does not provide adequate stiffness at the structural joint and alternative joints are sought. Bolts and pins (either wood or metal) are often used (Figs. 2-14c and d) along with metal or wooden gusset plates but also reduce the capacity of the bamboo component due to the potential for splitting failures at the joint. Since bamboo culms have variable cross sectional diameter, bolted connections are often designed with overlapping culms (Fig. 2-14d), which can create large joints, hinder modulation and prefabrication, and leads to eccentricities (Arce-Villalobos1993). On the other hand, well designed multiple pin joints may be used to develop efficient moment-resisting connections (Sharma 2010).

Plug connectors (Fig. 2-14b) of wood or cement mortar with an embedded metal component have an advantage of filling in open ends which helps to improve durability but, in the case of cement mortar, shrinkage and splitting (as the mortar draws moisture from the culm) are potential drawbacks (Janssen 2000). Mitch (2010) studied the performance of dowelled and grouted bamboo column bases (similar to Fig. 2-14b) subject to transverse forces and overturning moment. The connection was composed of the lower internodes being filled with cement mortar with a steel reinforcing bar embedded in the mortar plug. Due to shrinkage of the mortar, capacity was governed by the number of nodes engaged by the mortar plug; each node created a shear key of sorts. Arce-Villalobos (1993) proposed the used of wood plugs inserted into the open end of the culm affixed with various wood or steel connecting plates depending on the specific design of the central joint (Fig. 2-15). The joint works to take advantage of bamboo's strength properties in the longitudinal direction and protect the open end of the culm for infestation and moisture. Meanwhile, the wood and steel connectors can be glued into place with

51

an epoxy resin and adapted as needed for various joint applications. Arce-Villalobos (1993) also concluded that wood to bamboo connections also help to increase the flexibility of bamboo structures.

Arce-Villalobos (1993) reports that Duff (1941) suggested the use of forged steel or aluminum fittings for bamboo structures. Innovative joints have also been developed for use in bamboo grid and space structures. Metal connectors have been used in the study of bamboo space structures (Moreira and Ghavami 2009, Ghavami 2008, Ghavami and Moreira 1993, Spoer 1982). Albermani (2007) studied the use of novel Polyvinyl Chloride (PVC) joints for use as lightweight joints in bamboo grid structures. Another potential lightweight material option is to use glass fiber reinforced polymer (GFRP) materials for joints components.
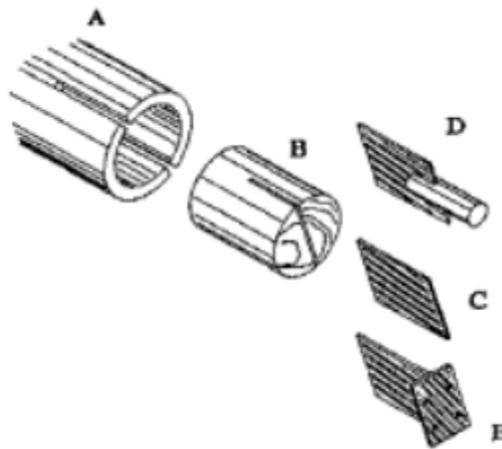
Figure 2-15: The Arce joint (Arce-Villalobos1993)

Ultimately, good joint design for bamboo structures must take into account the limits and strengths of the bamboo materials and components. Joints should, ideally, be located near nodes, seek to minimize holes, use seasoned culms, and be reinforced against splitting and crushing. Good joints should also be resistant to moisture and insect attack and consider the intended lifespan of the structure (Jayanetti and Follet 2008, Arce-Villalobos1993). Since bamboo components often perform best under axial loads, the best jointing techniques are those that can

resist these axial forces and their reactions in bamboo elements (Arce-Villalobos1993). Joints must also account for bamboo's weak splitting strength (at bolts) as well as its open ends. Standard design rules and good practice need to be established. Arce-Villalobos (1993) also argues that good joint design must be simple since the construction of bamboo structures often involves an untrained workforce and limited equipment.

2.2.3   Hazard Mitigation and Disaster Relief through Bamboo Structures

In many rural and developing areas, populations seek the conventional 'advanced' materials of steel, concrete, and masonry which are perceived to be durable and perform better during natural disasters like earthquakes. However, the technological knowledge and established methods of design practice often do not accompany the 'advanced' materials to these areas which leads to poorly built construction and ultimately greater damage and loss of life during seismic events. Another area of concern is the rebuilding of housing after a natural disaster and often the large shipments of conventional materials over long distances. Bamboo structures, which have the advantage of a lower mass than masonry and concrete structures (Vengala et al. 2008, Sharma 2010), have the potential to not only provide long term seismic performance of buildings but also to improve or expedite aid response in disaster relief efforts.

The effective seismic performance of bamboo housing has been illustrated in various field studies and research projects. Kaushik et al. (2006a, 2006b) conducted a field study of seismic damage following the magnitude 5.7 February 14, 2006 earthquake in Sikkim, India. As shown in Figure 2-16, masonry and reinforced concrete structures experienced significant damage while traditional Ikra style houses constructed of a bamboo frame with bamboo lathe infill performed well during the seismic event. The authors cited a lack of standard practices for

masonry and concrete construction as well as poor construction features such as floating columns, intermediate soft stories in reinforced concrete frames, and poor reinforcement detailing as the cause of seismic vulnerability in the region: "Except for a few [reinforced concrete] buildings involving major projects, analysis and design are generally not carried out; structural drawings are prepared simply based on previous experiences of engineers on the basis of a few [rules-of-thumb]" (Kaushik et al. 2006b). The authors also conclude that the amount of damage was disproportionate to the moderate magnitude of the earthquake. A larger, magnitude 6.9, earthquake struck northern Sikkim September 18, 2011. Similar damage patterns (although more significant) were reported in preliminary reconnaissance reports (Murty and Sheth 2012). Significantly, Murty and Sheth conclude: "There should be an aggressive promotion of traditional [Ikra] housing by development of a manual of good construction practices and inclusion of this as a formal housing construction typology eligible for bank loans".

a) damaged concrete structure   b) damaged masonry structure   c) traditional Ikra structure

Figure 2-16: Typical residential structures following the 2006 Sikkim earthquake (Kaushik et al. 2006)

Janssen (2000), in researching the National Bamboo Project of Costa Rica, notes the survival of 20 bamboo houses near the epicenter of the April 22, 1991 magnitude 7.5 earthquake. Vengala et al. (2008) notes that a bamboo test house, 2.7m^2 in size, was able to resist shake table-applied loads equivalent to the magnitude 7.8 Kobe earthquake without experiencing any damage. Bamboo bahareque structures, with varying combinations of timber, bamboo, and mortar, are also used extensively throughout Latin America, and are considered to have good performance during seismic events (Gonzalez and Gutierrez 2005, Guitierrez 2004). Work has been done to experimentally test and model the seismic performance of bamboo portal frames based on those found in and subject to the 2006 Sikkim earthquake (Sharma 2010).

In addition to long term seismic performance, bamboo structures also have potential as both temporary and permanent shelter in disaster relief efforts. Rather than shipping large quantities of conventional material, local bamboo can be used along with imported knowledge and construction guidelines/training to provide faster disaster responses (Brown et al. 2012). Bamboo gridshell structures are one potential option for these temporary shelters. The use of local building material may result in improved local resiliency and a more sustainable transition from temporary buildings to the construction of more permanent bamboo structures.

2.2.4 Engineered Bamboo Products

Bamboo has been used most often in its natural form much like timber but there is also a large amount of research addressing engineered bamboo products. These typically comprise a composite of bamboo and a binding resin. Glue laminated bamboo ('Glubam') or laminated bamboo lumber (LBL) is developed much in the same way as glue laminated lumber. Xiao et al. (2008, 2010) developed Glubam using 2,440 mm by 1,220 mm (8ft by 4ft) bamboo veneer sheets

(bamboo 'plywood') that are finger jointed and cold pressed. Through this process, girders were produced, tested, and used in the construction of a Glubam girder bridge able to carry an 8 ton two axle truck. Xiao et al. (2008) have also constructed a pedestrian bridge, a single story house, and a two-story house using Glubam components. LBL is used in the US for such non-structural components as flooring, countertops, and railings but has been shown to have structural properties and quality similar or better to wood lumber (Rittironk and Elnieiri 2008). Bamboo plywood is also formed from the lamination of bamboo strips into sheets (van der Lugt 2009). China is the leading producer of bamboo board and flooring material as well as woven bamboo mats. Other engineered products include bamboo mat board, bamboo mat veneer composite, bamboo mat corrugated sheets (roofing material), bamboo sliver laminated lumber, strand woven bamboo, and bamboo particle board similar to wood oriented strand board (OSB) which all attempt to optimize strength and utilize more of the raw bamboo culms in production (Guan and Zhu 2008, van der Lugt 2009, Vengala et al. 2008).

2.2.5   Composite Bamboo Products and Systems

Research has also been conducted on using bamboo in composite systems with other materials; these include bamboo reinforcement in concrete and in composite timber or steel assemblies. The US Navy studied the use of bamboo reinforcement in concrete in the 1960s (Brink and Rush 1966). Bamboo reinforcement in concrete has been studied in many different forms including split bamboo as reinforcement embedded in concrete beams, concrete slabs with permanent bamboo shutter forms, and bamboo reinforced columns with permanent shutter forms (Ghavami 2005, 2008). With permanent shutter forms (often also referred to as stay-in-place forms), the half-culm bamboo acts as formwork during the placement of the concrete and

remains afterward as permanent reinforcement. Ghavami (2005, 2008) studied bamboo shutter forms where the nodal diaphragms were left in place to act as shear connectors with the concrete. Strips of steel or bamboo can also be added close to nodal diaphragms to increase the shear transfer. Sudhakar et al. (2008) used vertically oriented concrete ties at intervals along the span to tie an arrangement of four bamboo culms into a composite bamboo beam. Gupta et al. (2008) used a similar approach using horizontal concrete ties to tie four culms together into a single composite column. Iyer (2002) investigated the use of bamboo strips as embedded reinforcement in masonry for improved seismic performance. One of the main concerns with using bamboo as concrete reinforcement is the high water absorption of bamboo which causes expansion of the reinforcement (and vice versa when dried) (Ghavami 2008).

In timber assemblies, bamboo boards and pins/nails have been used in timber structures for connections (Mori et al. 2008) and bamboo nails were often used in ancient Japanese construction. Modern bamboo connectors which also employ adhesive have been designed for timber pavilion structures (Inoue et al. 2008). Bamboo and timber plies have also been used to form composite sandwich panels. Finally, Li et al. (2008) studied a bamboo and steel composite floor slab composed of two bamboo panels and a profiled steel decking sheet.

2.3   THE PATH TO STANDARDIZATION

Standardization of testing and design practices is necessary not only to advance the use and acceptance of a technology but also to ensure the safety of the population using the technology. Standards provide a baseline reference as well as a benchmark requirement. Protection of the consumer, protection of the environment, reduction of production costs,

minimum standards of workmanship, occupant safety, and consideration of market requirements are all essential features of a good standard (Janssen 2000) as well as striving for performance-based metrics rather than prescriptive requirements. Therefore, standardization serves both a technical and social purpose as they must consider the context in which they will be implemented, taking into account of such things as local materials, local traditions, and the needs of the intended population.

Through standardization of non-conventional materials like bamboo, the triple bottom line of sustainable development can be realized, most notably in regard to equity. There is an increasing socio-technical-economic gap between advanced and developing societies as well as between urban and rural populations (Powell 2006). Standard field tests for non-conventional materials provide rural communities greater equity in terms of safe, adequate, and reliable housing and sustainable development using local resources resulting in an improved standard of living. Communities may wean themselves of unsustainable practices associated with transporting conventional materials to rural areas and renewable materials like bamboo reduce the strain on global construction resources.

2.3.1 Current Bamboo Standards

Currently, there are few standards and codes regarding the use of structural bamboo. In 2004, the International Organization for Standardization (ISO) in collaboration with the International Network for Bamboo and Rattan (INBAR) published a model standard for determining the mechanical properties of bamboo: ISO 22157-1 (ISO 2004b, 2004c). Illustrated in Figure 2-17, the document includes standard test methods for determining a) full-culm compressive strength (Fig. 2-17b); b) longitudinal tensile strength using a 'dogbone' specimen taken from the culm

58

wall (Fig. 2-17c); c) longitudinal shear using the 'bowtie test' (Janssen 1981) (Fig. 2-17d); and, d) flexural capacity based on a four-point bend test of a long culm (Fig. 2-17e). The latter test is typically governed by longitudinal shear behavior (i.e. *VAy/It* shear) and is therefore not a true modulus of rupture test. The standard also provides guidelines for determining moisture content, mass, and shrinkage properties of bamboo. Other tests focused on the longitudinal shear capacity of bamboo (often a critical behavior) include a typical 'S-type' shear coupon (INBAR 1999) (Fig. 2-17f) and a 'lap shear' test arrangement (Cruz 2002) (Fig. 2-17g). ISO and INBAR also have a model standard for bamboo structural design: ISO 22156 (ISO 2004a). Meanwhile, the National Building Code of India includes a section on bamboo construction covering requirements for minimum strength, suitable species, grading and seasoning, preservative treatment, as well as design and joining techniques (Bureau of Indian Standards 2005). ASTM International is considering bamboo in a proposed revision to its standard D5456, Specification for Evaluation of Structural Composite Lumber Products, but no consideration is currently given to bamboo used in its natural form (ASTM International 2010). The International Code Council Evaluation Service (ICC-ES) has published an evaluation report (ESR-1636) on the use of culms of *Bambusa Stenostachya* (Tre Gai) bamboo from Vietnam in construction and outlines design considerations and allowable design stresses (ICC-ES 2013).

a) culm dimensions   b) compression   c) tension

d) parallel shear   e) bending and longitudinal shear

detail for longitudinal shear flow

f) interlaminar shear   g) perpendicular shear   h) pin shear

i) transverse tension split-pin   j) edge bearing
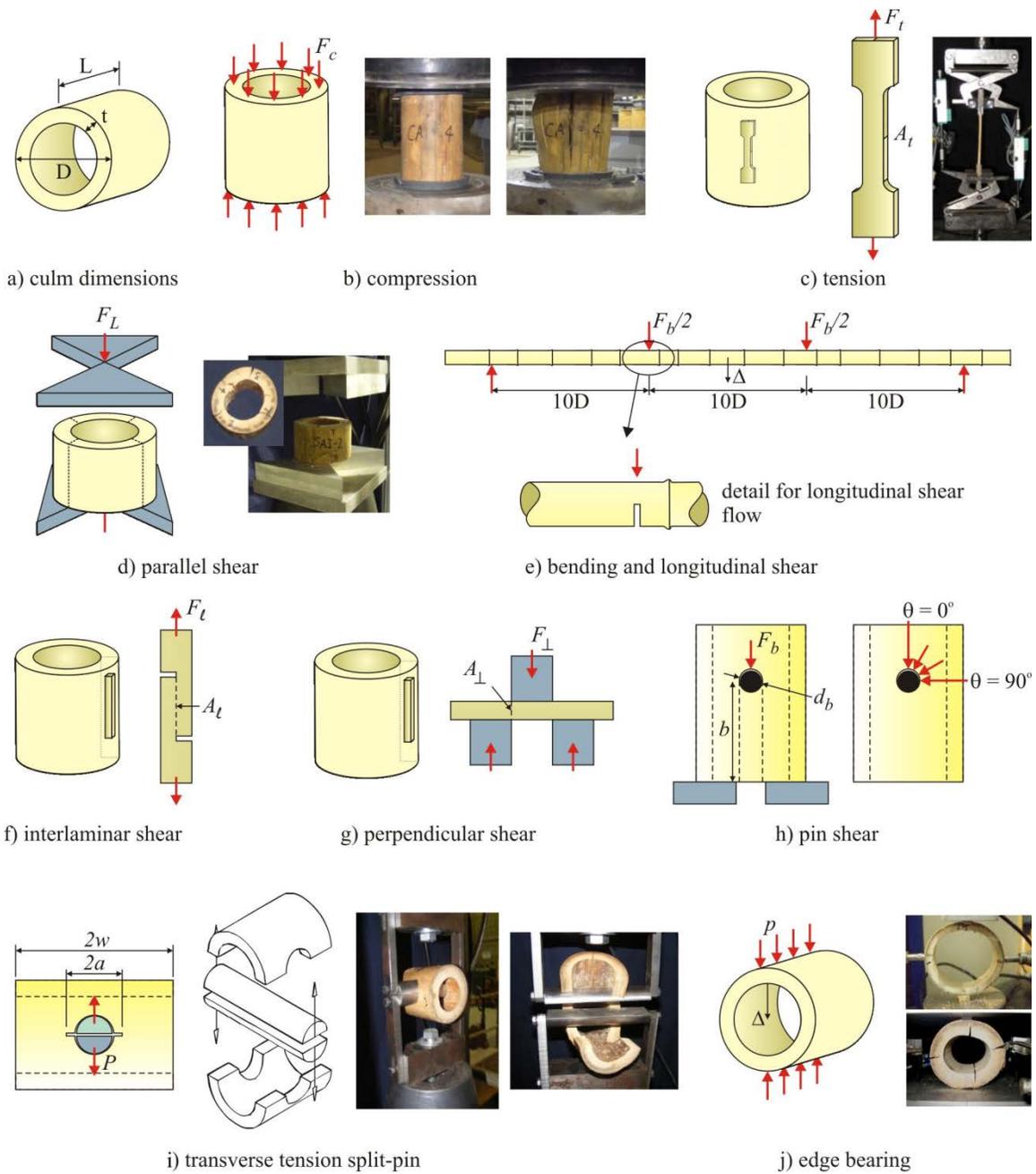
Figure 2-17: Current bamboo standards as well as proposed lab and field applicable tests (Harries et al. 2012)

2.3.2   Improving Standardization

While current standardized test methods and codes represent progress in the recognition of bamboo as a viable building material, they also highlight the need for further study and development. First, the currently available test methods do not address the splitting behavior of bamboo, which is the dominant limit state of full-culm bamboo. Second, while many of the testing procedures are applicable for laboratory settings, they cannot be implemented easily in the field where they are needed. Current field and laboratory research has sought to address these issues. Mitch et al. (2010) developed a split pin test (Fig. 2-17i) using a full bamboo culm section to determine the direct tensile rupture capacity perpendicular to bamboo fibers. The test uses a fracture mechanics approach that is based on the Mode I stress intensity factor which is a measure of the material's fracture toughness. This split pin test proved to improve the repeatability of bamboo test results as compared to other shear test methods (ISO 2004b, INBAR 1999 and Cruz 2002; Figs 2-17d, f and g, respectively). However, while the split pin test provides reliable results, it also requires a laboratory setting with capabilities to conduct tensile testing and precise machining. Therefore, Sharma et al. (2010) sought to develop a more field-friendly test with results comparable to the split pin test. The resulting edge bearing test (Fig. 2-17j) involves a full-culm section tested in compression perpendicular to its longitudinal axis to obtain the edge bearing (or diametric compression) strength. The failure mechanism of this test involves formation of multi-pinned arches in the culm cross section. The culm wall modulus of rupture, which represents a measure of transverse tension capacity of the culm wall and therefore the splitting behavior, may be calculated. Ultimately, this is one case of the synergy between development of a sound understanding of underlying bamboo mechanics and material behavior and development of practical/field-appropriate test methods.

Standardization of bamboo test methods is critical to the greater acceptance and utilization of bamboo structures. The capture of fundamental material properties permits comparison of bamboo behavior and performance across different species, geometry, weathering, and treatment processes. With respect to design, methods that reliably determine fundamental properties permit study of the calibration of material resistance factors as well as design guidance for various species. Standardized test methods can also be used in isolating factors and parameters that affect the material performance and behavior of bamboo. As with the progression from complex to field-applicable test methods discussed above, this calibration and isolation of factors affecting performance will help develop simpler design equations which will increase the acceptance, adoption, and utilization of bamboo construction in the field. Such a design approach for properties such as bamboo compression, tension, shear, and splitting capacity is consistent with those used for established materials (timber, concrete, steel, etc.) taking the general form of:

$$Q \leq \varphi F_i \left[C_1 x C_2 x \ldots x C_k \right] \tag{2-1}$$

Where the structural loading demand, Q, must be less than or equal to the capacity provided by the bamboo. This capacity is determined by considering a) the material property involved in resisting the load (compression, tension, etc.), F_i; b) a statistically derived material resistance factor, φ_i, based on standard tests and accounting for variation in material properties and confidence levels; and c) any other factors dependent on such things as species, geometry, exposure, etc. that may affect capacity, C_1 to C_k.

The goal of the current work is to further this progression of development from sound understanding of underlying bamboo mechanics and material behavior to more field applicable design and test methods. This will be accomplished through the investigation of structural

bamboo components, specifically bamboo axial and flexural members. The influence of bamboo fiber gradation on the standard bamboo tension test will be investigated with experimental tests. Bamboo columns will be tested and studied to investigate the column buckling behavior of bamboo culms and multiple-culm columns. Meanwhile, bamboo flexural tests will seek to investigate the longitudinal shear flow within the bamboo culm since this often drives splitting failures in bamboo flexural members.

# 3.0   INHERENT BENDING IN BAMBOO TENSION TESTS

Functionally graded materials (FGMs) like bamboo are important non-conventional materials in civil infrastructure that can be used for a variety of applications in both their natural and engineered forms. Standardized test methods and identification of critical limit states are crucial for increased use, reliability, and ultimately acceptance of bamboo structures. While the International Organization of Standards (ISO) has a model standard for bamboo (ISO 2004a) and a number of material test methods (ISO 2004b); these are often cursory and further study is warranted. ISO promulgates a standard coupon-based tension test method. It is the contention of the present study that, due to the functionally graded nature of bamboo, the test geometry for this test is inherently flawed and may result in additional non-uniform bending stresses being introduced across the breadth of the cross section during testing. The bending inherent in a standard coupon is due to the natural gradation of bamboo fibers through the radial direction of the culm wall. Additionally, coupon preparation: the orientation and location in the culm from which it is extracted, may significantly affect strength values reported from the test. This chapter investigates the inherent bending in bamboo tension specimens to quantify the influence of bending on tensile test results. Tensile specimens having different *in situ* orientation are prepared; these include 'radial' specimens engaging the full gradation of fibers through the culm wall thickness; and 'tangential' specimens taken from varying locations through the culm-wall thickness perpendicular to the radial direction. A Vic-3D (2010) imaging camera and electrical

resistance strain gages were used to measure variation in strain in the test specimens related to their original orientation in the bamboo culm. Experimental end conditions are also varied to explore effects of induced moment in the test specimens. Experimental values are compared with theoretical values for bending using a fiber element analysis approach. The experimental and analytical results show that current test methods for bamboo tension capacity do indeed develop stresses associated with specimen flexure; and the influence of bending is quantified for specimens of various sizes.

3.1 BAMBOO TENSILE STRENGTH

Model standards for bamboo published by ISO and the International Network for Bamboo and Rattan (INBAR), outline bamboo structural design strategies in ISO 22156 (2004a), and test methods for determining mechanical properties in ISO 22157 (ISO 2004b and c). The standard tensile test described in the latter involves the use of a 'dogbone' shaped specimen cut radially from the culm wall as shown in Figure 1-17c. The gauge portion of the specimen is required to have a rectangular cross section with dimensions of the culm wall thickness, t, or less in the radial direction and 10 mm to 20 mm in the culm tangential direction. The gage length is required to be 50 mm to 100 mm long (ISO 2004b). ISO 22157 also calls for the ends of the specimen to be "so shaped as to ensure that the failure occurs within the gauge portion" (ISO 2004b) which typically translates into a 'dogbone' shaped or tabbed specimen. Although ISO 22157 is silent on the issue, it should be clear that if a dogbone shape is used, the reduction should be made in the tangential direction of the specimen so as not to remove the extreme inner and outer culm wall fibers from the test coupon. The grips of the testing apparatus are required to

65

be aligned in the radial direction; that is: the specimen is gripped parallel to the culm wall thickness (t) dimension and through the width (w) of the specimen. If Young's modulus (modulus of elasticity or MOE) is desired, two strain gauges are placed on opposing sides of the specimen – although the ISO standard is not clear as to *which* opposing sides (the t or w faces). When testing for commercial purposes, the standard requires that specimens should have one node region located within their length, although this is not required (and is rarely done) for scientific research. Representative specimen dimensions and geometry given by ISO are shown in Figure 3-1.
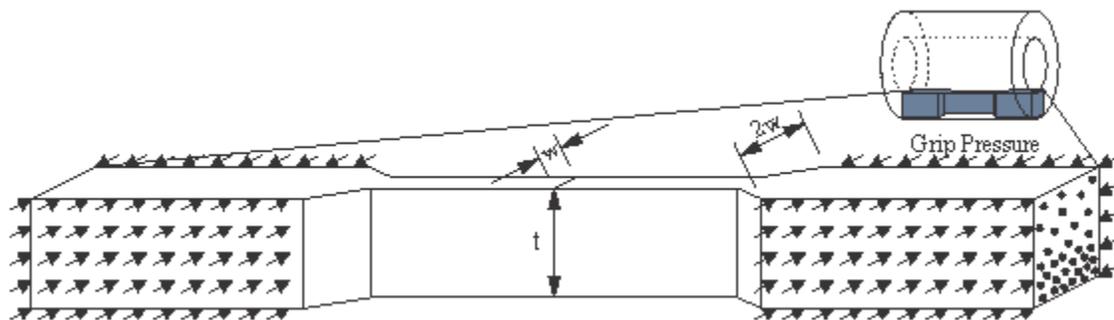
Figure 3-1: Representative bamboo dogbone specimen

In addition to the issues described above, the ISO standard tension test is silent on two critical issues: it does not consider or even mention the functionally graded nature of the bamboo fibers and their effect on specimen performance; or specify whether the loading grips of the testing apparatus should be fixed or free to rotate in order to take up any bending effects resulting from the specimen gradation. Furthermore, by specifying a specific tangential dimension of w = 10 – 20 mm with an unrestricted thickness value of t, the ISO standard is not giving consideration to the potential influence of shear lag which will effect specimens having w greater than t (Fig. 3-1) since gripping is prescribed to be through the w direction. Other standard tension test specimens for steel, (ASTM E8-11), timber, (ASTM D143-09), and fiber composites (ASTM D3039-08) also have prescribed values (timber) or recommended dimensions (steel and

fiber composites) but in most cases, in order to miminize shear lag effects, the t/w ratio is greater than 2. ASTM E8 requires that for specimens having non-conforming geometry to be considered comparable, the relationship between gage length and cross sectional area must be kept constant.

The tensile strength of bamboo has been studied for a variety of species and has been shown to vary widely. In this study, focus is placed on *how* tension strength is affected by the composition of the material, rather than on the quantitative values of tension strength for the species considered.

Tensile strength and modulus is influenced primarily by the volume fraction of bamboo fibers (Janssen 1981) since fibers are the primary source of strength (Ghavami 1988, Shao et al. 2009). Nonetheless, the lignin matrix effectively distributes stress between fibers (Shao et al. 2009). Shao et al. (2009) developed equations defining tensile strength and MOE based on the volume fraction of fibers and the rule of mixtures for a composite. In essence, this approach results in material properties averaged over the sectional area of the tensile specimen.

The elastic modulus on the outer layer of the culm wall has been found to be 3 times higher than the modulus at the inner wall (Duff 1941, Janssen 1981). Vaessen and Janssen (1997) stated that there was no evidence to show that these values varied other than linearly through the culm wall thickness. However, studies using imaging analyses have shown that the volume fraction of fibers (which can be related to tensile strength and modulus of elasticity, MOE) can vary in a parabolic fashion for some species (Amada et al. 1996, Amada et al. 1997, Ghavami et al. 2003). The resulting parabolic strength distribution is attributed by Amada et al. (1997) to the stress distribution (i.e.: bending due to wind load) experienced by bamboo in nature. Arce-Villalobos (1993) states that bamboo fails at a particular strain rather than a particular stress in the longitudinal and the tangential directions. Relationships between tensile

strength and moisture content (Ota 1950, Achá Navarro 2011), frozen moisture (Achá Navarro 2011) and density (McLaughlin 1979) have been studied. Cox and Geymayer (1969) reported that tensile strength depends on age, physiological variation of individual culms, habitat, liquid content of the soil, and 'external physical forces'. While most extant tests are made from specimens cut radially from the culm wall, many of the cited studies do not utilize the specimen dimensions and orientation promulgated by ISO. In particular, the orientation of the gripping mechanism and whether the machine grips are free to rotate often remain unreported.

3.2   INHERENT BENDING AND ROTATION OF TENSION SPECIMENS

While there has been research regarding the composition of bamboo as a functionally graded material, to the author's knowledge there has not been research on how this functional gradation affects the standard test for tensile strength. The variation in fiber density in the radial direction of the culm ultimately results in a non-uniform stress profile in specimens tested in the conventional manner. This non-uniform stress may produce a rotational moment in the specimen since the stress resultant in the specimen is not aligned with the axis of the test machine. While the ISO standard specifies a controlled displacement rate for the test, it does not give a specific requirement regarding the fixity of the specimen end conditions at the grips. Some test machines permit rotation at the grip locations by means of a ball joint or clevis. If permitted, this end rotation will result in bending deformation in a functionally graded tensile specimen.

The described behavior can be illustrated using a plane strain analysis of a representative bamboo tension specimen having a constant cross section with culm wall thickness, t, and

tangential width w, as shown in Figure 3-2a. In this case, the stress distribution in the radial direction (x in Figure 3-2a) is a function of modulus of elasticity and strain:

$$\sigma(x) = E_c(x)\varepsilon(x) \tag{3-1}$$

The composite modulus of elasticity $E_c(x)$ can be characterized using the rule of mixtures and the volume fraction of bamboo fibers, where E_f is the modulus of elasticity of a bamboo fiber, E_m is the modulus of elasticity of the lignin matrix, and $V_f(x)$ is the volume fraction of bamboo fiber as a function of x:

$$E_c(x) = E_f V_f(x) + E_m(1 - V_f(x)) \tag{3-2}$$

If strain is a constant across the section as is conventionally assumed for a tension test, the stress is found from Eq. 3-1 as a function of E_c. Once the shape of the stress profile is established, its resultant, F, and eccentricity with respect to the geometric centroid of the specimen (also the axis of the test machine), e, can be determined as shown schematically in Figure 3-2b. From these, the maximum and minimum stress in the cross section can be calculated as:

$$\sigma = \frac{F}{tw} \pm \frac{6Fe}{wt^2} \tag{3-3}$$

In which the first term accounts for the uniform distribution of tensile stress across the section area (A = tw) and the second term accounts for stress associated with the resulting moment Fe.

| a) Representative radial bamboo section | b) Representative stress profile, resultant force, and eccentricity |
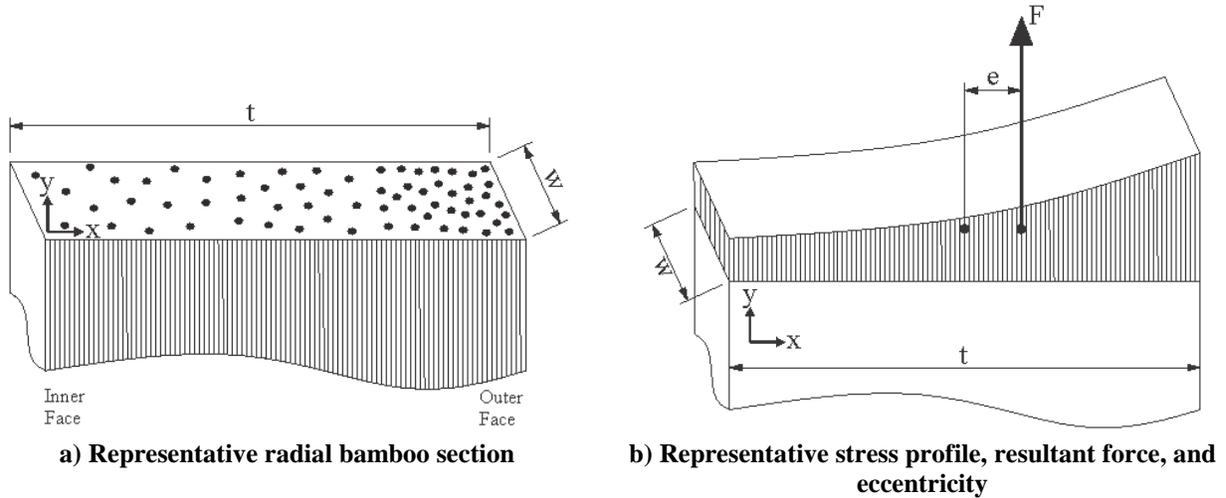
Figure 3-2: Illustrative fiber analysis of bamboo tension specimen

At this point, the continued analysis is dependent upon the specimen end restraint conditions. This can be illustrated by the conceptual spring model shown in Figure 3-3. The springs with varying stiffness, K represent the inner (K_1), middle (K_2), and outer (K_3) layers through the culm wall thickness (Fig. 3-3a). The spring stiffness increases from left to right ($K_1 < K_{2, <} K_3$), based on the increasing fiber volume fraction across the radial direction, x, of the culm wall. If the tension grips are restrained from rotation and displaced a value y (Fig. 3-3b), the strain across the section is constrained resulting in a stress variation in the section as described by Equation 3-3. However, if the tension grips are free to rotate (Fig. 3-3c), the induced moment, Fe, produced by the varying stiffness results in flexure of the section and a second-order strain distribution across the section. Considering this conceptual example, axial stress profiles across the normalized radial dimension (i.e.: t = 1) can be developed using representative distributions of fiber volume ratio, V_f.

70

a) 3 springs tested in parallel   b) springs tested in 'fixed' condition   c) springs tested in 'free' condition
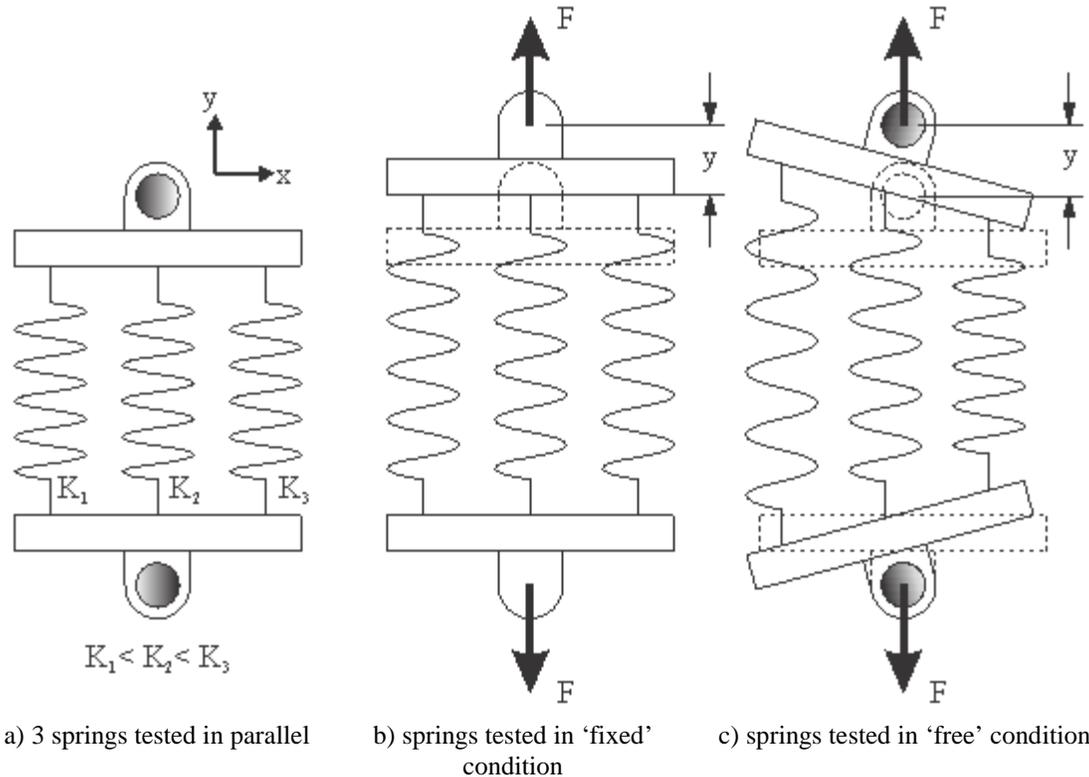
Figure 3-3: Rotation in representative spring model loaded in Tension

Janssen (1981, 2000) stated that the elastic modulus of a bamboo fiber is estimated as E_f = 35000 MPa, the elastic modulus of lignin is estimated as E_m = 1800 MPa, and that fiber volume fraction can be estimated as V_f = 0.60 at the outer face of the culm wall and V_f = 0.10 at the inner face for most species. Results from specimens of *Phyllostachys heterocycla pubenscens* (Moso) and *Dendrocalamus giganteus* by Ghavami et al. (2003) showed this conservative estimation of V_f to be valid. Ghavami et al. (2003) also found V_f to have a parabolic distribution in Moso and *Dendrocalamus*.

In our conceptual example, a constant, linear, parabolic, cubic, and square root distribution of fiber volume ratio, shown in Figure 3-4 – each resulting in an average fiber volume ratio in the cross section – V_f = 0.35, were selected (Eqns. 3-4 to 3-7). To ensure an average V_f = 0.35, the exterior V_f = 0.60 was held constant and the interior V_f was varied appropriately. Although admittedly artificial, but this is intended as an illustrative example only.

71

The value of E_f = 35000 MPa and E_m = 1800 MPa were used with Eqn. 3-2 resulting in a composite MOE averaged over the section area of E_c = 13420 MPa.

$$V_{favg.} = 0.35 \tag{3-4}$$

$$V_{flinear} = (0.60 - 0.10)x + 0.10 \tag{3-5}$$

$$V_{fparabolic} = (0.60 - 0.22)x^2 + 0.22 \tag{3-6}$$

$$V_{fcubic} = (0.60 - 0.26)x^3 + 0.26 \tag{3-7}$$

$$V_{fsquareroot} = (0.60 + 0.11)x^{\frac{1}{2}} - 0.11 \tag{3-8}$$
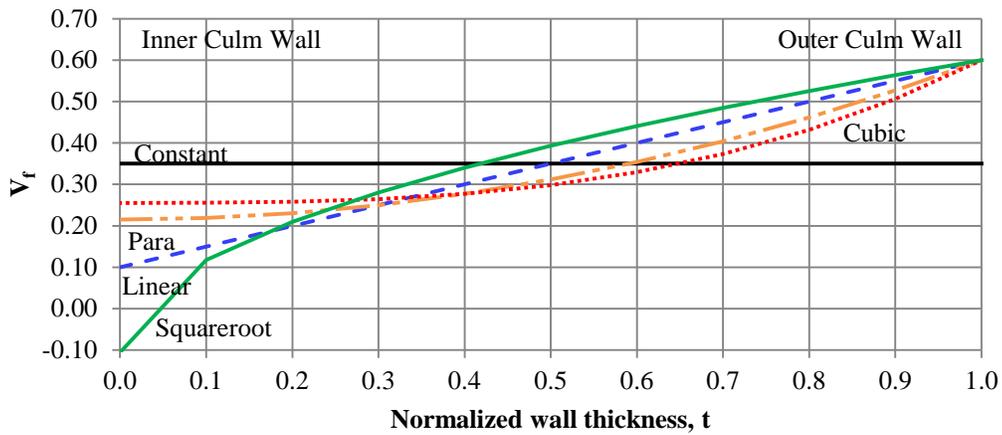
Figure 3-4: Representative fiber volume fraction distribution
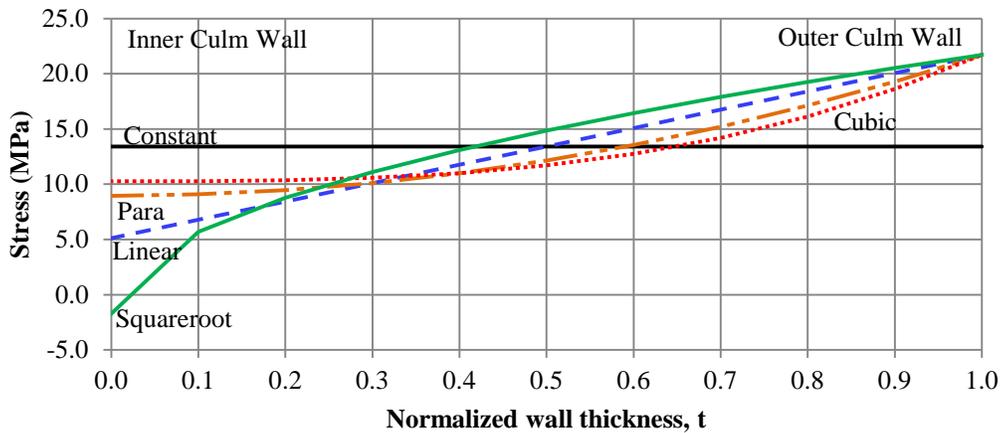
Figure 3-5: Stress due to uniform strain

72
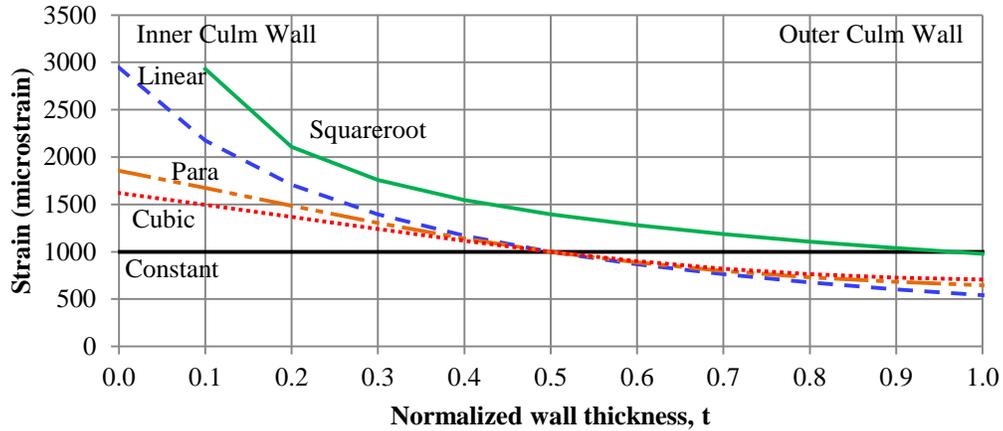
Figure 3-6: Total strain including rotation of moment Fe

Figure 3-5 illustrates that the stress caused by the application of a uniform tensile strain across the section exhibits a distribution similar to the distribution of the fiber volume fraction (which determines E-modulus). However, if the ends of the specimens are free to rotate; this stress results in the application of the moment Fe and the resulting strains, described by Eqn. 3-3, are shown in Figure 3-6 which accounts for the rotation in the specimen and shows that the maximum strain is occurring at the weaker interior face (see also Figure 3-3c). In addition to looking at the experimental strength results for the bamboo tensile specimens, the apparent strain profile through the culm wall thickness will be characterized using this approach as a guide to identify bending in the specimen.

3.3   EXPERIMENTAL PROGRAM

The experimental program consisted of bamboo tensile tests of specimens cut from the culm wall in both radial and tangential directions (Figure 3-7a). Radial specimens were cut through the entire culm wall thickness while tangential specimens were cut from the outer, middle, and inner layers of the bamboo culm thickness. Tests were conducted on a tension frame with locking self-

aligning grips allowing the specimen end restraint conditions to be either fixed or free to rotate. The test program sought to study the influences of fiber gradation of the culm wall and test machine end fixity on bamboo tensile strength results and the longitudinal strain profiles of the specimens. This program will identify factors affecting bamboo tension tests and permit these so-called 'interferences' to be quantified[1].

3.3.1   Specimens and Fabrication

Specimens were taken from 11 internodes of 2 culms of *Bambusa Stenostachya* (Tre Gai). Tre Gai bamboo, native to Vietnam, is a thick walled bamboo species which allowed for specimens to be cut in the radial direction of the culm wall as well as tangentially at three defined layers of the culm wall as shown in Figure 3-7a. The aspect ratio of specimen cross sectional area was targeted to be equal to 4, with the width equal to 20 mm (0.79 in.) and thickness equal to 5 mm (0.20 in.). The 'width' dimension of radial specimens is the culm-wall thickness. Tangential specimens were taken from the outer, middle, and inner portions of the culm wall as shown in Figure 3-7a. Unlike the radial specimens, tangential specimens have an essentially uniform gradation of fiber volume across their width. An average gage length of 80 mm was calculated for all specimens (minimum of 56 mm and maximum of 99 mm). Ultimately, 82 specimens were prepared following the test matrix shown in Table 3-1. A few specimens containing a node within the gage length were tested for each of the specimen orientations with the grip free to rotate and a final radial specimen containing a node was tested with fixed end conditions.

---

[1] 'Interferences' is the term used by ASTM to identify issues affecting the results of a test method. A section labeled 'Interferences' is now part of the ASTM Standard Test Method boilerplate text.

Specimens were fabricated using a horizontal milling machine as shown in Figure 3-7b. First, a rectangular block was removed from the culm wall of an internode. Radial and tangential specimens were then cut from the blocks using a band saw. Specimen geometry was measured at three locations along the gage length to determine an average value of width and thickness. Last, softwood gripping tabs were affixed to the specimens using an epoxy adhesive (Fig. 3-7c).
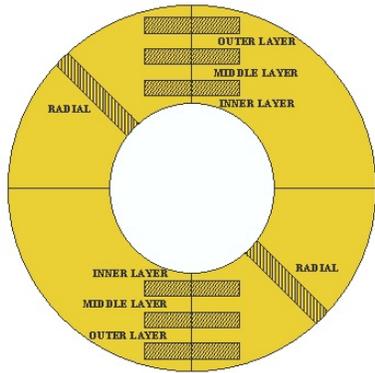
| a) specimen orientation | b) specimen fabrication in horizontal milling machine | c) application of softwood tabs |

Figure 3-7: Tensile test specimens

Table 3-1: Test Matrix

Specimen ID	internode tests	tests with nodes	orientation	end restraint
TRU1 to TRU12	10	2	radial	free
TRF13 to TRF23	10	1	radial	fixed
TOU24 to TOU3	10	1	tangential – outer	free
TMU35 to TMU43	8	1	tangential – middle	free
TIU44 to TIU54	10	1	tangential - inner	free
TOF55 to TOF64	10	-	tangential – outer	fixed
TMF65 to TMF72	8	-	tangential – middle	fixed
TIF73 to TIF82	10	-	tangential - inner	fixed

3.3.2 Testing Apparatus

Testing was conducted in an MTS 810 universal testing frame having an 89 kN (20 kip) capacity load cell (Fig. 3-8) and equipped with hydraulic wedge grips. Since the compression strength perpendicular to fibers is low (Janssen 1981), specimens were tested with a grip pressure of only 6.9 MPa (1000 psi) to minimize crushing and/or shear-related failures in the grip region. Occasionally adjustments to grip pressure had to be made during testing to account for specimen slip during testing. All specimens were placed in the grips such that the grip chucks were applied to the long side of the specimen; this is consistent with the ISO requirement for the radial specimens but not for the tangential. Nonetheless, the tangential specimens are expected to have more uniform cross section properties, in which case this change is not believed to be an issue.

Tests were conducted in displacement control at a rate of 0.0254 mm/s (0.001 in/s). ISO 22157 specifies a rate of 0.01 mm/s (0.0004 in/s), but this is impractically slow and cannot be reliably achieved with the test frame and controller used in this test program. The hydraulic wedge grips are self-centering, having a ball joint allowing rotation of the grip assembly. This joint may be fixed or be left free to rotate; thus affecting the end restraint noted in Table 3-1. Load and vertical displacement values were obtained directly from the MTS load cell and LVDT.
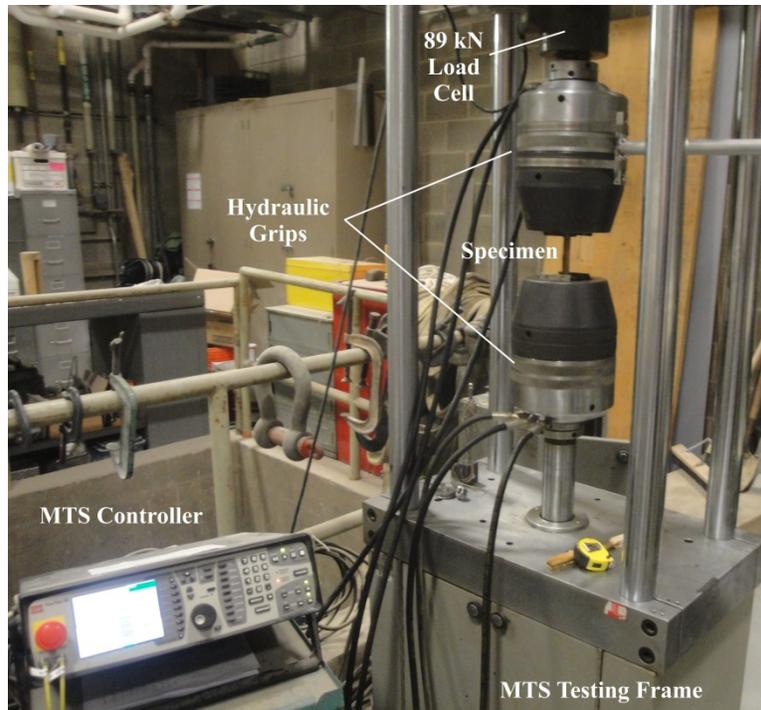
Figure 3-8: Experimental Test Set Up

3.3.3 Instrumentation

Surface strains in the bamboo specimens were measured using two forms of instrumentation. The primary instrumentation for the study was a VIC-3D digital image correlation system which captures the strain field in the specimen across either the radial or tangential dimension of the specimen. The VIC-3D system (shown in Figure 3-9) uses the concept of digital image correlation to determine the strain tensor on the material surface during the test. Specimens are painted with a speckle pattern prior to testing (photocopier toner broadcast onto wet white spray paint); during the test consecutive high resolution images are taken and deformation patterns (based on sampling of the speckle pattern) are recorded. Post processing allows specified strain fields to be plotted (Correlated Solutions 2010). Radial specimens were imaged to capture the

77

strain field in the radial direction while tangential specimens were imaged in the tangential direction; essentially; i.e.: the longer face of each specimen is imaged (Figure 3-9d).

a) test frame with VIC 3D system

b) VIC-3D cameras

c) test in progress

d) speckle pattern on specimen
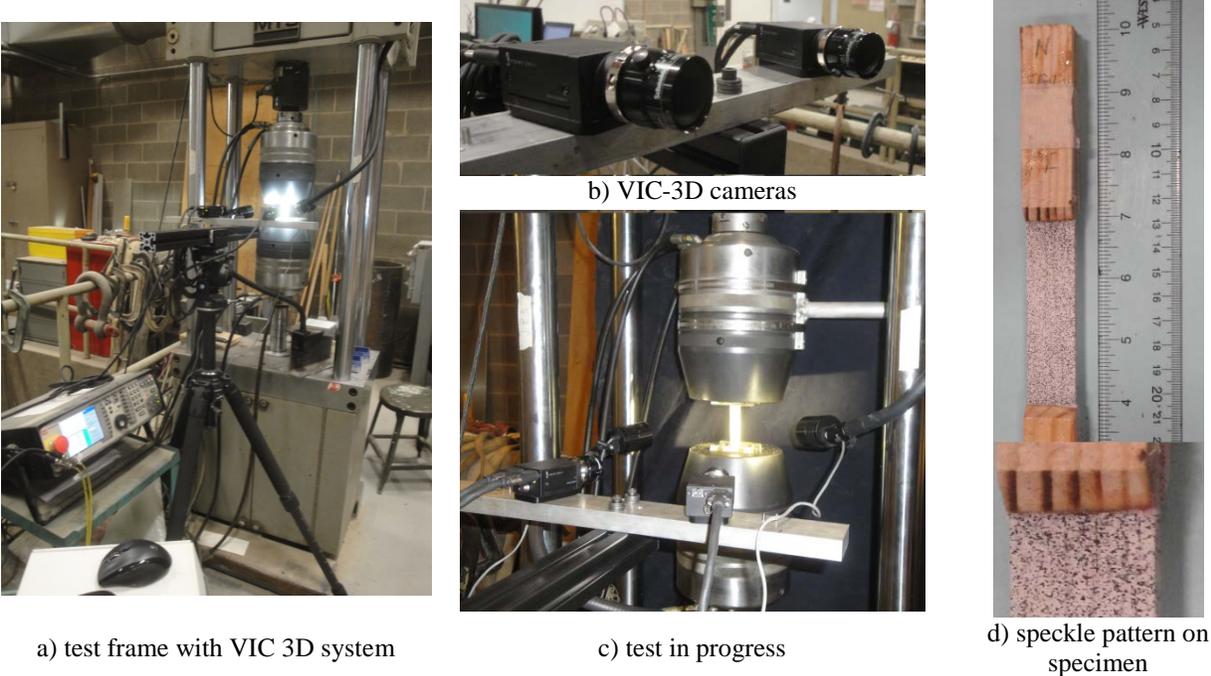
Figure 3-9: VIC-3D system.

Electrical resistance strain gages were also used on a set of radial free (TRU in Table 3-1) specimens and one radial fixed specimen (TRF in Table 3-1) to allow for comparison of directly measured strain values with results from the VIC-3D system. Two strain gages were placed at the mid-height of the specimen gage length; one placed at each of the interior and exterior edges of the radial dimension of the specimen as shown in Figure 3-10.
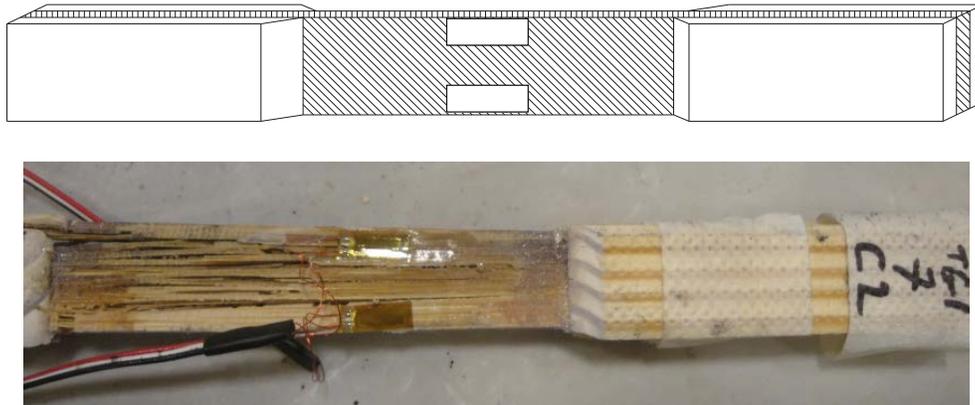
Figure 3-10: Location of strain gages on tension specimen and gages after testing

3.4   EXPERIMENTAL RESULTS

Reporting of the experimental results is organized into four sections. First, the failure modes observed during the testing are discussed and illustrated. Next, attention is given to a summary of tensile strength data observed. The observed experimental strain profiles are then discussed and the stress and modulus of elasticity across the radius are estimated using tangential specimens. Observed trends found in the experimental results are illustrated here using a representative set of specimen data. A complete catalogue of experimental tension test results is presented in the Appendix.

3.4.1   Failure Modes

The bamboo tensile test specimens exhibited six general categories of specimen failure as illustrated in Figure 3-10: Failure mode A involves specimen failure within the wood tabbed grip

length, while mode B represents failures at the interface of the grip and gage lengths. Failure mode C is a tensile rupture within the gage length of the specimen. Modes D and E both involve a longitudinal splitting failure through the gage length of the specimen; mode D is a single split, while mode E is referred to as a 'brooming' failure which engages the entire cross section. Finally, failure mode F represents cases where a combination of failure modes was observed. These are shown schematically and by example in Figure 3-10. Modes C through F are all considered 'good' failures in the sense of being mostly unaffected by the tabbing or gripping process. Failures C and E are the 'preferred' failure modes of unidirectional fiber reinforced polymer (FRP) materials having uniform fiber volume ratios. The single longitudinal splitting failures observed in modes D and F may result from the following two sources which cannot be avoided when testing bamboo:

Uneven grip pressure. While the gripping pressure applied to the softwood tabs is uniform, because the bamboo itself has varying material properties across the gripped width, the apparent 'gripping pressure' relative to the tested portion of the specimen may be uneven. This can result in single longitudinal splitting failures associated with regions of greater grip pressure. This type of failure is seen in hand-layed up FRP materials where the thickness of the specimen is not well controlled.

Longitudinal bending of specimen. If the specimen exhibits any flexure (see Section 3.2), longitudinal shear (i.e.: VAy/It shear) is present and may affect a longitudinal splitting failure.
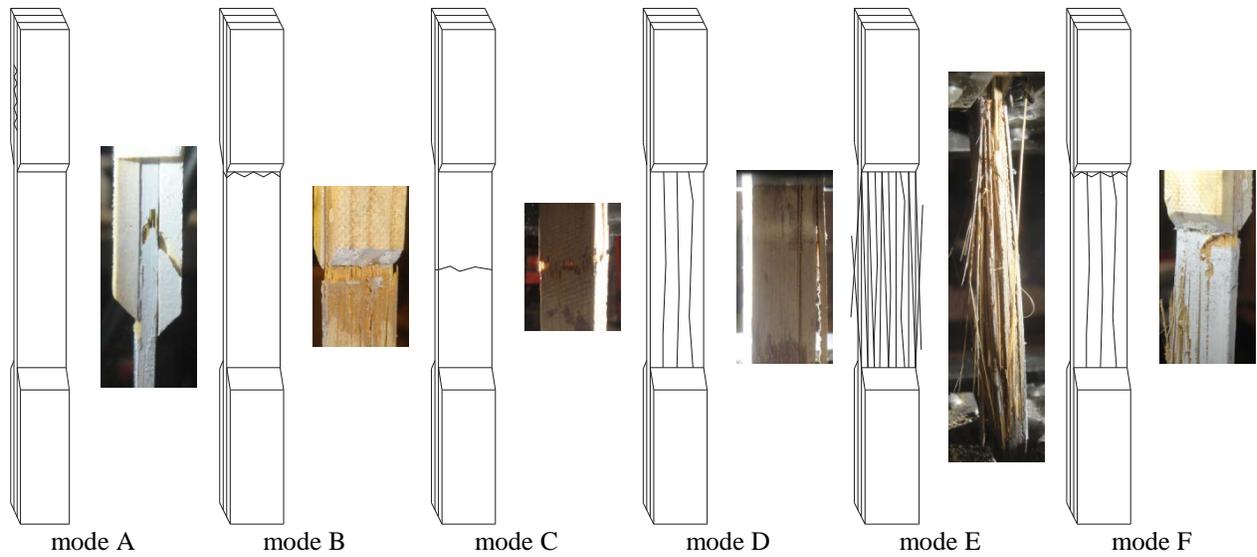
Figure 3-11: Representative Failure Modes

Considering the 76 internode specimens (Table 3-2), regardless of orientation or end restraint, 38 specimens (50%) experienced a mixed mode F failure. In each case, the combination consisted of a mode B or C rupture and a mode D or E splitting failure. Thirty-one specimens (41%) experienced a mode D or E longitudinal splitting failure only. One specimen (1%) and 6 specimens (8%) experienced failures in (mode A) or at (mode B) the wood tabs, respectively. Five of the six specimens having a nodal region in their gage length exhibited a mode C rupture failure exclusively; in these cases the failure was at the node. In comparing the failure modes with respect to specimen orientation and end restraint condition (Table 3-2), there was no significant difference between testing conditions. The dominant failure mode in each case was a mode D splitting failure or a mode F combination failure which included splitting. This observation, once again, highlights the issue of splitting as a dominant limit state for bamboo.

Table 3-2: Observed failure modes in tensile tests.

ID	orientation	end restraint	Test	observed failure mode					
				A	B	C	D	E	F
TRU	radial	Free	12	1	0	2	5	3	1
TRF		Fixed	11	0	0	1	3	0	7
TOU	tangential-outer	Free	11	0	0	0	4	2	5
TOF		Fixed	9	0	1	1	4	1	2
TMU	tangential-middle	Free	11	0	3	1	1	0	6
TMF		Fixed	10	0	0	0	5	1	4
TIU	tangential-inner	Free	8	0	0	0	2	0	6
TIF		Fixed	10	0	2	0	0	0	8

It should also be noted that during testing, many specimens experienced issues with slip occurring in the grip length between either the bamboo and wood tabs; or the wood tabs and hydraulic wedge grips. This was ultimately an issue with the grip system; therefore slip was not considered a failure mode in the testing; and displacement data for the tests was not considered in the following sections (since it necessarily includes slip).

3.4.2 Tensile Strength

The experimental tensile strength results are summarized in Table 3-3 and Figure 3-12 for the various orientation and end restraint conditions. Table 3-3 also presents the average tensile strengths for each condition normalized to the average strength of the radial-free (TRU) specimens. A few trends are immediately identified; while these may be expected, their implications are largely ignored in standardized bamboo tension tests:

1. In all cases, free end restraints result in higher tensile strengths than fixed restraints.

2. The tangential specimens capture the variation of expected tensile strength through the culm wall thickness. The outer specimens were about 1.87 times as strong as the inner and about 1.33 times as strong as the middle specimens. This result implies a higher order, rather than linear, fiber volume distribution.

3. The radial specimens exhibited results very close to (but marginally less than) the average of the three tangential locations which are also comparable to the results of the middle tangential specimens. Again, this result implies a fiber volume distribution having an order greater than 1.

4. COV values are typical of bamboo testing. The COV is seen to improve (i.e.: fall) for the fixed end restraint condition and with increasing fiber content (outer tangential specimens).

Table 3-3: Average Experimental Tensile Strength Summary and Normalization

End Restraint	Radial	Inner	Middle	Outer
Average Strength, MPa (COV)				
Free	141.2 (36.2%)	101.9 (41.4%)	139.9 (28.0%)	193.8 (18.9%)
Fixed	131.9 (28.9%)	94.3 (33.4%)	134.6 (24.1%)	172.8 (15.5%)
Free/Fixed	1.07	1.08	1.04	1.12
Average Strength Normalized to Free Radial Specimens				
Free	1.00	0.72	0.99	1.37
Fixed	0.93	0.67	0.95	1.22
Specimens Having Nodal Region, MPa				
Free	69.5 (25.7%)	29.3	68.8	125.4
nodal/internode	0.49	0.29	0.49	0.65

Specimens which included a nodal region within the gage length of the tensile coupon and tested in the free condition were also tested. Results, shown Table 3-3, showed much lower tensile strengths than the other specimens although exhibited similar trends. The detrimental effect of the node was less pronounced as the fiber volume ratio increased (inner to outer tangential specimens). The one radial specimen tested with a nodal region in the fixed condition (not reported in Table 3-3) experienced a tensile strength (42.9 MPa) lower than the free condition but it should be noted that a partial failure occurred at the node during test preparation.
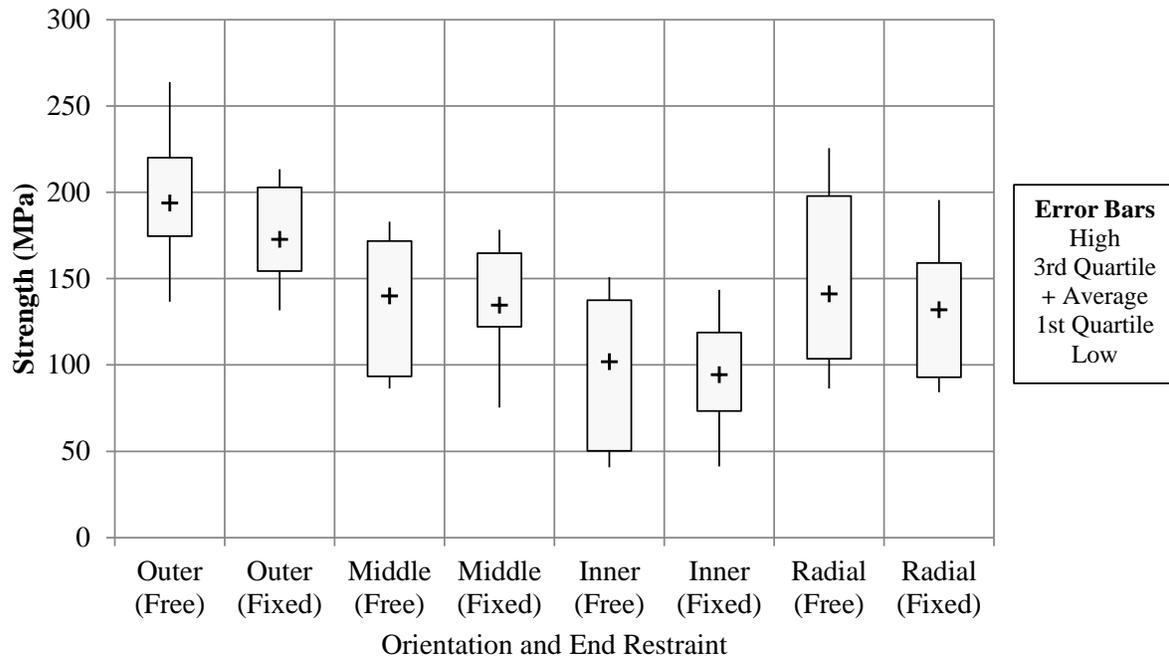
Figure 3-12: Experimental Tensile Strength

Tensile strength values are also known to vary with respect to the location of the specimen along the culm. Figure 3-13 illustrates the tensile strength results for specimens along the length of both culm TG1 (internodes 5 through 11) and TG21 (internodes 11 through 13). The results showed that for all orientations the tensile strength generally increased along the culm height although the results from TG1 are greater than those from TG21, indicating variation between culms. In culm TG1, this increase was more pronounced for the radial specimens, although this was not reflected in TG21. Nonetheless the trends indicated above were consistent regardless of the height along the culm at which specimens were taken.

The general increase in tensile strength along the height of the culm is believed to be a function of simple mechanics: The amount of fiber material in the culm section is essentially constant or increases marginally along the height of the culm (Janssen 2000) while the diameter and culm wall thickness generally decrease with height (see Section 2.1.2.1) reducing the area

over which the stress is determined. Since tensile strength is primarily imparted by the fibers, the apparent strength increases. Indeed, the fiber volume fraction increases along the culm height (Janssen 2000, Amada et al. 1996).

a) free end restraints   b) fixed end restraints
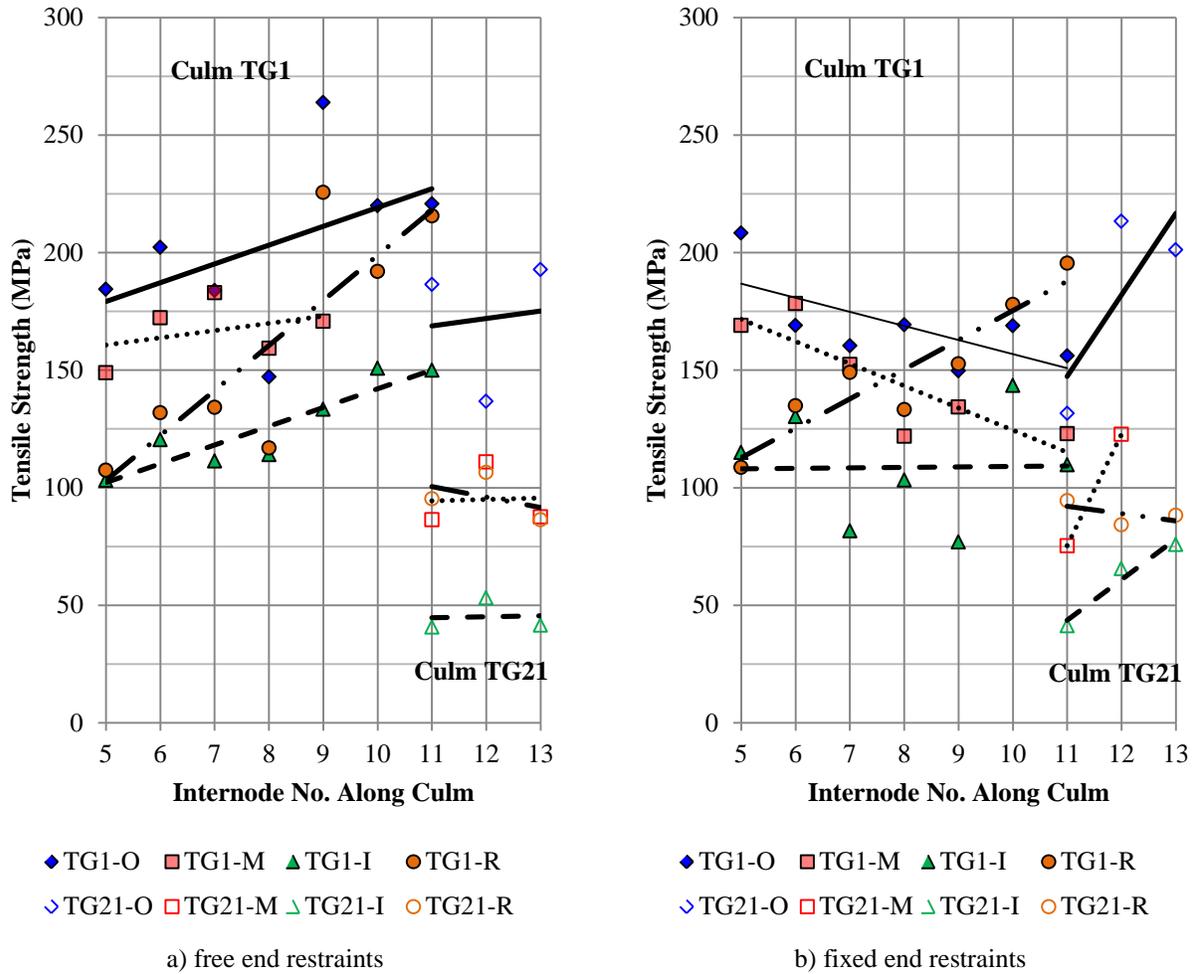
Figure 3-13: Tensile strength along the culm height.

In summary, the tensile strength results illustrate the influence of machine-imposed end restraints and the location and orientation within the culm from which the tension specimen is extracted. The latter affects the fiber volume ratio in the test specimen. The mechanisms affecting these general trends in tension behavior are explored further in the following section in which strain patterns in the specimens are investigated.

3.4.3   Experimental Strain Profiles

As stated previously, the goal of using the VIC-3D imaging system was to capture the experimental surface strain profiles across the width of the specimens (radial or tangential) relative to the culm wall orientation and ultimately capture rotation in the specimen. It is assumed that all tests exhibit plane strain behavior in the 'specimen thickness' dimension (i.e. the 'depth' direction for the VIC-3D system) which allows for study of the resulting experimental surface strains. Representative results and summaries are presented in this section while a complete summary of data obtained is presented in the Appendix.

Figures 3-14 and 3-15 show the strain profiles across the tension specimens cut from internode 5 of culm TG1 for the tangential and radial specimens in both the free and fixed end conditions, respectively. Strains at a number of stress levels are shown to indicate changes with test progression. The results for the free end condition (Fig. 3-14) show, apart from a break in the outer tangential specimen, a fairly uniform strain distribution in each of the tangential specimens as expected. Meanwhile, for the radial specimen with free end constraints, a nonlinear strain distribution decreasing from the inner face to the exterior highlights potential bending in the system as was illustrated in the earlier representative example (Figure 3-6). The radial specimen with fixed constraints (Fig. 3-15 bottom right) has a peak strain towards the center of the specimen, which does not suggest rotation, and tangential specimens once again show uniform strain results across their sections.

These results are reinforced by Figures 3-16 and 3-17 which compare the strain profile of the outer, middle, inner, and radial specimens for TG1-5 (free and fixed restraints respectively) at specific values of average applied stress. It should be noted, that due to preloading of some specimens by the machine grip pressure, strain values reported in Figures 3-16 and 3-17 should

be considered relative and not be compared directly across the sections; focus should be placed on the strain distributions. In Figures 3-16 and 3-17, the expected trends and behaviors are reinforced. In particular, the strain distribution at a given average stress level sees the interior strains greater than the exterior (see Figure 3-6) and the radial strains similar to the middle tangential strains.

Overall, the experimental strain distributions for all bamboo internodes tests (Appendix) exhibited mixed results. TG1-5 and TG21-12 radial specimens had evident rotation seen in the free specimen with more uniform strains in the fixed specimen. Two specimens (TG1-8 and TG21-13) saw rotation in both free and fixed radial specimens while specimen TG1-6 did not see pronounced rotation in either end restraint condition. Specimens TG1-7, TG1-10, and TG21-11 saw more evidence of rotation in the fixed condition while radial specimens for TG1-11 and TG1-9 saw higher strain values on their exterior side.
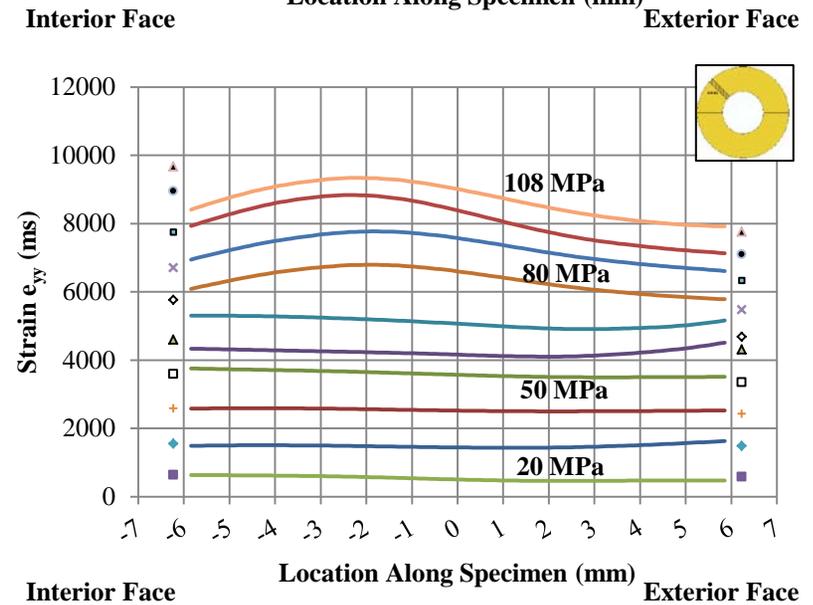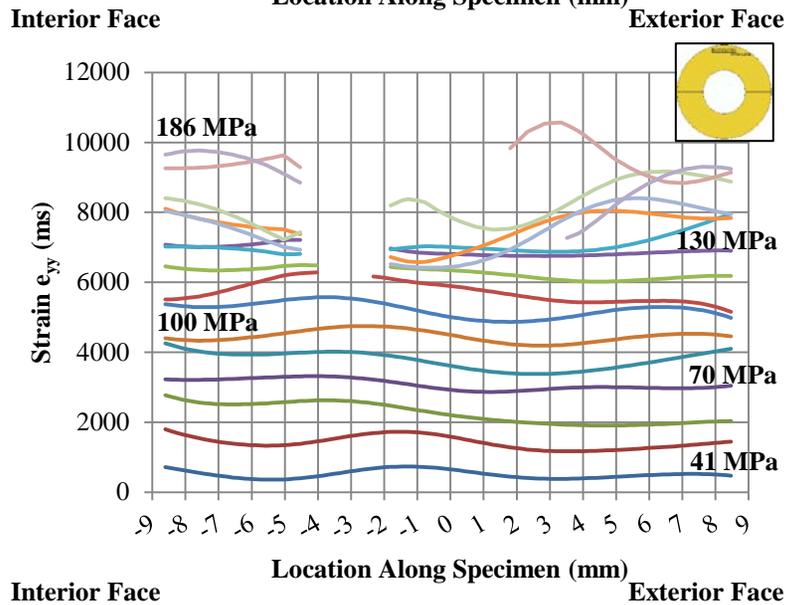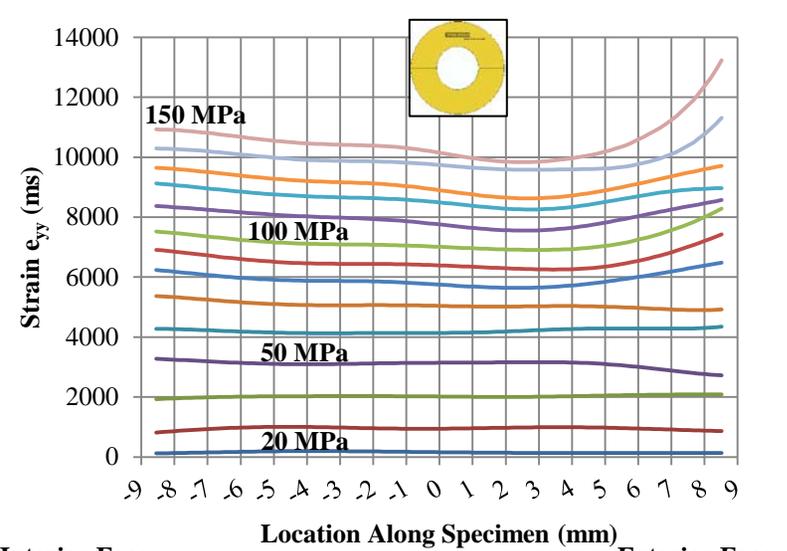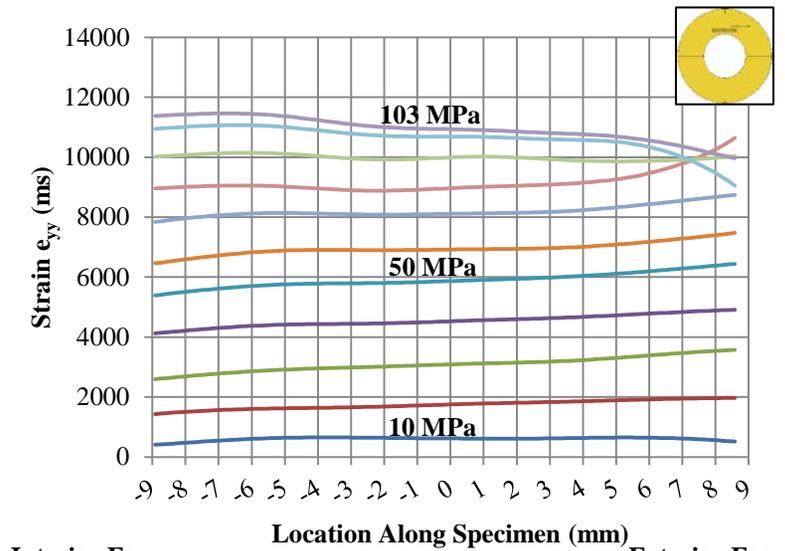
Figure 3-14: Specimen TG1-5 (Free): Inner (Upper Left), Middle (Upper Right), Outer (Lower Left), & Radial (Lower Right)

88
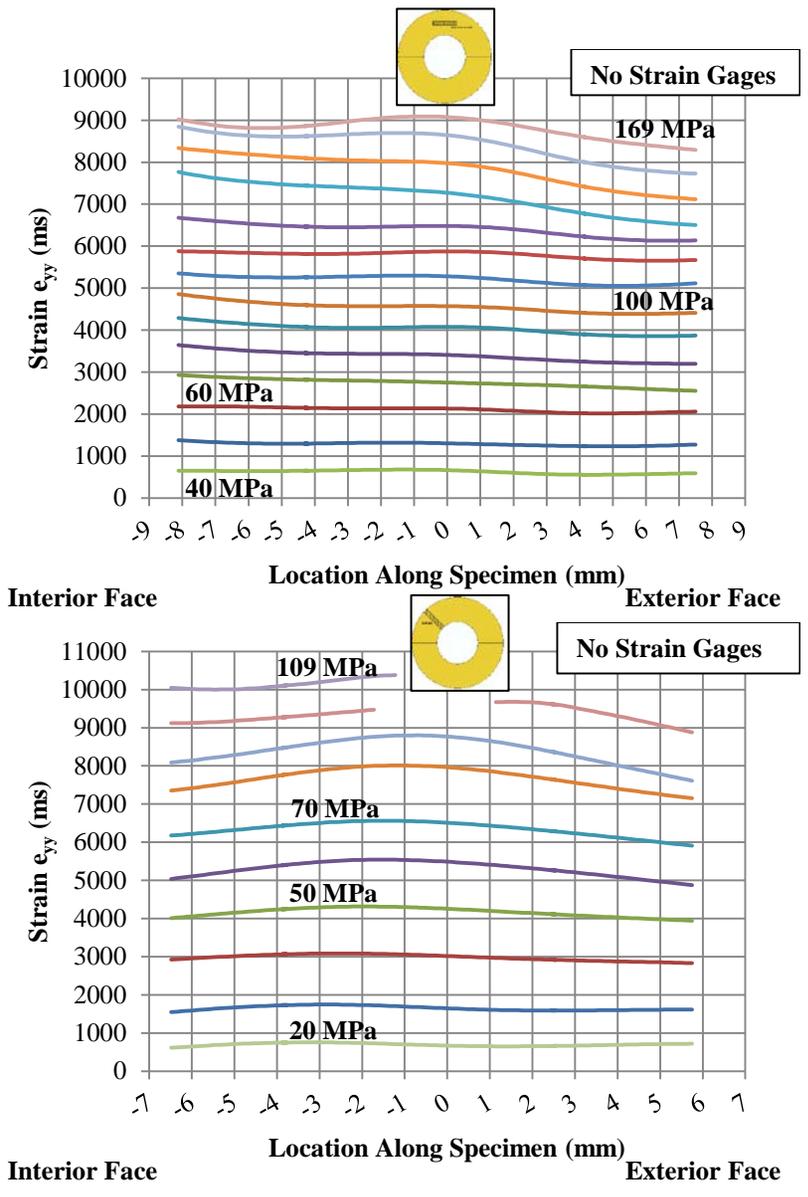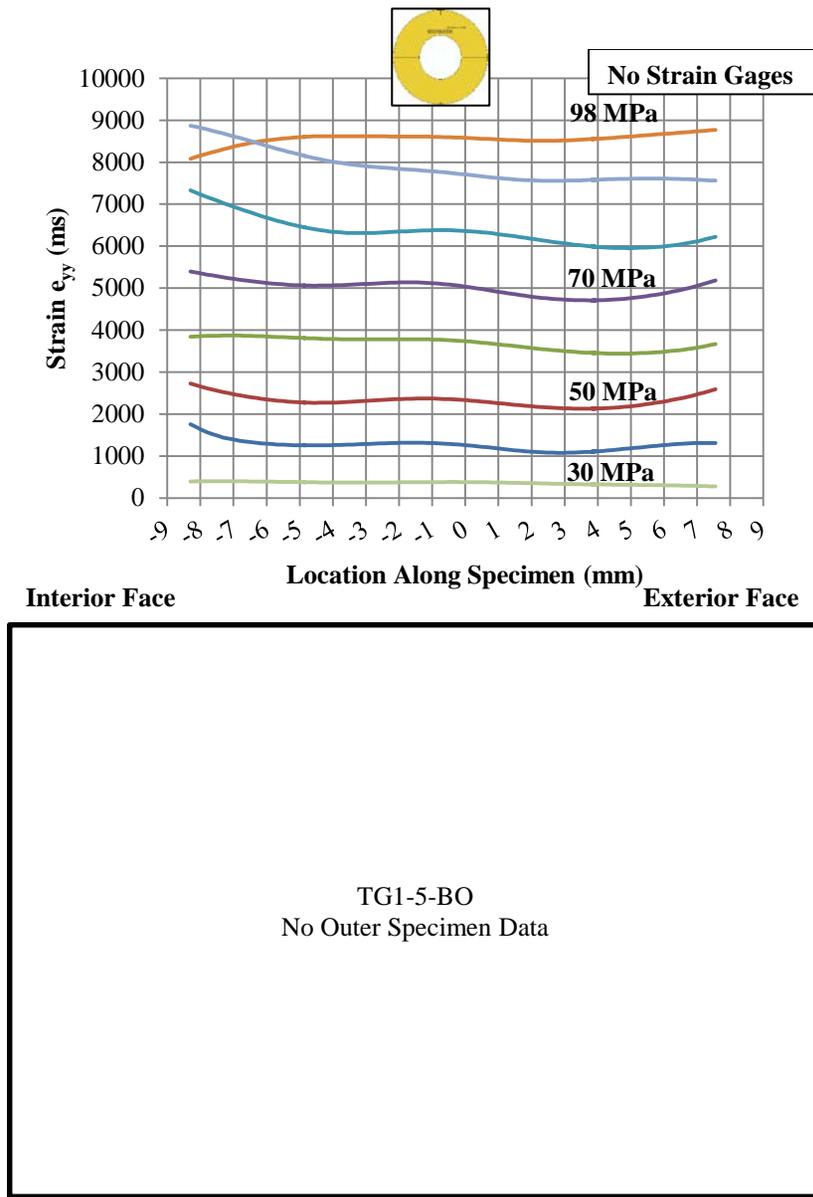
Figure 3-15: Specimen TG1-5 (Fixed): Inner (Upper Left), Middle (Upper Right), Outer (Lower Left), & Radial (Lower Right)
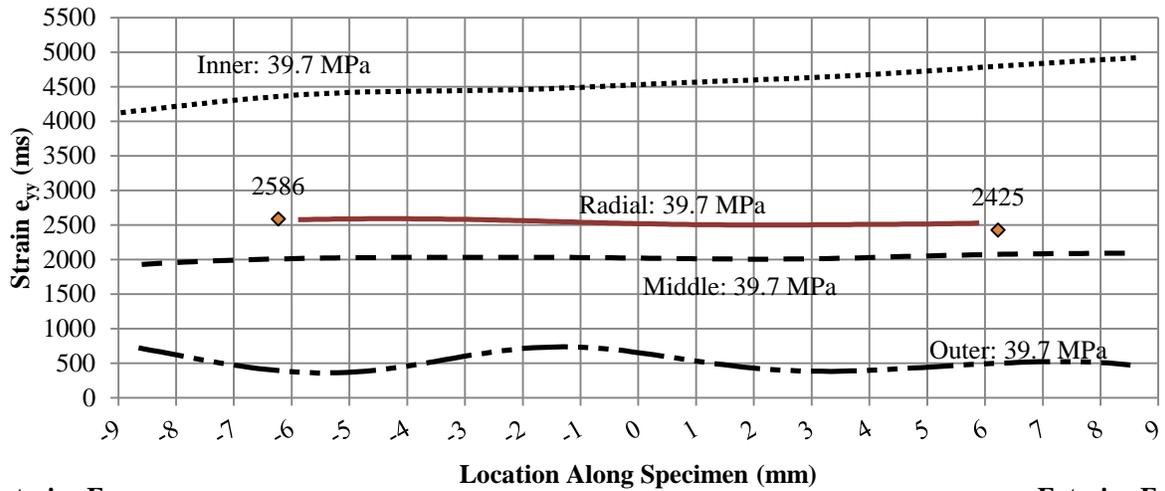
Interior Face

Exterior Face
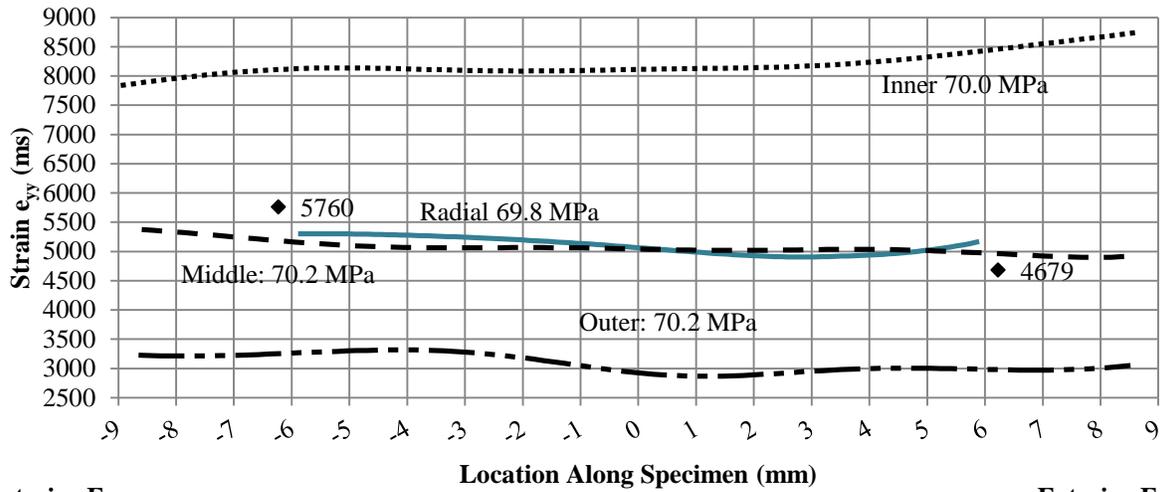
Interior Face
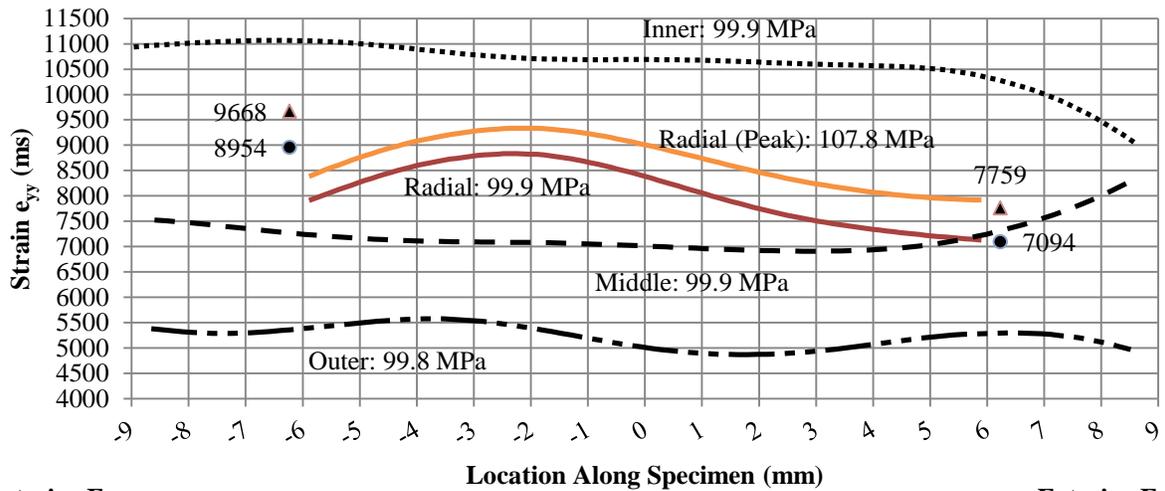
Exterior Face

Interior Face

Exterior Face

Figure 3-16: Strain profile for specimen TG1-5 (free): 40MPa (top), 70 MPa (center), and 100MPa (bot.)

90
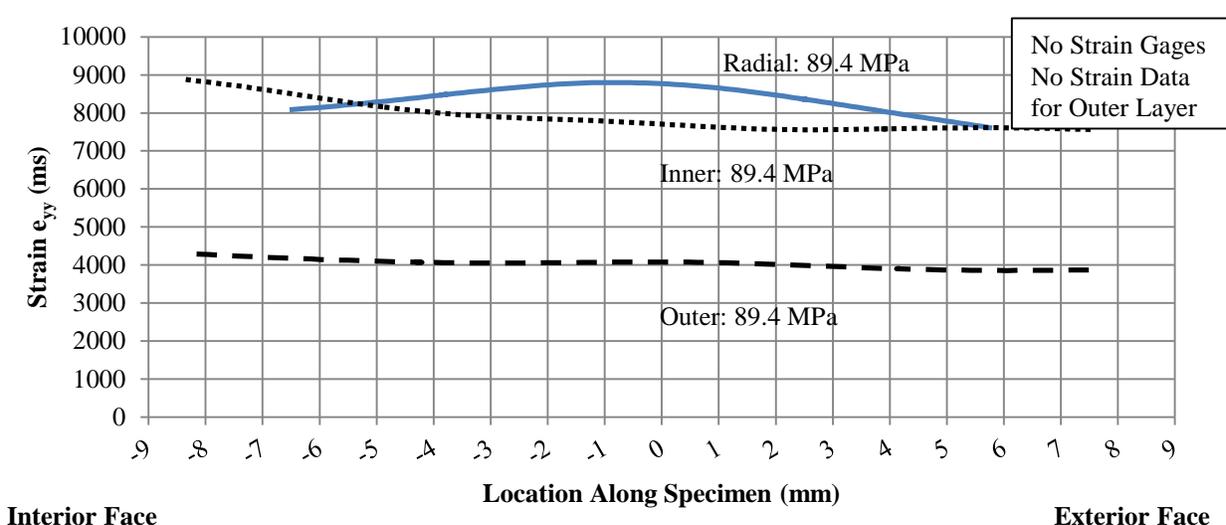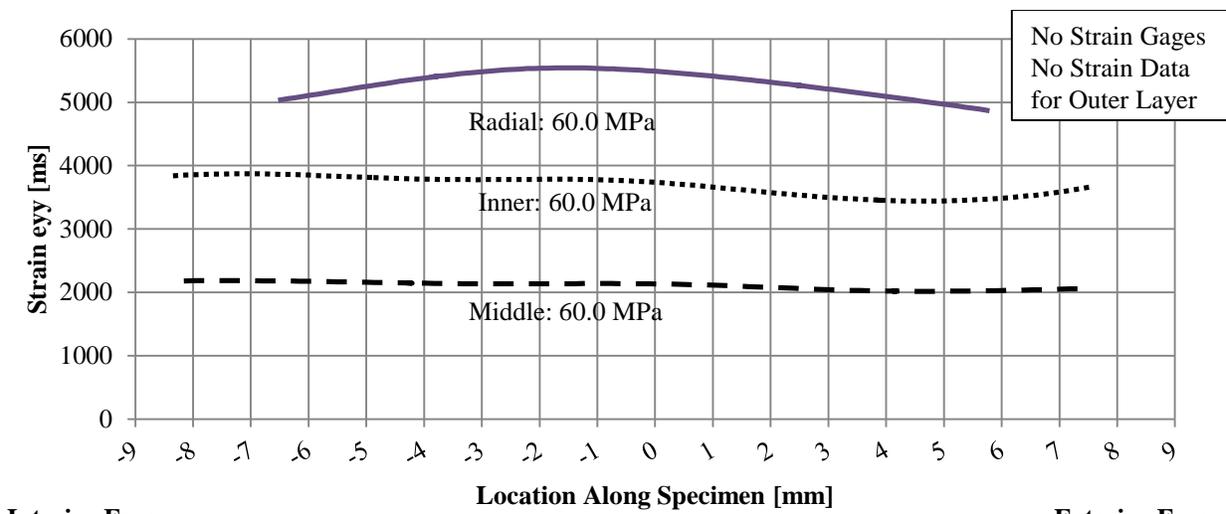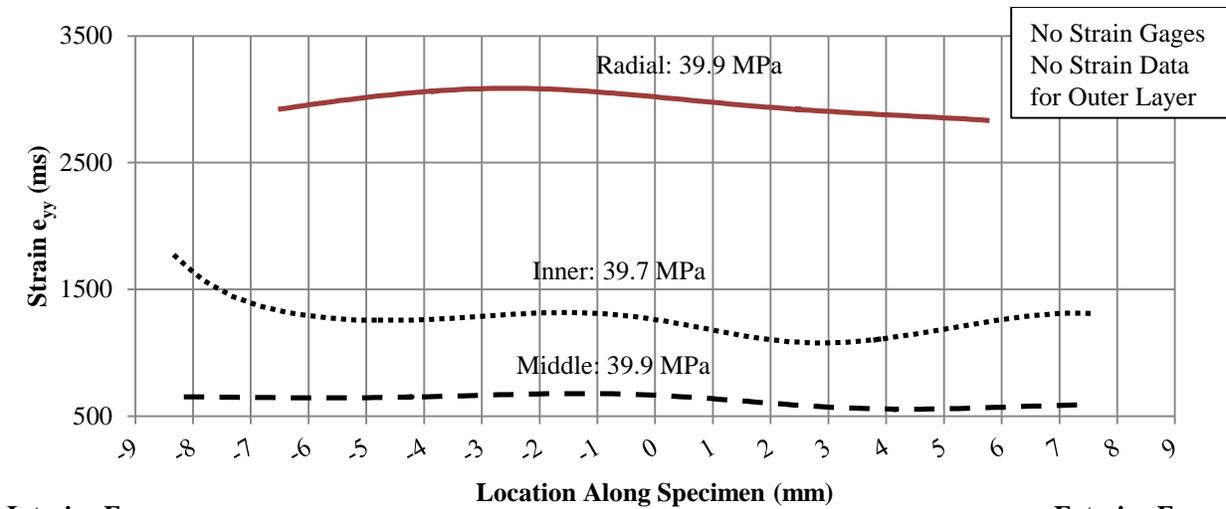
Figure 3-17: Strain profile for Specimen TG1-5 (fixed): 40MPa (top), 60MPa (center), and 89MPa (bot.)

3.4.4   Experimental Stress Profiles

The experimental tensile results were also used to estimate the uniform tensile stress distribution (not considering rotation) across the radial dimension (through the culm wall). Figure 3-18 plots the ultimate tensile stress for the inner, middle, and outer tangential specimens (free and fixed conditions) with respect to their estimated location along the normalized radial thickness dimension. To estimate the location of the tangential specimens, the middle specimen is assumed to be centered at 0.5t; specimen dimensions are known and a blade kerf of 2 mm (1/16 in) is assumed. From this, the location of the tangential specimens may be approximated. It is also acknowledged that the most extreme outer and inner fibers are lost due to milling of the tangential specimens. Figure 3-18 uses representative specimens TG1-5 and TG21-11 to illustrate common results.
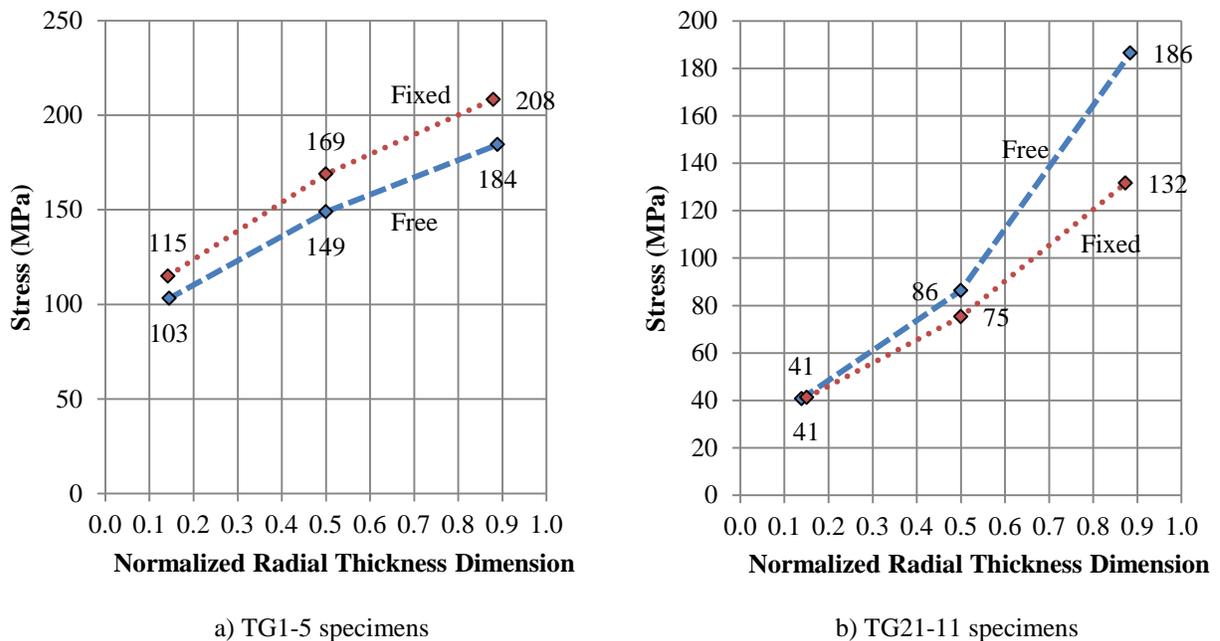
a) TG1-5 specimens   b) TG21-11 specimens
Figure 3-18: Representative stress profiles for specimens TG1-5 and TG21-11

Excluding the tests where no middle specimen (thinner walled culms did not permit three tangential specimens in every case) was fabricated (in which case only a linear distribution could

be graphed) for both free and fixed conditions, results clearly indicated a nonlinear stress distribution; albeit the relationship is by no means consistent. Three tests (TG1-5, TG1-6, and TG1-7) had exponentially decaying (i.e.: $\sigma \; \alpha \; x^y$; where y < 1) or near linear (y = 1) relationships similar to that shown in Figure 3-18a for both free and fixed conditions, while specimen TG21-11 (Fig. 3-18b) had an exponentially increasing (i.e.: $\sigma \; \alpha \; x^y$; where y > 1) relationship for both free and fixed conditions. Three specimens (TG1-8, TG1-9, and TG21-12) had a combination of curvature for free and fixed conditions. Specimens TG1-8 and TG21-12 saw exponentially increasing curvature in the fixed condition and decaying curvature in the free condition. The opposite was seen in specimen TG1-9. Specimen TG1-10 had no middle layer in either the free or fixed condition (only linear increasing relationships). Specimen TG1-11 has no middle layer in the free condition while specimen TG21-13 had no middle layer in the fixed condition. However, both showed exponentially increasing curvature in the case that included a middle layer. Finally, exponentially increasing curvature was seen in the nodal specimen (TG1-1) in the free condition.

3.4.5   Experimental Elastic Modulus Profile

Similar to the procedure used in Section 3.4.4 for determining the stress profiles, the experimental tangent modulus of elasticity distribution across the radial direction was also estimated using the results of tangential specimens from two internodes: TG1-8 and TG21-12. As mentioned previously, slippage in the grip length proved to be an issue in many tests which affected displacement results. These representative internodes were chosen based on their good load-displacement data from testing prior to the occurrence of slippage. Specimen TG1-8 exhibited a higher average apparent modulus in the fixed condition and had exponentially

increasing distributions. Meanwhile, specimen TG21-12 had near linear distributions and values for both free and fixed conditions. Results, once again, illustrate the influence of increasing fiber density across the radial dimension.
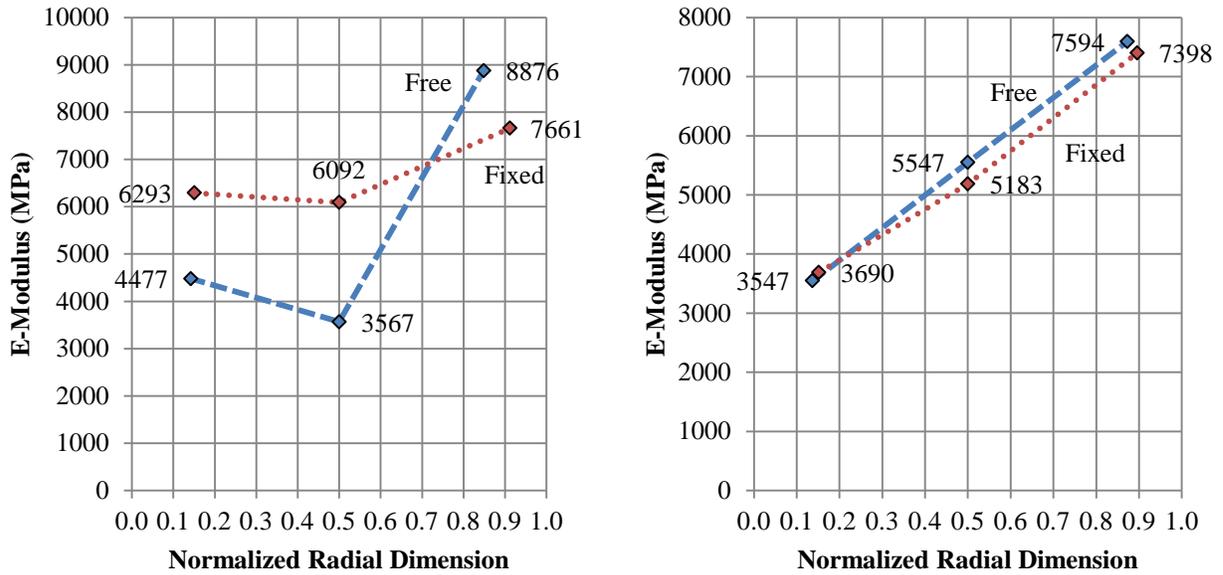
a) Specimen TG1-8   b) Specimen TG21-12
Figure 3-19: Representative E-Modulus profile for specimens TG1-8 and TG21-12

3.5   CONCLUSIONS

The goal of this experimental program was to highlight issues with and interferences present in current methods and practices regarding the tensile strength of clear bamboo specimens taken from the culm wall. The study not only investigated the influence of fiber gradation on the specimen behavior but also the end restraint condition provided by the testing machine – for which there is no guidance in applicable standards. The following conclusions are drawn from the experimental test results:

Tensile strength results obtained using a fixed end condition produced lower average strengths in all cases as compared to those tests that are free to rotate. It is envisioned that the specimen rotation when allowed in free end specimens causes longitudinal failures (splitting; failure modes D and E in Figure 3-11) as longitudinal splitting permits for redistribution of axial forces due to loss of strain compatibility across the section. Further, the tangential specimens capture the variation of expected tensile strength through the culm wall thickness and indicate a higher order, rather than linear, fiber volume distribution.

The radial specimens exhibited results very close to (but marginally less than) the average of the three tangential locations which are also comparable to the results of the middle tangential specimens. Again, this result implies a fiber volume distribution having an order greater than one.

COV values are typical of bamboo testing. The COV is seen to improve (i.e.: fall) for the fixed end restraint condition and with increasing fiber content (outer tangential specimens).

Experimental strain profile data illustrated that most radial tensile specimens had a nonlinear strain distribution, which could potentially be attributed to rotation due to variation of fiber volume in the section. However, nonlinear strain was also seen in some tangential and fixed specimens.

Experimental stress and E-modulus distributions illustrated that fiber gradation through the culm wall effects uniform tensile strength. As future work, fiber volume fraction could be estimated across the radial thickness to develop a refined E-modulus equation (which is species specific), which could then be used to calculate the total stress profile and resultant eccentric force. However fiber volume distributions are expected to vary from culm to culm as was apparently observed in this study. Thus to accomplish this task, either fiber distribution must be

measured for all specimens or a simplifying relationship adopted. Based on the present data, such a relationship will be nonlinear although, beyond this, no conclusion is warranted.

Overall, fiber density across the culm wall thickness and the end restraint conditions of the specimens were shown to have an influence on bamboo tensile test results and therefore must be considered in the development of improved standard test methods. It is recommended that tangential specimens from various regions within the culm wall be used since they possess a more uniform fiber density throughout their cross section and taken together can outline the fiber density and strength in the radial direction through the culm wall.

4.0   PERFORMANCE OF BAMBOO FLEXURAL COMPONENTS

Splitting or longitudinal shear failures in bamboo are a major concern with use of the material for construction applications and therefore must be addressed in standardized test methods and building practices. The present study investigates the longitudinal shear failure in full-culm bamboo flexural components through the use of a modified International Organization for Standards (ISO) bamboo flexure test (see Section 2.3.1 and Figure 22e). The objective is to develop a standardized test method for investigating splitting caused by flexure. Sixteen flexural specimens of *Dedrocalamus giganteus* (Dendrocalamus), *Phyllostachys pubescens* (Moso), and *Bambusa stenostachya* (Tre Gai) are tested. Data is recorded for ultimate strength, deflection, and strains at the location of the splitting failure. Smaller scale flexural specimens are taken from the culm wall of Tre Gai and Moso bamboo and tested in four-point bending. These smaller tests are used to capture splitting in the culm wall thickness and study correlations to the full-culm beam results. Test results are also compared with experimental test results for mode I (split-pin tests) and mode II (bowtie) failures.

4.1   BAMBOO FLEXURAL BEHAVIOR

While bamboo has been shown to have advantageous tensile and compressive strength properties in the direction of longitudinal fibers, better understanding is needed with regard to bamboo

97

flexural performance; specifically flexure-induced splitting in bamboo. As shown in Figure 4-1, splitting often occurs in bamboo components and connections due to the weak lignin matrix, lack of tangential fibers, and high rate of shrinkage due to drying.

(a) Beam splitting at joint   (b) Splitting at bolted connections
Figure 4-1: Examples of bamboo splitting (Sharma 2010)

While bamboo flexural, shear, and tension perpendicular to fibers have been studied, flexure induced splitting poses a unique concern as it comprises a mixed-mode failure with both tangential tension (Mode I) and in-plane shear (Mode II). The objective of the current study is to investigate a method for testing this dominate mode of failure.

4.1.1   Bamboo Flexural Behavior

The strength of a flexural element is determined from the maximum stress at either the extreme tension or compression fiber of the section, σ. This maximum stress or modulus of rupture is defined as:

$$\sigma = \frac{Mc}{I} \tag{4-1}$$

Where M is the moment at the section considered, c is distance from the neutral axis to the extreme fiber of the cross section, and I is the moment of inertia of the cross section.

Janssen (1981) defined the maximum flexural stress for bamboo as the maximum compressive stress corresponding to a controlling lateral tensile strain in the section. He conducted both short- and long-term flexural tests on 5 m long (3.60 m free span), full-culm bending specimens of *Bambusa blumeana*. A four-point bending test was chosen because this arrangement provides a region of constant moment. Tests demonstrated that the flexural neutral axis coincides with the centroid of the culm indicating that the tensile and compressive behaviors have the same effective stiffness. Additionally, the bending strength was shown to decrease from the bottom to the top of the culm while apparent modulus was shown to increase. Moisture content and density were also shown to be significant parameters affecting flexural strength. Creep behavior was shown to be described with a Burgers' model (Burgers 1935). However, Janssen also concluded that the ultimate bending strength is defined by both the ultimate shear stress in the neutral layer (splitting) and the ultimate tensile strain transverse to the fibers at the extreme compression fiber (resulting from the Poisson effect). The ratio of ultimate shear stress, τ to density was shown to increase with the age of the bamboo culms before cutting up to 5 years (Janssen 1981).

Since short flexural specimens can often fail in shear prior to a modulus of rupture being achieved, Vaessen and Janssen (1997) developed a theoretical equation for determining the critical length, l_c, of a four-point bamboo bending test to ensure that the modulus of rupture is achieved. They verified their approach with eight *Bambusa bluemana* test specimens. The theoretical model assumed that a) all cross sections were perfectly circular; b) each culm had a constant wall thickness; c) plane cross-sections remained plane after loading; d) Young's modulus remained constant over the length of the culm and varied linearly through the culm wall in the radial direction; and e) the material behavior is linear-elastic. Experimental results

(Janssen 1981) suggest that cracking occurs at either the neutral layer or extreme fibers. Therefore, the theoretical equation was developed based on the knowledge that "the specimen will fail due to pure shear stresses or pure bending stresses". The critical length is therefore the length resulting in simultaneous failure of the compression zone (maximum bending stress) and neutral layer (maximum shear stress) (Vaessen and Janssen 1997). Eight four-point bending tests were conducted with 5 long specimens (shear span to culm diameter ratio, a/D ≈ 8 to 13) and 4 short (a/D ≈ 4 to 8) specimens. Six of the specimens exhibited behavior that was predicted by the theoretical equation of critical length. Vaessen and Janssen also state that the functional gradation of fibers in a culm increase the apparent value of flexural stiffness, EI, by 10% as compared to a uniform distribution. While the bamboo can resist stress in the compression zone parallel to the fibers, this compressive stress causes a lateral tensile strain perpendicular to the fibers in the weaker lignin matrix. Using the critical value for this lateral strain determined by Arce-Villalobos (1993) of 0.0011 and a Poisson's ratio of 0.3 (Janssen 1981), Vaessen and Janssen estimated a critical compression strain of -0.0037 and a corresponding ultimate bending stress of 62 N/mm^2 for the culms they tested. Similarly, an ultimate shear stress of 2.2 N/mm^2 was determined from the same tests. The critical length for third-point bending was determined to be 26.3 (rounded to 30) times the bamboo culm diameter, D. The critical shear stress meanwhile is estimated as 2.3F/A (Janssen 2000). A specimen length of 30D, resulting in a shear span of 10D, is used in the current ISO bamboo material test standards (ISO 2004b and 2004c).

Ahmad and Kamke (2005) studied the physical and mechanical characteristics of *Dendrocalamus strictus* (Calcutta bamboo) using tension and bending tests. Calcutta bamboo is the most widely used bamboo in India and is found in every state of the country. It was found to have similar physical and mechanical characteristics to timber common in Malaysia and North

America. The authors studied the specific gravity (SG), equilibrium moisture content (EMC), dimensional stability, tensile strength, and bending strength. The tests were conducted using the ASTM standards for wood and wood-based materials D2395-93, D4933-91, and D143-94. Fifty 4.5 x 1.3 mm bending specimens, each 18 mm long, having both radial and tangential orientations were taken from along the culm height between nodes and at internodes. Specimens were conditioned at 20°C and 65% relative humidity for at least 3 weeks before the tests resulting in an average moisture content at testing of 9.4%. Analysis showed that there were no significant differences in modulus of rupture, MOR; stress at the proportional limit, SPL; or Young's modulus, E between the radial and tangential directions. The mean MOR in the radial direction was 137 MPa and 148 MPa in the tangential direction. Mean values of E were 9790 and 9880 MPa in the radial and tangential directions, respectively. Mean SPL values were 90.9 and 91.9 MPa respectively. Values of SPL and E were shown to differ significantly between internodes and nodes; MOR was not seen to vary for these locations. MOR, SPL and E were also shown to vary along the height of the culm. The authors concluded that Calcutta bamboo has bending strength and stiffness similar to or better than the timber species of Douglas-fir, yellow-poplar, aspen, pine, and hemlock. Generally, the top of the culm had the best mechanical properties.

Low et al. (2006) studied the structure, composition, and mechanical response of the Australian bamboo *Sinocalamus affinis* (Rendle) McClue using synchrotron radiation diffraction, Vickers indentation, three-point bend tests, and Charpy-impact tests. The bamboo tested included both one year old and mature five year old culms. Results showed that the young bamboo had a higher elastic modulus, flexural strength, impact strength, and fracture toughness. Hardness was

also found to be load and time-dependent. The major energy dissipative processes for producing high toughness in bamboo were fiber debonding, crack deflection, and crack-bridging.

Obataya et al. (2007) studied the flexural ductility of split bamboo culms and compared this with wood species through the use of cyclic bending tests. Three internodes of 150 mm diameter were obtained from the mid-height of 3-year-old *Phyllostachys pubescens* (Moso) culms. Internodes were cut into rods and then further divided into 240 mm long specimens from various radial locations through the culm wall thickness. Wood specimens were developed from spruce and beech woods. Four-point bending tests were conducted with strain gages placed on the compression and tensile faces of the beam. Five specimens were tested with the higher fiber density region (outer wall) acting in compression (type 1) while five others were tested with this region acting in tension (type II). Three-point cyclic bending tests were also conducted on bamboo and wood specimens. The results of the four-point bending tests showed that the bamboo specimens had a Young's modulus varying from 15 to 16 GPa irrespective of bending orientation. However, the maximum curvature was twice as high for type I bending specimens than for type II. This relationship was also shown for specimens from intermediate regions of the cross section. The authors conclude that bending orientation affects flexural ductility but has less impact on stiffness. Additionally, the flexural ductility of bamboo is best when the outer wall portion is placed in tension while the inner wall portion is compressed (this, of course is not possible in full-culm flexure). Studying the longitudinal compression behavior of the inner portion of the culm wall, Obataya et al. postulate that the parenchyma cells in which bamboo fibers are imbedded should be considered as a compressible foam-like structure. The behavior of the bamboo was not greatly influenced by the method of loading (monotonic or cyclic) and the modulus of elasticity of bamboo was shown to not be significantly different from that of wood

(Obataya et al. 2007). The combination of the multitude of fibers in the outer layer and the compressible inner layer results in excellent ductility of the split-culm specimens considered.

4.1.2   Bamboo Shear and Splitting Behavior

Flexure induced splitting results from longitudinal shear, τ, in a culm section defined as:

$$\tau = \frac{VAy}{It} \tag{4-2}$$

Where V is internal shear force at the location considered; I is the moment of inertia of the culm section; t is the width of the cross section resisting shear; A is the area above the section of interest; and y is the distance between the centroid of A and the neutral axis of the cross section. This is shown schematically for a hollow thick-wall tube in Figure 4-2a and shows that τ has a component in the plane of the cross section and in the longitudinal direction.

(a) Shear in thick-walled tube   (b) Shear flow in thin-walled tube
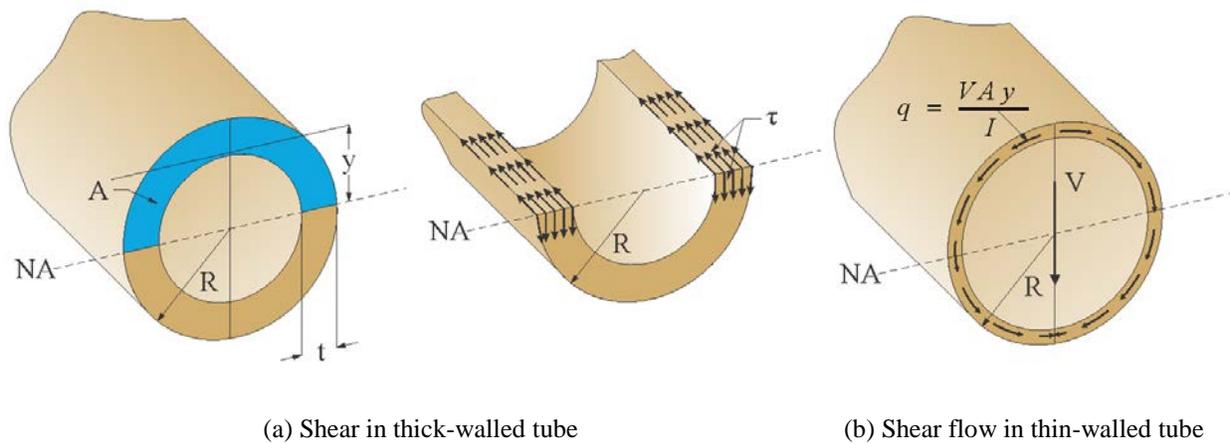
Figure 4-2: Longitudinal shear due to flexure

The value of τ reaches its maximum value at the neutral axis (NA), where A is equal to half of the culm cross sectional area. In this case Equation 4-2 becomes:

$$\tau_{max} = \frac{4V\left(3R^2 - 3Rt + t^2\right)}{3t\pi\left(4R^3 - 6R^2t + 4Rt^2 - t^3\right)}$$ (4-3)

For a thin-walled tube, where the thickness, t is assumed to be significantly smaller than the outer radius, R, (conventionally, thin-walled sections are those in which R/t > 20) the direction of the shear flow, q is always parallel to the walls of the tube (Fig. 4-2b) and the maximum shear stress is calculated as:

$$\tau_{max} = \frac{2V}{A_g}$$ (4-4)

Where A_g is equal to the area of the entire cross section.

The flexure induced shear stress, coupled with the bending stresses, results in a mixed mode I and mode II stress condition along the culm shear span. Mode I tensile opening stress (Figure 4-3a) perpendicular to the fibers results from the presence of a flexural gradient, while mode II in-plane shear (Figure 4-3b) results from the flexure-induced shear (i.e.: Equation 4-2). Mode III, out-of-plane shear (Figure 4-3c) of the culm wall would result from the addition of torsional loading but is not considered in the present study.

In many materials, Mode II is a relatively tough mode of behavior having a relatively high capacity in comparison to Mode I; however, in the presence of Mode I distortions, Mode II capacity and toughness deteriorate significantly. Thus, the Mode I component of flexure is believed to be the driving component of a splitting failure. Stated another way, splitting is more likely to occur in the high-moment region of the shear span (where there is a shear component, V) than in the constant moment region of a four-point bend test. However, direction of splitting is dictated by the higher curvature and moment closer to the mid-span.

a) Mode I, opening tension

b) Mode II, in plane shear

c) Mode III, out-of-plane shear
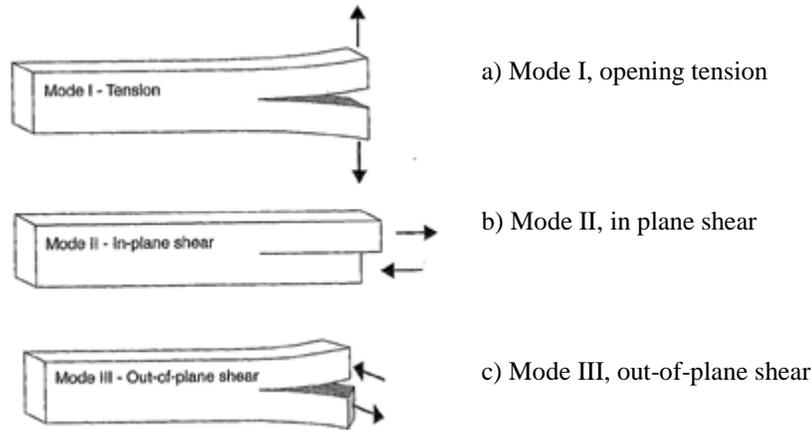
Figure 4-3: Standard definitions of fracture modes (Smith et al. 2003)

### 4.1.2.1 In-Plane Shear (Mode II Failure)

Currently, there are two standard test methods for determining bamboo shear strength parallel to longitudinal fibers as shown in Figure 4-4. Janssen (1981) developed the 'bowtie' test (Figure 4-4a) in an attempt to quantify in-plane shear capacity; this test is adopted in the model ISO standard for bamboo (ISO 2004b and 2004c). The test uses a full culm specimen tested in compression parallel to the fibers. The specimen length, L is equal to the culm diameter, D. 'Bowtie' loading plates as shown in Figure 4-4a create four longitudinal shear planes at which failure can occur. The shear strength is calculated from the culm wall thickness, t and the ultimate load, F as:

$$\tau = \frac{F}{\sum_{4\,quadrants} Lt} \tag{4-5}$$

Another accepted test is the 'S-type' test for inter-laminar shear, shown in Figure 4-4b which has been standardized by INBAR (1999). This test is based on ASTM standard D2733-70 (1976) *Method for Interlaminar Shear Strength of Structural Reinforced Plastics at Elevated Temperatures* and was adapted for bamboo by Moreira (1991). Coupons are taken from the culm wall and allow shear plane orientation either parallel or perpendicular to the through thickness of

the culm. Tested in tension, the coupon is notched halfway through the width of the specimen at two locations. This creates a plane of area A subject to direct shear (Fig. 4-4b); the inter-laminar shear strength is therefore:

$$\tau = \frac{F}{A}$$ (4-6)

a) bowtie test for in-plane shear
(Janssen 1981, ISO 2004b)

b) S-type inter-laminar shear test
(INBAR 1999, Cruz 2002)
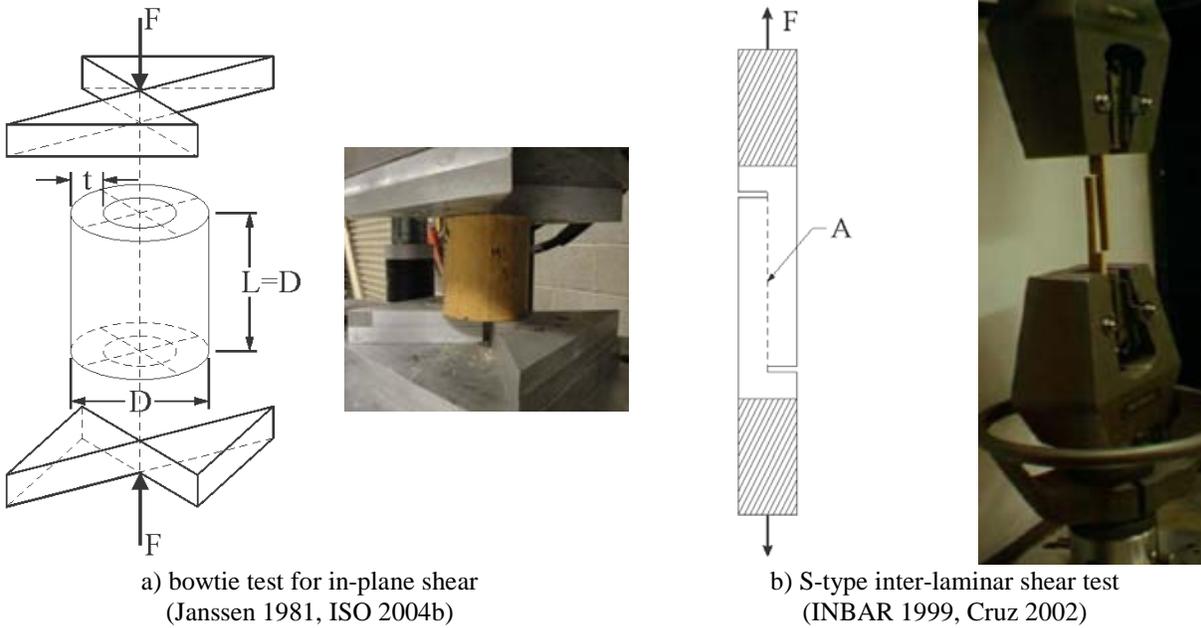
Figure 4-4: Current test methods for in-plane shear strength of bamboo

Cruz (2002) also developed a 'lap shear' test arrangement to study shear strength perpendicular to the longitudinal fibers. Sharma (2010) provides an extensive review of available bamboo test methods. Nonetheless, current available standardized tests do not investigate bamboo splitting characterized by the tensile strength perpendicular to the bamboo fibers (Mode I) or mixed-mode failures.

4.1.2.2 Bamboo Splitting (Mode I and Mixed-Mode Failures)

Research has been conducted to understand the strength characteristics and to develop test methods for bamboo tensile strength perpendicular to the fibers: the Mode I component of

splitting resistance. The susceptibility to longitudinal splitting due to drying of thick-walled bamboo can also be attributed to the presence of both longitudinal and tangential stresses and weak tensile strength perpendicular to fibers. The low tensile strength perpendicular to fibers is due to the fact that only the lignin matrix resists stresses in the tangential and radial directions of the culm. Arce-Villalobos (1993) concluded that there is no correlation between the density of bamboo and its transverse tensile strength implying that the capacity of the lignin is relatively universal. Arce-Villalobos also states that bamboo samples fail at a specific tangential strain: 0.0011. Recognizing that Poisson's ratio of 0.3 is also relatively constant for bamboo (Janssen 1981), the tangential strain can be related to longitudinal strain and ultimately to design criteria. However, this limiting tangential strain approach can also be framed simply as relating to the density and strength of the weak lignin matrix in the tangential direction. As reported by Shao et al. (2009), Zeng et al. (1992) found that the tensile strength perpendicular to the longitudinal fibers was only about 2% of that parallel to the fibers.

As discussed in Section 2.3.2, Mitch et al. (2010) and Sharma (2010) sought to develop laboratory and field tests for tensile strength perpendicular to the longitudinal fibers. Mitch et al. developed the split-pin test shown in Figure 4-5a. Based on fundamental linear elastic fracture mechanics, the test consists of a full culm specimen having a transverse hole. Horizontal notches are made at the edge of the holes in order to initiate failure in the horizontal plane. A split steel pin is inserted and loaded such that a transverse tension failure of the culm results. Ultimately, the test determines the direct tension capacity perpendicular to the longitudinal bamboo fibers (Eqn. 4-7) and can be used to assess the fracture toughness of the culm (Eqn. 4-8). Results showed that the test improved upon the repeatability of test results as compared to the 'bowtie'

or S-specimen tests shown in Figure 4-4. The tension capacity perpendicular to the longitudinal fibers, $\sigma\perp$, is given as:

$$\sigma_{\perp} = \frac{F}{2Lt - 4at}$$
(4-7)

Where the specimen dimensions are shown in Figure 4-5b. The Mode I strain energy release rate (a measure of fracture toughness), G_I, is given as:

$$G_I = \frac{K_I^2}{E}$$
(4-8)

Where E is the elastic modulus of the material and K_I is the crack intensity factor for the specimen geometry:

$$K_I \approx \frac{F}{2Lt} \sqrt{\pi a} \left(\frac{L}{\pi a} \tan\left(\frac{\pi a}{L} \right) \right)^{\frac{1}{2}}$$
(4-9)
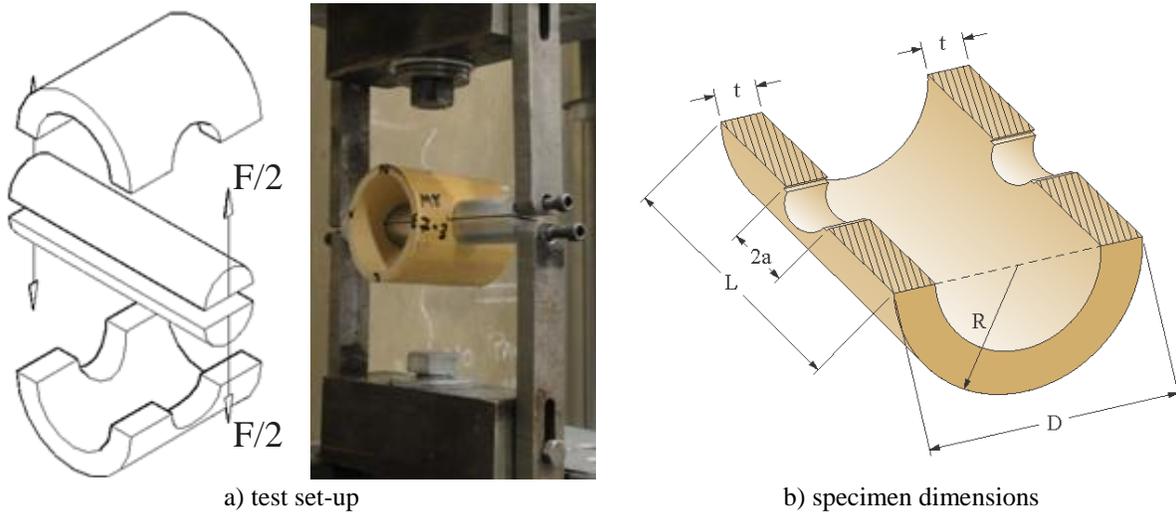
a) test set-up   b) specimen dimensions
Figure 4-5: Split-Pin Test (Mitch 2009)

Sharma (2010) sought to develop a less complex test that could be applied in the field and correlate with the split-pin test which requires specimen machining, a complex test apparatus and a method of applying tension; all impractical in a field test. The edge bearing test, shown in Figure 4-6, was proposed as a surrogate for the more complex split-pin test, since a compression

test is more easily implemented. The edge bearing test is composed of a full culm specimen loaded in compression perpendicular to the bamboo fibers. The test is used to determine the transverse modulus of rupture for the culm walls, f_r (Eqn. 4-10) – a measure of transverse tension capacity:

$$f_{rNS} = \frac{M_{NS}(c_r + h_r)}{I_r}$$

$$f_{rEW} = \frac{M_{EW}(c_r + h_r)}{I_r}$$

(4-10)

Where the applied moments are given as:

$$M_{NS} = \frac{wLR_c}{\pi}\left(1 - \frac{I}{AR_c^2}\right)$$

$$M_{EW} = \frac{wLR_c}{\pi}\left(1 - \frac{I}{AR_c^2}\right) - \frac{wLR_c}{2}$$

(4-11)

In Equations 4-10 and 4-11, the NS and EW subscripts refer to the specimen quadrant indicating applied moments in which the tension is along the inner or outer culm wall, respectively (see Figure 4-6 for moment directions and rupture patterns).The subscript r in Equation 4-10 refers to the culm properties at the quadrant at which the rupture occurs. In Equation 1-10, $c_r = t/2$ and refers to the distance from the midline of the culm wall to the edge of the wall section at the location of rupture while h_r is the distance from the culm wall midline to the elastic neutral axis of the culm wall measured toward the center of curvature at the location of rupture (Sharma 2010). In Equation 4-11, $A = Lt$ and $I = Lt^3/12$ are the area and moment of inertia of the single culm wall in through-wall flexure. R_c is defined as the culm radius measured to the midwall thickness; that is $R_c = (D-t)/2$.
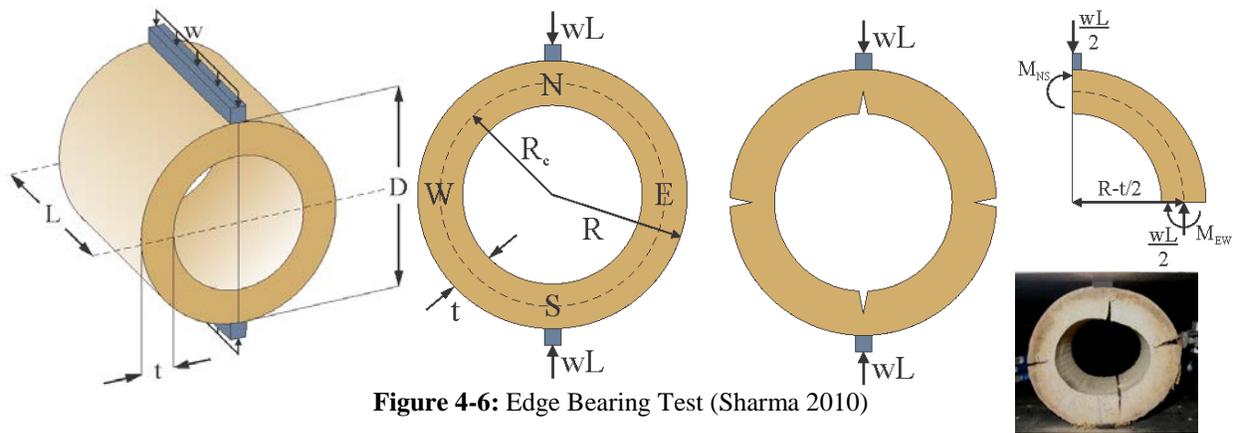
Figure 4-6: Edge Bearing Test (Sharma 2010)

Amada and Untao (2001) also studied the fracture toughness of bamboo culms and nodes at the macroscopic level using notched tensile tests from 2 year old *Phyllostachys edulis* (Mousou). The fracture characteristics of bamboo were considered to be first fiber-cracking. Dog-bone specimens having a width equal to the culm wall thickness and a gauge length of 50 mm were used. A 0.4 mm thick notch was cut perpendicular to the fibers from the outer surface of the specimen using a razor blade. The fracture toughness calculated based on this specimen geometry had the highest value at the outer surface of the culm and decreased towards the inner surface. The average fracture toughness was determined to be 56.8 MPa·m$^{1/2}$ which is higher than most wood species. The authors concluded that the fracture toughness is proportional to the volume fraction of the fibers, V_f, through the culm wall thickness. Furthermore, the fracture toughness in the outer layer and the average value increased marginally with height in the culm. Finally, the fracture toughness of bamboo nodes was found to be 18.4 MPa·m$^{1/2}$, which was lower than that at the inner surface (Amada and Untao 2001). It is important to note that the specimen geometry used by Amada and Untao measures the toughness of the longitudinal bamboo fibers and matrix across the cross section and says little of the toughness associated with longitudinal splitting.

110

Shao et al. (2009) studied the Mode I inter-laminar fracture properties of *Phyllostachys pubescens* (Moso) bamboo. The Mode I inter-laminar fracture toughness, G_I was measured based on the energy method using double cantilever beam specimens and a scanning electron microscope to study fracture surfaces. According to the authors, once there are cracks in bamboo, the delaminating propagation is not controlled by the strength but by interlaminar fracture toughness which is a basic characteristic of the bamboo. The Moso used in the study was 4 years old and had a total height of approximately 15 m. Seventeen double cantilever specimens were taken from the culm wall at heights of 1.3, 3, and 5 m along the culm. The moisture content was approximately 11% during testing. The mean value of Mode I inter-laminar strain energy release rate was determined as $G_I = 358$ J/m^2 (COV = 17%). No significant difference in fracture toughness was found for specimens located at different heights along the culm. Crack propagation was shown to develop along the longitudinal interface between fibers or ground tissue and the crack was a self-similar fracture without fiber-bridging (Shao et al 2009) which is consistent with a pure Mode I failure. The authors also concluded that the resistance arresting crack propagation is controlled by the inter-laminar strength between fibers or ground tissue.

Tan et al. (2011) conducted a multi-scale study on the fracture behavior and resistance properties of Moso bamboo as a functionally-graded material. First, the study used nano-indentation experiments to study the variation of Young's modulus in the radial and longitudinal directions of the culm as well as to study micro-scale tensile properties. Next, the resistance curve behavior of bamboo was investigated with four point bending experiments. Specimens were 4.2 x 4.0 x 40.0 mm in size and had notches (notch to width ratio of approximately 0.45) at midspan. Specimens were composed of three groups: those having notches on the outer culm face with the highest fiber density (outside crack); notches on the inner culm face with lowest

fiber density (inside crack); and notches on the side face (side crack). The tests were conducted under displacement control with a loading rate of 0.01 mm/s. The finite element method was then used to calculate the energy release rates for crack geometries used in the experimental testing. Crack bridging models were used to investigate bridging effects in the bamboo fracture behavior. Energy release rates for crack bridging models as well as the finite element models were shown to have good agreement with results from the experiments. Inside crack specimens were shown to exhibit the highest energy release rates or toughness followed by the side crack specimens and outside crack specimens respectively. The authors concluded that this was due to high cellulosic bridge densities in the inside crack specimens (Tan et al. 2011). Meanwhile the intermediate behavior in the side crack specimens was attributed to crack tip shielding caused by ligament bridging.

Zhao et al. (2011) studied mixed-mode cracking in the fracture of bamboo flexure specimens using digital speckle correlation method (DSCM) instrumentation. Specimens were taken from the culm wall of four year old *Phyllostachys pubescens* (Moso). Flexural specimens had a length of 160 mm, a test span of 120 mm, and were 10 mm square. One specimen category (Bamboo-O) had the outside face of the culm wall in tension while another (Bamboo-I) had the inner face of the culm wall in tension. A 4 mm crack was placed at mid-span in the tension face of the flexural member and load was applied 15 mm to the left of mid-span according to Chinese National Standard GB/T15780-1995 (as reported by Zhou et al). A CCD camera was used to capture the speckle image continuously during the test. DSCM was then used to determine the crack opening displacement (COD). The stress intensity factors K_I and K_{II} were also calculated. Results showed that the COD for Bamboo-O was less than that for Bamboo-I while the stress

intensity factors for Bamboo-O were greater than those for Bamboo-I. The authors conclude that the gradient distribution of bamboo has a protecting function for a static crack in the inner layer.

The objective of the current study is to investigate the mixed-mode longitudinal shear behavior of full culm bamboo flexural components and work to develop methods for a testing procedure of full culm specimens. While studies by Tan et al. (2011) and Zhou et al. (2011) investigated small-scale specimens taken from thin walled bamboo species, the current study investigates full-culm specimens of both thin-walled and thick-walled bamboo species. In addition, the work seeks to correlate the mixed-mode strength behavior with Mode I and Mode II behavior seen in split-pin and bow-tie tests in order to estimate the primary driver of the flexural splitting failure.

4.2   EXPERIMENTAL PROGRAM

The experimental portion of this investigation was composed of three phases: a) estimation of the Mode I and Mode II capacities of the bamboo using bowtie and split-pin tests; b) small scale beam tests of rectangular specimens taken from the culm wall; and c) full-culm modified ISO flexural tests to determine longitudinal splitting strength. The specimens, test methods and results of these phases are described in the following sections.

4.2.1   Bamboo Species and Test Locations

Three species of bamboo were used for the full-culm modified flexural tests. *Dedrocalamus giganteus* (Dendrocalamus) and *Phyllostachys pubescens* (Moso) were tested in the Structures

and Materials Laboratory at the Pontifícia Universidade Católica de Rio de Janeiro (PUC) during the author's tenure as a visiting researcher from February to June 2012. Moso specimens tested at PUC were supplied from an off campus facility while 10 to 12 year-old Dendrocalamus culms were harvested from the PUC campus in 2010. Eight Dendrocalamus culms were harvested and cut into 4 m sections; test specimens were selected from this group. It should be noted that the Dendrocalamus culms were stored unsheltered outside the laboratory. This did not allow the untreated bamboo to dry properly and resulted in infestation of the bamboo by insects that eat the starches as they tunnel through the culm.

Additional full-culm specimens of *Phyllostachys pubescens* (Moso) and *Bambusa stenostachya* (Tre Gai) were tested in the Watkins-Haggart Structural Engineering Laboratory (WHSEL) at the University of Pittsburgh. Specimens were ordered from a bamboo importer in Portland, Oregon (www.bamboocraftsman.com) with Moso specimens shipped from China and Tre Gai specimens from Vietnam. Specimens for the bowtie, split-pin, and small beam tests were fabricated from the same batch of Moso and Tre Gai culms as the full-culm tests in Pittsburgh and were also tested in the WHSEL Lab.

4.2.2 Bowtie Tests

'Bowtie' tests (Fig. 4-4a) were conducted in accordance with ISO standard 22157-1:2004(E) (ISO 2004b) on six Moso and five Tre Gai specimens to estimate the Mode II in-plane shear strength (τ) of each species. Specimens were taken from undamaged regions of full-culm beam specimens after testing. For each specimen, measurements of wall thickness and specimen length were taken at each quadrant (N, S, E and W) at each end of the specimen; these dimensions are summarized in Table 4-1. The length of each specimen was equal to

114

approximately one culm diameter as required by the ISO standard. Specimen ends were cut parallel and at right angles to the axis of the specimen.

Table 4-1: Bowtie Test Specimen Geometry and Results

Bowtie Test	Culm	Avg. diameterD	Avg. length, L		Avg. Culm Wall Thickness, t				Shear Area	Ult. Load	Shear Stress (Eq. 4-5)
		(mm)	(mm)	L/D	N (mm)	S (mm)	E (mm)	W (mm)	mm^2	kN	MPa
M1	M8-7-1	65.0	68.6	1.06	5.48	5.35	5.23	5.42	1473	20.83	14.14
M2	M8-8-1	63.6	67.4	1.06	5.31	5.70	4.91	4.89	1402	20.62	14.71
M3	M8-8-2	63.0	68.8	1.09	5.31	5.10	5.53	5.74	1491	19.61	13.15
M4	M9-14	60.5	62.0	1.02	5.79	6.06	6.04	5.74	1464	25.22	17.23
M5	M12-9	64.7	67.7	1.05	6.47	6.83	6.71	6.78	1814	23.99	13.23
M6	M12-10	64.2	67.0	1.04	6.58	6.91	6.62	7.07	1822	23.59	12.94
										Avg. (COV)	**14.20 (0.104)**
T1	T7-2	65.2	70.2	1.08	23.54	21.34	25.29	22.47	6503	58.36	8.98
T2	T7-3	65.7	66.6	1.01	23.91	22.71	21.27	23.25	6071	56.89	9.37
T3	T7-10	64.1	80.4	1.25	20.14	22.19	18.10	20.01	6463	48.89	7.56
T4	T7-11	64.2	66.8	1.04	16.07	19.48	18.68	20.40	4985	45.15	9.06
T5	T11-1	65.9	65.7	1.00	20.50	20.47	24.58	25.29	5966	49.42	8.28
										Avg. (COV)	**8.65 (0.075)**

Specimens were tested in an Instron universal testing machine with 'bowtie' compression loading plates as shown in Figure 4-4a. Specimens were oriented in the testing apparatus so that shear planes occurred at the cardinal designations. A specified loading rate of 0.01 mm/sec was used as prescribed by ISO. The maximum load and location(s) of failure were noted for each specimen and testing stopped automatically when the load fell to 50% of the peak.

4.2.2.1 Bowtie Tests Results

Results of the bowtie tests are shown in Table 4-1. In-plane shear stress is calculated from Equation 4-5. Moso specimens had an average ultimate shear strength of 14.23 MPa with a COV of 0.104, while Tre Gai specimens displayed an ultimate shear strength of 8.65 MPa with a COV of 0.075. This latter value is close to the value of 8.8 MPa determined by Mitch (2009) for

the same species (although a different batch of culms). The COV from the current tests is considerably better than the 0.30 value reported by Mitch.

Failure of bowtie specimens generally occurred along two of the shear planes created by the loading plates. The first failure typically occurred at the peak load. In two of eleven tests, after the initial failure and load reduction, the specimen carried additional load until a second failure occurred in the shear plane opposite of the initial failure (Fig. 4-7a). In two tests, the first failure occurred and the load dropped below 50% of that peak, ending the test. Five specimens failed initially at a shear plane but experienced multiple additional cracks at a second peak, breaking the specimen into three separate pieces. The additional cracks in this category of failures occurred both at shear planes and between shear planes (Fig. 1-7b). Finally, two tests saw cracking between shear planes. This failure indicates a degree of flexure across the unsupported quadrant and may indicate initial flaws in the test specimens. In most cases, the ultimate load and shear stress were similar for each specimen. In all cases, the shear failure ruptures along the entire length of the specimen.

(a) Failure at shear plane   (b) Failure between shear planes
Figure 4-7: Examples of Bowtie Test Failure Planes

4.2.3 Split-Pin Tests

Split-pin tests were conducted on four Moso and three Tre Gai specimens in order to determine the Mode I tensile strength perpendicular to fibers ($\sigma\perp$) of each species as well as the Mode I stress intensity factor (K_I). Similar to the bowtie tests, specimens were taken from full culm beam tests after testing and measurements of wall thickness were taken at the East and West quadrants at both ends of the specimen. Specimen length and diameter at both ends were also measured. All dimensions are summarized in Table 4-2 and Figure 4-5b. The length (L) of each specimen was equal to approximately one culm diameter as recommended by Mitch (2009). Each specimen has a 25.4 mm diameter hole drilled through the east and west sides. Both holes were created with a single pass of a drill press to maintain symmetry of the specimen. The diameter of the hole is required to be between 0.1D and 0.5D. Crack initiators 3 mm in length were cut parallel to the length of the culm on either side of the drilled hole with a fine toothed hacksaw blade resulting in a dimension 2a = 31.4 mm (see Fig. 4-5b).

Table 4-2: Split Pin Test Geometry and Results

Split-pin Test	Culm	Avg. D	Avg. length, L		t_{east}	t_{west}	F_{ult}	$\sigma\perp$ (Eq. 4-7)	K_I (Eq. 4-9)
		(mm)	(mm)	L/D	(mm)	(mm)	(kN)	(MPa)	(MPa•m$^{1/2}$)
M1	M8-1	80.5	110.6	1.37	6.19	6.15	1.69	1.73	0.28
M2	M8-5-1	69.9	73.1	1.05	5.46	5.34	1.05	2.33	0.32
M3	M8-7-3	66.3	74.6	1.12	4.95	5.21	0.97	2.21	0.31
M4	M8-7-4	65.8	63.0	0.98	5.38	5.32	1.13	3.34	0.42
							Avg. (COV)	**2.40 (0.244)**	**0.33 (0.178)**
T1	T11-2	66.0	69.2	1.05	19.56	19.11	2.46	1.68	0.22
T2	T11-3	66.4	70.5	1.06	20.31	19.51	1.83	1.18	0.16
T3	T11-8	67.8	73.6	1.09	15.34	15.43	2.23	1.71	0.24
							Avg. (COV)	**1.52 (0.162)**	**0.21 (0.166)**

The specimens were loaded at a rate of 0.005mm/sec using an Instron universal testing machine and the ultimate load was recorded for each test.

117

4.2.3.1 Split-Pin Test Results

Results from the split-pin tests are presented in Table 4-2. The tensile capacity perpendicular to the length of the fibers ($\sigma\perp$) and stress intensity factor (K_I) are calculated from Equations 4-7 and 4-9, respectively. An average ultimate tensile strength of 2.40 MPa having a coefficient of variation of 0.244 was calculated for the Moso specimens while Tre Gai specimens had an average ultimate tensile strength of 1.52 MPa and a coefficient of variation of 0.162. The stress intensity factors for Moso and Tre Gai specimens were 0.33 MPa•m$^{1/2}$ and 0.21 MPa•m$^{1/2}$, respectively. The coefficient of variation was 0.178 and 0.166 for both species respectively. The results observed for the Tre Gai specimens were comparable (although slightly higher) to results presented by Mitch et al. (2010) for similar Tre Gai tests which had an average ultimate tensile strength of 1.06 MPa and a stress intensity factor of 0.17 MPa•m$^{1/2}$, both with a COV of 0.22.

4.2.4   Small Scale Flexural Tests

Small beam tests were conducted to determine the longitudinal shear strength of bamboo within the culm wall. Four specimens of Moso and five specimens of Tre Gai were cut from the culm wall internodes (Fig. 4-8a) using a milling machine. Specimen dimensions are reported in Table 4-3. Specimens were oriented in such a way that the width, b was measured in the radial direction of the culm and the height, h was oriented in the tangential direction (Fig. 4-8a). The height to width ratio of the specimens was kept as close to a value of 2 as was possible (Table 4-3). As shown in Figure 4-8, the specimens were tested in four point bending with a 0.5h deep laser-cut notch (Figure 4-8c) cut into the tension face under one load point. The first specimen in each species series was tested without a notch as a control. The notched orientation was selected to result in similar orientation as in full-culm specimens described in the following section.
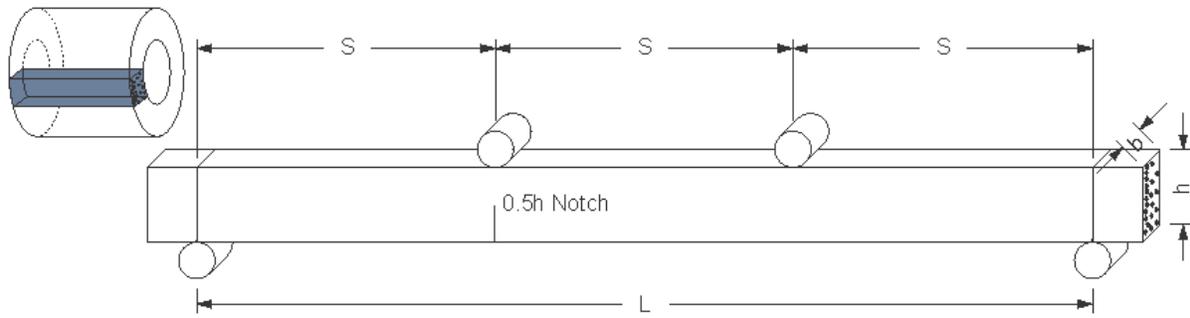
a) test set-up orientation and dimensions

b) test set-up (Specimen T4 shown)
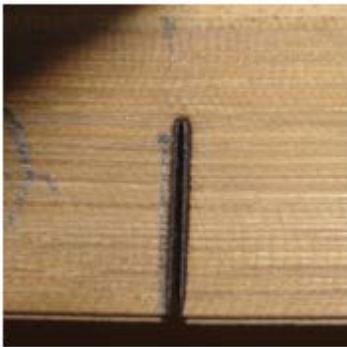
c) notch

d) typical failure (Specimen T4 shown)

**Figure 4-8:** Small Beam Flexural Specimen Configuration

Table 4-4 provides the average geometry of the beam specimens tested. Moso specimens were tested over a simple span of L = 152 mm with shear span lengths of 51 mm. The Tre Gai specimens were tested over a simple span of L = 229 mm with shear span lengths of 76 mm. The variation in sizes was due to the larger internode lengths in the Tre Gai culms. A Vic-3D imaging system (described in Section 3.3.3) was used in order to investigate the stress concentration at the notch location and capture splitting in the specimen.

Table 4-3: Small Beam Geometry and Results

| Small Beam Specimen | Notched | dimensions at notch | | | | Shear, V | Shear Stress, τ (Eq. 4-2) |
| | | b | H | h/b | Area | at crack initiation | |
		(mm)	(mm)		(mm^2)	(N)	(MPa)
M2	N	5.88	12.13	2.06	71.3	334	7.02
M6	Y	5.64	12.65	2.24	71.3	56	1.19
M7	Y	5.97	12.67	2.12	75.7	114	2.25
M9	Y	5.98	12.37	2.07	74.0	99	2.01
						Avg. (COV)	**1.28 (0.307)**
T4	N	12.01	19.13	1.59	230	905	5.90
T5	Y	11.47	18.75	1.63	215	77	0.54
T6	Y	10.86	19.39	1.79	211	145	1.04
T8	Y	10.99	17.97	1.64	197	107	0.81
T10	Y	10.46	17.69	1.69	185	95	0.77
						Avg. (COV)	**0.788 (0.260)**

4.2.4.1 Small Scale Beam Test Results

The results of the small scale flexural tests are presented in Table 4-3 and Figure 4-9 for the Moso and Tre Gai specimens. First, un-notched specimens M2 and T4 were shown (as expected) to have much higher shear capacity than notched specimens (Table 4-3); this value is characteristic of the species and test geometry. In the notched specimens, failure occurred at the notch at the first peak of loading as shown in the applied shear versus stroke diagrams. For Moso specimens M7 and M9, this peak also corresponded with maximum shear stress for the entire test (Fig. 4-9a). All Tre Gai specimens except T5 experienced a secondary loading phase (Fig. 4-9b) indicating a very tough post-peak behavior.
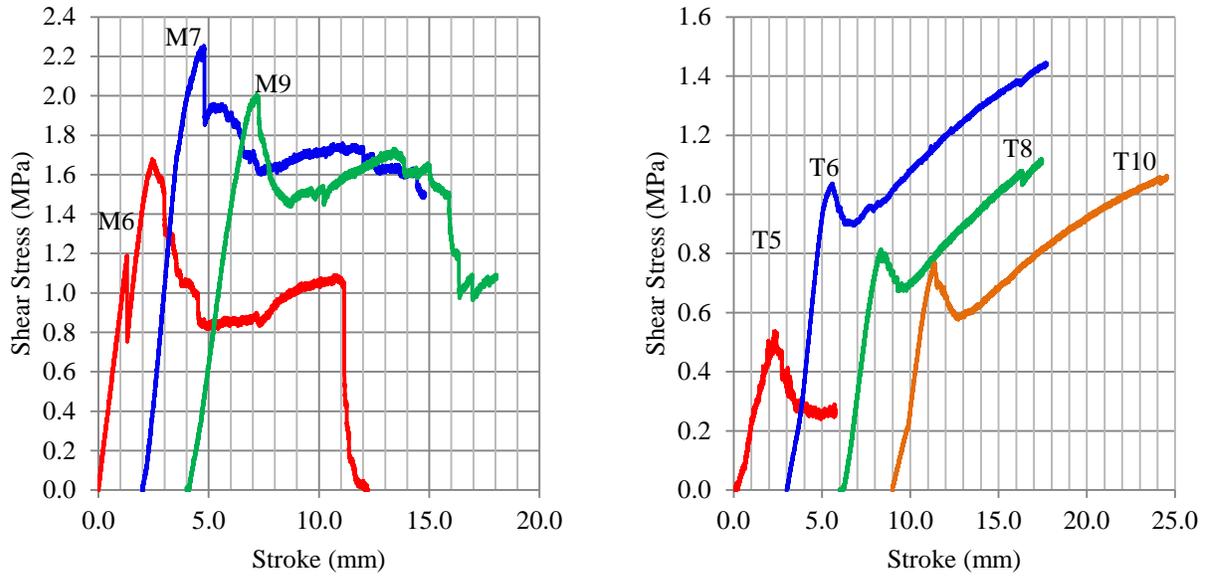
a) Moso Specimens   b) Tre Gai Specimens

Figure 4-9: Shear Stress (MPa) v. Stroke (mm) for Small Notched Flexural Specimens (curves offset for clarity)

It is noted that several Tre Gai tests were ultimately stopped due to the maximum deflection limit of the test arrangement being reached (the beams 'bottomed out' on the test frame). Notched Moso specimens had an average shear stress, τ_1 at splitting of 1.82 MPa with a COV of 0.31, while Tre Gai specimens had an average shear stress value of 0.79 MPa with a COV of 0.26.

Representative results of the failure mode and strains estimated using the VIC-3D imaging system are shown in Figure 4-10 for an un-notched Tre Gai specimen (T4) and in Figure 4-11 for a comparable notched specimen (T8). The un-notched specimen (Fig. 4-10a) shows bending strains (ε_{xx}) increasing during the test as expected with compression at the top face and tension on the bottom face of the beam (Figs. 4-10b - e). Meanwhile, in the photos of the representative notched specimen, the primary failure mode was for an initial crack to propagate from the notch towards midspan (Figs. 4-11b and 4-8d). As the cracking towards midspan became substantial (in some cases through the entire constant moment region) cracking towards the support would develop. Figure 4-11d shows strain associated with bending (ε_{xx}) and the concentration of stress at the location of the notch. Meanwhile, Figure 4-11e illustrates the

concentration of vertical strain (ε_{yy}) along the crack as it continues to open. The failure behavior of the small beams will be compared with the results of the full-scale specimens described in the following section.
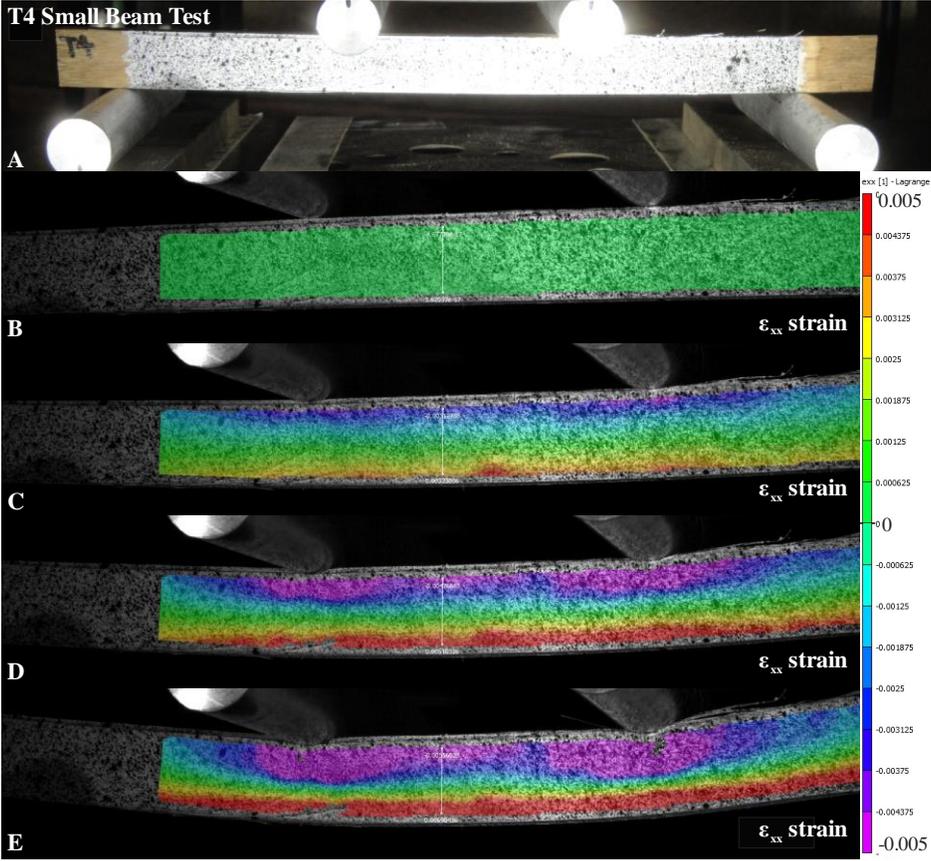
Figure 4-10: VIC-3D contour images for un-notched Tre Gai beam specimen
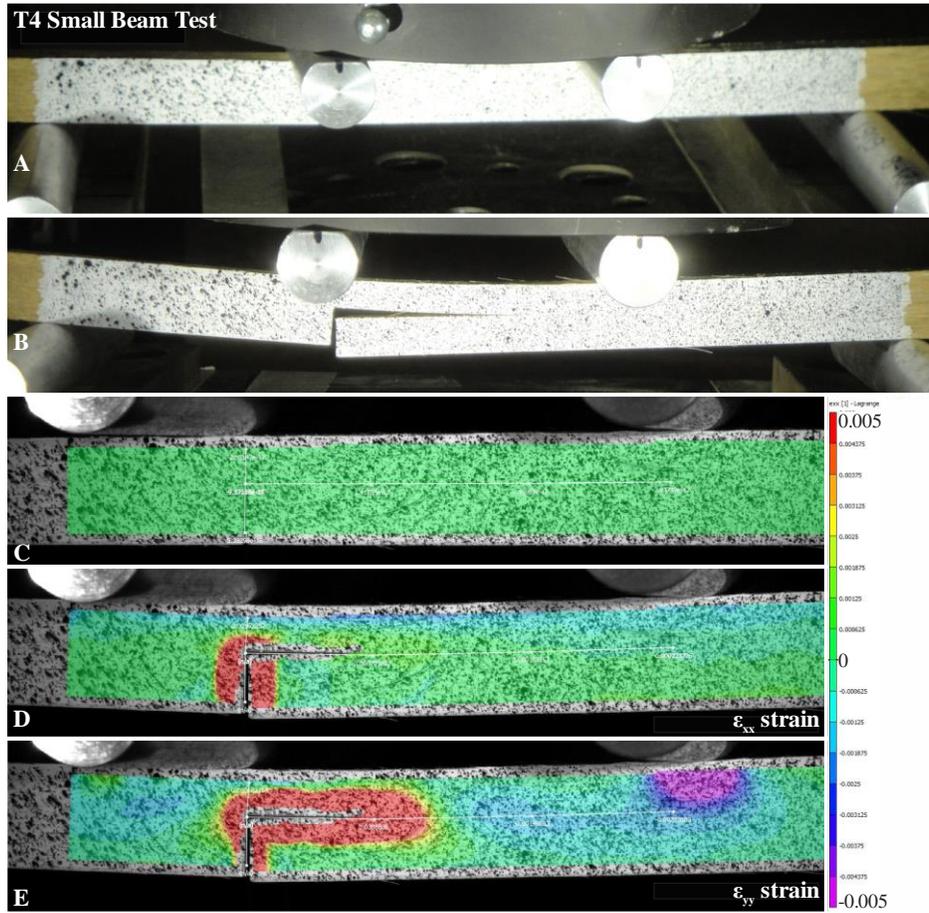
Figure 4-11: VIC-3D Contour Images for Notched Tre Gai Specimen

4.2.5 Full-Culm Flexural Tests

Full-culm flexure tests were conducted both at the University of Pittsburgh (UPitt) and the Pontifícia Universidade Católica de Rio de Janeiro (PUC) using three different species of bamboo (Dendrocalamus, Moso, and Tre Gai). As described in the following section, the tests consisted of four-point bending tests (ISO 2004b) modified with a notched specimen in order to better measure the longitudinal shear behavior of the culm in flexure and investigate the potential of the modified test as a reliable standard test method. The full-culm results were also correlated with the results of the smaller scale tests for Mode I, II, and mixed mode failures.

4.2.5.1 Specimens

Full-culm flexure specimens were selected from batches of *Dedrocalamus giganteus* (Dendrocalamus) and *Phyllostachys pubescens* (Moso) and *Bambusa stenostachya* (Tre Gai). Specimens of Dendrocalamus and Moso culms tested at PUC were tested over simple spans of 3000 mm and 2760 mm, respectively. Moso and Tre Gai culms tested at UPitt were tested with simple spans of 2896 mm and 2286 mm, respectively. Span lengths were selected to meet the 30D span requirements of ISO 22157 (2004b) and were also dictated to some extent by culm lengths available from suppliers.

For geometric measurements, the section quadrants of the bamboo culm cross sections were assigned cardinal directions (North, South, East, and West) and each internode was numbered from the base to the top of the culm. The initial variability in geometry was catalogued prior to testing. Measurements were taken along each culm's length for diameter, variation from a plumb axis (to determine initial out-of-straightness), wall thickness (wall thickness

124

measurements were taken following testing when the culms were cut into sections), and internode length. Measurements were taken by placing the bamboo in a specially designed jig as shown Figure 4-12. The culm is placed between two parallel string lines set a constant distance apart; measurements were taken between each string and the culm. From this, both the culm diameter and deviation from centerline or "out-of-straightness," can be determined. Measurements were taken at the center of each internode, load/notch points, and support points in both principle axes (N-S and E-W; i.e.: each culm was rotated 90 degrees in the jig for a second set of measurements). Table 4-4 summarizes values for culms used in this study. The gross cross section area (A_g) and moment of inertia (I) are based on the average diameter (D) and wall thickness (t) values measured at each internode, averaged over the culm length.

| a) support condition of measuring jig. | b) culms that are (top) relatively straight and (bottom) significantly curved in jig. |

Figure 4-12: Jig for measuring bamboo culms

Twenty specimens were tested in flexure and their geometric properties are summarized in Table 4-4. With the exception of one specimen of Dendrocalamus (DB2 0.0125S), all specimens had maximum out of straightness less than 1% of span length. Based on culm diameter to wall thickness, Moso and Dendrocalamus are considered thin-walled species, having D/t > 10, while Tre Gai is a thick-walled species. Specimens tested at PUC had larger cross sections than those tested at Pitt. Finally, all efforts were made to maximize the test span and respect the S > 30D requirement (ISO 2004a); due to culm availability, this was not always possible with some of the specimens tested at PUC.

Table 4-4: Geometric Properties of Bamboo Flexure Specimens and Test Details

Test	Culm	Test Span, S	D	T	Max. out of straightness, δ		Area, A	Moment of Inertia, I	notch location (see Fig. 1-5)	Shear V = F/2	Shear Stress, τ (Eq. 4-12)[1]
										at initiation of failure at notch	
		(mm)	(mm)	(mm)	(mm)	δ/S	(mm^2)	(mm^4)		(N)	(MPa)
						Moso tested at UPitt					
1	MP9	2896	67	8	7	0.0025	1434	652864	none	1526	2.66
2	MP4	2896	75	7	7	0.0025	1401	822364	none	2156	3.55
3	MP1	2896	72	5	15	0.0052	1135	625468	P2	244	0.50
3B									P1	293	0.48
4	MP2	2896	71	8	13	0.0044	1505	756185	P2+D	375	0.66
4B									P1+D	456	0.64
5	MP12	2896	62	7	8	0.0026	1188	467654	none	1124	2.23
6	MP8	2896	71	6	15	0.0053	1181	630323	P2+D	337	0.63
6B									P1+D	119	0.19
										Avg. (Notched)	**0.52**
										COV	**0.348**
						Tre Gai tested at UPitt					
7	TP7	2286	65	21	5	0.0023	2896	873988	none	4306	2.07
8	TP8	2286	67	16	11	0.0049	2587	930004	P2+D	402	0.33
9	TP2	2286	66	12	8	0.0035	2060	783247	P2+D	293	0.33
10	TP3	2286	63	16	9	0.0038	2382	715878	P1+D	440	0.32
										Avg. (Notched)	**0.33**
										COV	**0.031**
						Dedrocalamus tested at PUC					
11	DB1	3000	95	9	25	0.0084	2453	2292217	none	1928	1.50
12	DB2	3000	109	10	38	0.0125	3137	3849267	none	5227	3.53
13	DB3	3000	145	16	16	0.0052	6600	13859277	P1	1468	0.38
14	DB4	3000	136	13	13	0.0042	4944	9576049	P1	1707	0.69
15	DB5	3000	109	19	20	0.0065	5437	5746187	P2	1082	0.43
										Avg. (Notched)	**0.50**
										COV	**0.332**
						Moso tested at PUC					
16	MB5	2760	105	10	2	0.0008	3057	3476649	none	5014	3.48
17	MB3	2760	95	9	19	0.0069	2531	2380560	none	2593	2.37
18	MB4	2760	95	9	24	0.0085	2433	2276357	P2	536	0.47
19	MB2	2760	83	8	9	0.0033	1941	1409975	P2	164	0.19
										Avg. (Notched)	**0.33**
										COV	**0.598**

[1] calculated using dimensions measured at notch location

4.2.5.2 Experimental Flexural Test Arrangement

The configuration of the flexural tests follows the guidelines of ISO 22157 (2004b) with a specimen having a span, S ≥ 30D, and equal shear spans, S/3 ≥ 10D. This specimen geometry is necessary to ensure a flexure-dominated behavior (Vaessen and Janssen 1997). In order to

study longitudinal shear behavior, the test is modified as shown in Figure 4-13c with a vertical notch of length 0.5D cut into the tension side of the flexural member at the end of the constant moment region. When loaded, the notch will initiate a longitudinal shear failure at its root. The maximum longitudinal shear flow at the notch root corresponding to this geometry can then be calculated from equations 4-3 or 4-4 for thick or thin-walled species, respectively. As shown in Table 4-4, some specimens of each species/location group were tested without a notch to determine the apparent flexural capacity of the material and observe any longitudinal shear failures. This was followed by tests using notched specimens to investigate the longitudinal shear flow capacity. As shown in Figure 4-13c, some specimens were notched directly under a load point (P1 or P2) while other specimens were notched at a distance of one culm diameter, D from the load in the adjacent shear span (P1+D or P2+D). Notches approximately 2 mm wide were cut using either an electric circular saw (UPitt) or hand saw (PUC). Vertical deflection was recorded at load and support points using draw wire transducers (DWT). Electric resistance strain gages were placed at the root of the notch, as shown in Figure 4-14c in an effort to capture the tangential strain at the moment of initial splitting. All notched specimens had two strain gages located at the notch on the side of the support. Tests 6 (MP8), 6B (MP8), 8 (TP8), 9 (TP2), and 10 (TP3) also had two strain gages located at the notch on the side towards mid-span. Strain gages at the mid-span of the culm (i.e.: within the pure-moment region) were used to measure extreme compressive and tensile strains or tangential strain (Fig. 4-13d) depending on the specimen. Un-notched specimens at PUC had mid-span strain gages measuring the extreme compression and tension strains due to bending while un-notched UPitt specimens had mid-span gages measuring tangential strains. Finally, the first test failures of three UPitt Moso specimens

127

were repaired using pipe clamps, the culms re-notched at the other support, and the culms retested; these second tests are designated 3B, 4B and 6B in Table 4-4.

a) Full-culm flexure test configuration used at UPitt.

b) Full-culm flexure test configuration used at PUC.

c) Notch detail at point P1 or P2

d) Strain gage detail at point M
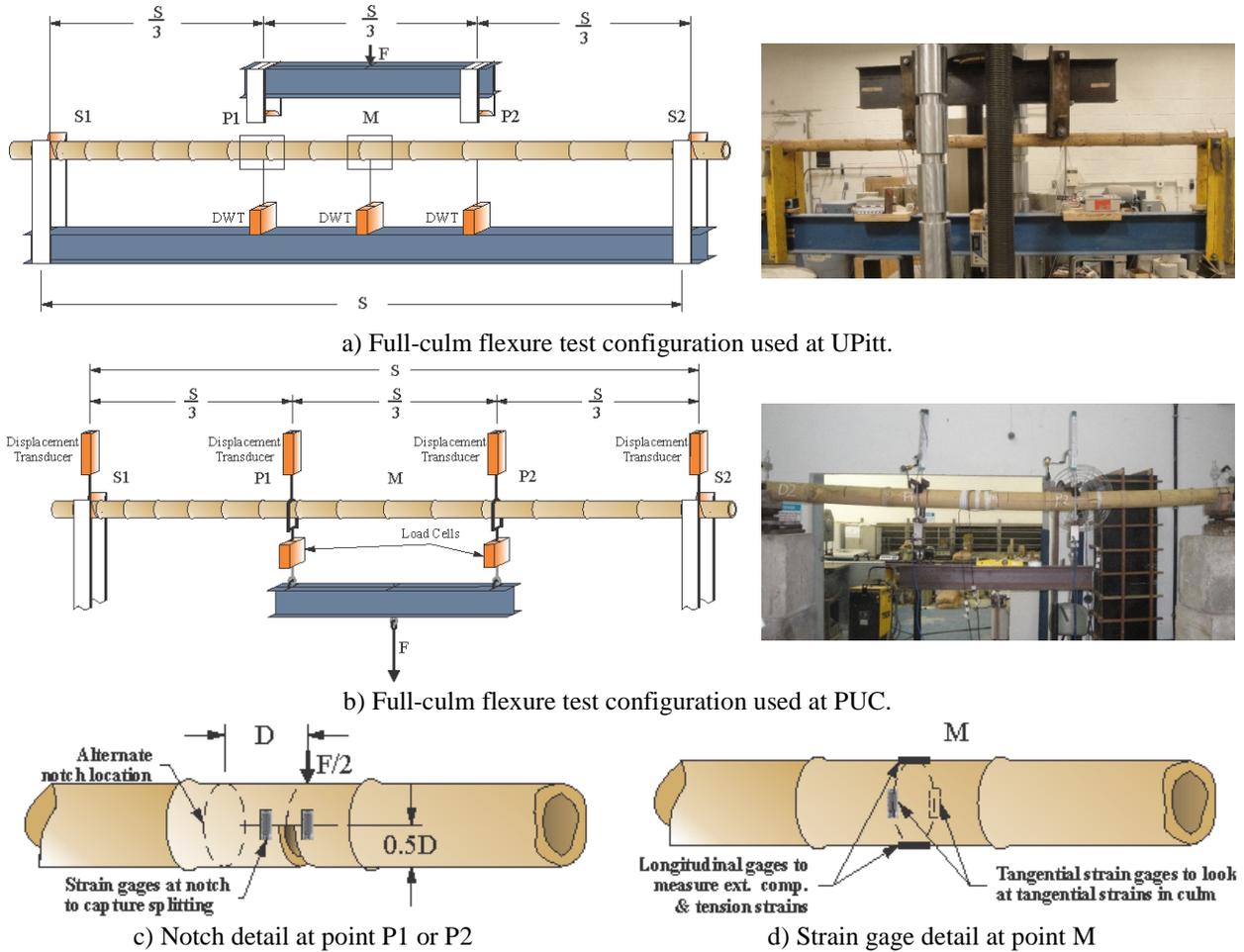
Figure 4-13: Modified flexure test for full scale culms

The test configuration varied between the two testing locations as shown in Figure 4-13. At UPitt, the testing configuration was arranged as shown in Figure 4-13a with the culm supported in saddles made of lifting-sling straps and loaded from above with a spreader beam. DWTs measured displacement directly at the mid-span, load points, and at the supports. Specimens were tested in a Baldwin universal testing machine under displacement control. At PUC, a manual loading apparatus was designed as shown in Figure 4-13b. Using a manual crank and loading plate beneath the testing floor, a spreader beam was pulled downward to load the culm in

flexure. Two load cells and displacement transducers measured load and displacement at each loading point while two additional transducers measured displacement at the supports. In both set ups, care was taken to ensure that loading and support points provided sufficiently large bearing area and flexibility in order to mitigate local crushing of the culm walls; this is crucial in the design of such tests.

4.2.5.3 Experimental Full-Culm Test Results

The results of the full-culm tests provided information not only on the longitudinal shear strength of bamboo culms in flexure but also on the functionality of the proposed modified test arrangement. In the case of the PUC test arrangement (Fig. 4-13b), all specimens were able to achieve failure. However, the test is unstable in nature; the culm could become unseated from the roller support and the spreader beam can become inclined (thereby applying unequal load) as the splitting progresses at the notch. For the UPitt orientation, the test was more stable, yet had issues of the culm surface coming off the loading saddle at the notch location after sufficient cracking had occurred (although this only affects post-peak behavior) . Most un-notched specimens tested at UPitt also reached the maximum deflection limit allowed by the test configuration before failure (i.e.: specimens 'bottomed out'; the test requires greater clearance than was provided). However, all notched specimens were able to reach their ultimate failure before 'bottoming out'.
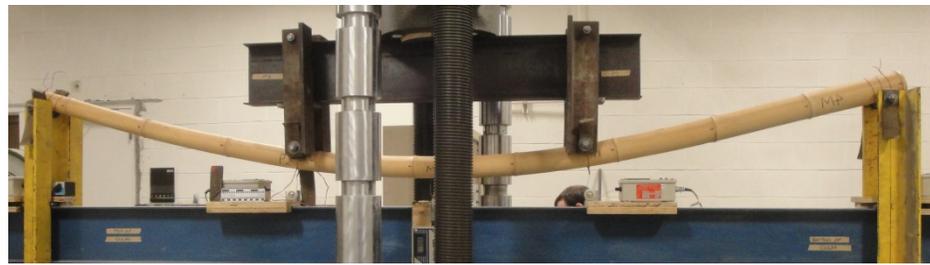
a) Unnotched specimen (M4) under load

b) Notched specimen (T8) under load

c) Notch before test (T8)

d) Notch during test (T8)

Figure 4-14: Representative test pictures

Figure 4-14 illustrates both an un-notched specimen (M4) under loading (Fig. 4-14a) and a notched specimen (T8) at failure (Fig. 4-14b). Un-notched specimens showed a smooth load-displacement curve as illustrated in Figure 4-15a. These also illustrated a stable hysteretic behavior and permanent deformations when tested over several cycles. This is in contrast to the behavior of notched specimens which exhibited several peaks before ultimate load is reached (Fig. 4-15b). These intermediate peaks are believed to coincide with initial cracking and discrete propagation of the crack developed at the root of the notch (Fig 4-14d). Nine of fourteen notched specimens exhibited this 'sawtooth' behavior.
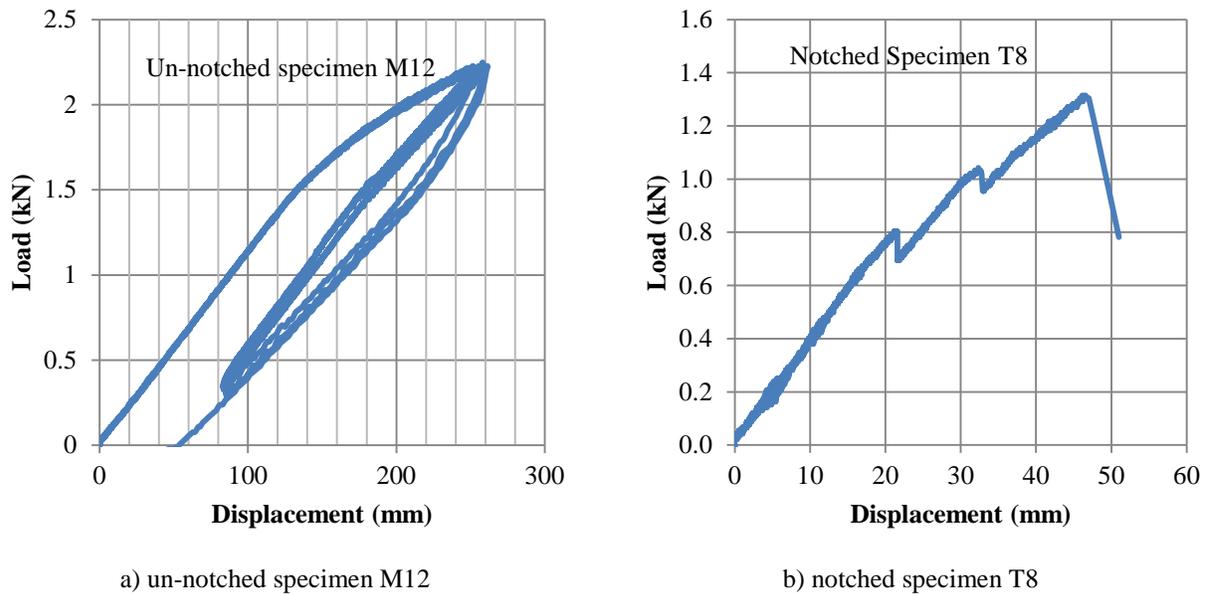
a) un-notched specimen M12   b) notched specimen T8
Figure 4-15: Representative load-displacement curves

Figure 4-14 illustrates the notch detail in a representative Tre Gai specimen (fully shown in Figure 4-14b) both before testing (Fig. 4-14c) and during testing after cracking has occurred (Fig. 4-14d). For the majority of specimens regardless of species or notch location, initial cracking was directed towards the midspan of the culm. In some specimens, further loading resulted in a second crack developing on the other side of the notch which propagated towards the near support. As discussed in the next section, the dominant direction of cracking is driven by the direction of increasing moment and curvature in the beam, which is towards mid-span and the constant moment region.

The test results are summarized in Table 4-4 for all tests and catalogued by species. Specimens of Moso tested at UPitt and PUC are listed separately due to the fact that material properties of bamboo can vary between different batches of culms. Shear, $V = F/2$, is shown for the ultimate strength or for the first peak if a 'sawtooth' load-displacement curve was observed. Shear stress, τ at the notch at initial splitting for the thick-walled Tre Gai is calculated from

Equation 4-3 which may be simplified for the given test geometry (i.e.: notch depth = 0.5D and notch at edge of shear span) as:

$$\tau = \frac{F\left(D^3 - (D - 2t)^3\right)}{48It} \qquad (4-12)$$

Shear stress for thin-walled Moso and Dendrocalamus may be calculated using Equation 4-4 which was found to agree very well with Equation 4-12 for the specimens whose D/t ratios were generally 10 or greater (Table 4-4). Equation 4-4 over-estimated the experimentally observed shear stress by about 7% for the Tre Gai, whose D/t ≈ 4.2 clearly indicates thick-walled specimens. Nonetheless, as an approximate estimate, Equation 4-4 is suitable.

As expected, the strength of the un-notched specimens was significantly higher than the strength of notched specimens. Recall, that testing with L/D > 30 is intended to mitigate the splitting mode of failure in a beam test (Vaessen and Janssen 1997). Nonetheless, some longitudinal cracking was seen to develop in some un-notched specimens (MP9, MP4, and TP7). Specimen MP9 did have some existing cracks in two locations that were then propagated during testing, while specimens MP4 and TP7 began testing with no major cracks identified. While most culms had surface cracking due to drying shrinkage, a major crack was defined as a deep crack going through most of the wall thickness and extending over an entire or multiple internodes. Notched specimens did not have any major cracking but notched Tre Gai specimens did have some pre-existing gashes and surface cracks due to harvesting and drying.

Based on initial cracking capacity, splitting shear strength for all notched specimens was similar: Moso tested at UPitt had an average value of shear stress, $\tau_{avg.}$ of 0.52 MPa (COV = 0.348), while Moso tests at PUC had a value of 0.33MPa (COV = 0.598). Dendrocalamus specimens exhibited an average shear stress of 0.50 MPa (COV = 0.332) while the thicker-walled Tre Gai specimens had an average value of 0.33 MPa (COV = 0.031). The lower average

value and higher COV for the two PUC Moso tests is due to the lower experiment stress value (0.19 MPa) of specimen MB2. A small crack at the notch developed during test preparation of this specimen when the load of the spreader beam was applied to the beam. This crack (or the weak conditions to initiate a preliminary crack) could have been caused during cutting and preparation of the notch. In addition to naturally large variation exhibited by bamboo materials, this latter point identifies specimen handling as a potential source of error, particularly with relatively fragile notch tests. Discounting the result from MB2, the shear stress of the single remaining notched Moso specimen tested as PUC is essentially the same as Moso specimens tested at UPitt.

4.3   DISCUSSION

The full-culm flexural tests exhibited lower strength values than the bowtie, split-pin, and smaller clear bamboo flexural specimens. Table 4-5 summaries the results for all four of the tests conducted at UPitt. These specimens were from the same batch of culms and therefore are directly comparable. Shear strength values determined from small clear specimens were 2.4 – 3.5 times stronger than the values determined from full culm tests. Much of this difference may be attributed to 'scale effects' and the high quality of the clear specimens used. Comparing bowtie tests to the full culm results, the normalized values show similar ratios for both the Moso and Tre Gai. In both cases, the bowtie tests yielded longitudinal shear strengths 26-28 times greater than the full culms and 8-11 times greater than the clear specimens. The differences are believed to reflect the fact that the bowtie test is 100% Mode II distortion while the crack initiation of the beam tests is dominated by Mode I behavior (see Figure 4-3). Comparison of the bowtie and

split-pin test results, that compare Mode II to Mode I behavior directly, illustrates that the Mode I (split-pin) capacity is only about 17% of the Mode II (bowtie) capacity. This result is typical of many brittle materials especially unidirectional fiber-reinforced materials. The notched beam tests exhibit some mixed mode behavior but are dominated by mode I response. The relationships demonstrated in Table 4-5 may provide insight into the underlying ratio of Mode I and Mode II components contributing to mixed mode failure. More importantly, they may be leveraged to develop simpler test methods which may be used as surrogates for determining other material properties: as concrete tensile strength may be estimated from compressive strength, bamboo splitting behavior may be estimated from simple to conduct tests such as the bowtie test.

Table 4-5: Summary of strength results (UPitt specimens only)

Species	Bowtie	Split-Pin	Clear	Full
	τ, MPa (COV)	$\sigma_\perp$ MPa (COV)	τ, MPa (COV)	τ, MPa (COV)
Moso	14.20 (0.10)	2.40 (0.24)	1.82 (0.31)	0.51 (0.35)
Tre Gai	8.65 (0.075)	1.52 (0.16)	0.79 (0.26)	0.33 (0.031)
Normalized values				
Moso	27.8	4.7	3.6	1.0
Tre Gai	26.2	4.6	2.4	1.0

The geometry of the splitting in the full culms also confirms the mixed mode nature of the failure. Figure 4-16 shows images taken after testing with a handheld high magnification camera of the splitting failure in Dendrocalamus specimens tested at PUC. Images were taken on the same face of the culm on either side of the notch following testing. The images show crack-bridging occurring as the crack propagates towards mid-span and the support; this is an indication of a mixed-mode failure. As noted in Section 1.1.2.2, Shao et al. (2009) did not see crack-bridging in double cantilever tests which is consistent with pure Mode 1 fracture exhibited using this test method.
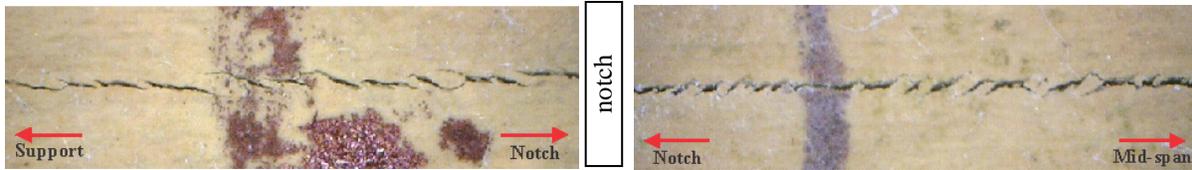
Figure 4-16: Magnified images of crack bridging on either side of notch in *Dendrocalamus* specimen DB3

4.3.1   Applicability as a Field Test

It was hoped that strain gage data would help in capturing splitting behavior, although strain gages provide data only up to the point of splitting. Unfortunately, due to a perceived acquisition error, strain gage data collected at UPitt was potentially corrupted. Nonetheless, as the foregoing demonstrates, sufficient data to identify and quantify longitudinal splitting behavior is available simply from load-deflection behavior. This demonstrates the potential utility of this relatively simple test in a field (rather than laboratory) environment. As shown in Figure 4-13, multiple test arrangements may be used depending on availability of resources and only simple instrumentation is required to measure applied load and deflection. For instance, using the test arrangement designed at PUC (Figure 4-13b), free weights may be used to apply load and sufficiently accurate deflection measurements (precision of 1 mm is adequate for culms of the size tested here) may be made using a tape or ruler.

4.4   CONCLUSIONS

The modified full-culm tests for assessing longitudinal shear behavior illustrate the need for a standardized test method to characterize the longitudinal splitting strength of bamboo tested in flexure. Results showed that full-culm tests produced lower shear strength values than current

135

standardized or proposed tests. This is believed to be partially the result of the complex mixed mode behavior occurring at the notch. Full-culm results were also lower than similar values obtained from small clear through-wall specimens.

The current work also strove to better understand the relationship of Mode I and Mode II failure components in the mixed-mode failure of bamboo beams. Results in Table 4-5 suggest that Mode I tangential tensile strength perpendicular to the fibers is the main driver of longitudinal splitting and showed that a ratio between Mode I, Mode II, and mixed mode capacities may exist. As future work, research should be conducted on developing an interaction relationship between Mode I and Mode II components so that an interaction equation may be developed for longitudinal splitting strength in a form similar to Equation 4-13:

$$\frac{a\sigma_\perp}{\sigma_{\perp max}} + \frac{b\tau}{\tau_{max}} \leq 1 \tag{4-13}$$

In which a and b are empirical or theoretically derived coefficients. This would allow values from smaller standard tests such as the bowtie and split-pin tests to be used in design of full-culm flexural components yet still account for the mixed-mode splitting. Alternatively, with such a relationship established, simple-to-conduct tests (such as the bowtie or the edge bearing tests) may be able to be used as surrogate measures of more-difficult-to-obtain values.

The notched beam test configuration had several drawbacks. First, once significant cracking occurred at the notch location, some specimens deformed (kinked) sufficiently to change the boundary conditions of the test – removing contact at the loading saddle above the notch. This caused all load to be placed on the un-notched side of the beam, thereby changing the configuration of the test. This can be corrected with a three-point bending test with a single load and notch at the midspan. Second, effort was made to meet the 30D length requirement of the ISO 22157 four-point bending test (ISO 2004b); ensuring flexural behavior of the specimen and

thereby isolating shear failure at the notch location. It is also noted that the bending stress component at the notch was the majority contribution to the principal shear stress value calculated at the notch and shows the influence of flexural rotation in the test. A shorter shear span would reduce this influence and increase the influence due to flexural induced shear. One area of future work would be to investigate the performance and repeatability of shorter shear span specimens tested in three-point bending as a standard test for longitudinal mixed-mode splitting strength of bamboo. In such a test, the shear span length may be adjusted to modify the ratio of Mode I and Mode II failure components. Removing the notch altogether in shorter specimens and permitting a shear failure to occur 'naturally' should also be investigated. In this case, geometric parameters associated with the Ay term of VAy/It (Equation 4-2) would need to be determined at the location of failure following the test and will be vary from specimen to specimen. Monitoring such behavior may be cumbersome in this case.

5.0   PERFORMANCE OF BAMBOO COLUMNS

This chapter presents the experimental results of an investigation of the buckling capacity of single-culm and multiple-culm bamboo column elements. Single-culm columns of species *Bambusa Stenostachya* (Tre Gai) were tested to obtain single-culm column capacities as well as control tests to determine the behavior of short-doweled end-conditions. Three multiple-culm columns were then tested in order to investigate the ultimate capacity and buckling behavior of these elements. Specifically of interest was the effect of 'bamboo stitching' on improving column behavior in the bamboo culms. Experimental values were compared with theoretical predictions for buckling capacity. The effective strength behavior of multiple-culm columns was shown to exhibit load redistribution and to mimic the sum of individual culm capacities rather than composite column behavior. Stitching was shown to be beneficial in enforcing column geometry yet detrimental due to the introduction of lateral loading to culms.

5.1   BACKGROUND

The structural behavior of bamboo is not nearly as well understood as more conventional construction materials, which results in the use of bamboo often being relegated to non- and marginally-engineered construction. Moreover, the specific behavior of either common or necessary structural elements or details is only understood anecdotally. This study investigates

full-culm bamboo column behavior. While studies of single culm columns (compression elements) have been conducted (Arce-Villalobos 1993, Ghavami and Moreira 2002, Yu et al. 2003, Yu et al. 2005), multiple-culm columns are largely unstudied. Multiple-culm columns have a number of advantages including: a) accommodating relatively simple concentric connections of framing members to be made; b) allowing increased axial capacities and improved lateral force resistance; and, c) allowing, due to increased capacity, smaller individual culm sizes to be used.

This study presents a series of experiments of full-scale axially-loaded single and multiple-culm bamboo columns. Ultimate behavior and buckling capacities are assessed and contrasted with fundamental mechanical theory in an effort to establish rational design guidance for such columns. A specific parameter of interest is the improved behavior that may be developed in multiple-culm columns by the provision of 'stitches' and/or connections to transverse members. It is hypothesized that well-designed multiple-culm columns may provide sufficient capacity to permit multi-story bamboo frame structures to be engineered.

5.1.1   Bamboo Column Buckling

The elastic buckling capacity (P_{cr}) of a uniform, initially straight concentrically loaded column is described by the Euler buckling equation (Eqn. 5-1):

$$P_{cr} = \frac{\pi^2 EI}{(KL)^2} \tag{5-1}$$

Where E is Young's modulus, I is the moment of inertia of the cross section and KL is effective length, where K modifies actual column length, L, to account for end restraint conditions.

Applying Equation 5-1 to bamboo requires a number of modifications to account for a) the variation in section (I) over the height (L); b) initial out-of-straightness; and c) material

variability (E). Nonetheless, these factors can be accounted for using fundamental mechanical principals. From a design perspective, however, these modifications are conventionally addressed partially through permitted tolerances and partially though the use of modification and material resistance factors.

In his 1993 doctoral thesis, Arce-Villalobos used energy methods to study the critical buckling load of single-culm bamboo columns. A critical buckling load equation was developed for a straight bar of tapered cross section and variable Young's modulus. A second equation for a "Southwell plot of deformations" (Southwell 1932) was proposed to remove the influence of crookedness from the equation for critical buckling load during an experiment of a crooked strut. An experimental program was conducted on a sample of *Guadua s.p.* culms to develop experimental Southwell plots which were compared with theoretical predictions. Statistically compared, experimental and theoretical results had a correlation of R^2=0.81. Arce-Villalobos also proposed an equation using average properties of I and E, but states that, while most critical load values for a tested sample were conservative estimates, critical load was over-estimated for some culms. Arce-Villalobos lists buckling of bamboo columns as an area for future research and outlines recommendations. First, initial lateral culm deformation must be considered as a major source of lateral deformation in axially loaded members. Second, buckling load is affected by the change in cross-section dimensions and elastic modulus along the height of the culm. The variation in the cross section itself also effects the calculation of an effective value for the sectional stiffness (EI). Finally, due to randomly-positioned nodal regions being more flexible (in the axial direction), the critical buckling load will be reduced. Thus, the average influence of nodes should be studied (Arce-Villalobos 1993).

Ghavami and Moreira (2002) investigated the column buckling behavior of single bamboo culms for use in a space structure. Eleven specimens of *Dendrocalamus giganteus* with a diameter of 100 mm and a length of 2 m were first measured to determine initial curvature and deviation of the centroid from the longitudinal axis along the culm using a special measuring device developed for the purpose. The moment of inertia, I_f, was also calculated considering that a higher fiber density exists in the outer 25% of the culm wall (Fig. 2-2) rather than considering the gross section (I_g) for a homogeneous cross section. Specimens were tested in compression as pin-ended columns (i.e.: K = 1). The buckling load for the specimens was determined using a Southwell plot and the modulus of elasticity, E, was determined experimentally for the specimens. Results showed that a) experimentally determined values of apparent moment of inertia (I_{exp}) were close to those predicted considering I_f; and b) failure and ultimate load were governed by compression failure of bamboo fibers in the concave section of the element (resulting from global buckling deformation) followed by local buckling of the culm wall. The authors concluded that the stress corresponding to this failure phenomenon is the limit of proportionality in uniform compression (Ghavami and Moreira 2002).

Column buckling is one of the critical limit states for failure in bamboo scaffolding. Yu et al. (2003) investigated the buckling behavior of two bamboo species, *Bambusa pervariabilis* (Kao Jue) and *Phyllostachys pubescens* (Mao Jue) with 72 column buckling tests. A limit state design method against column buckling of structural bamboo based on empirically modified slenderness was developed based on calibration against buckling tests conducted over a wide range of practical member lengths. Tests considered height-to-diameter ratio, diameter variations over member length, and moisture content of the bamboo. Bamboo specimen lengths were 400, 600, and 800 mm for Kao Jue and 1000, 1500, and 2000 mm for Mao Jue. Moisture content was

considered to be the most important property in determining mechanical properties and was taken as either natural (N) or wet (W); the latter was achieved by immersing the bamboo in water for 1 week prior to testing. Pin-ended (i.e.: K=1) compression tests were conducted on small specimens of bamboo cut from the buckling specimens after the buckling test to better determine material properties. Applied load, axial shortening, and horizontal displacements were measured continuously throughout the large-scale buckling tests. Both global buckling (most Mao Jue members) and local buckling (wet and short Kao Jue specimens) were observed during the tests. Reduction of load-carrying capacity due to buckling was shown to be severe. A buckling design method was developed based on the method for structural steel promulgated in the British steel code BS5950 (British Standards Institution 2000). This approach adopts the Perry-Robertson (Robertson 1925) interaction formula for compressive buckling strength with initial imperfections. To account for the variation of Young's modulus along the member length, the average Young's modulus was used for the entire member length. Variations of external diameter and thickness are also apparent and the variation in moment of inertia was considered in the analysis with a non-prismatic parameter α (evaluated through the classical energy method). To calibrate the proposed design method, an analysis was conducted against the test data with all partial safety factors equal to 1. The analysis determined Robertson constants, modified slenderness ratios and average model factors for each species. The non-prismatic parameter was found not to be insignificant for Kao Jue but significant for Mao Jue; thus, with respect to the cross section properties, a Kao Jue culm can be viewed as being non-tapered while Mao Jue is tapered. The authors also proposed limits for culm out-of-straightness in order for their design method to be applicable (Yu et al. 2003).

In a subsequent study, Yu et al. (Yu et al. 2005) constructed 4 full-scale double-layer bamboo scaffolds and tested them to failure to assess bamboo culm buckling within such a structural system. The scaffolds were composed of both Kao Jue and Mao Jue bamboo species. All 'lashed' or 'tied' joints were fashioned using bamboo or plastic strips and were therefore considered as pins in analysis and design. Secondary and bracing members provided effective load distribution in the event of axial buckling of a post. The test scaffolds were 9 m high, 6 m wide and 0.6 m deep and had four working platforms (including the top). Each consisted of varying arrangements of bamboo species and lateral restraint configurations. Test scaffolds were loaded on the topmost working platform with sand bags near the central post. Results of the test exhibited the inner central post (Kao Jue) buckling either between main horizontal ledgers or globally across the four working platforms. However, no global collapse of the structure was observed. Using this experimental data, the authors developed a finite element model to examine and predict the buckling behavior of the scaffold systems (Yu et al 2005).

5.1.2   Standard Design Procedures

Currently, the International Organization for Standardization (ISO) document ISO 22156: *Bamboo Structural Design* (ISO 2004a) provides guidance for determining the culm moment of inertia and ultimately determining the buckling load for bamboo columns. As a conservative estimate, diameter and wall thickness should be measured at both ends of the culm and the mean values used in the calculation of I_{culm}. ISO 22156 specifies the use of the Euler buckling equation (Eqn. 5-1) but with a 10% reduction in I_{culm} to account for tapers in diameter of less than 1 on 170. Additionally, column designs must consider bending stresses due to initial curvature, eccentricities and induced deflections (ISO 2004a). The National Building Code of India (Bureau

143

of Indian Standards 2005) provides similar requirements for determining the moment of inertia of bamboo columns. It is understood that the Indian standard is an adoption of the ISO model standard.

5.2   EXPERIMENTAL PROGRAM

The experimental program to investigate the buckling behavior of multiple-culm bamboo columns encompassed five main stages: a) cataloguing the culm geometry; b) experimental determination of compression strength; c) determination of effective length factor, K based on the column end conditions used; d) experimental buckling tests of single-culm specimens; and e) experimental buckling tests of multiple-culm columns. These stages are described in the following sections.

5.2.1   Specimens

Bambusa Stenostachya (Tre Gai) harvested in Vietnam was used for the experimental tests. The bamboo was purchased commercially in 3 m lengths; the author has no control over culm selection and the harvesting and storage history of the culms is unknown. Specimens were first cut to length and the section quadrants assigned a cardinal designation (North, South, East and West). The initial variability in geometry was then catalogued prior to testing. Measurements were taken along each culm's length for diameter, variation from a plumb axis (to determine initial out-of-straightness), wall thickness (wall thickness measurements were taken following

testing when the culms were cut into sections), and internode length. Measurements were taken by placing the bamboo in a specially designed jig as shown in Figure 5-1.

a) support condition of measuring jig.

b) culms that are (top) relatively straight and (bottom) significantly curved in jig.

Figure 5-1: Jig for measuring bamboo columns

The culm is placed between two parallel string lines set a constant distance apart, measurements were taken between each string and the culm. From this, both the culm diameter and deviation from centerline or "out-of-straightness," can be determined. Measurements were taken at the center of each internode and in both principle axes (N-S and E-W; i.e.: each culm was rotated 90 degrees in the jig for a second set of measurements). Table 5-1 summarizes the values for the culms used in this study. The gross cross sectional area (A_{culm}) and moment of inertia (I_{culm}) values are based on the average diameter (D) and wall thickness (t) values measured at each internode and are based on the gross cross section dimensions. For the batch of Tre Gai used, the culm diameter did not vary significantly over the culm height, although the wall thickness did decrease from bottom to top. The typical ratio of bottom to top diameter (D_{bot}/D_{top}) was 1.01 whereas the ratio of bottom to top wall thickness (t_{bot}/t_{top}) was 1.7; therefore, these culms must be treated as being tapered (Yu et al. 2003). Average initial out-of-straightness of this batch of Tre Gai bamboo was relatively small: 0.006L, with no value exceeding 0.010L. As indicated in Table 5-1, culms having a larger section were selected for single-culm column tests (tests S1-S4); while marginally smaller culms were selected for the four-culm column tests (tests M1-M3).

145

Table 5-1: Column Specimen Geometry Data

Column Test	Culm ID	Length, L (mm)	Avg. Diameter, D (mm)	Avg. Wall Thickness, t (mm)	Max. Deviation from Straight (mm)	Max. Deviation from Straight Ratio of L	A_{culm} (mm^2)	I_{culm} (mm^4)
S1	TG-5	2600	89	15	23	0.009L	3,400	2,440,000
S2	TG-8	2600	87	15	13	0.005L	3,400	2,283,000
S3	TG-9	2590	88	17	11	0.004L	3,800	2,521,000
S4	TG-4	2600	86	16	17	0.006L	3,600	2,263,000
SH1	TG-3-6'	1830	88	16	17	0.009L	3,600	2,390,000
SH2	TG-21-4'	1218	83	25	7	0.006L	4,600	2,314,000
SH3	TG-3-2'	609	82	24	4	0.006L	4,300	2,122,000
M1	TG-13	2590	77	16	7	0.003L	3,000	1,526,000
M1	TG-15	2590	77	15	22	0.009L	2,900	1,448,000
M1	TG-23	2590	73	12	11	0.004L	2,300	1,102,000
M1	TG-25	2590	72	18	14	0.005L	3,100	1,255,000
M2	TG-10	2590	78	16	12	0.005L	3,100	1,599,000
M2	TG-12	2590	80	13	14	0.005L	2,700	1,594,000
M2	TG-14	2590	83	15	13	0.005L	3,100	1,927,000
M2	TG-24	2590	78	14	12	0.004L	2,800	1,491,000
M3	TG-6	2590	85	15	19	0.007L	3,300	2,100,000
M3	TG-7	2590	83	13	26	0.010L	2,900	1,786,000
M3	TG-18	2600	85	16	25	0.010L	3,500	2,210,000
M3	TG-19	2590	82	20	11	0.004L	3,900	2,084,000

5.2.2   Compression Tests

Compression test specimens were fabricated from the off-cuts of the culms and conducted in accordance with ISO standard 22157-1:2004 (ISO 2004b) from which the experimental compressive strength, σ_c and the modulus of elasticity, E were determined. Fourteen inter-nodal specimens having a length-to-diameter ratio (L/D) of 1.25 were prepared from seven randomly selected culms. Sulfur capping compound was used to prepare the cylinder ends, resulting in an aspect L/D ratio for the test specimen clear height greater than 1 in every

case. Two electrical resistance strain gages were applied at the N and S locations on the section. A compressive strength of 54.7 MPa having a coefficient of variation (COV) of 30.4% and a Young's modulus of 13,450 MPa having a COV equal to 31.8% were found for the bamboo tested. These values compare well with experimental values reported for Tre Gai specimens by Mitch (2009) and were used in the calculation of predicted and experimental buckling behavior.

5.2.3 Column End Connections

Due to the desire to test both single and multiple-culm columns with the same end conditions, the nature of the test machine and fixtures used, and laboratory safety considerations, all culms were provided with a short-doweled end condition (Fig. 5-2). The end conditions consisted of a 12.7 mm diameter threaded rod embedded 60 mm into each culm and grouted with a high-strength, quick setting plaster. The culm walls were carefully cut to ensure uniform bearing on the steel end plate. The threaded rods form a dowel connection (or shear key), preventing unwanted lateral movement of the culm ends while also providing a convenient connection to the test frame.
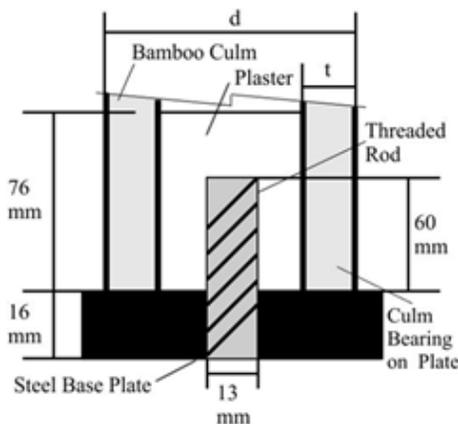
a) schematic view of connection

b) view of four-culm connection showing culms bearing on steel end plate

Figure 5-2: Short-doweled end condition

147

5.2.4   Determination of Effective Length of Columns

To establish an appropriate effective length factor (K) for the column end conditions used, two 2590 mm long specimens of 88.9 mm diameter schedule 80 poly vinyl chloride (PVC) pipe were tested as column elements. These specimens a) were provided with identical end conditions as described in the previous section; b) were initially straight; and c) have effectively no variation in known dimensions or material properties along their length or through their section. Thus, by applying Equation 5-1 to experimental results, the effective length factor (the only unknown) may be calculated. Results from duplicate control tests are shown in Table 5-2. The average effective length factor found for the end conditions used was K = 0.55. Evaluation of photographs (Figure 5-3) of buckled shapes confirms this value.

Table 5-2: Results for control columns used to establish value of effective length factor, K

Specimen	Length, L	outside diameter, D	wall thickness, t	I	E	P_{CR}	K_{eff}
	(mm)	(mm)	(mm)	(mm^4)	(MPa)	(kN)	
PVC1	2591	88.9	7.62	162 x 10^4	2812	25.0	0.52
PVC2	2591	88.9	7.62	162 x 10^4	2812	20.8	0.57

As will be discussed, the apparent value of K for the bamboo specimens may be greater than for the PVC since, due to initial out-of-straightness-induced flexure, the end of the bamboo specimens was observed to rotate against the steel end plate prior to the onset of buckling. The PVC did not exhibit this behavior.
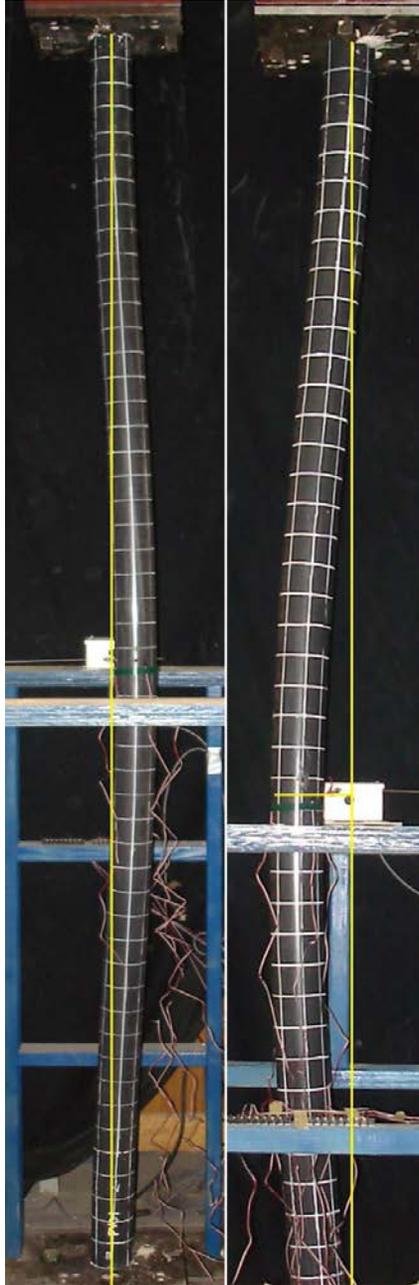
Figure 5-3: Buckled shaped of PVC columns 1 and 2

149

5.2.5 Column Buckling Test Program

All buckling tests (including the PVC tests described previously) were conducted in a servo-hydraulic controlled universal test machine (UTM) having a capacity of 900 kN. All tests were run in displacement control (to ensure controlled failures) at a rate of 2.54 mm per minute. Applied load and crosshead displacement were obtained from the UTM controller; lateral displacement in both NS and EW directions of individual culms at mid height were obtained using draw wire displacement transducers (DWT) as shown in Figure 5-4d; and bamboo flexural strains at mid-height were obtained using electrical resistance strain gages (also seen in Figure 5-4d). All data was collected electronically at a rate exceeding 1 Hz. It is acknowledged that use of crosshead travel for column axial displacement is not entirely correct since this value includes the compliance of the test machine. However this data is only used directly to identify the onset of bifurcation and buckling; the small error introduced does not affect such results. The test frame compliance is known to be 0.015 mm/kN when testing specimens of the height tested here.

Seven single culm and three four-culm column tests were conducted as shown in Table 5-1. Conducting the single-culm tests was intended to establish a baseline for the culm behavior. The four-culm columns were assembled such that the culm spacing in both principle directions was equal and adequate to allow transverse members of a size similar to the longitudinal culms to pass (see Figure 5-4c). All culm end conditions were identical as described above and shown in Figure 5-2. Test M1 was a simple arrangement of four culms. Only the doweled end conditions enforced the multiple culm geometry (spacing) over the height of the specimen. Thus, M1 may be thought of as testing four single culm columns in parallel. All things being equal, the capacity of M1 should be four times the lowest individual culm capacity. It is hypothesized that

as the weakest culm in the four-column arrangement fails, the load is redistributed to the remaining culms and these will then buckle in rapid succession.

Specimen M2 and M3 are provided with bolted 'stitches' (Fig. 5-4c) which effectively enforce the initial column geometry at their locations. M2 had a stitch located at mid-height (i.e.: L/2) and M3 had stitches at its third points (L/3). These stitches, it is proposed, will help to inhibit single culm buckling and thereby improve the overall column load carrying capacity. Each stitch consists of two short lengths of bamboo having an outside diameter of about 75 mm (same material as columns in this case) connected through the entire assembly with four 12.7 mm threaded rods (or carriage bolts). The holes for these rods are drilled *in situ* using a 300 mm long drill bit, thus ensuring alignment.

c) detail of bolted column stitch of specimen M3

a) single culm specimen prior to test S1

b) four culm specimen prior to test M2

d) DWT instrumentation at mid-height of single culm (top) and four-culm (bottom) test.
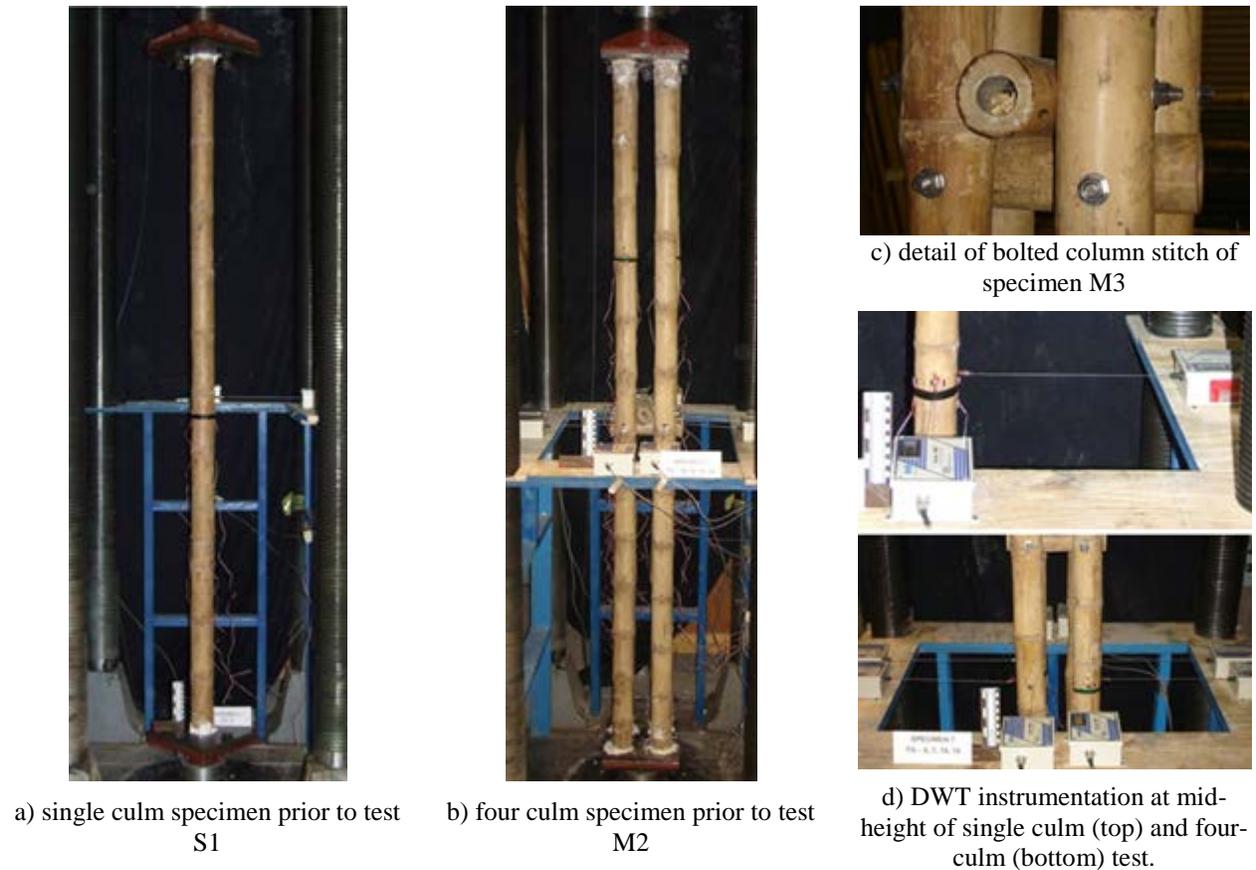
Figure 5-4: Test set-up and instrumentation

5.3   EXPERIMENTAL RESULTS

A summary of axial load capacities of the seven specimens tested is provided in Table 5-3. In this test program, behavior was dominated by single culm buckling behavior. As noted in Table 5-1, the culms used to form the four-culm specimens were marginally smaller than those used for the single culm tests. The average slenderness (L/r) of culms used for the single-culm tests was 100, whereas that for the four-culm tests was 111. The slenderness of the short bamboo columns ranged from 27 to 71. Thus, in addition to normalizing results by column area (A_{culm}) to determine the axial stress carried by the bamboo, an additional normalization by slenderness is also required to allow direct comparisons of behavior.

Table 5-3: Specimen axial load capacity

Specimen	Column Area ΣA_{culm}	Slenderness $(L/r)_{average}$	Critical Load P_{cr}	Critical Stress $\sigma_{cr}=P_{cr}/\Sigma A_{culm}$	Normalized Critical Stress $\sigma^*=\sigma_{cr}(L/r)_{average}$
	(mm^2)		(kN)	(MPa)	(MPa)
S1	3400	97	52	15.2	1484
S2	3400	100	50	14.7	1473
S3	3800	101	96	25.0	2521
S4	3600	103	63	17.6	1809
SH1	3600	71	65	18.2	1286
SH2	4600	54	131	28.6	1548
SH3	4300	27	95	22.1	607
M1	11200	119	140	12.5	1482
M2	11700	109	159	13.6	1482
M3	13600	106	138	10.1	1071

5.3.1 Full Height Columns

Figure 5-5 shows the normalized axial stress (σ^*) versus axial displacement curves for all full-height specimens. Normalized axial stress accounts for both the variation in column area (ΣA_{culm}) and slenderness of the individual culms (L/r), where r is the radius of gyration of the culm section:

$$\sigma^* = \frac{P}{\sum A_{culm}} \left(\frac{L}{r}\right)_{average} \tag{5-2}$$

a) single culm columns

b) multiple culm columns
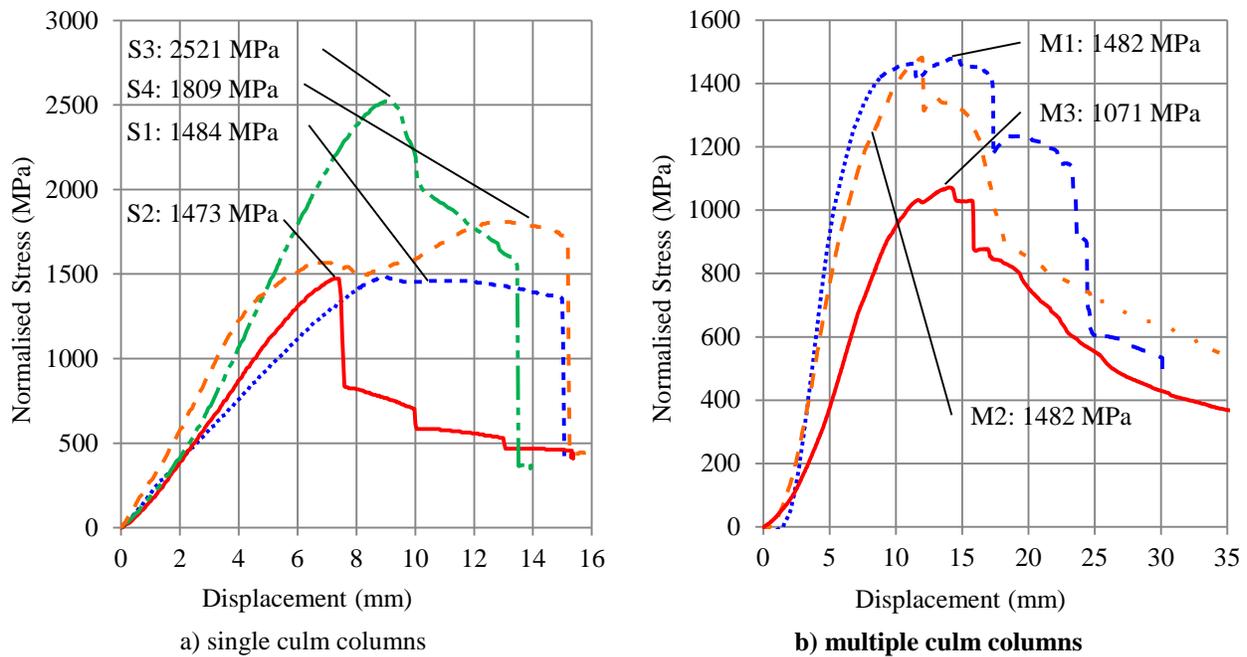
Figure 5-5: Normalized stress v. displacement plots.

Because the tests are conducted in displacement control, critical buckling is identified as occurring at the load plateau in Figure 5-5 although lateral displacements of the culms is evident at lower loads. Eventual culm splitting (described below) corresponds to the subsequent, almost instantaneous, loss of capacity evident in the curves shown in Figure 5-5.

Specimens M1 and M3 exhibit initial small drops in capacity which are recovered prior to the critical (peak) load being achieved. Specimen M2 exhibits similar behavior, although the initial peak is never regained. This behavior is attributed to load redistribution in the multiple-

culm specimens, where the initial peak represents the behavior of the 'weakest' culm; this is discussed further below.

Single culm capacities were relatively consistent with the exception of specimen S3. This culm, in addition to being the largest section tested, was also among the straightest (Table 5-1); both factors are believed to contribute to this specimen's superior performance. The four-culm specimen behavior was similarly consistent.

Figure 5-6 illustrates the failure modes of one single-culm specimen (Fig. 5-6a) and all three of the multiple-culm specimens (Figs. 5-6b to 5-6d). The photos all show specimens under load at a large displacement. All single culm specimens were observed to buckle over their entire length. As the axial displacement increased, the culms exhibited a longitudinal splitting failure generally at the top end of the culm where the culm wall thickness is at its minimum (Fig. 5-6e). The splitting, in this case, is a longitudinal shear failure of the culm resulting from the flexure induced by buckling; a so-called VAy/It failure. Since natural vertical orientation of culms was maintained, this always occurred at the top of columns where culm wall thickness, t, is smallest.

The initial flexure-induced rotation at the culm ends results in local crushing of the bamboo and, as it progresses, loss of bearing contact on the 'tension' side of the culm. This has the effect of increasing the effective length factor, K, of the culm. Similar behavior was observed in column base connection tests (Mitch 2010). Once splitting occurs, culm capacity is lost.

Individual culm behavior in the four-culm specimens also reflected this general behavior. This is dramatically illustrated in Figure 5-6b of specimen M1. In this photo all four culms have buckled independently and a significant longitudinal splitting failure of one is clearly seen.

The presence of stitches enforces the four-culm geometry at the stitch location(s). Thus each individual culm is 'forced' to buckle in the same direction (Figs. 5-6c and d). This effect is

seen in Figure 5-7 which shows, in plan, the lateral displacement traces at mid-height of each culm in the four-culm columns. The unstitched culms of specimen M1 are able to displace laterally (buckle) as their individual geometries dictate. The stitched culms of M2 and M3, on the other hand, must 'track' each other. The stitches, as it were, restrain the initial buckling of the 'weakest' culm while 'drawing' the remaining culms in the direction of the weakest buckling culm. This, in essence, results in a collection of self-equilibrating lateral point loads being applied to all culms at the stitch locations. These loads (and their resulting moments) may be initially restrained or drive buckling. As a result of the stitch-induced lateral loads, some of the culms formed a 'kink' at the location of the stitch. Figure 5-6f, for instance, shows a clear kink in the left-hand culm while the right-hand culm shows more uniform curvature. In the case shown in Figure 5-6f, the kink resulted from the local buckling of the culm wall at the location of the threaded rod. Although the rods were only installed 'thumb tight', the column's lateral deformation, in this case, resulted in the rod being 'pulled through the culm wall'. Finally, minor longitudinal splitting, associated with the stitch bolts was also observed (Fig. 5-6g).

Considering the foregoing discussion and the results shown in Table 5-3, it is evident that beneficial effects of the stitch (restraining section behavior) are counteracted by the additional lateral loads they introduce. Thus the need for stitches is inconclusive, particularly for relatively slender columns dominated by individual culm behavior. Nonetheless, transverse or in-plane bolted connections to such multiple-culm columns are de facto stitches. Thus the stitch behavior must be considered where such connections exist.

155

a) S4   b) M1   c) M2   d) M3   e) splitting at top (M2)

f) kinking at braces (M3)

g) splitting at bolts (M3)

Figure 5-6: observed behavior of bamboo column specimens

a) M1 (no stitching)   b) M2 (stitch at mid-height)   c) M3 (stitching at 1/3rd points)

Figure 5-7: Lateral displacement of culms in multiple-culm columns (figures drawn to scale on a grid 50 mm)

In Table 5-4, experimental column capacity is compared to that predicted using the Euler buckling equation (Eqn. 5-1). For the multiple-culm columns, the effective buckling load determination is based on the sum of the culm moments of inertia (i.e.: ΣI_{culm}), rather than the gross column moment of inertia (I_g). This is consistent with the observed column behavior and would appear to be consistent with findings from previous research and available standards, as described above. As shown in Table 5-4, the calculations were made using both the theoretical pin-ended capacity ($K = 1$) toward which the culm behavior deteriorates, and the initial, experimentally determined value of $K = 0.55$. It is clear from Table 5-4, that the observed column behavior falls between these limits, although generally closer to the pin-ended limit of K = 1. As a measure of column behavior, the apparent value for effective length factor is shown in Table 5-4; this value is the K required to calculate the experimentally observed critical load using Eqn. 1. The difference between this value and $K = 0.55$ may be attributed to the following: a) variability of the test specimen section and material properties; b) initial out-of-straightness; and c) degradation of the column end condition described above. To separate and quantify these effects, additional analyses and research is required. Nonetheless, the universal use of $K = 1$ is shown to yield conservative predictions.

Table 5-4: Predicted Column Behavior

Specimen	ΣI_{culm}	P_{cr} (Eqn. 1)			Apparent K
		Experimental	Predicted		
			K=1	K=0.55	
	(mm^4)	(kN)	(kN)	(kN)	
S1	2,440,000	52	48	159	0.96
S2	2,283,000	50	45	149	0.95
S3	2,521,000	96	50	165	0.72
S4	2,263,000	63	45	147	0.84
M1	5,331,000	140	105	348	0.87
M2	6,611,000	159	131	432	0.91
M3	8,181,000	138	162	534	1.08

5.3.2 Short Column Tests

The purpose of the three "short" column tests was to investigate how the ultimate load of the column was affected by changes in column slenderness. As noted in Table 5-1, the short columns were single culm columns having lengths of 1830 mm, 1218 mm, and 609 mm. These were tested using the same procedure as the full height columns (Section 5.2.5). Results presented in Table 5-3 show that the shorter columns generally experience a higher critical stress (as expected) as compared to the full height single-culm and multiple-culm columns. Specimen SH1, having a length of 1830 mm, had a critical stress similar to full-height specimen S4 (18.2 and 17.6 MPa respectively). The two columns also had similar column areas. Meanwhile, specimen SH3, having a length of only 609 mm, performed poorer than expected. A possible explanation for this is differences in performance at the end conditions which would influence apparent strength.

Figure 5-8 illustrates the initial and final shapes for the three short column tests. Similar to the full-height specimens, the failure in all three tests occurred near the top connection and involved longitudinal splitting. Kinking is also seen in the 1830 mm specimen SH1 (Fig.5-8b) and the 1218 mm specimen SH2 (Fig. 5-8d). Finally, the 609 mm specimen SH2 illustrated a splitting failure combined with a crushing/squashing failure (Fig. 5-8f) in which the top of the culm split into four pieces which then buckled/crushed individually. This may have been due to the plaster plug (Figure 5-2a) driving through the node near the top connection and then acting as a wedge, splitting the culm into four segments. Figure 5-8 also illustrates that global buckling behavior is limited in the shorter columns; each exhibited a kinked shape rather than a relatively uniform buckling displacement.

a) SH1 pre-test (1830 mm)

b) SH1 buckled

c) SH2 pre-test (1218 mm)

d) SH2 buckled

e) SH3 pre-test (609 mm)

f) SH3 buckled

Figure 5-8: Original and buckled shapes for single-culm bamboo short columns

The results of the short column tests indicate some additional limitations of such tests and emphasize the sensitivity of bamboo material and member tests to support or boundary conditions. Such sensitivity, one assumes, is carried into real structures and must be addressed in design standards – most likely through reduced material reduction factors.

5.3.3   Summary of Column Tests

The critical stress, σ_{cr} versus the column slenderness, L/r results of all the column tests are summarized in Figure 5-9. The plot also includes the results from the compression tests (L=1D) specimens used to calculate the average crushing strength (Section 5.2.2). This average crushing strength is plotted until it intersects with the Euler curve, which is plotted for values of effective length of K=1 and K=0.55 (based on PVC column tests reported in Section 5.2.4). As described above, the plot illustrates that the full-height single culms and multiple-culm columns (excluding specimen M3) are well-predicted using K = 1.
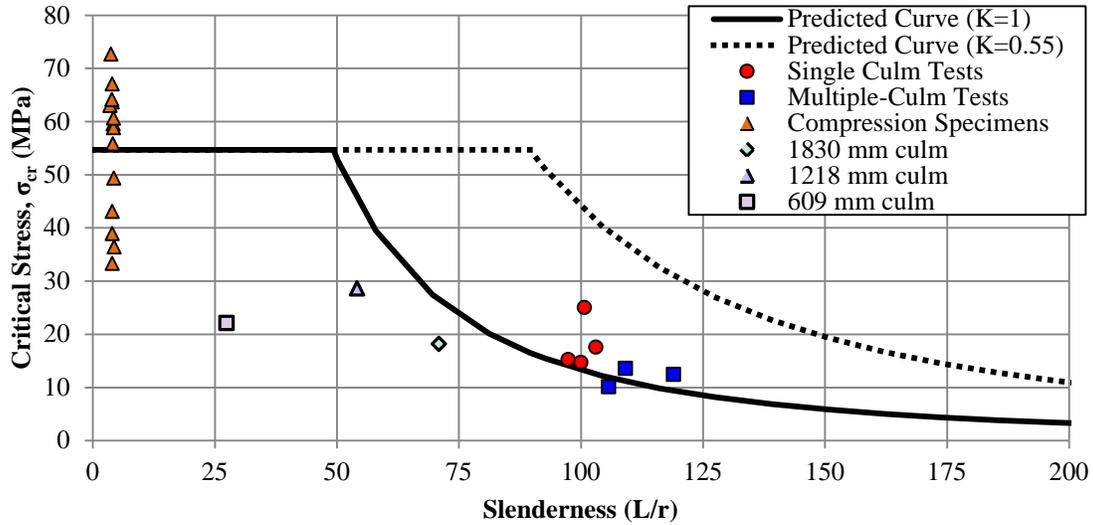
Figure 5-9: Plot of critical stress versus slenderness (L/r)

For K=1, critical buckling stress as calculated by the Euler equation is equal to the crushing strength at a slenderness of L/r = 49, which agrees well with the critical slenderness value of 50 determined by Arce-Villalobos (1993). Arce-Villalobos concluded that this value can be used directly to determine when full capacity of a bamboo compression element can be obtained. However, the short column specimens illustrate a significant reduction from predicted values L/r < 75. This behavior is typical of 'intermediate height columns' that experience interaction between local and global buckling and also is seen in columns having large imperfections or eccentric loads. Additional short column specimens are needed in order for a predictive curve to be estimated for L/r < 75 that captures this apparent reduction in strength.

5.4   CONCLUSIONS

Bamboo has great potential as an alternative and sustainable building material yet more understanding is needed of its structural behavior in order for the use of bamboo to extend

beyond marginally-engineered structures. Understanding the behavior of multiple-culm columns offers a pathway to building larger and perhaps multi-story structures. The intent of this chapter was to present the experimental results for the buckling behavior of single-culm and multiple-culm specimens and characterize these with respect to the Euler equation which is typically used in design. The results of the single culm specimens confirmed the need for initial out-of-straightness and taper to be considered for Tre Gai culm specimens. Multiple-culm column specimens exhibited load redistribution as weaker culms began to fail and observed column behavior was best represented by the sum of the individual culms, ΣI_{culm}, rather than by the gross section properties, I_g, of the multiple-culm column. Bamboo stitching was shown to enforce the geometry of the multiple-culm column yet their benefit of restraining weaker culm buckling was counteracted by their introduction of lateral loads to the individual culms. While these results proved inconclusive, the effect of this stitch behavior must be considered where transverse or in-plane bolted connections to these columns exist in the field. The apparent effective length factor, K for the full-height specimens was shown to be closer to 1 than to the value predicted in the control tests. This was potentially due to flexure-induced rotation causing local crushing at culm ends as well as variability in the cross section and initial culm out-of-straightness. The flexure-induced rotation also caused longitudinal splitting failures at the top end condition. These effects need to be considered in the field for cases were culms are subject to end bearing loads. Finally, short column tests exhibited similar longitudinal shear failures but showed a kinking behavior as opposed to global buckling. Short columns also highlighted a significant reduction in load capacity for slenderness ratios L/r < 75. More tests are necessary to refine and develop predictive performance curves for future design.

162

6.0   SUSTAINABILITY OF BAMBOO STRUCTURAL COMPONENTS

Bamboo has been recognized for many years as a potentially sustainable alternative to conventional building materials. This assertion has been made based on such qualitative advantages as bamboos' rapid growth rate, rapid renewability, material strength, and multitude of species across the globe. However, few studies have attempted to quantify the sustainability of bamboo alternatives in construction; particularly full-culm bamboo. This study seeks to quantify the environmental impacts of a representative structural bamboo component; specifically the four-culm bamboo column studied in Chapter 5. Those impacts are then compared with the impacts of similar representative timber and steel columns. First, using a life cycle assessment methodology, a representative comparative life cycle assessment (LCA) is conducted for the use of bamboo columns and comparable solid timber or built-up box timber columns. The LCA conducted follows a cradle-to-consumer approach that will study material extraction, processing, delivery and erection of the product. The LCA will be considered with respect to column use in the United States, which has a large supply of timber resources, as well as use in Brazil, which has both timber and bamboo resources available. The representative comparative LCA example is then expanded by adding representative steel columns for comparison, specifically standard hollow box and round shapes (HSS). Ultimately, with a functional unit defined as a comparable structural capacity, the intent of the work is also to investigate the potential of better integrating environmental impacts into the structural design process.

6.1   BACKGROUND ON LIFE CYCLE ASSESSMENT OF BAMBOO

Bamboo has been widely recognized qualitatively as a sustainable material with advantages including carbon sequestration and erosion control. Yet few studies have tried to quantify the sustainable benefits of bamboo. The following section reviews some of the previous studies regarding environmental impacts of bamboo use and the research basis for the current study. As mentioned previously, the current midpoint LCA of full-culm bamboo seeks to determine quantitatively whether a representative bamboo column is a relatively more sustainable alternative to structurally comparable timber or steel columns of comparable capacity. The current study is also based on the structural behavior of bamboo columns as described in Chapter 5 of this work, previous work on comparable timber components, and representative steel alternatives designed based on AISC (2011) capacity calculations.

6.1.1   Life Cycle Assessment Methodology

Life cycle assessment (LCA) is defined as "a technique for assessing the environmental aspects and potential impacts associated with a product" or process (ISO 14040 2006). The first LCA study is considered to be a 1970 study done for the Coca-Cola Company investigating the environmental impacts of soda container alternatives and most early LCA studies involved packaging materials (Baumann 2004). The LCA process involves assembling an inventory of all the inputs and outputs associated with a product or process, assigning environmental impacts to these inputs and outputs, and then analyzing/interpreting the resulting impacts. The LCA methodology outlines four major steps: definition of the goal and scope; life cycle inventory (LCI) analysis of all inputs and outputs, life cycle impact assessment (LCIA) which converts

inventory data into a set of environmental impact categories, and interpretation of the results. Standard guidelines for conducting an LCA are outlined in the International Organization of Standards (ISO) document *ISO 14040: Environmental management – Life cycle assessment-Principles and framework* (ISO 14040 2006). The goal and scope definition is critical to the process as it not only outlines the intended outcome of the LCA study but sets the boundaries of what inputs and outputs are considered in the study of a specific process. Common boundaries include cradle to grave (considering impacts from material extraction to disposal), cradle to consumer or cradle to site (considering impacts from material extraction until the hand-off to the consumer), and cradle to cradle (considers impacts from material extraction to reuse of the product). As discussed in Section 6.2, the system boundary of this study involves a cradle to consumer or site approach.

6.1.2   Previous LCAs on Bamboo and Wood

As discussed in Chapter 1, the rapid growth rate of bamboo and its accessibility throughout the world make full-culm bamboo an appealing construction material alternative for building when compared with conventional materials, specifically timber. De Flander and Rovers (2009) sought to quantify the global potential of bamboo as a modern construction material by comparing the volume of timber and laminated bamboo lumber needed to construct a representative house with a floor area of 175 square meters. They found that one hectare of *Guadua angustifolia* (Guadua) bamboo in Colombia can produce enough volume per year to construct the model house. A similar hectare of timber only produces enough volume of lumber to construct the model house every four years. Lobovikov et al. (2012) suggest that increasing stands of bamboo culms could be used as biomass carbon sinks in regions, although the concept requires further study.

Ultimately, quantified environmental impacts of bamboo are needed to assess environmental sustainability.

van der Lugt et al. (2006) used a cradle-to-grave LCA to compare the environmental impacts of beam and column components in a bamboo pedestrian bridge in the Netherlands with timber, steel, and concrete elements required for a similar load bearing capacity. Guadua bamboo was sourced from plantations in Costa Rica and even with sea transport was shown to be the most sustainable alternative. However, conducting a life cycle costing (LCC) analysis, it was found that steel was more cost effective than bamboo due to the shorter life span and higher labor costs of the bamboo option.

van der Lugt et al. (2009) again investigated the environmental impacts and sustainability of using various bamboo materials (both natural culms and engineered bamboo products) as compared to timber products in Western Europe. The data used in this study for determining the eco-costs/kg was obtained from the IDEMAT-2008 (www.idemat.nl) and Ecoinvent-v2 (www.ecoinvent.org/database/) databases. The study investigated both the environmental impact or 'eco-burden' of bamboo products using the Eco-cost model and the regenerative nature of bamboo with its annual yield. The LCA study considered mostly products made of Moso bamboo but also looked at species *Guadua spp.* and *Dendrocalamus asper*. This report looked at bamboo materials that are already available (or have the potential to be available) in the Western European market: bamboo culms, Plybamboo (comparable to plywood), Strand Woven Bamboo (SWB), Bamboo Mat Board (BMB; comparable to oriented strand board), and bamboo composites (fibers). The LCA reported was based on a 'cradle-to-site' approach as it was assumed that the use and end-of-life phases were similar for bamboo and timber products. The products were assumed for use in the Netherlands and to have originated from sustainably

166

managed plantations in China. The functional unit (FU) varied for each product. For the LCA of an unprocessed bamboo culm, the FU was taken to be a table leg 0.8 m long with a diameter of 9 cm. The eco-costs/kg were first calculated for the production and transportation of a 5.33 m long Moso culm and results showed that 94.5% of the eco-costs were from sea transport from China to the Netherlands. For the comparison with timber, the bamboo table leg was compared with the same table leg built of various softwood and hardwood species. Results showed that sea transportation caused the bamboo to have higher eco-costs than most woods except FSC tropical hardwood (van der Lugt et al. 2009). Vogtländer et al. (2010) also compared the environmental impacts of raw bamboo culms from the van der Lugt et al. (2006) study and Plybamboo and Strand Woven Bamboo from China with similar timber products in terms of eco-costs/kg. Calculations were based on the Ecoinvent-v2 and IDEMAT 2008 databases and the eco-costs 2007 method for LCIA (Vogtländer 2001). As expected and similar to previous studies, results showed that sea transport gave bamboo a higher eco-cost/kg value compared to local timber but bamboo performed better as compared to FSC hardwood.

van der Lugt et al. (2012) investigated the environmental impact (i.e.: global warming potential in kg CO_2 equivalents) for industrial bamboo products, specifically carbonized 3-layer laminated bamboo board. An LCA was conducted considering a cradle-to-warehouse plus end-of life boundary for the bamboo board production. The use phase was not included since "emissions in this step are less than 1%" (van der Lugt et al. 2012) in comparison to production and disposal. The product was considered to be produced in China and then shipped to Europe, specifically the Netherlands. In addition to quantifying the environmental impacts of laminated bamboo board, the authors also sought to address how carbon sequestration is dealt with in the life cycle analysis of bamboo. Considering a cradle-to-grave scope, biogenic CO_2 was considered

by van de Lugt et al. (2012) to have a net zero effect on global warming unless the bamboo is burnt to generate electricity or heat as replacement for other fuels. On a global scale, van der Lugt et al. also state that bamboo carbon sequestration is a function of land transformation (i.e. if global forest area is increasing and the wood and/or bamboo volume in buildings is increasing, then carbon sequestration increases). Therefore, effects of carbon sequestration from bamboo plantation area growth over a 5 year period as well as credit from burning bamboo at disposal for heat were considered and laminated bamboo board was found to be viable as a sustainable alternative even after transportation to Europe.

A 2011 project by undergraduate students at the University of Pittsburgh also involved a comparative LCA of bamboo and timber; specifically bamboo and timber portal frames. Portal frames were selected as these are often seen in residential timber construction. In timber construction, these are composed of dimensional lumber and plywood sheathing to provide lateral stiffness. The functional unit of this study was defined as equivalent lateral stiffness and experimental testing was conducted to determine the lateral stiffness of a timber portal frame sheathed in plywood and a bamboo portal frame sheathed using a bamboo woven mat (Choi et al. 2011). The equivalent stiffness ratio was determined to be 6.8 bamboo frames = 1 timber frame. The timber frame was composed of 2 X 4 hem fir stud timber with nailed connections and 3/8" plywood sheathing while the bamboo frame was composed of *Pseudosasa amabilis* (Tonkin Cane) from China. The impacts of the bamboo woven mat could not be studied due to a lack of manufacturing data. Tonkin Cane was selected for the study because even though it has a small diameter it has thick and stiff culm walls like large diameter bamboo. Additionally Tonkin Cane is available from producers in the United States. This allowed the authors of the study to investigate three cradle-to-consumer scenarios: locally produced and used in Brazil; domestically

produced and used in Pittsburgh, PA, USA; and internationally produced and used in Pittsburgh. The bamboo process phases included agriculture, treatment, and transportation. The study used established LCA data for the timber frame reported by Puettmann et al. (2010a, 2010b). Bamboo produced locally and domestically was found to be potentially more sustainable than timber based on the functional unit of equivalent lateral stiffness. Results also showed that transportation was the major phase limiting the sustainability (i.e.: internationally produced bamboo) followed by the cultivation impacts. The authors concluded that using larger diameter bamboo (i.e.: stiffer culms) may improve the equivalent stiffness ratio between the two frames and therefore increase the relative sustainability of the bamboo portal frame (Choi et al. 2011).

A second 2012 study by undergraduates at the University of Pittsburgh conducted a comparative LCA of bamboo and glass fiber reinforced polymer GFRP gridshell structures for use as rapidly deployable relief shelters in response to natural disasters (Brown et al. 2012). As with the 2011 study, the functional unit was the structural stiffness of the gridshell structure. Results showed that if bamboo is farmed in a sustainable manner, located in a favorable climate, and transportation distance for delivery is limited, bamboo can be a sustainable material alternative to GFRP for the gridshell structures considered (Brown et al. 2012).

With regard to US timber production, Milota et al. (2005) conducted a gate-to-gate life-cycle inventory of softwood lumber production for both the US Pacific Northwest (Oregon and Washington) and the US South (Georgia, Alabama, Mississippi, and Louisiana). The objective of the work was to determine the energy and material inputs and outputs associated with the production of planed dry lumber. The research was part of the development of a wood products LCA database by the Consortium for Research on Renewable Industrial Materials (CORRIM). The functional unit for the study was 1000 board feet or 2.36 m^3 of planed, dry dimension

lumber (Milota et al. incorrectly cites a value of 1.623 m^3 as equivalent to 1000 board feet; it is unclear how or if this affects their results and conclusions). The system boundary encompassed the sawmill complex (gate-to-gate) and includes the process units of sawing, drying, energy generation, and planing. Transportation from the various process units (i.e.: via forklift) is also included. Consideration was also taken of the co-products produced such as sawdust, wood chips, green lumber, bark, etc. (Milota et al. 2005). Other CORRIM-sponsored studies include Puettmann et al. (2010) who conducted an LCI on US wood products in the Inland Northwest and the Northeast regions and Wilson (2010) who conducted a scope 2 LCI for resins in wood composites. The results of these studies and other data in the CORRIM LCA database are publically available in the Department of Energy's National Renewable Energy Laboratory (NREL) USLCI database (CORRIM 2011). This database will be used in the present study for the timber column data.

6.1.3 Research Basis for Current LCA

In Choi et al. (2011), it was found to be difficult to compare equivalent lateral stiffness of the varying bamboo and timber systems due to scaling issues with the frames. Being constructed in Pittsburgh, availability of appropriate culms or sheathing to 'match' dimensional lumber properties is limited; hence the ratio of relative frame stiffness of 6.8. Axial column capacity is a much more direct structural parameter for study as a functional unit and if column capacity is similar, the column itself can directly serve as a functional unit. The multi-culm bamboo column reported in Chapter 5 is the basis for this study. Harries et al. (2000) reported comparable tests of built-up timber columns which will serve as a primary basis for comparison. Additional comparable hot-rolled steel shapes are also considered for comparison. Table 6-1 provides a

comparison of these comparable column members while the following sections briefly summarize each material selection.

Table 6-1: Column sections considered

	four culm bamboo column	6 X 6 built up timber column	6 X 6 dimensional timber column	Steel	
				HSS3x3x1/8	HSS3x0.203
data source	Chapter 5	Harries et al. (2000)	NDS (2005)	AISC (2011)	
	test data	test data	design data	design data	
E (MPa)	13,450[e]	12,400[d]	12,400[d]	200,000[d]	
KL (mm)	2600	3050	2600	2600	2600
A (mm^2)	12,200	13,070	17,420	839	1077
I (mm^4)	6,700,000	23,700,000	25,300,000	740,000	690,000
r (mm)	23.4	42.6	38.1	29.7	25.3
P (kN)	159[e]	179[e]	246[d]	160[d]	164[d]
$f_{cr} = P/A$ (MPa)	12.1[e]	13.5[e] 6.05[d]	14.1[d]	$f_{cr} = 190^d$	$f_{cr} = 152^d$
$\pi^2 EI/(KL)^2$ (kN)	131	312[e]	579[d]	216	201
$f_{comp=}$ (MPa)	54.7[e]	13.8[d]	14.5[d]	317[d]	290[d]
weight of 2600 mm column (kg)	24.3	19.7	23.6	17.3	22.1
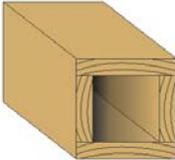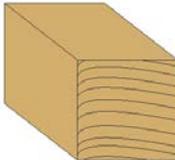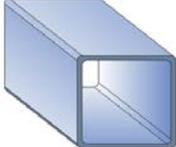
E = modulus of elasticity; KL = effective length; A = cross section area; I = moment of inertia; r = radius of gyration; P = critical applied force; P/A = critical applied stress; $\pi^2 EI/(KL)^2$ = theoretical Euler buckling load; f_{comp} = crushing stress; f_{cr} = critical buckling stress.
[e] = experimentally determined; [d] = code-prescribed design data

6.1.3.1 Four-culm bamboo columns

The four-culm columns reported in Chapter 5 of this work are the basis for this comparative LCA study. The bamboo culms of species *Bambusa Stenostachya* (Tre Gai) were harvested and treated in Vietnam and transported to the US via a supplier in Portland, Oregon. The columns were composed of four 2600 mm high Tre Gai culms that were 'stitched' together

with bamboo cross stitches and threaded steel rods. The columns were designed and tested according to ISO 22156 and ISO 22157-1:2004 guidelines.

6.1.3.2 Timber columns

Harries et al. (2000) conducted axial, flexural, and squash load capacity tests on built-up timber elements. The columns and flexural members were constructed out of pressure-treated 2 in. nominal Southern Pine sawn dimensional lumber connected with Resorcinol resin adhesive. The columns were 3048 mm in height and of various cross sectional area. Predicted capacity was calculated using the allowable stress values from the 1995 National Design Standard (NDS) Supplement. Experimental results showed that the built-up members had significant over-strength to allowable design values and therefore could be designed conservatively with the NDS provision for solid sawn timber columns (Harries et al. 2000). The average ultimate capacity values were 119.1 kN for four 5 X 5 columns; 178.7 kN for two 6 X 6 columns and 217.6 kN for two 8 X 8 columns. Since the boxed timber column used only 2 in nominal dimensional lumber, it is a potential sustainable alternative to using larger solid timbers. Although not considered in the present study, the columns tested by Harries et al. also included columns made of finger-jointed dimensional lumber, which itself allows greater utilization of the harvested timber. Due to the comparable capacity, the 6 X 6 column, shown in Table 6-1, will be considered in the comparative LCA. A comparable 6 X 6 solid timber column was also designed using ASD equations from the 2005 NDS Supplement (AF&P Assoc. 2005) and Breyer et al. (2007) for consideration in the comparative LCA.

172

6.1.3.3 Structural Steel Columns

Representative hot-rolled steel columns were designed based on American Institute of Steel Construction (AISC 2011) guidance for an unbraced length of 2600 mm and required nominal capacity of 160 kN (experimental capacity of four-culm bamboo column). Only doubly symmetric HSS sections were considered since the smallest available wide flange shape has a capacity of more than 350 kN. Singly- or non-symmetric shapes were not considered due to the complexity of their behavior and the difficulty of integrating these into a simple design. Steel is priced by weight; therefore the columns were designed to minimize the steel weight (cross sectional area) in each case.

6.2   METHOD AND INPUTS

The comparative LCA presented will assess the environmental impacts of the structural bamboo, boxed timber, solid timber, and steel columns. A 2600 mm tall column will be considered as the functional unit. This column has an axial load bearing capacity of approximately 160 kN (18 tons). The columns are not assumed to be part of a lateral load resisting system in this comparison since the effects of lateral load will affect each column capacity differently. It is assumed that the footing beneath the column is adequate. The footing and its connection to the column are excluded from the LCA since the details of these may vary widely and will depend on the structural context of the column (i.e.: gravity only or part of a lateral load-resisting system). The results of this midpoint LCA will be the LCIA profiles for the columns. A cradle-to-consumer approach will be used as it is assumed that the use and disposal phases for both the bamboo and the timber columns will be similar; the disposal and/or re-use of the steel columns

will depend greatly on context. Durability (and thereby service life) will also vary for each material and will be highly dependent upon context. In particular, whether the columns are interior columns or exposed to the elements will affect service life. The varying service lives and reuse options for each material as well as analysis of sensitivity to changes in service life and reuse are major components for a 'cradle-to-grave' assessment and objects of future study; these are not considered in the current comparison. The process flow diagram in Figure 6-1a illustrates the six processes included in the system boundary: extraction (i.e.: harvesting), transportation to the processing site, processing and preservative treatment, transportation to erection site, fabrication of fastener system, and erection. For timber box columns (Fig. 6-1b), erection is conducted before delivery to the site. For steel columns, extraction, transportation to the processing site, and processing are combined into one life-cycle step (Fig. 6-1c).

a) bamboo columns

b) timber box columns
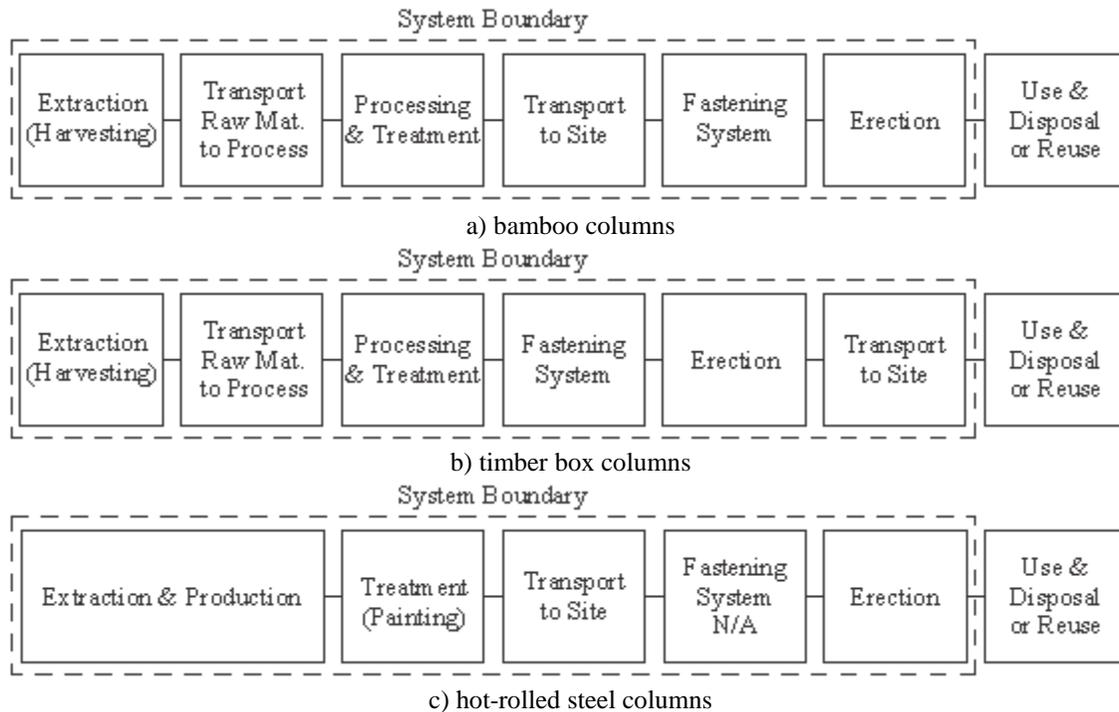
c) hot-rolled steel columns
Figure 6-1: Process Flow Diagram for Columns

Two scenarios are considered: 1) columns used in the USA, which has stockpiles of steel and timber components; and 2) columns used in Brazil which has steel, timber, and bamboo

174

material available. Large diameter bamboo is not native to North America, and thus transportation costs to receive bamboo from Asian plantations (or elsewhere) are expected to drive the impacts of the use of bamboo in the USA. Nonetheless, with appropriate incentive, large culm species *could* be grown in the USA, addressing the issue of availability. Brazil, however, offers a more sustainable context since the number of native large diameter bamboo species is greater. In terms of timber, Brazil is facing issues of deforestation in the tropical forests of the Amazon as well as protecting what areas remain of the coastal Atlantic Forest. Therefore, it is envisioned that in Brazil, there is both the incentive and opportunity for greater structural use of bamboo.

Table 6-2 illustrates the LCI databases used to characterize the six major processes in the system process flows. The LCI databases used were the USLCI (www.nrel.gov/lci/), IDEMAT 2001 (www.idemat.nl), and ecoinvent (www.ecoinvent.org/database/) databases. The LCIA tool TRACI 2 version 3.01 from the US EPA (www.epa.gov/nrmrl/std/traci/traci.html) was used for the life cycle impact assessment.

Table 6-2: Included Processes for Comparative LCA and Corresponding LCI Databases

Process Flow	Mat.	Scenario 1 (USA)		Scenario 2 (BRAZIL)	
		Included Process Names	Database	Included Process Names	Database
Extraction	Bam.	Carbon sequestration estimate	van der Lugt (2012)	SAME AS SCEN. 1	
		Chain sawing I	IDEMAT		
	Timber	Softwood logs with bark, harvested at avg. intensity site, at mill, US SE/US	USLCI	Roundwood, paraná pine (SFM), under bark, u=50%, at forest road/BR U	ecoinvent
Transport to Processing	Bam.	Transport, lorry 3.5-7.5t, EURO3/RER S	ecoinvent	SAME AS SCEN. 1	
	Timber	Transport, combination truck, average fuel mix/US	USLCI	Included in Processing & Treatment	
Production	Steel	1 lb, Fe360 I (construction steel)	IDEMAT	SAME AS SCEN. 1	
Processing and Treatment	Bam.	Energy Asia I	IDEMAT	Electricity, low voltage, production BR, at grid/BR U'	ecoinvent
		Borax, anhydrous, powder, at plant/RER U	ecoinvent	SAME AS SCEN. 1	
		Boric acid, anhydrous, powder, at plant/RER U	ecoinvent	SAME AS SCEN. 1	
	Timber	Rough green lumber, at sawmill, US SE/kg/US	USLCI	Sawn timber, paraná pine (SFM), kiln dried, u=15%, at sawmill/BR U	ecoinvent
		Dry rough lumber, at kiln, US SE/US	USLCI	Preservative treatment, sawn timber, pressure vessel/RER U (Adjusted for Brazil Electric Grid)	ecoinvent
		Surfaced dried lumber, at planer mill, US SE/kg/US	USLCI		
		Preservative treatment, sawn timber, pressure vessel/RER U	ecoinvent	Analyzing 1 kg 'Wood preservative, organic salt, Cr-free, at plant/RER U'	ecoinvent
		Wood preservative, organic salt, Cr-free, at plant/RER U	ecoinvent		
	Steel	1 oz Alkyd paint, white, 60% solvent, at plant/RER U	ecoinvent	SAME AS SCEN. 1	
Transport to Site	Bam.	Transport, ocean freighter, average fuel mix/US	USLCI	Transport, lorry 3.5-7.5t, EURO3	ecoinvent
		Transport, single unit truck, diesel powered/US'	USLCI		
		Transport, combination truck, diesel powered/US'	USLCI		
	Timber	Transport, single unit truck, diesel powered/US	USLCI	Transport, lorry 3.5-7.5t, EURO3	ecoinvent
	Steel	Transport, combination truck, diesel powered/US'	USLCI	Transport, lorry 3.5-7.5t, EURO3	ecoinvent
Fasteners	Bam.	Galvanized steel sheet, at plant/RNA	USLCI	SAME AS SCEN. 1	
	Timber Box Only	Phenol-resorcinol-formaldehyde resin, at plant/US (Cradle - Gate)	USLCI	SAME AS SCEN. 1	
		Phenol-resorcinol-formaldehyde hardener, at plant/US (Cradle - Gate)	USLCI	SAME AS SCEN. 1	
Erection	Bam. Timber	Electricity, at grid, Eastern US/US	USLCI	Electricity, low voltage, production BR, at grid/BR U	ecoinvent

6.2.1 Extraction (Harvesting)

For timber, the species investigated were Southern Yellow Pine (specific gravity 0.55) for the USA scenario and Paraná Pine for the Brazilian scenario. The extraction process for bamboo and timber focused on the harvest of the grown product for industrial use, although agriculture processes are included in the LCI figures. In terms of US timber, CORRIM data in the USLCI database considers the production of seedlings which includes fertilization, planting, and forest management including fertilization during stand growth (Johnson et al. 2005, Oneil et al 2010, and Puettmann et al. 2010). Agriculture is also included in values for the Paraná Pine planation-grown product (Athaus et al. 2007). In the case of bamboo agriculture, it is assumed that there is no fertilizer used and the agriculture process is not otherwise included; this assumes initial manual planting and regenerative growth of culms; thus no 'reforestation' process is required. These assumptions are based on a case study of a bamboo plantation in Costa Rica (van der Lugt 2009) and interviews with a plantation owner in Brazil conducted by the author (Inglês 2012). However, it is acknowledged that bamboo agriculture processes vary between plantations of different sizes as well as by regions globally and future study on variability between bamboo harvesting practices is needed. Although bamboo is harvested by hand in many areas, the use of a chain saw was assumed as a practical method for harvesting both the culm size and volume of culms practically required for structural applications. For the southern pine case, reforesting and carbon sequestration is included as part of the harvesting process. It is noted that native Paraná pine is an endangered species due to historical over-logging but the process used considered pine harvested from a sustainably managed plantation (and is also representative of other plantation pine species) and therefore implicitly also includes reforestation and carbon sequestration. Presently, there is no data available for bamboo reforestation or carbon sequestration in standard

LCIA databases; this is a significant weakness of the presently available databases and should be addressed by future (agricultural-related) researchers in order that timber and bamboo alternatives may be compared on even more comparable bases. Recently, however, van der Lugt et al. (2012) proposed quantification of the beneficial effects of carbon sequestration and reforesting for bamboo. They propose a value of 1.83 kgCO$_2$/kg of bamboo culm harvested. This value becomes 5.72 kg CO$_2$/kg when it is considered that the culms only constitute 32% of the plant (Zhou and Jiang (2004) as reported by van der Lugt); underground rhizomes account for the majority of sequestered carbon. This value is used in the present analyses as an estimate of carbon sequestration in order that analyses of each material are comparable.

6.2.2   Transportation to Processing

The Tre Gai bamboo used in this study was locally harvested and processed near Ho Chi Minh City, Vietnam. The timber box column was processed by Cox Industries of Orangeburg, South Carolina (Harries et al. 2000). Transportation of harvested logs to the processing facility and sawmill is included in the data from both the USLCI and ecoinvent data bases. For scenario one, raw logs are assumed to travel 130 km to the sawmill for lumber production (Puettmann et al. 2010). For scenario 2, a transport distance of 90 km for Paraná pine is included in the processing step (Athaus et al. 2007). This latter inconsistency results from the use of multiple LCI databases which classify processes differently using data from multiple studies. This may affect the ultimate comparability of results but represents current best-practice. For harvested bamboo, it was assumed that culms are transported a similar distance as timber – 130 km and 90 km in each scenario, respectively – by a single unit lorry.

6.2.3 Processing and Treatment

The processing for bamboo includes sun drying and preservative treating using the Boucherie Method. The Boucherie Method uses borates (i.e.: borax powder and boric acid) to impregnate the bamboo with a pump and is described in Section 2.1.4.3. An estimated 1kWh of energy is used per culm (Choi et al. 2011) and the amount of chemical per weight of bamboo is given by van der Lugt (2003).

For timber scenario 1, processing includes sawing, kiln drying, planing, and preservative treatment. For pressure treating, a creosote free preservative is impregnated into the timber using an industrial pressure chamber (Southern Pine Association, 2006). These steps include such processes as transport through the mill as well as sorting and stacking. The Paraná pine scenario includes similar processes; therefore the preservative treatment process from scenario 1 is used with an adjustment for the Brazilian electricity grid. For sawn timber intended for only interior exposure, typically no treatment is required. The intended use of the column: interior or exterior exposure should be considered in interpreting impacts.

6.2.4 Transportation to Site

For scenario 1, it is assumed that bamboo columns are assembled in Pittsburgh, PA. The treated Tre Gai bamboo is shipped via ocean freighter from Ho Chi Minh City to a supplier in Portland, OR (12875 km). A single unit truck is used to deliver the bamboo from the shipyard to the supplier (9 km). The shipment is then transported cross country by tractor-trailer to Pittsburgh (4184 km). The completed timber columns are transported by single unit truck from South Carolina to Pittsburgh (946 km).

For scenario 2, specific locations of bamboo and pine suppliers in Brazil are unknown although sustainable options should be supplied locally. Therefore, both materials are assumed to travel via lorry 805 km to the erection site.

6.2.5 Fasteners

Fasteners are considered only when they are used in the construction of the column itself. End connections and footings used to connect the column 'into' the structure are not considered. Therefore, no fasteners are considered for the solid timber and steel cases. The fastening systems for the bamboo and timber box column are steel bolted connections and a phenol-resorcinol-formaldehyde resin adhesive, respectively. The galvanized steel components (threaded rods, nuts, and bolts) used to connect the bamboo test columns (Chapter 5) were weighed and their impacts determined based on the weight of the material. Transportation to site of the connection components is assumed to be coincident with final domestic transportation of the culms.

It was assumed that a 2 mm layer of resin is applied to all contact areas for the built-up timber columns and a 1:5 ratio of hardener to resin was used to determine the mass of each (Wessex Resins 2011). Erection of the built-up columns is completed during the plant-processing phase; the columns are shipped in their final form.

6.2.6 Erection

The erection process for the bamboo and timber columns primarily involves the use of sawing equipment and drilling equipment. Bamboo columns are assembled in the field, whereas built-up timber columns are assembled in the plant; following and preceding shipping to the site,

respectively. For the bamboo column, a miter saw was used to trim culms to their proper height when required (study assumes culms were supplied came in standard 3 m (10 ft) lengths) and a cordless drill was used to drill the holes for bolted connections. Power, voltage, and amps from each piece of equipment were used along with estimated usage times to calculate the amount of electric energy required. A band saw was used for cutting threaded steel rod to length for the through-bolts. For the solid timber and the timber box columns, only the miter saw was utilized for cutting timber to their proper length when required. Steel sections are assumed to be cut to length at their respective mills and require no further assembly within the scope of this analysis. Once on site, individual columns have similar weights (Table 1-1) and thus handling equipment requirements will be similar; all columns considered can be carried by one manual laborer and certainly erected by two.

6.2.7   Steel Process Inputs

The IDEMAT 2001 database considers construction steel environmental impacts based on the 1999 average world production and considers delivery in Europe, specifically the Netherlands. It is unclear what percentage of the environmental impacts is due to final delivery in this dataset. Steel is a truly global commodity with raw materials coming from all corners of the globe and final products shipped to all markets. The industry in 2013 is also considerably different than that in 1999; for instance, between 1999 and 2012, US steel production has increased 190% and global production has increased 287%. The US share of global production has fallen from 8.6% in 1999 to 5.7% in 2012 (World Steel Association 2012, USGS 2010, and Figure 1-2). Nonetheless, noting that representative steel samples are being used for comparison in this study, the environmental impacts values from IDEMAT 2001 are used directly.

Steel sections are painted with an Alkyd paint to prevent rust and it is assumed that 32 ounces of paint covers 100 square ft. Transportation to site is similar to the timber cases for both scenarios 1 and 2; it assumed that the final columns travels 805 km by truck. No assembly is considered as the steel columns are assumed to arrive on site cut to the required length.

6.3   LCIA PROFILES

LCIA profiles are organized by the nine impact categories associated with the TRACI LCIA tool:

- global warming potential of greenhouse gas emissions measured in units of kg CO_2 (carbon dioxide) equivalent (eq)

- acidification: H+ moles eq

- carcinogens: kg benzene eq

- non-carcinogens: kg toluene eq

- respiratory effects: kg PM2.5 (particulate matter less than 2.5 microns) eq

- eutrophication (e.g. excess nitrates and phosphates) : kg N eq

- ozone depletion: kg CFC-11 (chlorofluorocarbons) eq

- ecotoxicity (e.g. pesticides, fertilizers, and energy emissions): kg 2,4-D eq and,

- smog (e.g. nitrous oxide, sulfur dioxide, and carbon monoxide): kg NO_x eq

First, the bamboo and timber options are compared as they are considered to have the greatest similarity in harvesting, production, and treatment. Additionally, bamboo and timber may be considered to be more comparable and appropriate for structures in which bamboo may be considered. Impacts for bamboo and timber options are therefore each divided into major

processes. Following this, total impacts for categories are compared for the bamboo, timber, and steel alternatives.

6.3.1   Bamboo and Timber Columns

Figures 6-2 and 6-3 illustrate the cumulative LCIA profiles for the bamboo and timber columns for scenario 1 and scenario 2 respectively. Values are normalized to the maximum value in each category; thus comparison cannot be made between impact categories. For the first (US) scenario (Fig. 6-2), the bamboo column has the highest impact value in the two categories of, carcinogens and non-carcinogens resulting from the use of galvanized steel fasteners which have a significant impact in these categories. For global warming potential, reforestation and carbon sequestration considered during the harvesting process has the largest environmental impact contribution for bamboo but these net environmental benefits count as a credit in this case (i.e.: a negative impact value in Fig. 6-2). However, if carbon sequestration was not considered, bamboo would have the largest environmental impact due to long shipping distance required. Ultimately, transportation to site and the use of steel fasteners are the dominant processes for bamboo in all impact categories except global warming potential. Without these processes, bamboo would have the least environmental impact of the three natural product alternatives in all categories. In this study, it must be acknowledged that transportation effects are estimated and relative only to this specific study. Clearly, for bamboo construction to be viable in North America local planation must take place; this will significantly reduce environmental and financial impacts.

The timber box column has the highest impacts in the five categories of acidification, respiratory effects, eutrophication, ecotoxicity, and smog due to the impact of the adhesive resin (fastener) used. Timber processing and treatment as well as transportation also have noticeable

impacts for the performance of both timber columns, although if the timber is destined for interior use, treatment becomes unnecessary. In the case of global warming potential, the timber columns also have a net environmental benefit (negative number in Fig. 6-2) but this is not as significant as the bamboo case.

Only in the impact category of ozone depletion does the solid 6x6 timber column have the highest impact due to timber processing (since the solid column has more material). However, if a more environmentally friendly adhesive system were used for the built up column, it would have lower impacts in all categories as compared to the solid timber column. Overall, scenario 1 results illustrate that bamboo is a potentially sustainable option despite not being locally grown. This conclusion is dependent on the carbon sequestration allowance used; in this study the value reported by van der Lugt et al. (2012) was adopted in lieu of an alternative value provided within the available LCA data bases. Additionally, although less lumber is used, the impacts associated with the adhesive resin in the built-up timber column adversely affect its overall environmental performance compared to solid timber. However, not factored into the equation is that large dimensional lumber (solid timber column) must come from larger and older trees, while smaller dimensional lumber (2 in nominal thickness) used in the built-up column can be sawn from smaller, younger trees, sustainable farmed trees and more boardfeet (lumber volume) can be produced per harvested tree.
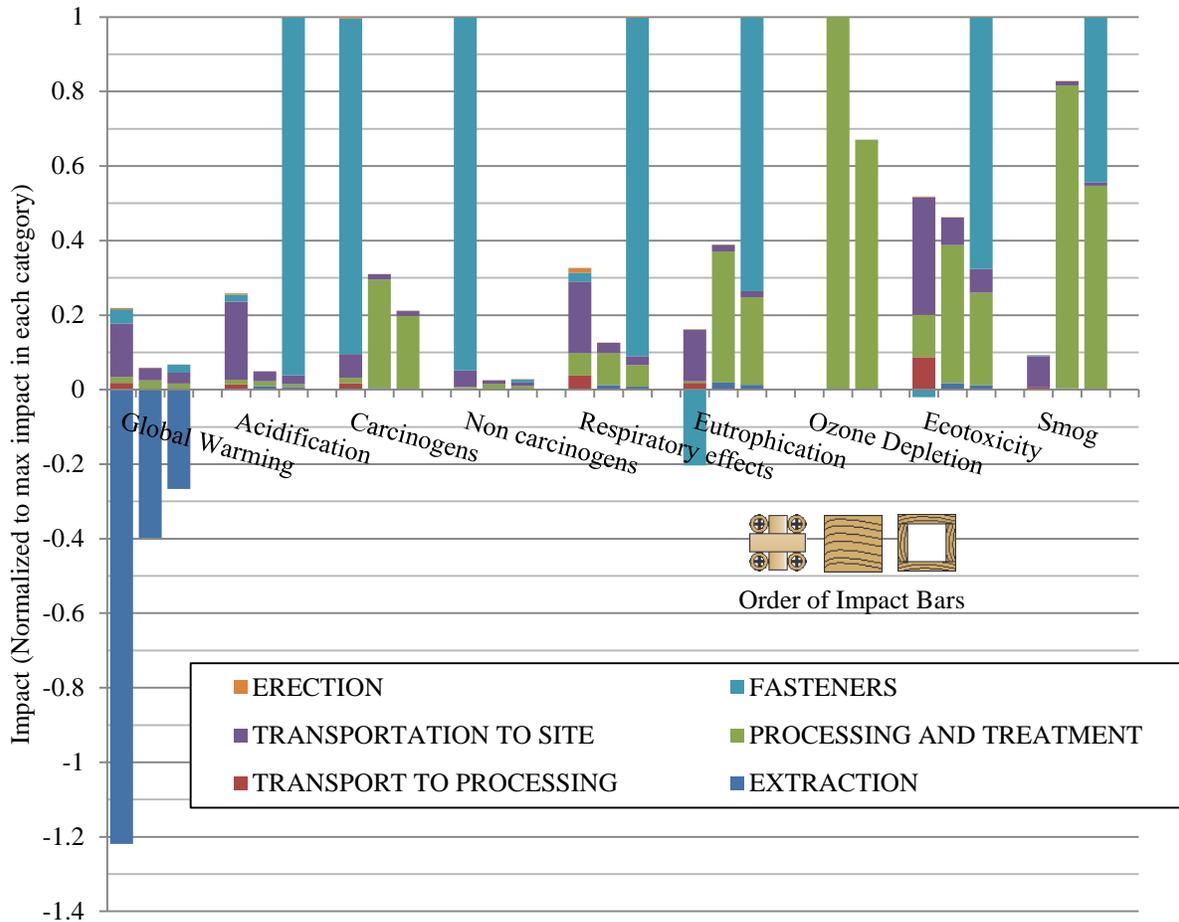
Figure 6-2: LCIA profile for 2600mm bamboo and timber columns (scenario 1)

For scenario 2, set in Brazil, the bamboo column only has the higher environmental impacts in the category of non-carcinogens and the lowest impacts in all other categories but carcinogens. Galvanized steel fasteners and transport were the major processes impacting bamboo performance yet transport now only includes 805 km of truck transport to site. If bamboo is local to a community, the impact of transportation would fall even further. The built-up timber box column has the higher impacts in the categories of acidification, eutrophication, ecotoxicity, and smog due, once again, to the influence of the adhesive resin. The solid timber column has the higher impacts in the categories of carcinogens, respiratory effects, and ozone depletion, although these values may fall if the wood remains untreated for interior use.
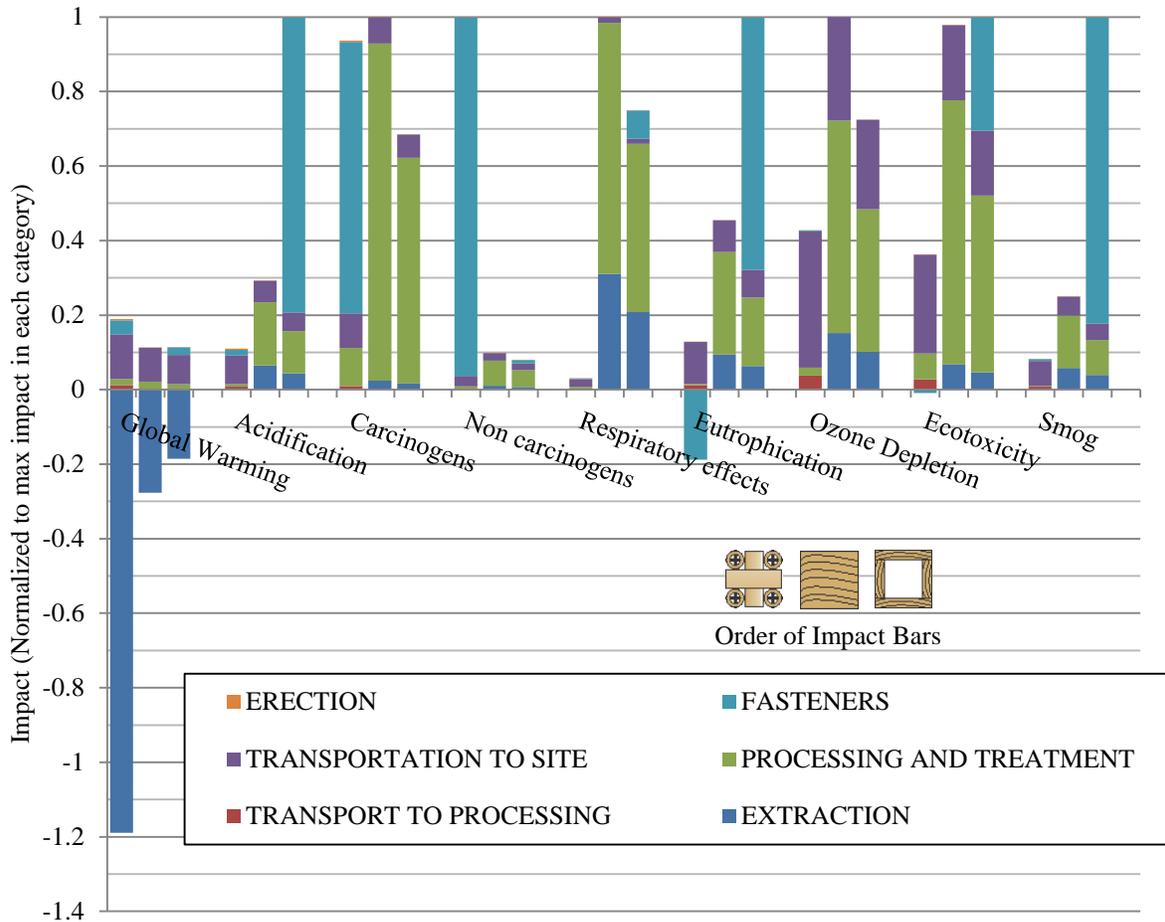
Figure 6-3: LCIA profile for bamboo and timber columns (scenario 2)

Ultimately, bamboo becomes a much more sustainable alternative relatively the closer it is to the building site since it has lower impacts due to initial processing and treatment. Therefore, since bamboo is found locally in Brazil, it has greater potential in that region (as compared to competing with established sustainably managed pine forests/plantations in the US). Fastening systems used for columns also proved to be a significant component of impacts in both scenarios.

6.3.2 Comparison with Steel Columns

While the first portion of the LCIA study considered bamboo and comparable timber columns, the second portion adds hot-rolled steel column sections that were optimized to use the least material (i.e.: lowest cost). The environmental impacts of representative box, and round HSS columns were assessed for both the US and Brazil scenarios. The results of the LCIA for representative steel sections are then compared with the environmental impacts of the bamboo and timber columns in Figures 6-4 and 6-5.

The results in Figure 6-4 for scenario 1 (again normalized to the greatest impact value in each category) illustrate that there is nominal difference between the square and round HSS shapes and is attributable to the greater sectional area (and therefore section weight) of the round HSS (see Table 6-1). The HSS sections are shown to out-perform both timber columns in four impact categories: eutrophication, ozone depletion, ecotoxicity, and smog (built up timber is worst case in five categories, solid timber in one) and to outperform bamboo in five categories: acidification, non-carcinogens, ozone depletion, ecotoxicity, and smog.
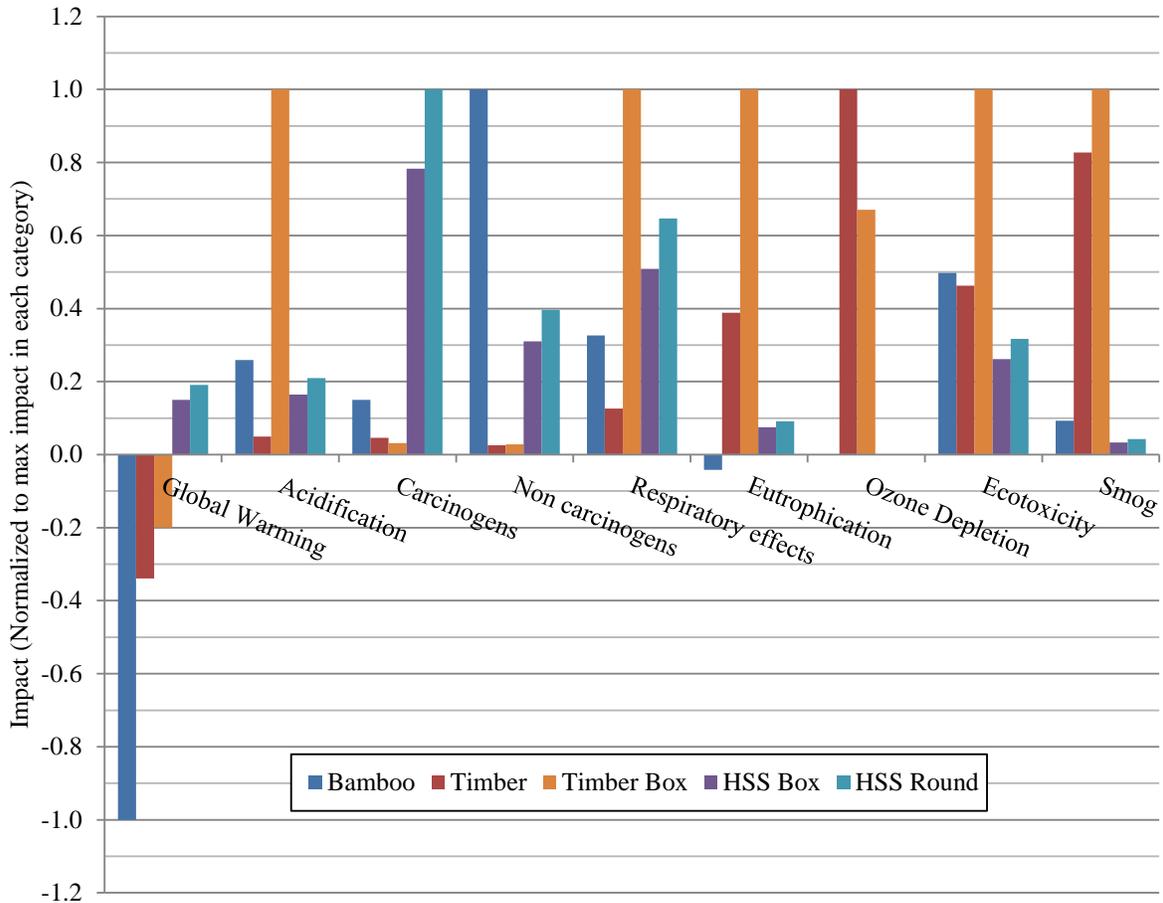
Figure 6-4: LCIA profile for bamboo, timber, and steel columns (scenario 1)

In scenario 2 (Fig. 6-5), the performance of steel components appears to improve compared to timber alternatives yet decreases slightly in relation to the bamboo column. The HSS sections out-perform the timber alternatives in 6 categories: acidification, respiratory effects, eutrophication, ozone depletion, ecotoxicity, and smog. The HSS sections only out-perform bamboo in 3 categories: non-carcinogens, ozone depletion, and ecotoxicity.
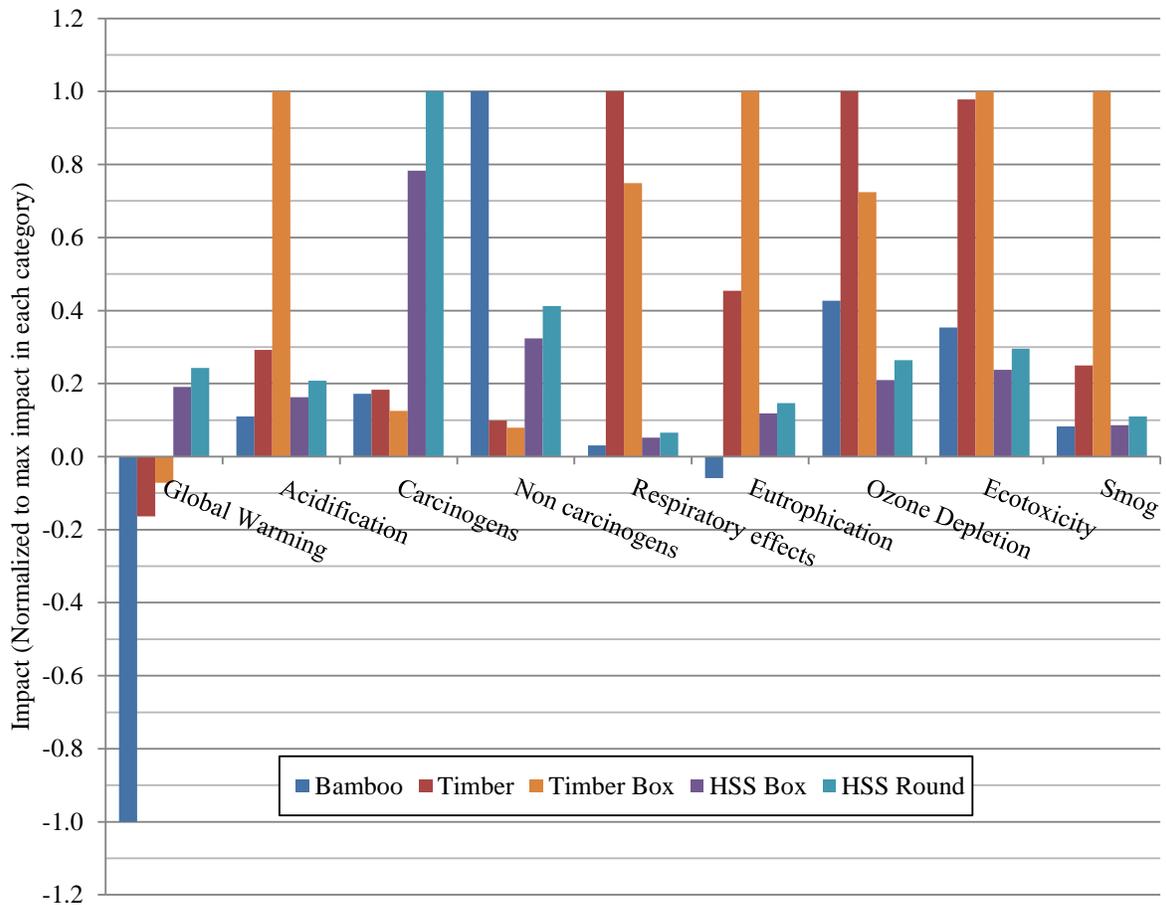
Figure 6-5: LCIA profiles for bamboo, timber, and steel columns (scenario 2)

6.3.3 Discussion

Table 6-3 summarizes the quantitative environmental impacts for all column alternatives in both scenarios. The table, as with Figures 6-2 through 6-5, illustrate that there is no clear sustainable option between the bamboo, timber, and steel columns. This is due to the fact that no weighting is given to the nine impact categories outlined in the midpoint LCIA study. A single sustainability metric similar to the eco-costs/kg used by van der Lugt et al. (2006, 2009) or Vogtländer et al. (2010) is therefore needed to define the more sustainable option. Ultimately, van der Lugt et al. (2009) determined that only domestically produced bamboo products were

potentially more sustainable than domestic European lumber in some cases. A similar finding appears to be the case in the present study in which the results presented did show that the bamboo column had improved performance in the second scenario: domestic production in Brazil. This highlights the conclusion that bamboo is sustainable when used locally rather than when it is shipped long distances and is likely true for most commodities when monetary cost is excluded from the analysis. The environmental impacts of shipping outweigh the benefits of the bamboo material. This agrees with findings of Choi et al. (2011) which considered the TRACI impact categories of only global warming potential, acidification, non-carcinogens, and ecotoxicity in their final report. The LCIA profile results reported by Choi et al. also showed that internationally shipped bamboo had higher impacts than timber in the categories of global warming, acidification, and non-carcinogens based on equivalent frame stiffness. Additionally, the midpoint LCIA points to the large impact of fasteners on environmental impacts of both bamboo and timber components. Considering the *relative* weight of categories in which fasteners impact may change this conclusion as fasteners represent a relatively small part of either column.

The results also illustrated the comparable performance of representative steel components as compared with the bamboo and timber columns. Janssen (1981) states that steel production requires 50 times more energy than bamboo and Ghavami (2008) reports that two tons of CO_2 are produced for every 1 ton of steel. Certainly, if one kilogram of steel and bamboo were compared one would assume that the bamboo would perform better. However, when looking at structural elements having comparable capacities, the smaller HSS sections exhibited environmental impacts (depending on category) on par with those of bamboo and timber. Nonetheless, the bamboo impacts were driven by transportation and fastening systems while steel impacts were driven by production.

Table 6-3: LCIA results for all column alternatives

	Section	four-culm bamboo column		6X6 sawn timber		6X6 built-up timber Box		HSS3x3x1/8		HSS3x0.203	
Impact Category	**Unit**	**Scen. 1**	**Scen. 2**	**Scen. 1**	**Scen. 2**	**Scen. 1**	**Scen. 2**	**Scen. 1**	**Scen. 2**	**Scen. 1**	**Scen. 2**
Global Warming	kg CO_2 eq	-149.8	-153.6	-50.8	-25.1	-29.9	-10.9	22.5	29.3	28.6	37.2
Acidification	H+ moles eq	16.7	8.6	3.2	22.9	64.5	78.3	10.6	12.8	13.5	16.2
Carcinogens	kg benzene eq	0.109	0.126	0.034	0.134	0.023	0.092	0.568	0.574	0.726	0.733
Non carcinogens	kg toluene eq	3324.5	3274.7	83.9	322.8	92.3	259.2	1032.0	1059.6	1316.5	1351.8
Respiratory effects	kg PM2.5 eq	0.024	0.027	0.009	0.866	0.072	0.649	0.037	0.045	0.047	0.057
Eutrophication	kg N eq	-0.004	-0.006	0.036	0.046	0.093	0.101	0.007	0.012	0.008	0.015
Ozone Depletion	g CFC-11 eq	0.0005	0.0033	64.6	0.0077	43.3	0.0056	0.0001	0.0016	0.0001	0.0020
Ecotoxicity	kg 2,4-D eq	6.4	10.1	6.0	27.9	12.9	28.5	3.4	6.8	4.1	8.4
Smog	kg NO_x eq	0.32	0.15	2.88	0.47	3.48	1.87	0.12	0.16	0.15	0.21

6.4   FUTURE WORK

The goal of the current midpoint LCA was to compare the environmental impacts of a representative bamboo column with comparable timber and steel alternatives designed for the same axial capacity and to demonstrate advantages and drawbacks of the adoption of a structural capacity or element as a functional unit. In terms of the bamboo LCIA, information on the environmental impacts for available agriculture, harvesting, and treatment processes (as well as uses) of various bamboo species must be compiled and refined into a standard database for future assessments.

In this study, the carbon sequestration allowance for bamboo was adopted from an independent study: van der Lugt et al. (2012). It is not entirely clear that this value is determined considering the same parameters as those provided in standard datasets for timber. Nor, one assumes, has the value been 'vetted' to the same degree as those formalized in the datasets. For example, the carbon sequestration data for bamboo and timber are not directly comparable without knowing the harvest cycle for both. In general, structural bamboo may be harvested every two or three years whereas softwood lumber is harvested on cycles on the order of ten years or more. Thus the carbon sequestration advantage of bamboo may be three to five times that of timber. It is understood that the present data and study accounts for the single harvest cycle required to produce the bamboo or timber column considered.

Study of impacts due to bamboo connection methods would also be useful as the column fastening system for the four-culm column was a large contributor in the total impact values. The sensitivity of results to changes in the bamboo processes (as well as those of timber and steel) is

also necessary once an improved database is available. Improved, and perhaps regionalized impact data on steel production is required since steel production can vary with location as different production processes and national energy mixes will affect results. Yet steel is a globally traded commodity, raw materials for steel production are also harvested and traded on a global scale, and the end of life and recycling of steel varies considerably. For example, ore may be extracted in Australia of Brazil (and mixed with recycled feed stock from India and Europe) for steel milled and fabricated in China intended for a bridge structure in the USA or UK (current examples include the San Francisco Bay Bridge and the second Forth Road Bridge in Edinburgh). At the end of the bridge's life – which may be 100 years hence, the steel may be recycled in India or another region not presently considered. Although the environmental impact data for construction steel from the IDEMAT 2001 database was used as being representative, determination of the sensitivity to process changes is necessary.

Inclusion of masonry and reinforced concrete construction, which bamboo construction often competes with in rural areas such as Northeast India, would also benefit the overall comparison. In terms of column elements considered here, masonry piers, cold-formed steel built-up columns, and timber cluster posts should also be included as alternatives. Replacing full-length lumber in the box columns with finger-jointed lumber (assembled from offcuts when lumber is sawn to length) should also be investigated. (While not reported in Harries 2000, finger-jointed box columns were also tested and the results reported in the sponsor report.)

6.4.1   Single metric for environmental impact

A single metric of environmental impact would also improve the overall assessment as the nine impact categories of the midpoint LCA did not necessarily provide a clear 'sustainable'

option. Weighting of the impact categories into a single parameter would allow for more straight forward comparison with structural parameters and ultimately better integration into the structural design process. Nonetheless, it must be acknowledged that any single measure is necessarily flawed and, itself, must address regional priorities. Janssen (1981) calculated the ratio of embodied energy (MJ/m^3) and design stress (MPa) for concrete, steel, wood, and bamboo to show an order of magnitude between materials for comparison. However, this approach does not account for design parameters such as shape of the cross section and required stiffness (e.g. deflection limits). For example, column design is driven by stability measured by the length (m), moment of inertia (mm^4) and radius of gyration (mm), rather than by stress.

Instead, a parameter could be developed in the form of 'environmental impact'/structural property, ηQ, where Q is a measure of eco-cost/kg such as those used by previous studies: kg CO_2/ft, or embodied energy/ft (van der Lugt et al. 2009, Vogtländer et al. 2010). Like geometric properties, values could then be calculated for specific or representative structural materials or shapes and be compiled into a design aid for use in comparing structural design alternatives. An example might be a column of data quantifying environmental impact vs. unbraced column length added to Table 3-10 used for column design in the AISC Steel Construction Manual. Tabulating a generalized case associated with production, adjustment factors could then be developed for impact parameters based on location specific process (e.g. European, US, or Asian steel production) or material (e.g. domestic softwood, domestic hardwood, international hardwood, or sustainably harvested wood) as well as a generalized transportation adjustment factor (e.g. 100, 500, or 1000+ km, transport radii factor). Such an approach might take the form of design Equation 6-1similar to Equation 2-1.

$$\eta Q = Q \left[C_{process\ factor} x C_{transport\ factor} x \ldots x C_k \right]$$
(6-1)

6.4.2 Inclusion of a transportation adjustment

Another key issue with the LCA of structural sections is the issue of accounting for shipping volume as well as weight – essentially considering the shape or form of the element being shipped. Currently, transportation environmental impacts are given in terms of material weight multiplied by distance traveled in units of tons-kilometer (tkm) or similar. This assumes that two similarly weighed structural components (in this case, a column) generate the same impacts (for a specific vehicle and distance travelled) regardless of structural shape. Yet standard trucks have a finite shipping volume (and load capacity) and different columns vary in size and shape. As an illustrative example using the columns considered in this study, consider a standard shipping unit volume of 2.6 m long and 2.44 m square; i.e.: 2.6 m long columns bundled into a 2.44 m square pallet for shipping on a flatbed truck thereby accommodating conventional roadway vertical and horizontal clearances. For this case, Table 6-4 provides a summary of the number of columns that may be shipped in each unit and their approximate weight. In each case, it is assumed that the total product weight may be carried by the truck; another threshold that must be respected.

Table 6-4: Example of transportation volume and weight.

	Bamboo	built-up timber	solid timber	HSS3x3x1/8	HSS3x0.203
Unit dimension	100 mm dia. culms	132 mm square	140 mm square	76 mm square	76 mm dia.
Weight of 1 column (kg)	24.3	19.7	23.6	17.3	22.1
Number of 2600 long columns in 2.4 x 2.4 m unit	648 culms 130 columns	324	289	1024	1152
Total weight per truck (kg)	3,536	6,400	8,500	17,700	25,400
tkm/km (1 truck)	3.54	0.64	0.84	1.77	2.54
Number of trucks or trips required to transport 1152 columns	9	4	4	2	1
Total shipped weight (kg) of 1152 columns	27,993	22,694	27,187	19,929	25,400

It is easily seen from Table 6-4 that the column form will affect transport impact. Bamboo and timber require approximately nine and four times the number of vehicles (or

individual trips), respectively, to ship an equivalent number of columns as the steel HSS round section despite the total shipped weight being similar. In this case, the weight of a full truck varies significantly between columns. However, each trip includes the impact of moving the truck itself (a 'fixed' impact per km) and perhaps, the impact of the truck returning to the depot empty. These factors cannot be easily accounted for in the present LCIA which bases transportation impact on shipped weight only. The column form, and its effect on the transportation *volume* required, must be accounted for in the comparative LCIA. An appropriate form factor must be developed so as the varying shape of structural columns can be considered in environmental costs of shipping. In the present example, at least two variations clearly demonstrate the variability of transportation impact:

1. In the example shown in Table 6-4, the bamboo columns are shipped as individual culms and assembled on site. If the culms were pre-assembled, the volume taken up by one column would not be that of five individual 100 mm culms (approximately $0.03m^3$) but a square unit approximately 300 mm on a side (0.23 m^3), almost eight times the shipping volume.

2. In some cases tubular steel is shipped nested into larger sections; this will decrease the number of columns in our hypothetical shipping unit but increase the shipment density; therefore the shipping impact per column may fall assuming that the truck capacity is not exceeded and that there is a demand for shipping sections of different size.

6.4.3   Consideration of service life

Last, consideration of structural component design life must also be considered in future studies. As natural fiber materials, bamboo and timber have a limited service life, especially if untreated. Even steel will corrode in time if not treated properly. However, if properly maintained and

recycled, all three alternatives can offer potential longevity and reuse, which reduces the amount of new material needed for replacement or new construction. Therefore, impact benefits associated with reuse and consideration of service life (whether directly applied in the environmental impact parameter or through an adjustment factor) should be considered in the analysis. Efforts in this realm have been made by a number of researchers including Aktas and Bilec (2012).

6.5   CONCLUSIONS

The goal of this study was to quantify the potential environmental sustainability impacts of a structural bamboo column in comparison to a solid timber, built-up box timber, and two representative steel column sections. An additional objective was to demonstrate, by example, advantages and drawbacks of the adoption of a structural capacity or element as a functional unit. A comparative midpoint LCA considering a scope 2 (cradle-to-consumer) approach was conducted for these elements with respect to two scenarios: use in the United States (scenario 1), where bamboo must be imported and use in Brazil (scenario 2) where bamboo species are locally grown. It was initially hypothesized that the boxed timber column would be the more sustainable option in the United States while bamboo would prove the more sustainable option in Brazil.

The results of the study ultimately did not produce a clear sustainable option between the bamboo, timber, and steel columns in either of the scenarios studied. LCIA profiles did show that transportation to erection site contributed the most to the environmental impacts of the bamboo column in both scenario 1 and 2. Specifically, the long distance transport of bamboo in scenario 1 appears to negate the benefits of using bamboo seen in categories and therefore bamboo is best

197

used only in a domestic context. The bamboo column had larger environmental impacts than timber in the categories of carcinogens (scenario 1) and non-carcinogens (scenario 1 and 2); this is attributed to the use of galvanized steel fasteners used (consistent with the experimental work presented in Chapter 5). Further research on non-steel fastener alternatives for the bamboo column could significantly reduce environmental impacts. The Brazil scenario ultimately decreased bamboo environmental impacts in five of the nine categories: global warming, acidification, non-carcinogens, eutrophication, and smog.

The phenol-resorcinol-formaldehyde resin and related processing contributed the most to the environmental impacts of the built-up box timber column in both scenarios 1 and 2, allowing the solid timber column, despite having more wood material, to outperform the timber box column in some categories. An alternative adhesive may significantly reduce these impacts. The use of finger-jointed timber may also reduce the timber-related impacts of the box columns since finger-jointed lumber is assembled from what is essentially waste in the dimensional lumber fabrication process. The HSS box and HSS round sections outperformed the timber columns and even the bamboo in some impact categories for both scenarios and are potential options for use. The erection process in all cases had negligible impacts as compared with other process steps.

The midpoint LCA results show that bamboo could be a sustainable alternative relative to other columns studied in both the US and Brazil but grouping and weighting of TRACI impact categories is needed to better compare the bamboo, timber, and steel alternatives. Furthermore, these results highlight the need for development and refinement of a database for bamboo life cycle inventories and the potential of future work in developing an environmental impact quantification based on structural parameters than can be integrated into the structural design process and standard design aides.

7.0   CONCLUSIONS

The objective of this work was to describe a research program aimed at assessing the performance of full-culm structural bamboo use in construction from perspectives of standard test method development, structural component strength, and environmental impact. Research is focused on the use of bamboo in its natural full-culm form rather than fabricated bamboo products and consideration is given to the appropriate social context of such bamboo construction: use as a locally available non-conventional building material. In consideration of this objective, several experimental studies were conducted. Detailed conclusions are found in each chapter.

7.1   ASSESSMENT OF STANDARD MATERIALS TEST METHODS

In the effort to highlight interferences present in current methods and practices in standard testing methods, the tensile tests presented in Chapter 3 sought to investigate the influence of bamboo fiber gradation and end restraint conditions on specimen performance since these factors are not currently considered in applicable standard test methods. Radially cut specimens were shown to have strengths similar to, yet nominally less than, the average strength values of tangentially cut specimens from the inner, middle, and outer layer of the culm wall thickness. Results of tests of radially-cut specimens were shown to be comparable to the strengths of

middle layer tangential specimens which imply a nonlinear fiber distribution with an order greater than one. Specimens with rotationally free end conditions were shown to have a higher average strength in all cases than those with fixed end conditions and it is believed that allowing end rotation caused longitudinal splitting failure which permitted redistribution of axial forces since strain compatibility across the section was no longer valid. The effects of restraining rotation were illustrated in the non-linear strain distributions captured with a VIC-3D imaging system for the free end constrained radial specimens. However, nonlinear strain was also seen in some tangential and fixed specimens. Overall, fiber density across the culm wall thickness and the end restraint conditions of the specimens were shown to have an influence on bamboo tensile test results and therefore must be considered in the development of improved standard test methods.

Modified ISO flexural tests, as discussed in Chapter 4, were conducted to assess the longitudinal shear strength (splitting) of bamboo resulting from flexure and to investigate development of standard testing practices for this mixed-mode failure. Flexural specimens, tested in four-point bending, were modified by cutting a notch having a depth equal to the culm radius, in the tension face of the culm at or near one loading point in order to isolate the point at which shear failure initiates. Full-culm tests produced lower shear strength values as compared to smaller clear specimens machined from the culm wall or current standard or proposed tests for Mode I (split-pin test) and Mode II (bowtie test) shear. This was found to be partially due to the mixed-mode nature of the splitting failure. Mode I tangential tensile strength perpendicular to the fibers was shown to be the main driver of longitudinal splitting and results suggested a ratio between Mode I, Mode II, and mixed mode capacities may exist. Development of an interaction ratio would potentially allow simple-to-conduct tests (such as the bowtie or the edge bearing

tests) to be used as surrogate tests for more-difficult-to-obtain values. Several drawbacks of the notched beam test configuration highlight the need for further testing in developing a standard test configuration for longitudinal splitting caused by flexure.

7.2   ASSESSMENT OF STRUCTURAL AND ENVIRONMENTAL PROPERTIES

As discussed in Chapter 5, understanding the behavior of multiple-culm columns offers a pathway to building larger and perhaps multi-story bamboo structures. Experimental buckling tests were conducted on full-scale single- and multiple-culm columns having slenderness ratios on the order of $L/r \sim 100$; these were characterized with respect to the Euler equation. The apparent effective length factor, K, for the full-height specimens was shown to be closer to 1 than to the value predicted in control tests for the end restraint considered. This was potentially due to flexure-induced rotation causing local crushing at the culm ends as well as variability in the cross section and initial culm out-of-straightness. Results from single culm specimens appeared to confirm the need for initial out-of straightness and taper to be considered for the thicker-walled Tre Gai specimens. Multiple-culm column specimens exhibited load redistribution as weaker constituent culms began to fail and observed column behavior was best represented by the sum of the individual culms (apparent moment of inertia $I_{column} = \Sigma I_{culm}$) rather than by the gross section properties ($I_{column} = I_g$) of the multiple-culm column. Three shorter columns tested suggest a significant reduction in load capacity for slenderness ratios $L/r < 75$ as compared to the experimentally determined crushing strength and expected Euler buckling loads.

In terms of environmental impacts associated with material use, bamboo has many perceived qualitative benefits but only a limited number of studies have looked at quantifying the

relative environmental impacts of bamboo use. The intent of the midpoint life-cycle-analysis reported in Chapter 6 was to compare the environmental performance of the structural bamboo column from Chapter 5 with structurally comparable timber and steel alternatives. While the results did not produce a clear sustainable option between the bamboo, timber, and steel columns or the two scenarios studied (fabrication and use in US and Brazil), LCIA profiles did show that transportation to the erection site and the steel bolt fastening system used contributed the most to the environmental impacts of the bamboo column in both the US and Brazilian scenarios. When used in a domestic context (Brazil scenario), environmental impacts of bamboo decreased in five of nine impact categories: global warming, acidification, non-carcinogens, eutrophication, and smog as compared to US use, where bamboo must be imported. The phenol-resorcinol-formaldehyde resin and processing contributed the most to the environmental impacts of the built-up box timber column alternative in both scenarios. The HSS box and HSS round sections outperformed the timber columns and even the bamboo in some of the impact categories for both scenarios and therefore remain potential options for use.

7.3   FUTURE WORK

The current work highlights the need for further development of standard testing methods as well as design criteria for bamboo structural components. One of the primary limit states seen in all the experimental studies undertaken in this work (tension, flexure, and buckling tests), and in most other studies cited throughout this dissertation, was longitudinal splitting failures induced by flexure. Therefore, further tests are needed to create a larger data set in order that this limit state can be characterized properly using a refined standard test method. However, in addition to

specific recommendations made based on each of the experimental studies herein and reported in each chapter, the work also points to broader future areas of research that can aid in furthering the body of knowledge on the utilization of structural bamboo.

7.3.1   Modeling of bamboo as a functionally graded material

The bamboo tensile testing conducted illustrated the influence of culm wall fiber gradation on the strength results of the standard test procedure. The functionally graded material (FGM) nature of bamboo must be considered in the development of standard test procedures and design criteria. Therefore, modeling the mechanical behavior of FGMs like bamboo is an important area of future study, specifically, characterization and modeling of the fracture and splitting behavior of bamboo. Fracture and fatigue modeling has been studied for wood and a summary is provided in Smith et al. (2003). Techniques for fracture modeling of wood include statistical fracture models (SFMs); fictitious crack models and bridging models that use Linear Elastic Fracture Mechanics (LEFM); finite element models; morphology-based models; lattice models; and damage models. With respect to bamboo, Silva et al. (2006) developed a finite element model of a bamboo culm section (Fig. 7-1a). The study considered the use of a) graded finite brick elements; b) a homogeneous orthotropic model; and c) an isotropic homogeneous model. Results showed the homogenized orthotropic model to be the stiffest while the graded elements capture the highest stresses at the bamboo wall exterior. Nonetheless, the isotropic homogeneous model was found to be suitable for capturing global behavior. Sharma (2010) developed a beam element model of a bamboo frame which was used to compare model results with results from an experimental pushover frame test (Fig. 7-1b). However, the beam element model only considered deterioration of the bamboo column base connections and no degradation in the

stiffness of the bamboo elements. Villalobos et al (2011) developed a proposed 2D SFM based on the drying fracture process in specimens of bamboo *Quadua angustifolia*. Ultimately, development of bamboo structural component models will provide a crucial tool in helping to predict the behavior and performance of a multitude of bamboo species and bamboo structural systems in addition to studying modification factors to future design equations. They would also serve as a foundation for future more comprehensive models.

a) Bamboo internode finite element model by Silva et al. (2006)

b) Beam element model frame (Sharma 2010)
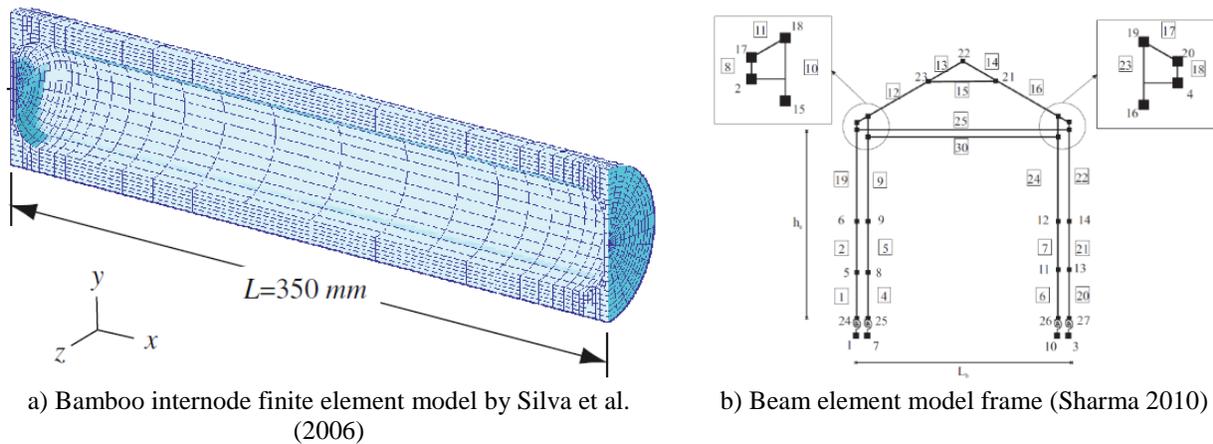
Figure 7-1: Modeling of structural bamboo components

7.3.2   Performance of bamboo jointing techniques

The longitudinal splitting seen in the experimental buckling capacity of bamboo columns (chapter 5) occurred in all cases at the short-dowel end condition at the top of the column. Ultimately, as discussed in Section 2.2.2, the development of effective jointing techniques for bamboo structures and understanding their performance and capacity is crucial to understanding the performance of an entire bamboo component or structural system. Sharma (2010), in the study of the seismic performance of a representative bamboo portal frame, also states that research on bamboo jointing, specifically force-displacement relationships of connections and identification of limit states, is crucial for understanding the performance of bamboo building

systems. Furthermore, the results of the LCIA in chapter 6 of this work illustrate that the fastening system currently considered for multiple-culm columns (galvanized steel bolts), contributed significantly to the environmental impacts of the entire column. Therefore, conventional (steel bolts), traditional (wrapping or binding), and non-conventional jointing techniques for bamboo must also be assessed with respect to environmental impacts.

7.3.3   Bamboo LCI Database and Structural Design LCA Parameter

As discussed in chapter 6, the establishment of a bamboo LCI database which compiles data for various agriculture, treatment, production, use, and disposal processes for bamboo would allow for environmental impacts to be better determined for the multitude of bamboo species, products, and uses. A standard database would also allow for better comparison between studies of the environmental sustainability of using bamboo products in a variety of domestic and global contexts. A bamboo LCI database would also eliminate many process assumptions that currently need to be made in assessments and highlight areas requiring more research and data collection. Further, the LCIA studied in chapter 6 highlights the need for environmental impact parameters that can be linked to structural design properties of structural components allowing for easier comparison of environmental impacts for building alternatives and determining sustainable options during the structural design process.

7.4   SUMMARY

With the benefits of rapid renewability, global accessibility, and good strength properties, bamboo has great potential as an alternative structural building material that can add to the global construction resource base. The pathway to standardization is the development of standard testing procedures that are applicable both in laboratory and field settings as well as establishment of design criteria for dominant limit states, particularly longitudinal splitting. The current study sought to assess standard bamboo testing methods as well as the performance of structural bamboo components (beams and columns). Standard tensile tests as prescribed by ISO 22157 (2004b) were conducted to assess the test interferences associated with the functionally graded nature of the bamboo culm. Resulting strength and nonlinear strain distributions showed that behavior is affected by these variables and therefore must be considered in the standard test procedure. Full-scale single- and multiple-culm column tests were also conducted to investigate the experimental buckling strength with respect to the Euler equation commonly used in design. Column tests showed that multiple-culm columns had an effective moment of inertia equal to the sum of individual culm components and that shorter columns exhibited a reduction in strength beyond that predicted by the Euler equation. Further tests are needed to better characterize the strength versus slenderness curve for bamboo columns.

The study also illustrated that longitudinal splitting is a dominant limit state for bamboo components tested in various manners and longitudinal splitting induced by flexure was seen in both the tensile and buckling tests. Therefore, a modified ISO flexural test for full-culm bamboo was developed and tested as a standard longitudinal splitting test prototype. The tests showed a reduction in shear strength as compared to smaller clear bamboo specimens testing in bending or bowtie shear tests. Similar ratios between results of the mixed mode failure seen in the full-culm

206

tests and results of the split-pin test (Mode I failure) and the bowtie test (Mode II failure) for two different bamboo species suggest that an underlying relationship may exist that could be used in establishing future design or material testing criteria.

A comparative midpoint life-cycle-impact-analysis (LCIA) was conducted to compare environmental impacts associated with constructing the experimental bamboo column studied with timber and steel alternatives of similar capacity. Results, although requiring weighting of impacts to reach a definitive conclusion, suggest that bamboo is best used in a domestic setting where it is readily available. Steel alternatives were also shown to be a viable alternative (depending on impact category considered) as compared with the bamboo and timber options considered. The need for environmental impact parameters related to structural capacity properties and to account for structural shapes was cited. Overall the work highlights the need for further testing and characterization of bamboo structural components to aid in furthering the standardization and utilization of this promising non-conventional building material.

APPENDIX A

SUMMARY OF RESULTS FROM BAMBOO TENSION TESTS

The following appendix presents the complete strength and strain profile results from the experimental tension test program conducted in Chapter 3.

Table A-1: Tension Test Strength Results

Specimen	Culm	Internode	Quadrant	Layer	Area	Area	Peak Load	Peak Load	Peak Strength	Peak Strength
					sq mm	sq in	kN	kips	MPa	ksi
1	TG1	1	C1	Radial	92	0.142	7.5	1.7	82.2	11.9
2	TG1	5	C1	Radial	80	0.124	8.7	1.9	108.6	15.8
3	TG1	6	C1	Radial	73	0.114	9.7	2.2	131.8	19.1
4	TG1	7	C1	Radial	71	0.110	9.5	2.1	134.1	19.5
5	TG1	8	C1	Radial	73	0.113	8.5	1.9	116.8	16.9
6	TG1	9	C1	Radial	63	0.097	14.2	3.2	225.7	32.7
7	TG1	10	C1	Radial	64	0.099	12.3	2.8	192.0	27.8
8	TG1	11	C1	Radial	54	0.083	11.5	2.6	215.6	31.3
9	TG21	11	C1	Radial	80	0.124	7.6	1.7	95.3	13.8
10	TG21	12	C1	Radial	77	0.120	8.2	1.8	106.4	15.4
11	TG21	13	C1	Radial	78	0.120	6.7	1.5	86.3	12.5
12	TG1	1	D1	Radial	82	0.127	4.7	1.1	56.9	8.2
13	TG1	5	C2	Radial	73	0.114	7.9	1.8	107.4	15.6
14	TG1	6	C2	Radial	75	0.116	10.1	2.3	134.9	19.6
15	TG1	7	C2	Radial	69	0.106	10.2	2.3	149.1	21.6
16	TG1	8	C2	Radial	71	0.110	9.4	2.1	133.2	19.3
17	TG1	9	C2	Radial	61	0.095	9.4	2.1	152.7	22.1
18	TG1	10	C2	Radial	63	0.098	11.3	2.5	178.0	25.8
19	TG1	11	C2	Radial	56	0.087	11.0	2.5	195.5	28.4
20	TG21	11	C2	Radial	80	0.125	7.6	1.7	94.5	13.7
21	TG21	12	C2	Radial	76	0.118	6.4	1.4	84.2	12.2
22	TG21	13	C2	Radial	75	0.116	6.6	1.5	88.2	12.8
23	TG1	1	D2	Radial	83	0.129	3.6	0.8	42.9	6.2
24	TG1	1	A (North)	Outer	103	0.159	12.9	2.9	125.4	18.2
25	TG1	5	A (North)	Outer	113	0.175	20.8	4.7	184.5	26.8
26	TG1	6	A (North)	Outer	109	0.169	22.0	4.9	202.3	29.3
27	TG1	7	A (North)	Outer	107	0.166	19.7	4.4	183.8	26.7
28	TG1	8	A (North)	Outer	103	0.159	15.1	3.4	147.1	21.3
29	TG1	9	A (North)	Outer	93	0.144	24.6	5.5	263.9	38.3
30	TG1	10	A (North)	Outer	105	0.163	23.2	5.2	219.9	31.9
31	TG1	11	A (North)	Outer	111	0.172	24.5	5.5	220.7	32.0
32	TG21	11	A (North)	Outer	107	0.166	20.0	4.5	186.4	27.0
33	TG21	12	A (North East)	Outer	107	0.166	14.7	3.3	136.7	19.8
34	TG21	13	A (North East)	Outer	94	0.145	18.1	4.1	192.8	28.0
35	TG1	1	A (North)	Middle	100	0.155	6.9	1.5	68.8	10.0
36	TG1	5	A (North)	Middle	110	0.170	16.3	3.7	148.9	21.6
37	TG1	6	A (North)	Middle	110	0.170	18.9	4.3	172.2	25.0
38	TG1	7	A (North)	Middle	102	0.158	18.7	4.2	183.0	26.5
39	TG1	8	A (North)	Middle	68	0.105	10.8	2.4	159.3	23.1
40	TG1	9	A (North)	Middle	91	0.141	15.5	3.5	170.7	24.8

209

				Table A-1 (continued)						
41	TG21	11	A (North)	Middle	107	0.165	9.2	2.1	86.4	12.5
42	TG21	12	A (North East)	Middle	105	0.163	11.7	2.6	111.0	16.1
43	TG21	13	A (North East)	Middle	68	0.105	5.9	1.3	87.6	12.7
44	TG1	1	A (North)	Inner	86	0.134	2.5	0.6	29.3	4.3
45	TG1	5	A (North)	Inner	86	0.134	8.9	2.0	103.2	15.0
46	TG1	6	A (North)	Inner	81	0.125	9.7	2.2	120.4	17.5
47	TG1	7	A (North)	Inner	72	0.112	8.0	1.8	111.3	16.1
48	TG1	8	A (North)	Inner	110	0.171	12.6	2.9	114.1	16.8
49	TG1	9	A (North)	Inner	68	0.105	9.1	2.0	133.4	19.3
50	TG1	10	A (North)	Inner	116	0.179	17.5	3.9	150.8	21.9
51	TG1	11	A (North)	Inner	103	0.159	15.4	3.5	150.0	21.8
52	TG21	11	A (North)	Inner	88	0.137	3.6	0.8	40.8	5.9
53	TG21	12	A (North East)	Inner	100	0.155	5.3	1.2	53.1	7.7
54	TG21	13	A (North East)	Inner	90	0.140	3.7	0.8	41.6	6.0
55	TG1	5	B (South)	Outer	110	0.170	22.8	5.1	208.4	30.2
56	TG1	6	B (South)	Outer	101	0.156	17.0	3.8	169.1	24.5
57	TG1	7	B (South)	Outer	107	0.166	17.2	3.9	160.3	23.3
58	TG1	8	B (South)	Outer	106	0.165	18.0	4.1	169.3	24.6
59	TG1	9	B (South)	Outer	105	0.163	15.7	3.5	149.7	21.7
60	TG1	10	B (South)	Outer	107	0.166	18.1	4.1	168.9	24.5
61	TG1	11	B (South)	Outer	91	0.141	14.2	3.2	156.0	22.6
62	TG21	11	B (South)	Outer	105	0.163	13.8	3.1	131.6	19.1
63	TG21	12	B (South)	Outer	111	0.172	23.7	5.3	213.4	30.9
64	TG21	13	B (South)	Outer	110	0.171	22.2	5.0	201.1	29.2
65	TG1	5	B (South)	Middle	104	0.162	17.6	4.0	169.0	24.5
66	TG1	6	B (South)	Middle	94	0.146	16.8	3.8	178.3	25.9
67	TG1	7	B (South)	Middle	79	0.122	12.0	2.7	152.4	22.1
68	TG1	8	B (South)	Middle	105	0.163	12.8	2.9	121.9	17.7
69	TG1	9	B (South)	Middle	65	0.100	8.7	2.0	134.3	19.5
70	TG1	11	B (South)	Middle	50	0.077	6.1	1.4	123.0	17.8
71	TG21	11	B (South)	Middle	77	0.119	5.8	1.3	75.3	10.9
72	TG21	12	B (South)	Middle	97	0.150	11.9	2.7	122.7	17.8
73	TG1	5	B (South)	Inner	93	0.144	10.7	2.4	115.0	16.7
74	TG1	6	B (South)	Inner	91	0.142	11.9	2.7	130.3	18.9
75	TG1	7	B (South)	Inner	87	0.135	7.1	1.6	81.6	11.8
76	TG1	8	B (South)	Inner	63	0.098	6.5	1.5	103.3	15.0
77	TG1	9	B (South)	Inner	84	0.130	6.5	1.5	76.9	11.2
78	TG1	10	B (South)	Inner	126	0.196	18.1	4.1	143.5	20.8
79	TG1	11	B (South)	Inner	78	0.122	8.6	1.9	109.7	15.9
80	TG21	11	B (South)	Inner	89	0.138	3.7	0.8	41.2	6.0
81	TG21	12	B (South)	Inner	76	0.117	5.0	1.1	65.6	9.5
82	TG21	13	B (South)	Inner	132	0.204	10.0	2.2	75.9	11.0
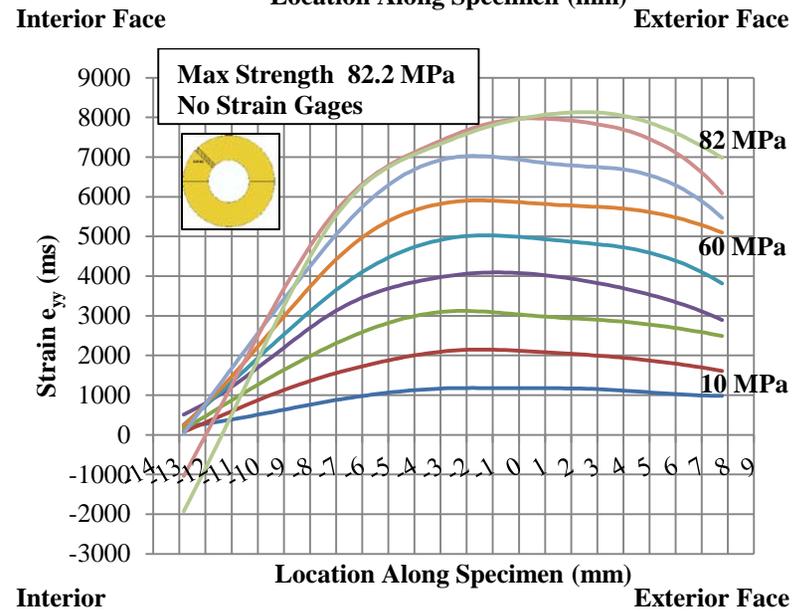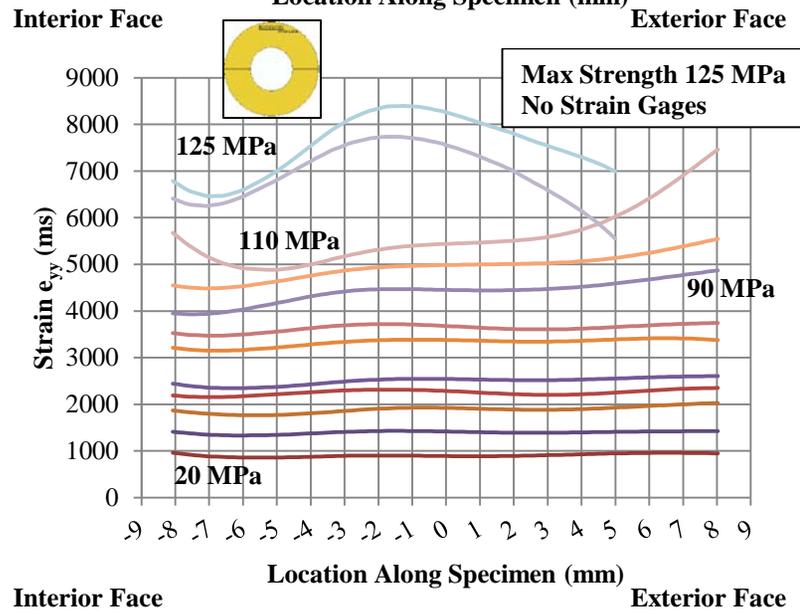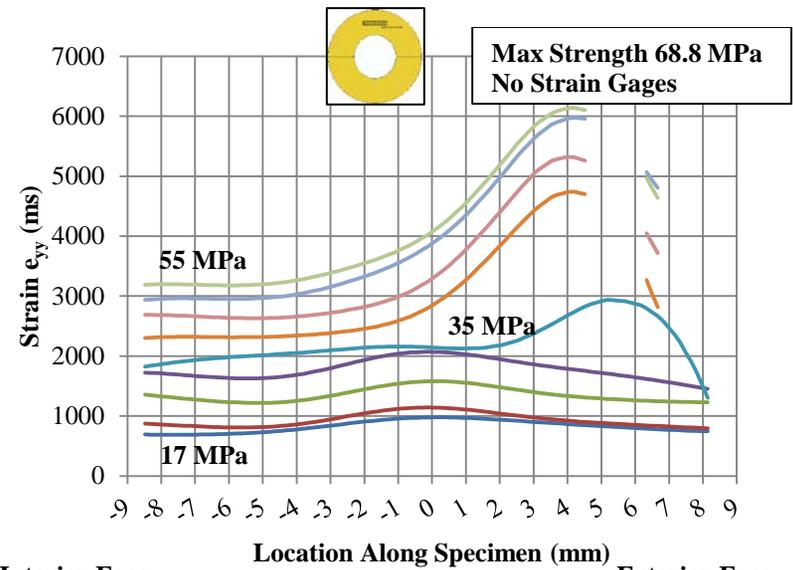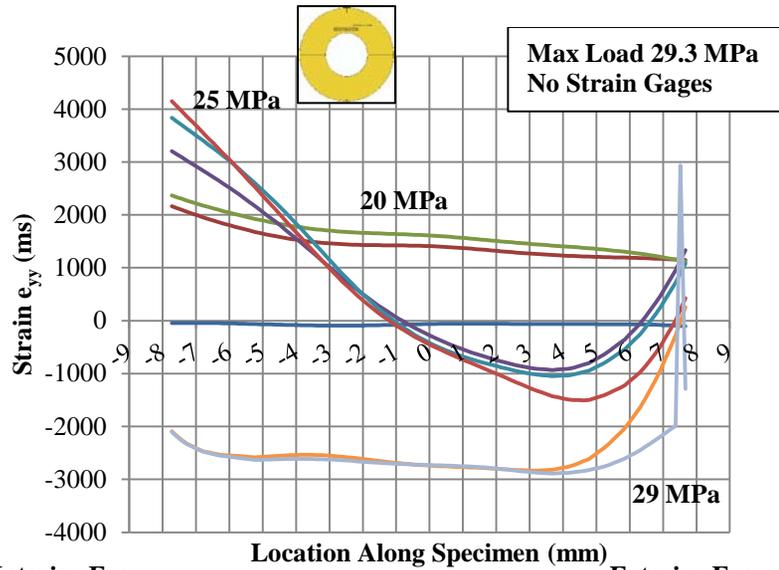
Figure A-1: Specimen TG1-1 (Free): Inner (Upper Left), Middle (Upper Right), Outer (Lower Left), & Radial (Lower Right)

211
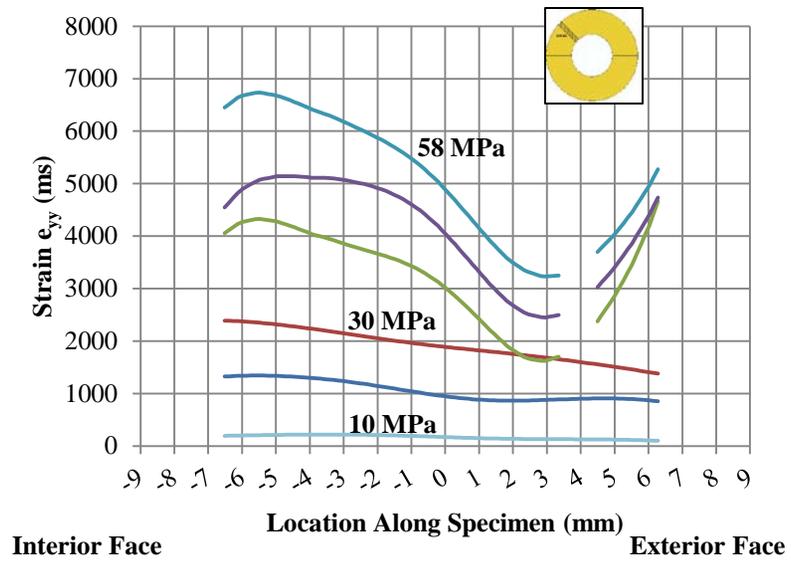
Figure A-2: Specimen TG1-1 (Free): 2nd Radial
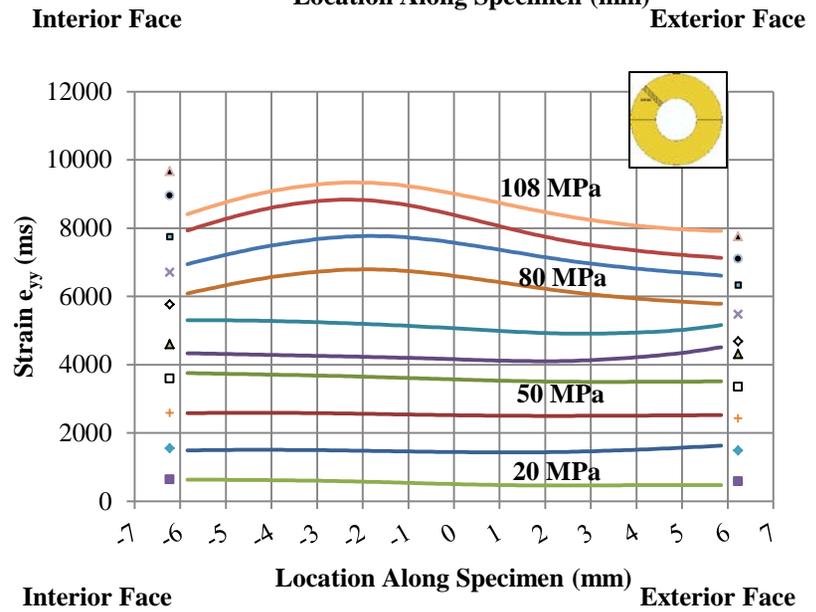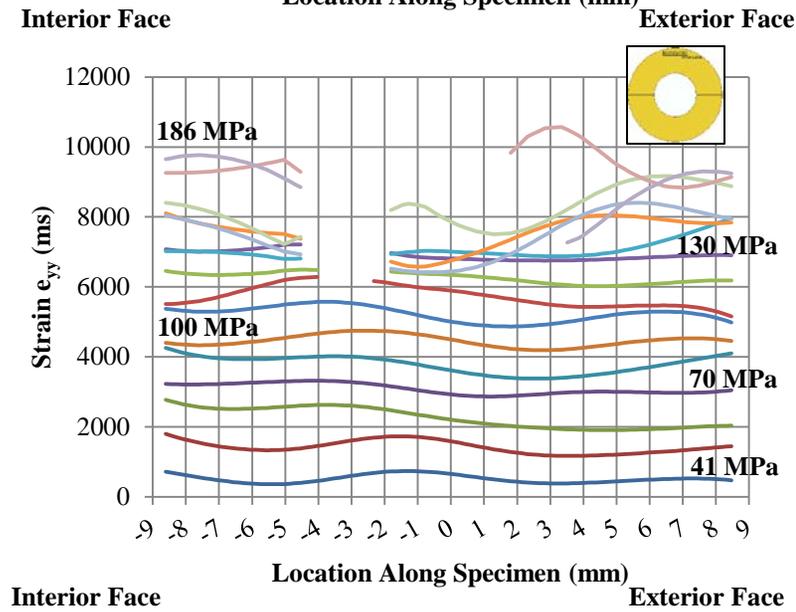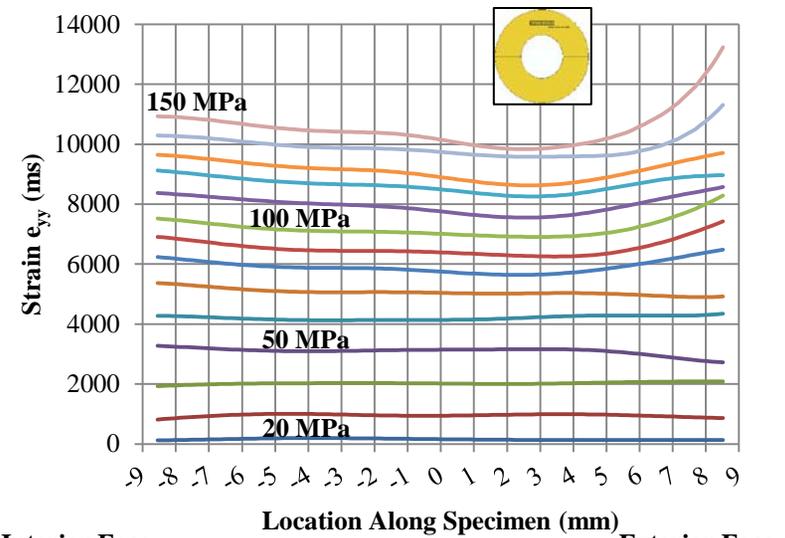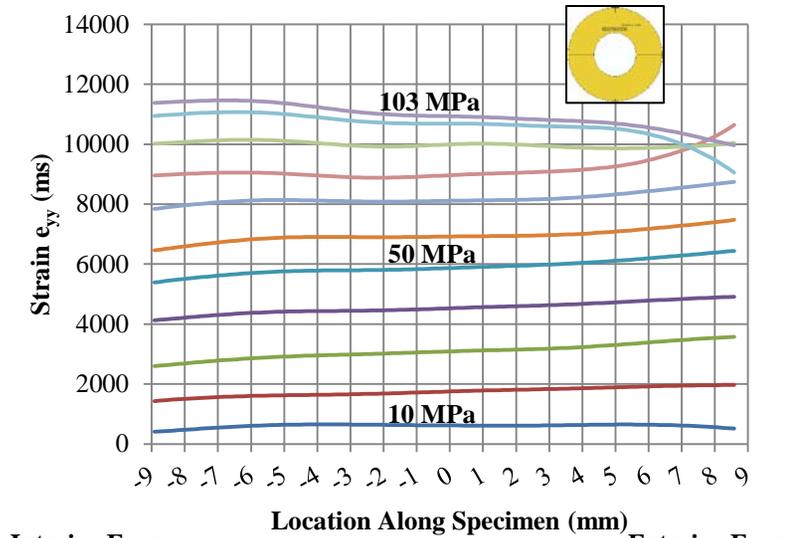
Figure A-3: Specimen TG1-5 (Free): Inner (Upper Left), Middle (Upper Right), Outer (Lower Left), & Radial (Lower Right)

213
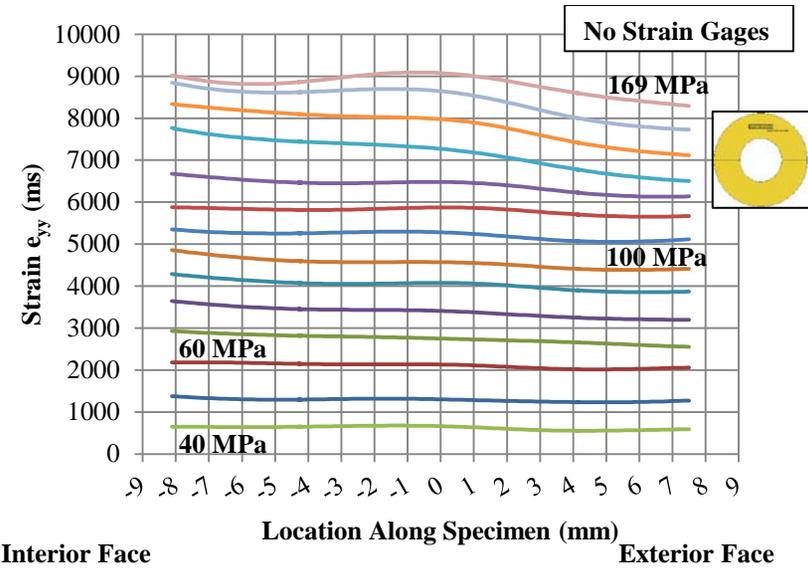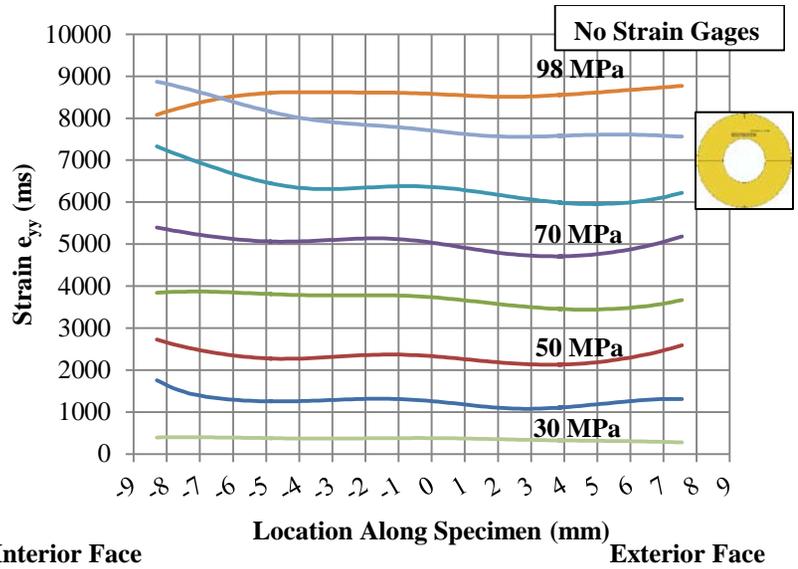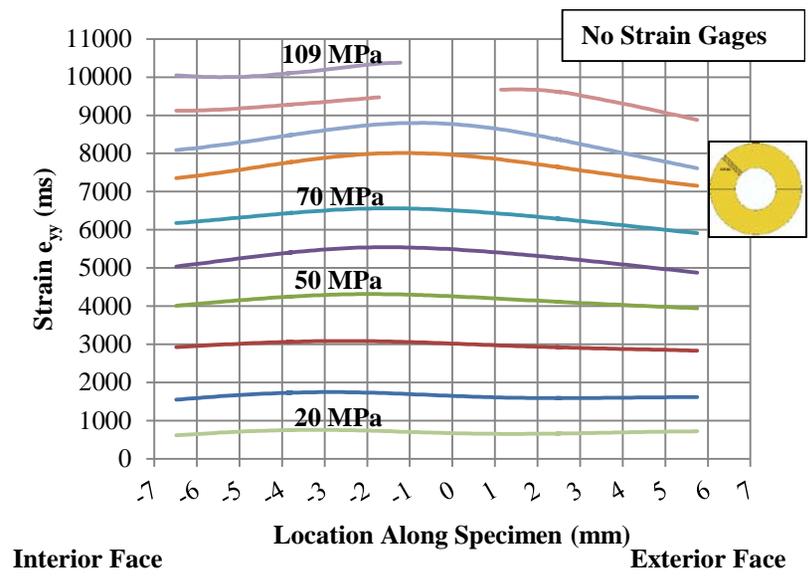
Figure A-4: Specimen TG1-5 (Fixed): Inner (Upper Left), Middle (Upper Right), Outer (Lower Left), & Radial (Lower Right)

214
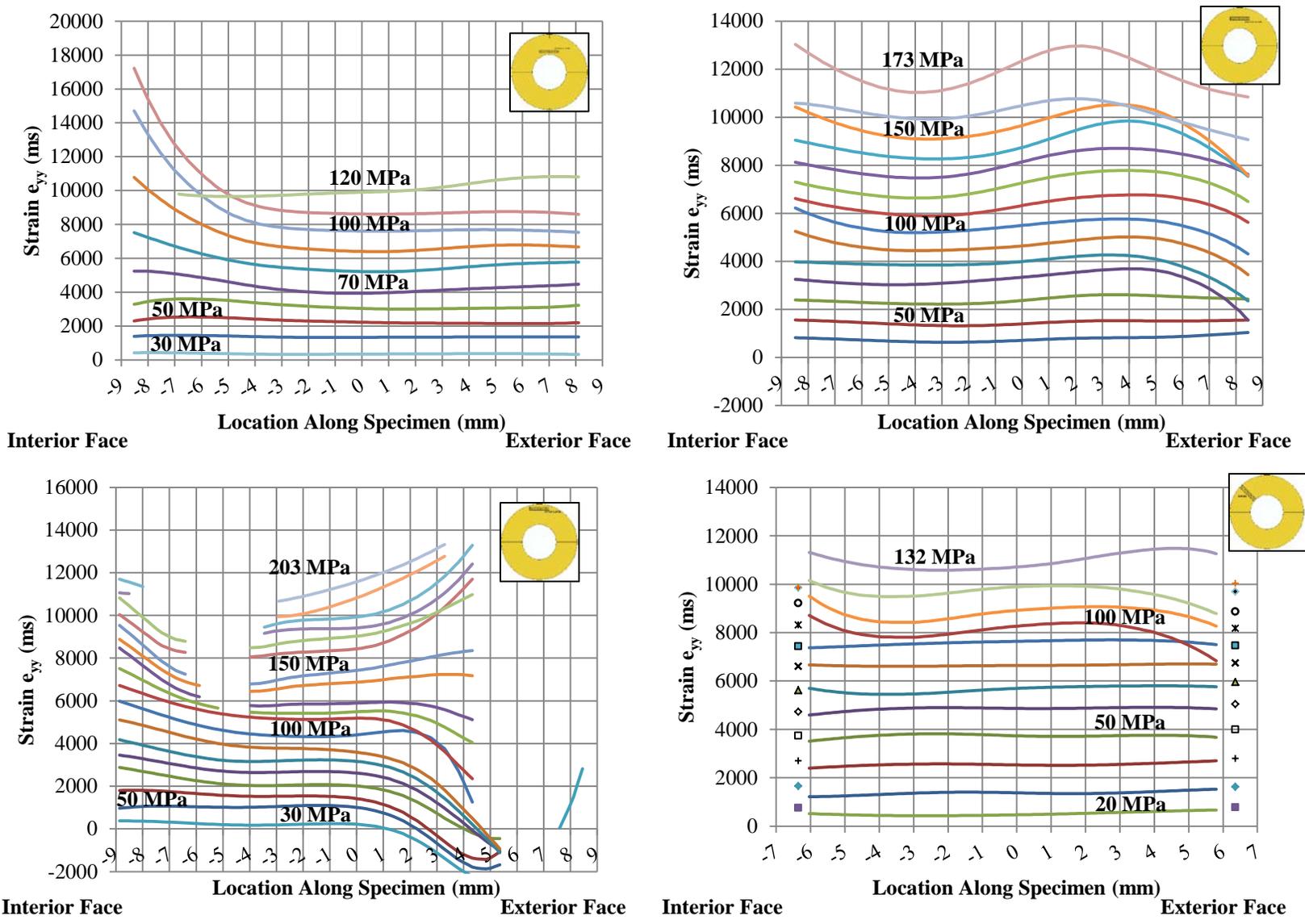
Figure A-5: Specimen TG1-6 (Free): Inner (Upper Left), Middle (Upper Right), Outer (Lower Left), & Radial (Lower Right)
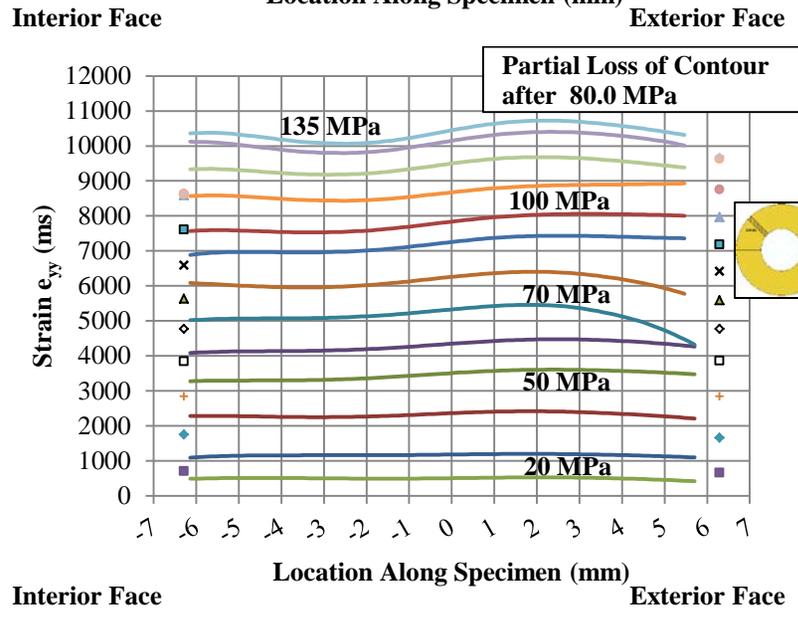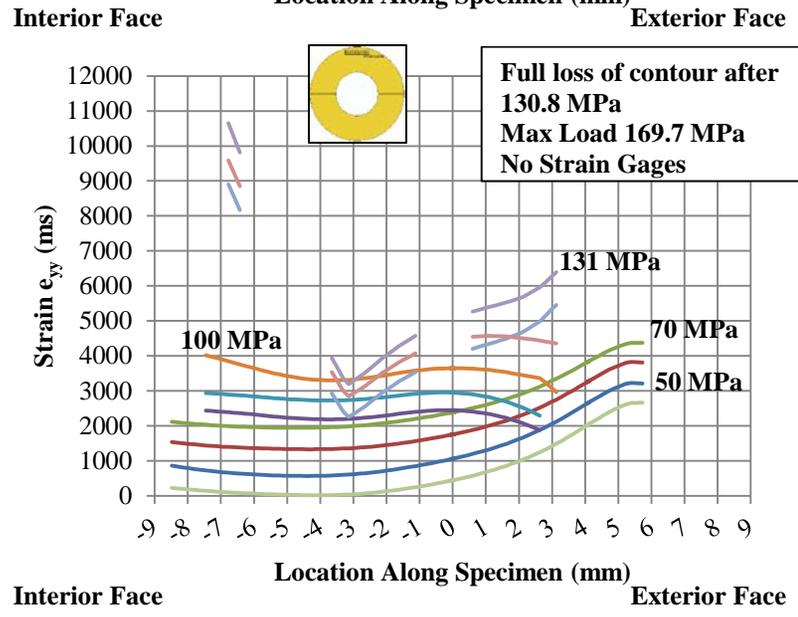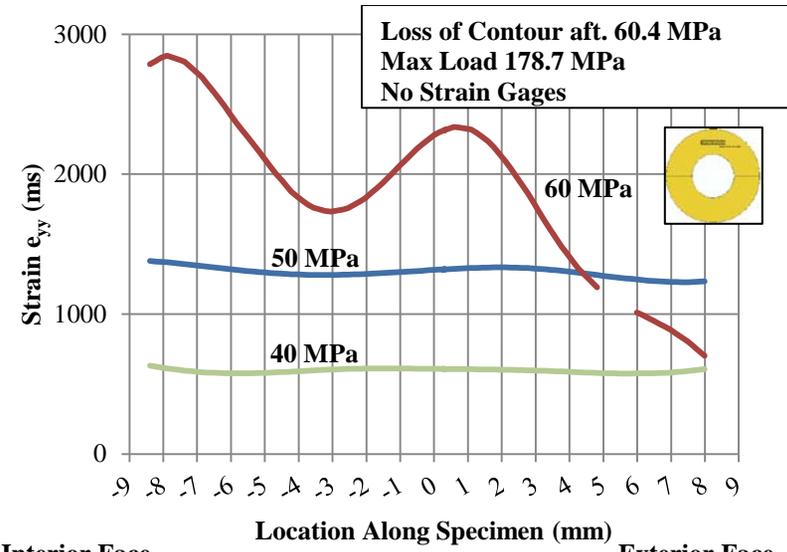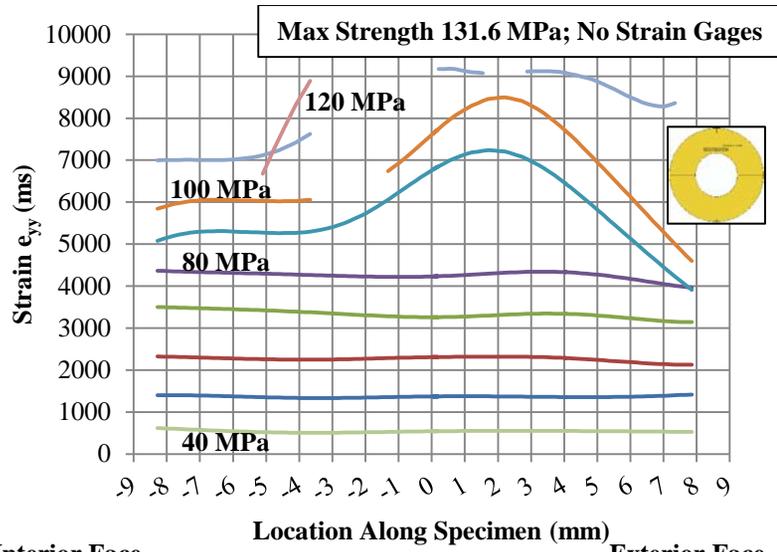
Figure A-6: Specimen TG1-6 (Fixed): Inner (Upper Left), Middle (Upper Right), Outer (Lower Left), & Radial (Lower Right)
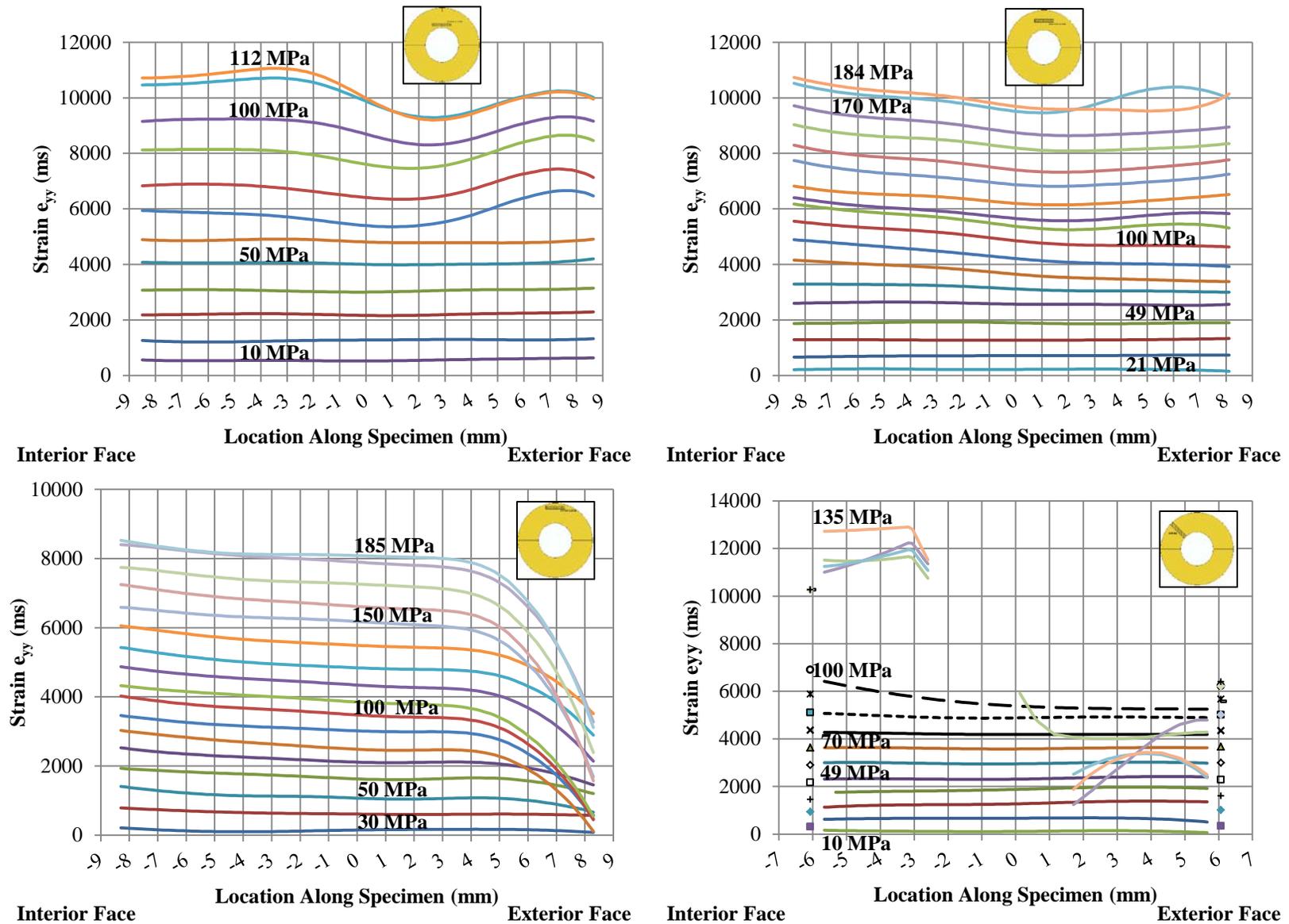
Figure A-7: Specimen TG1-7 (Free): Inner (Upper Left), Middle (Upper Right), Outer (Lower Left), & Radial (Lower Right)
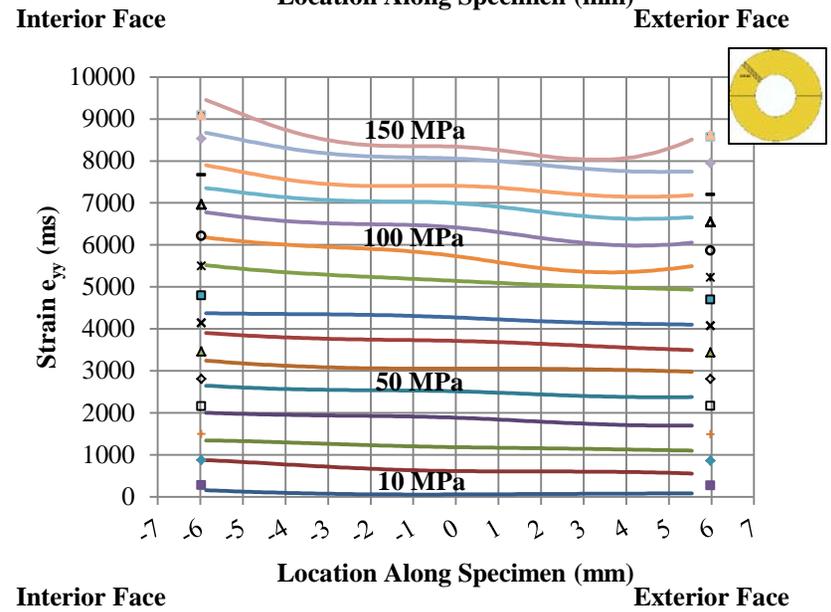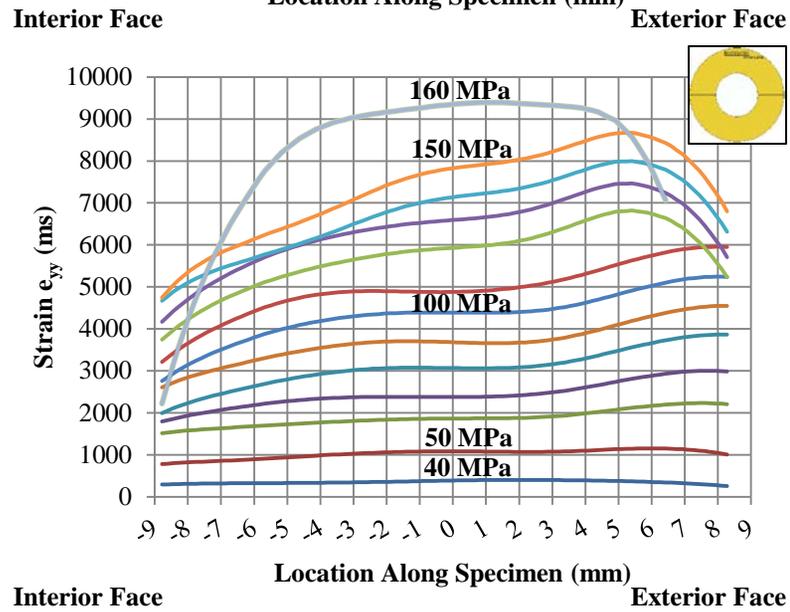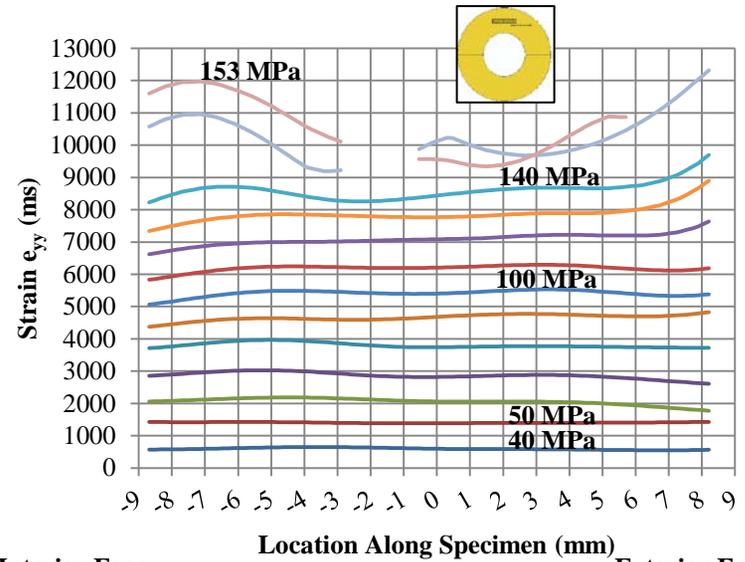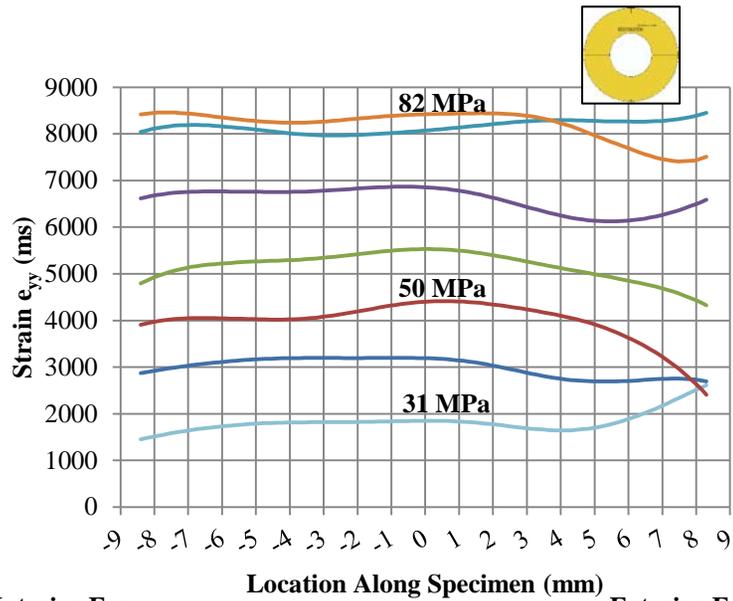
Figure A-8: Specimen TG1-7 (Fixed): Inner (Upper Left), Middle (Upper Right), Outer (Lower Left), & Radial (Lower Right)

218
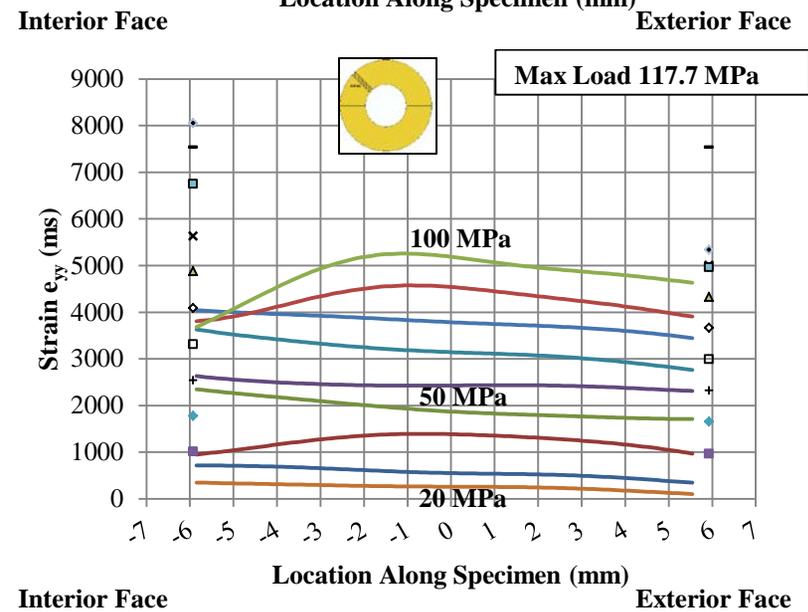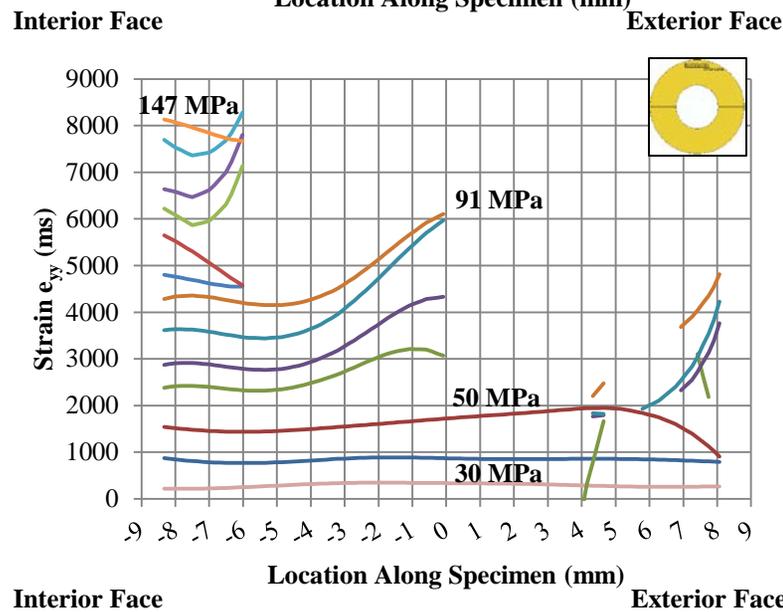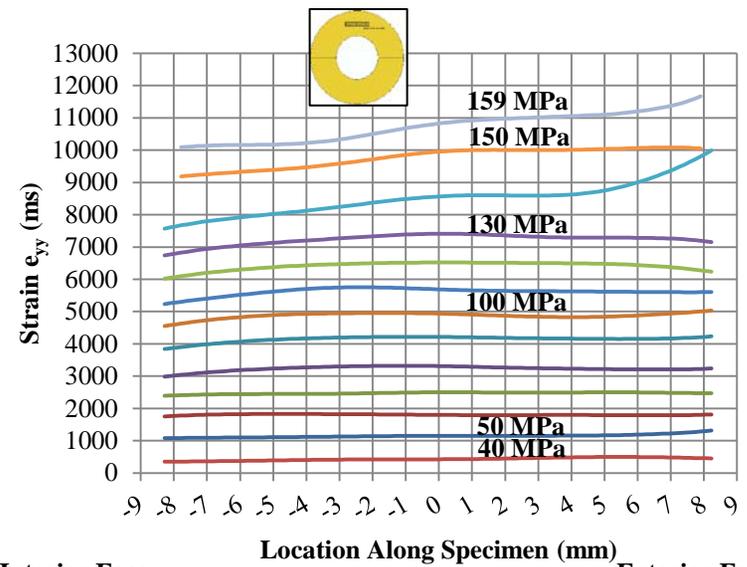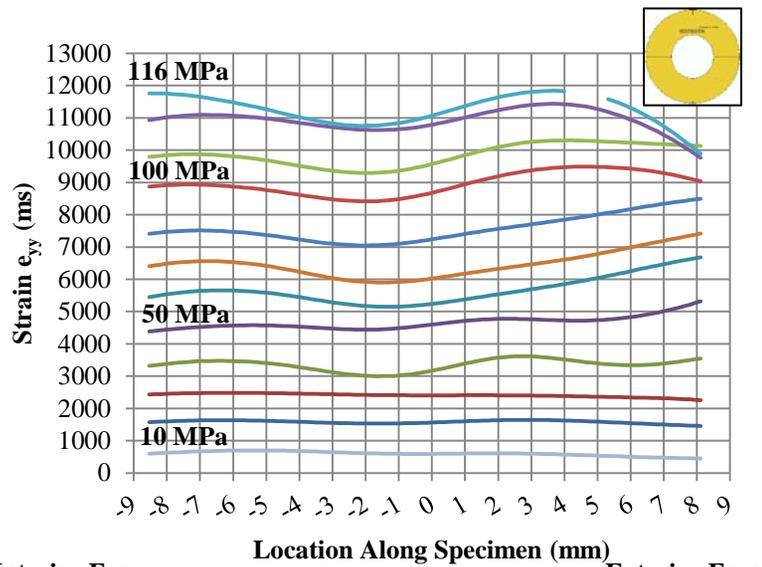
Figure A-9: Specimen TG1-8 (Free): Inner (Upper Left), Middle (Upper Right), Outer (Lower Left), & Radial (Lower Right)

219
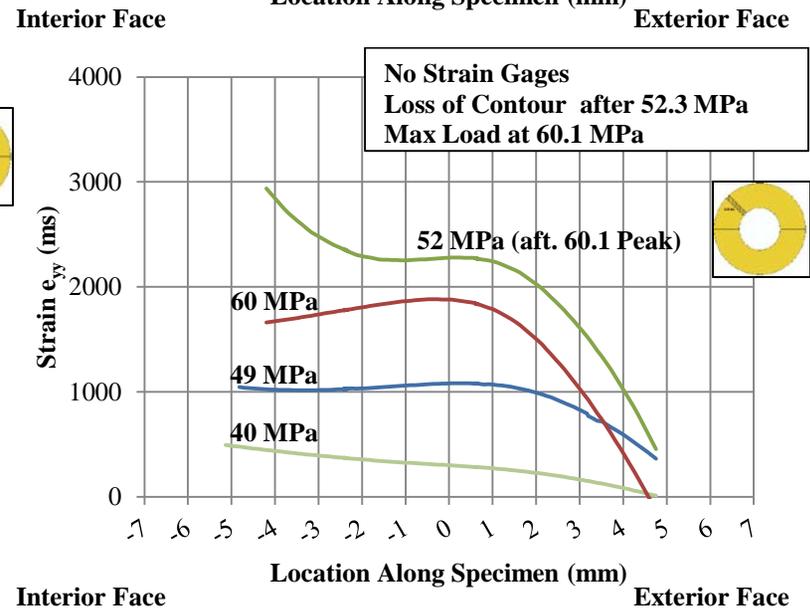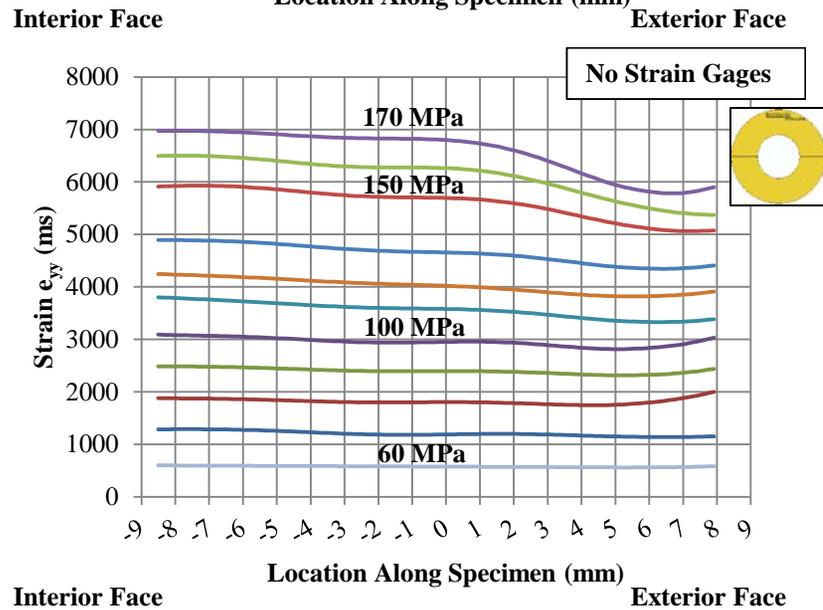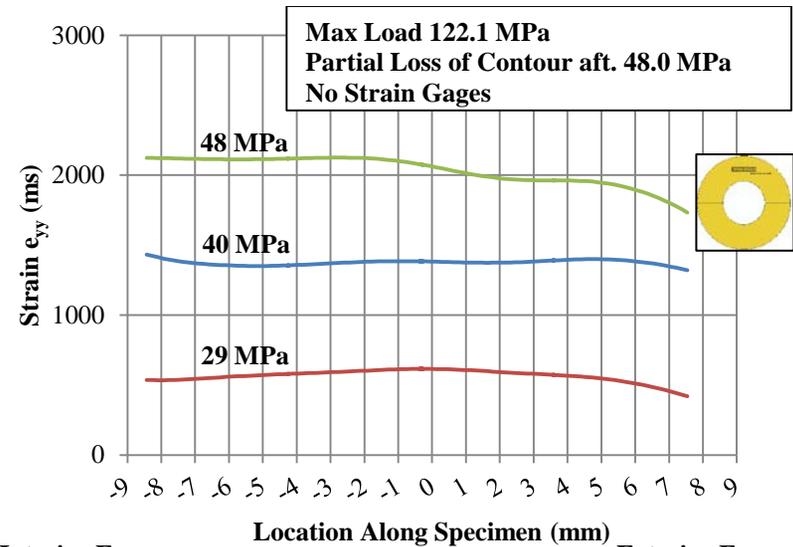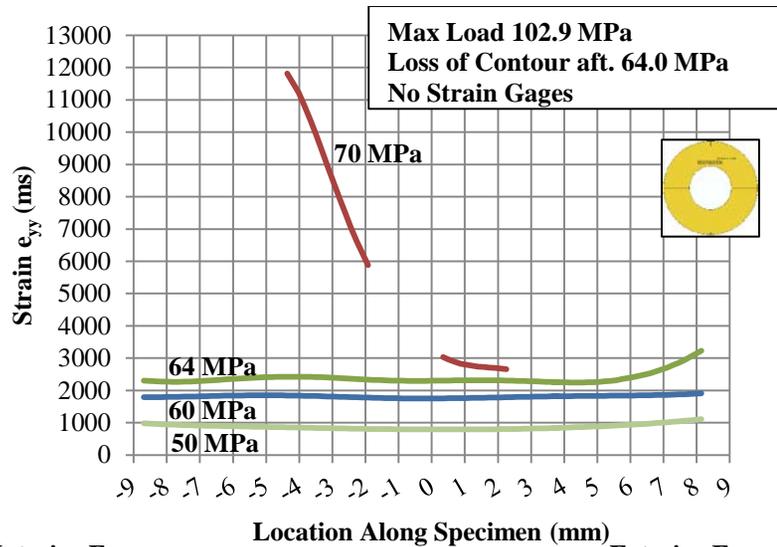
Figure A-10: Specimen TG1-8 (Fixed): Inner (Upper Left), Middle (Upper Right), Outer (Lower Left), & Radial (Lower Right)
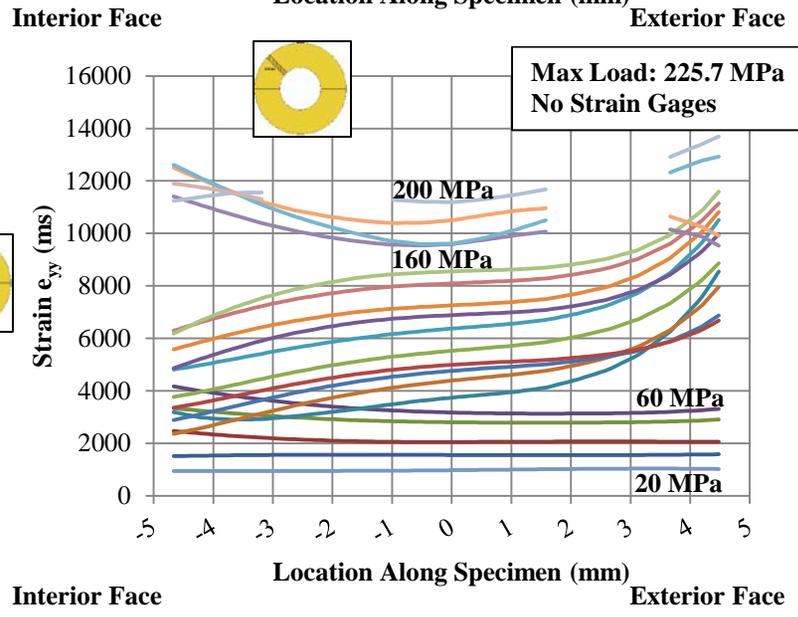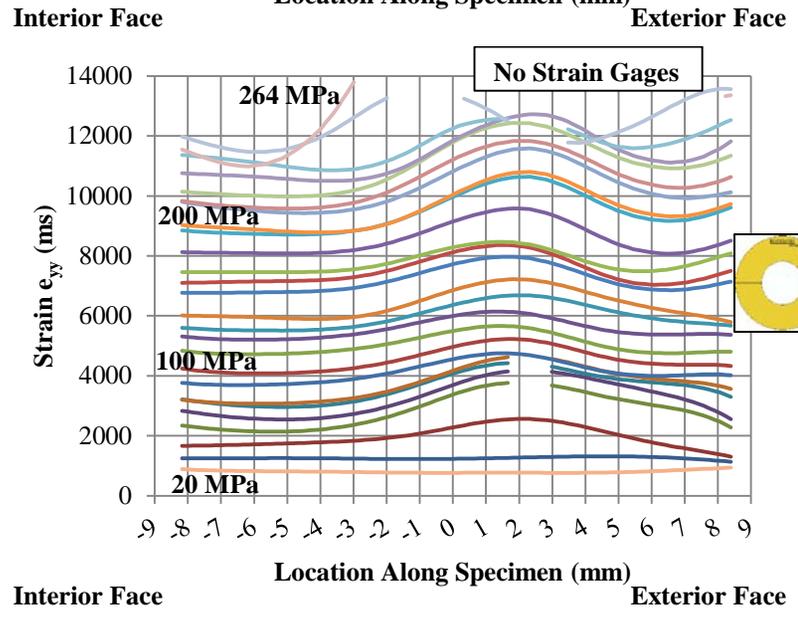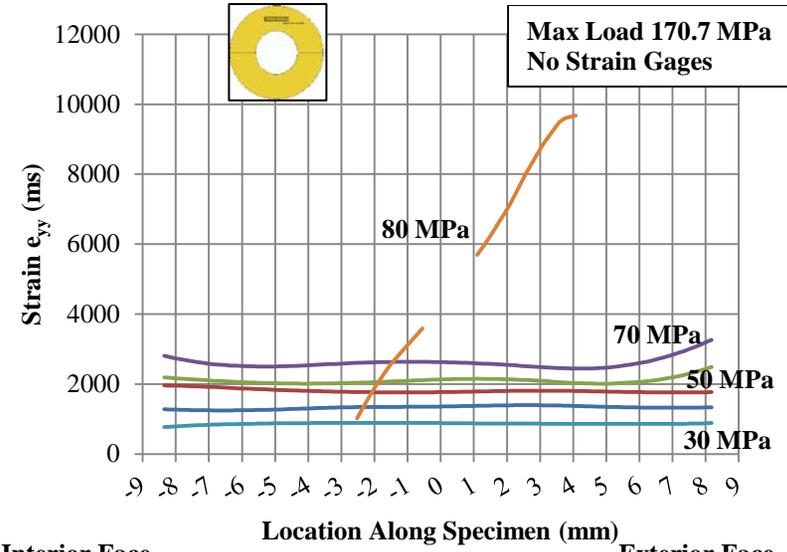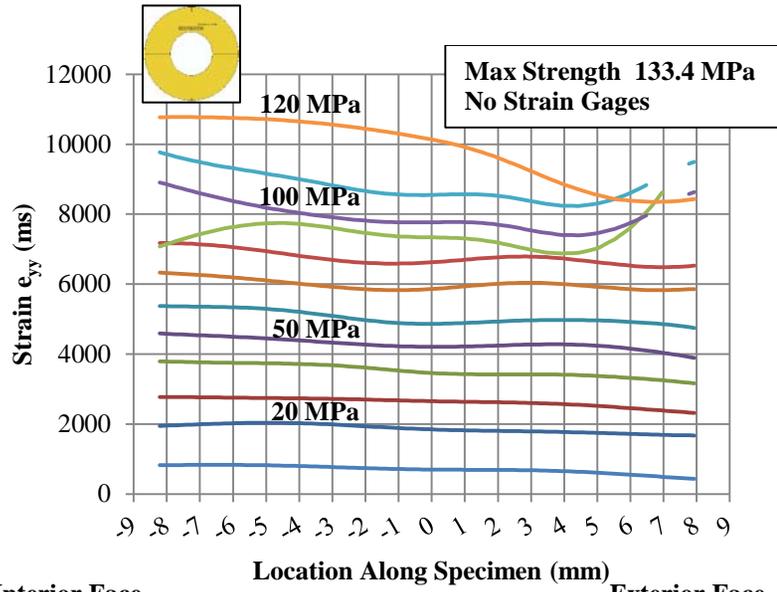
Figure A-11: Specimen TG1-9 (Free): Inner (Upper Left), Middle (Upper Right), Outer (Lower Left), & Radial (Lower Right)

221
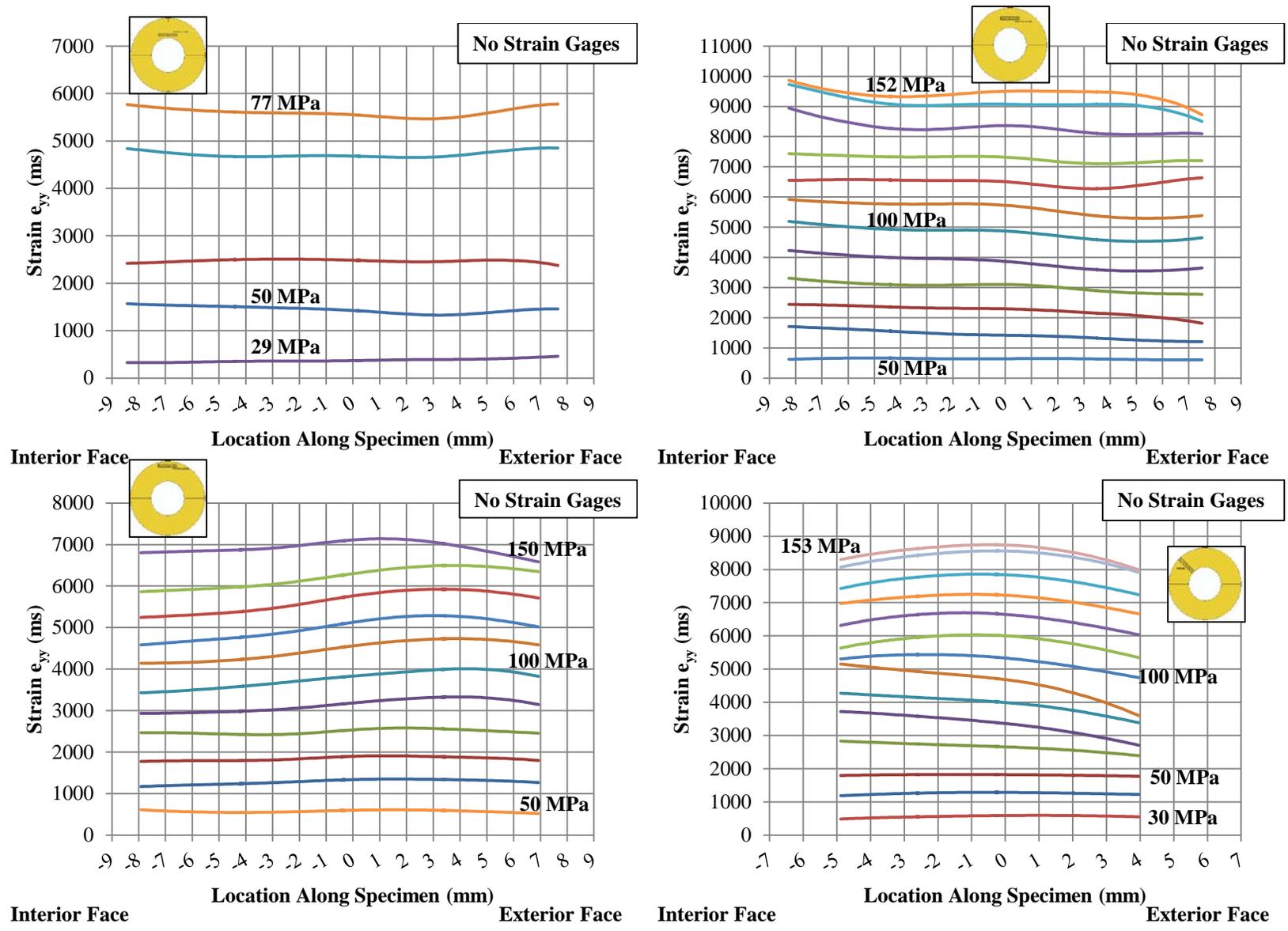
Figure A-12: Specimen TG1-9 (Fixed): Inner (Upper Left), Middle (Upper Right), Outer (Lower Left), & Radial (Lower Right)
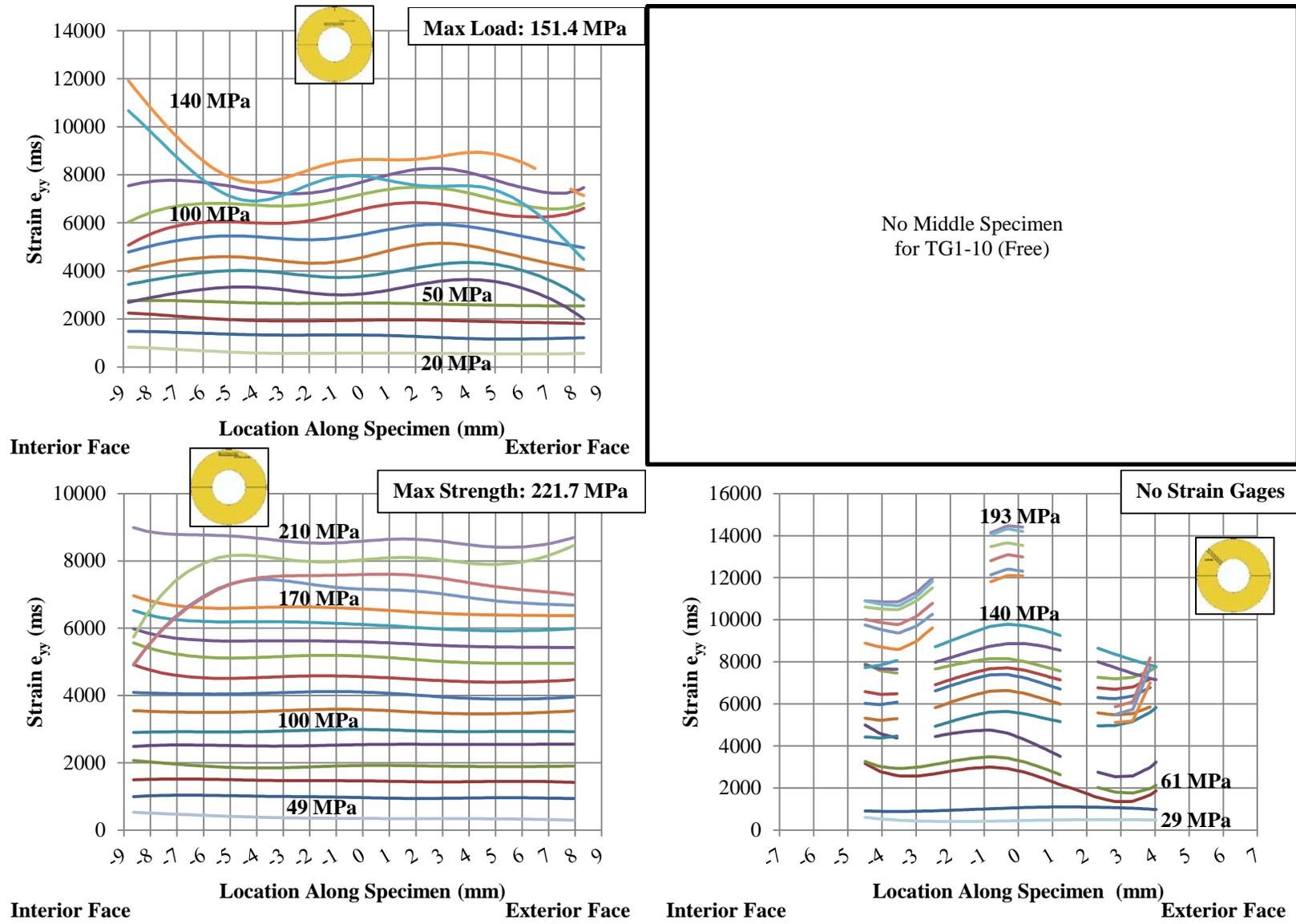
Figure A-13: Specimen TG1-10 (Free): Inner (Upper Left), Middle (Upper Right), Outer (Lower Left), & Radial (Lower Right)

223
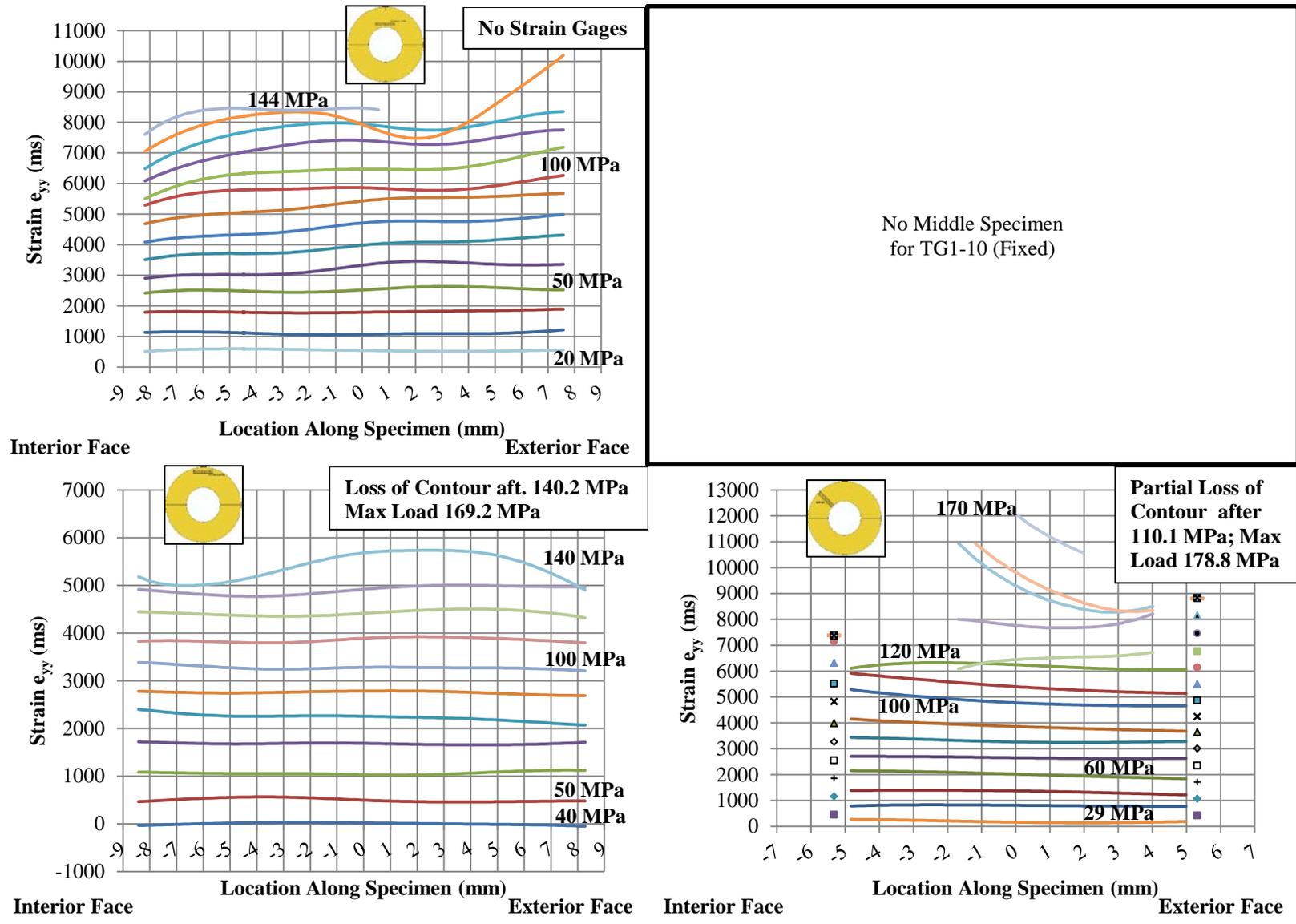
Figure A-14: Specimen TG1-10 (Fixed): Inner (Upper Left), Middle (Upper Right), Outer (Lower Left), & Radial (Lower Right)

224
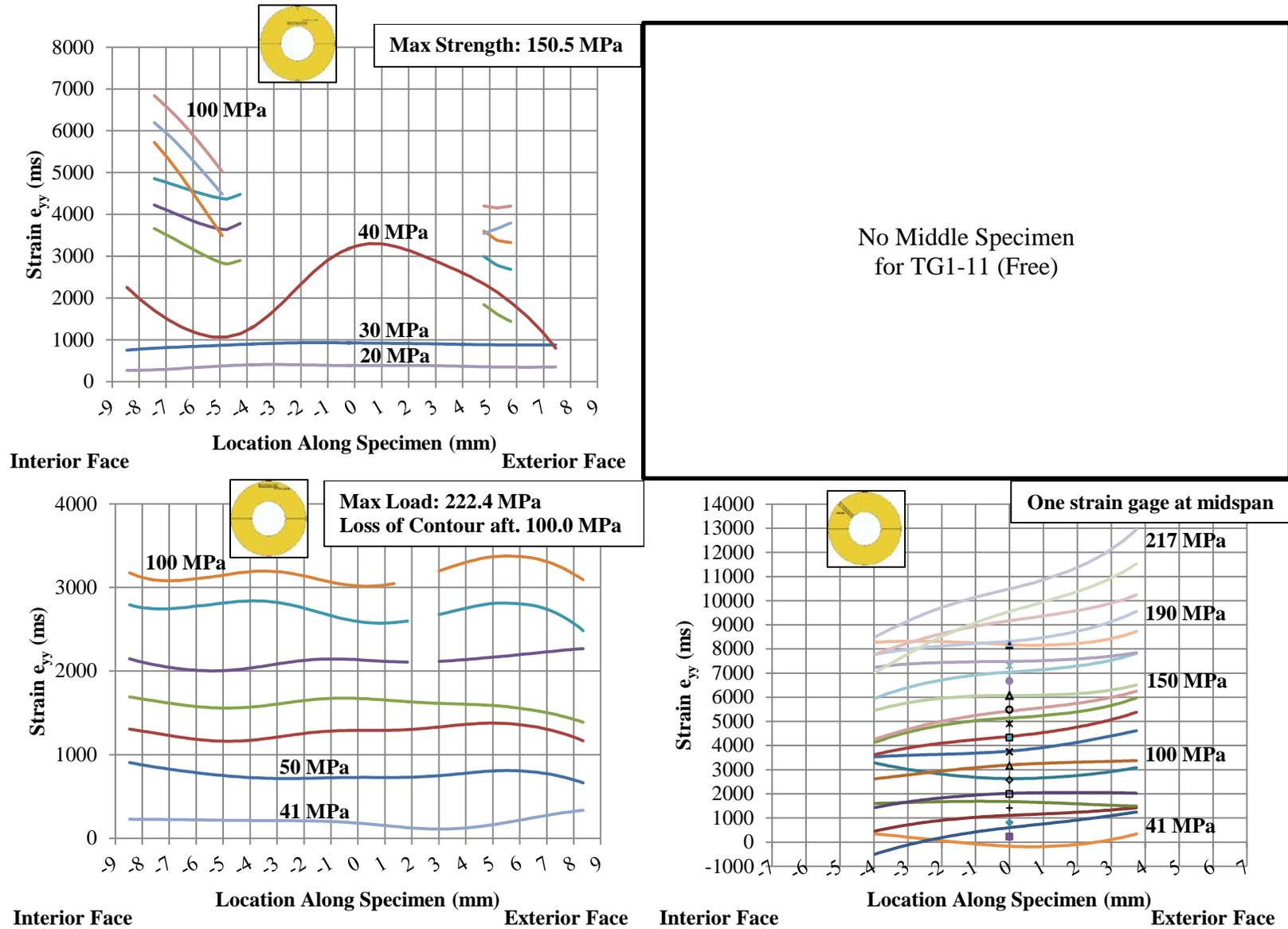
Figure A-15: Specimen TG1-11 (Free): Inner (Upper Left), Middle (Upper Right), Outer (Lower Left), & Radial (Lower Right)

225
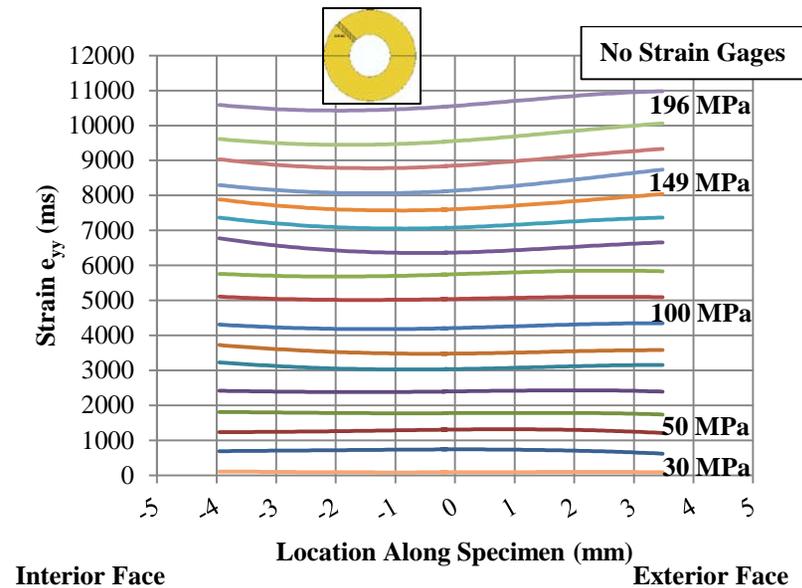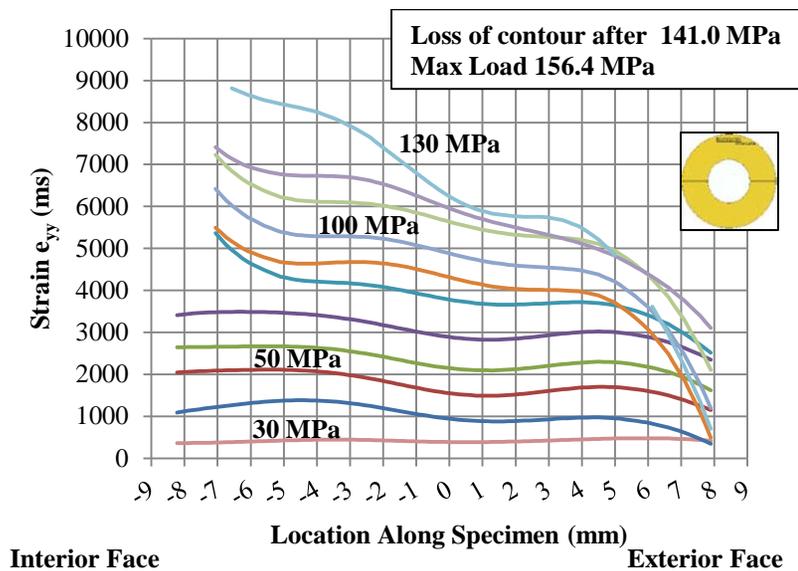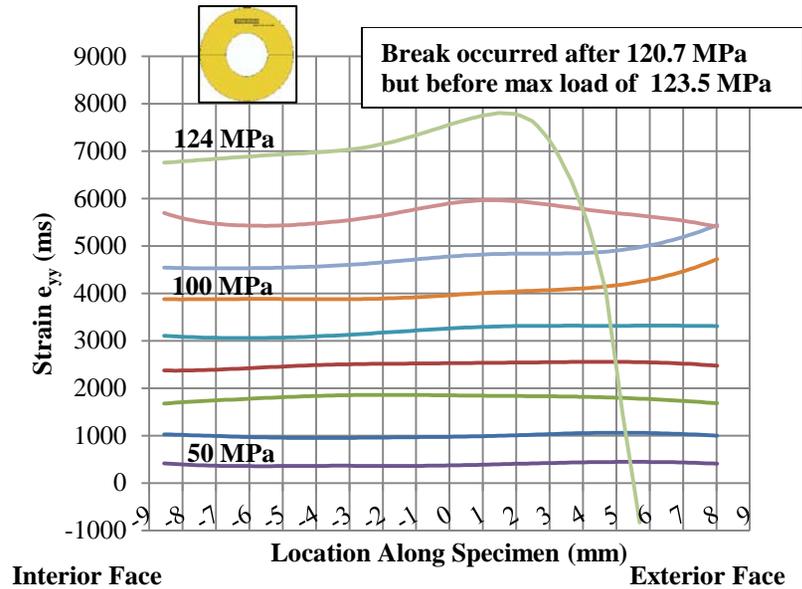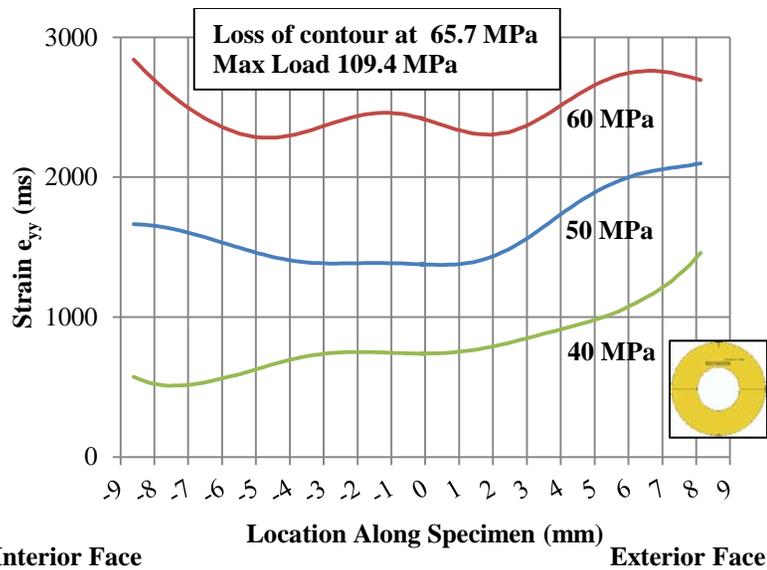
Figure A-16: Specimen TG1-11 (Fixed): Inner (Upper Left), Middle (Upper Right), Outer (Lower Left), & Radial (Lower Right)
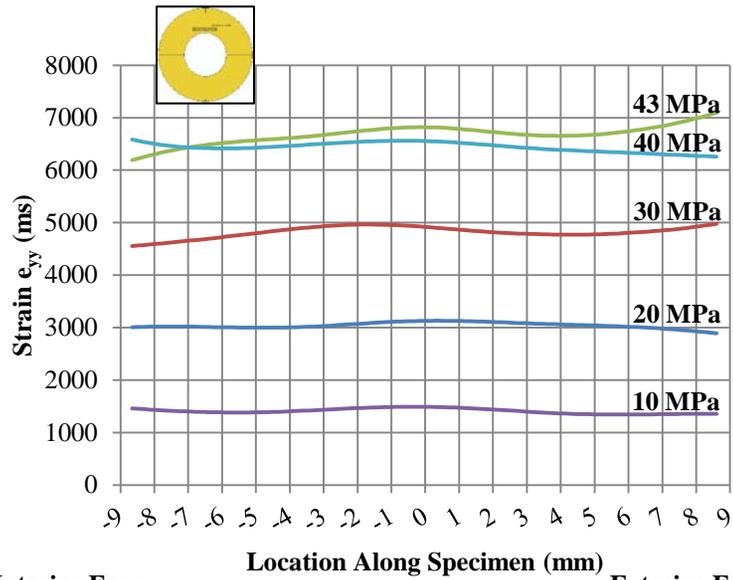
226
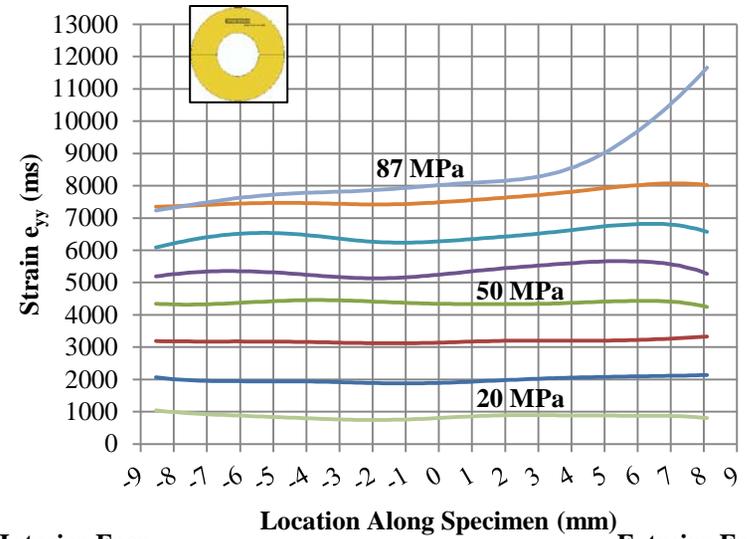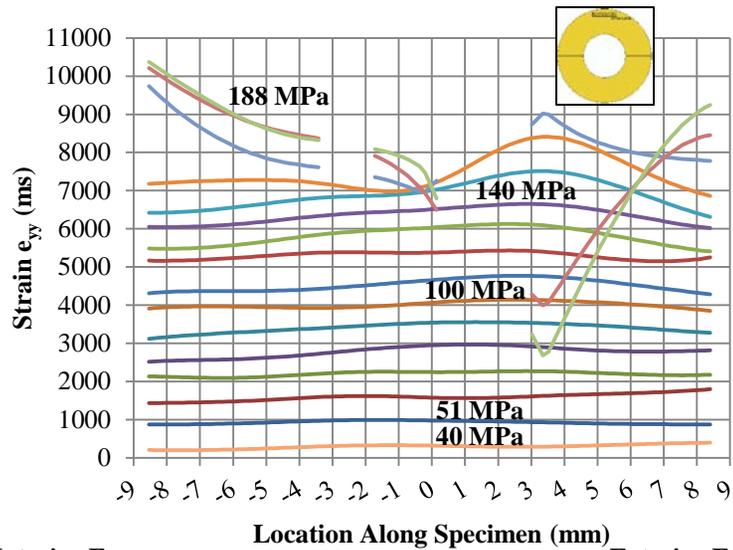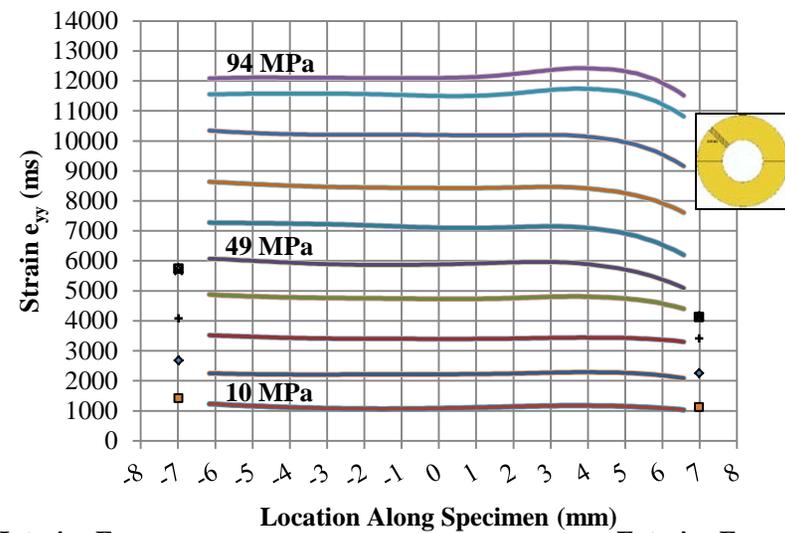
Figure A-17: Specimen TG21-11 (Free): Inner (Upper Left), Middle (Upper Right), Outer (Lower Left), & Radial (Lower Right)

227
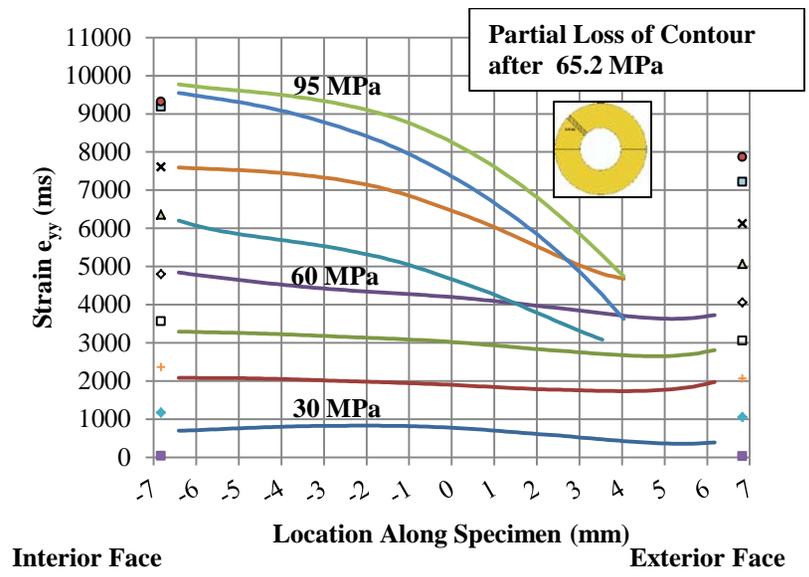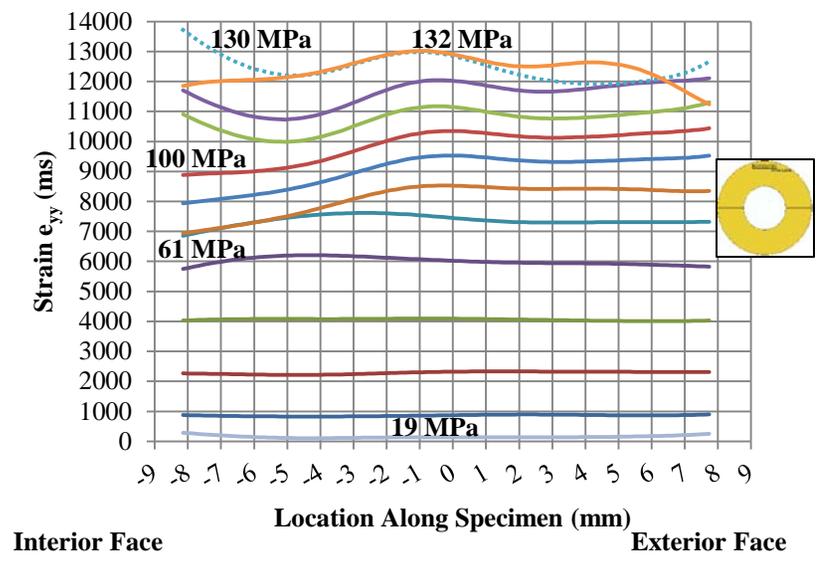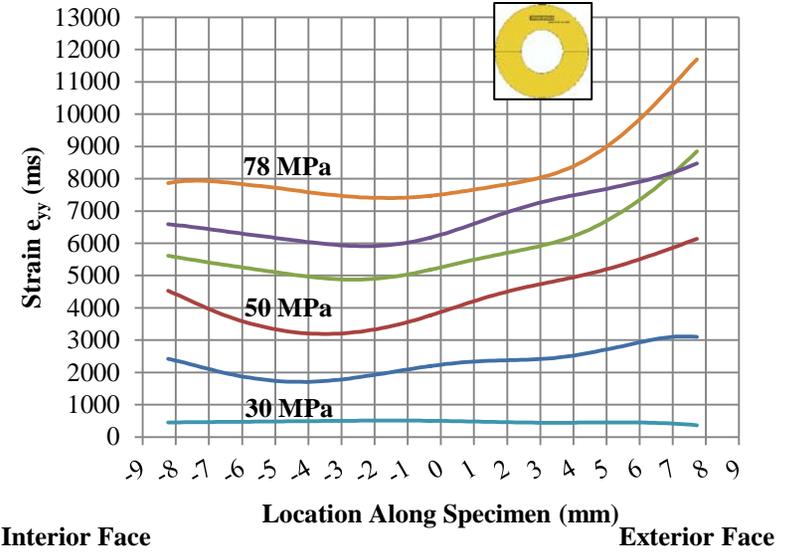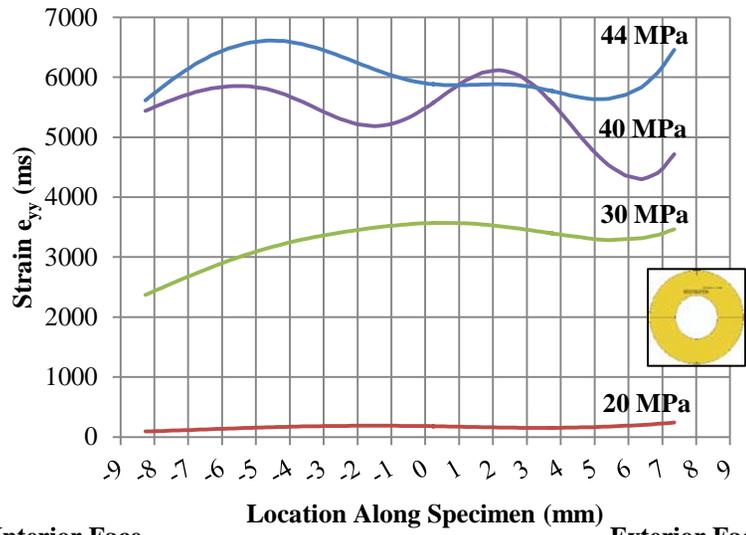
Figure A-18: Specimen TG21-11 (Fixed): Inner (Upper Left), Middle (Upper Right), Outer (Lower Left), & Radial (Lower Right)
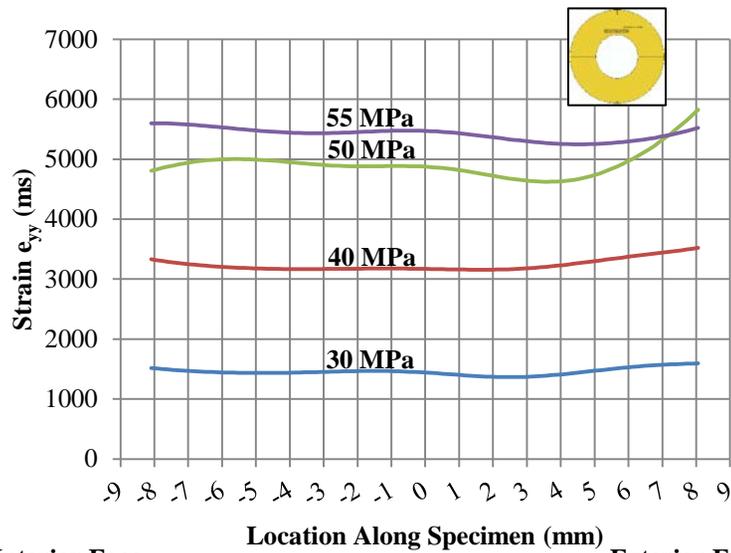
228
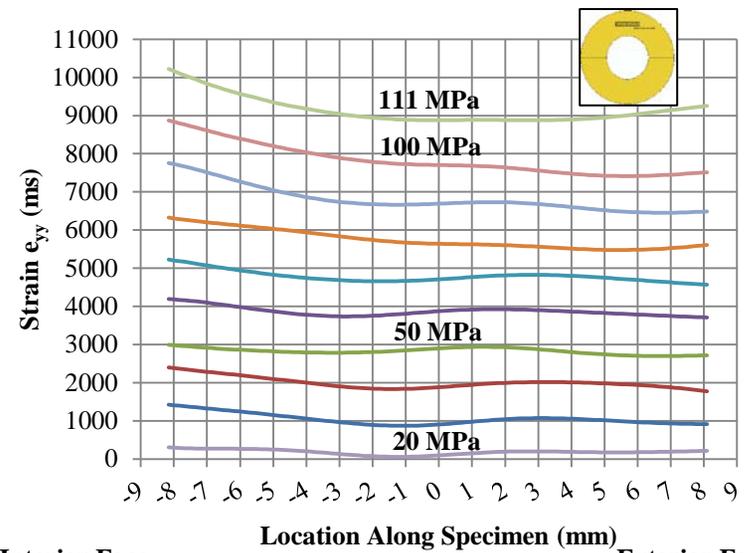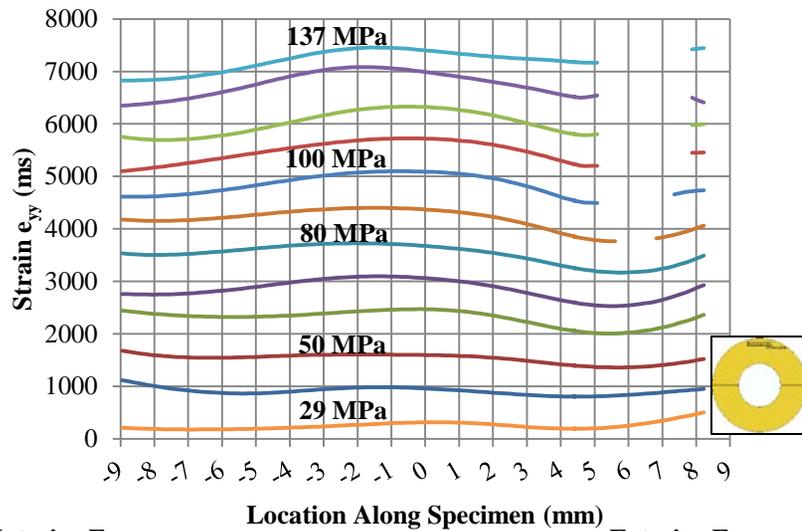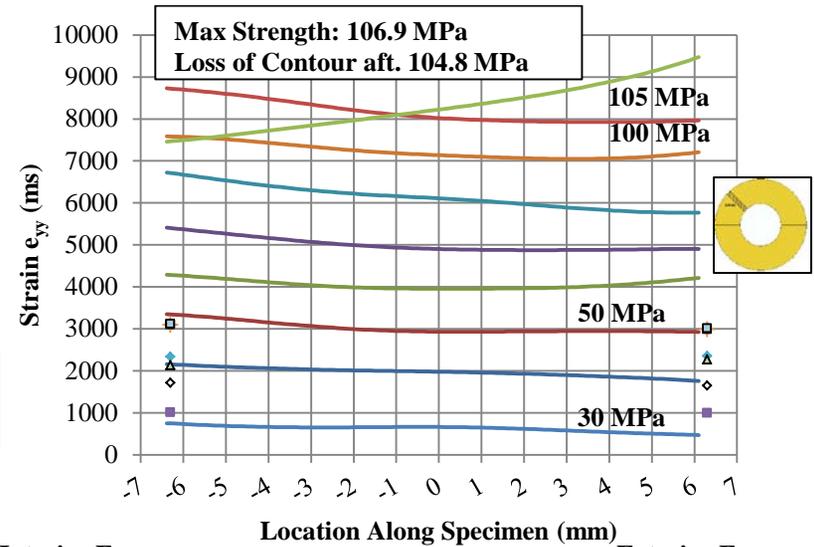
Figure A-19: Specimen TG21-12 (Free): Inner (Upper Left), Middle (Upper Right), Outer (Lower Left), & Radial (Lower Right)

229
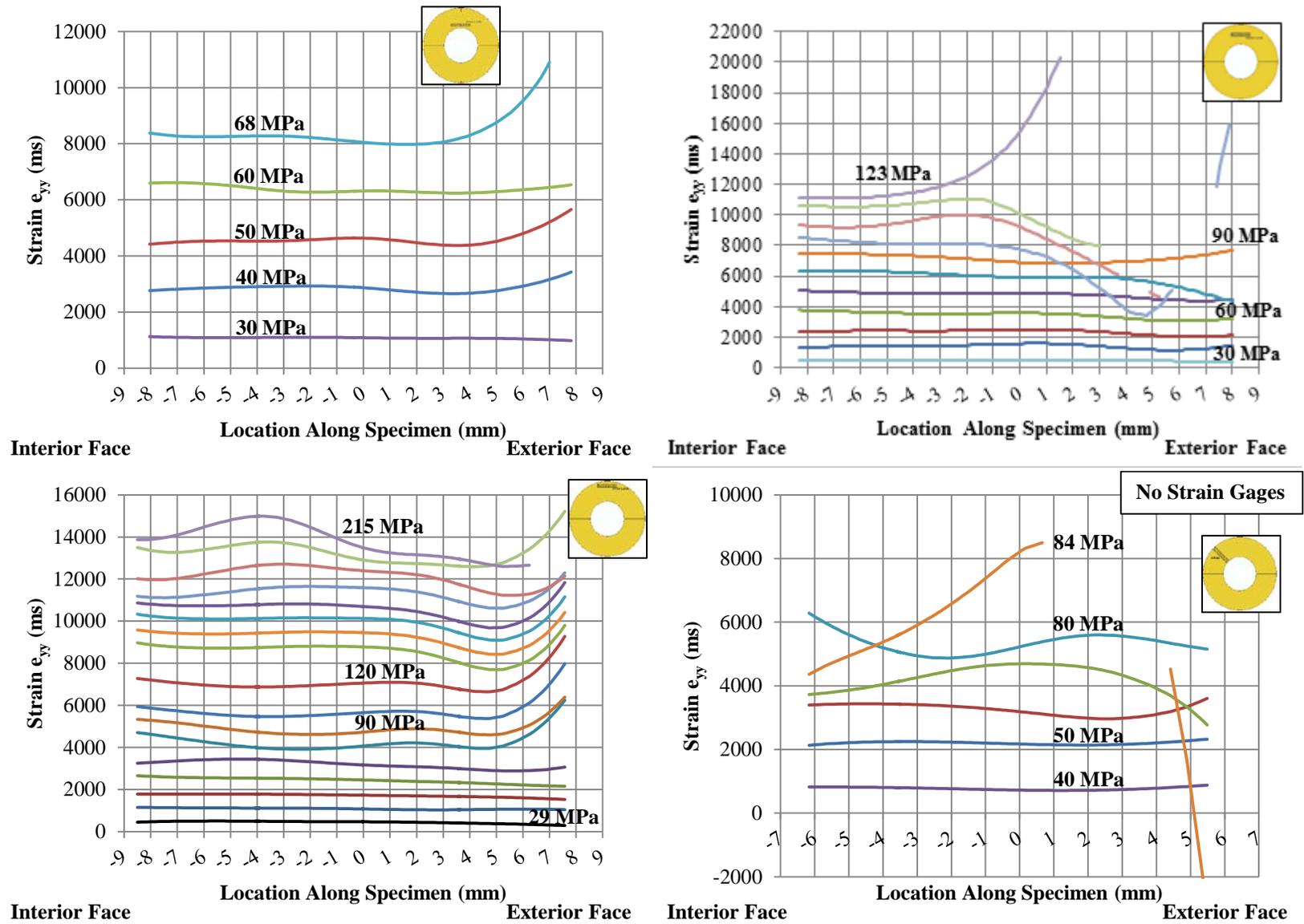
Figure A-20: Specimen TG21-12 (Fixed): Inner (Upper Left), Middle (Upper Right), Outer (Lower Left), & Radial (Lower Right)

230
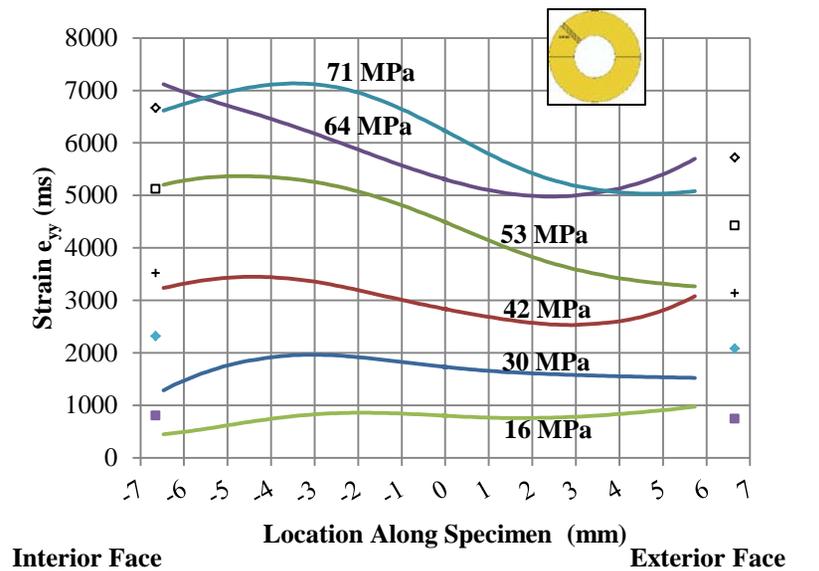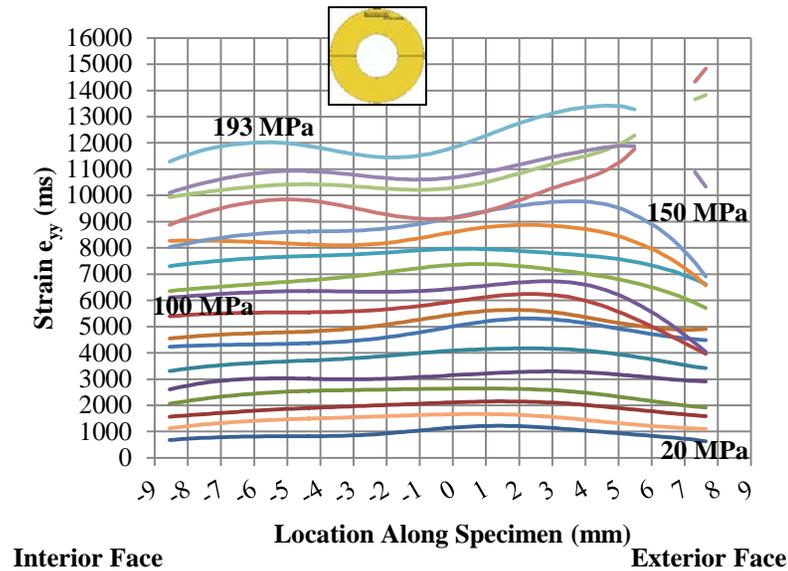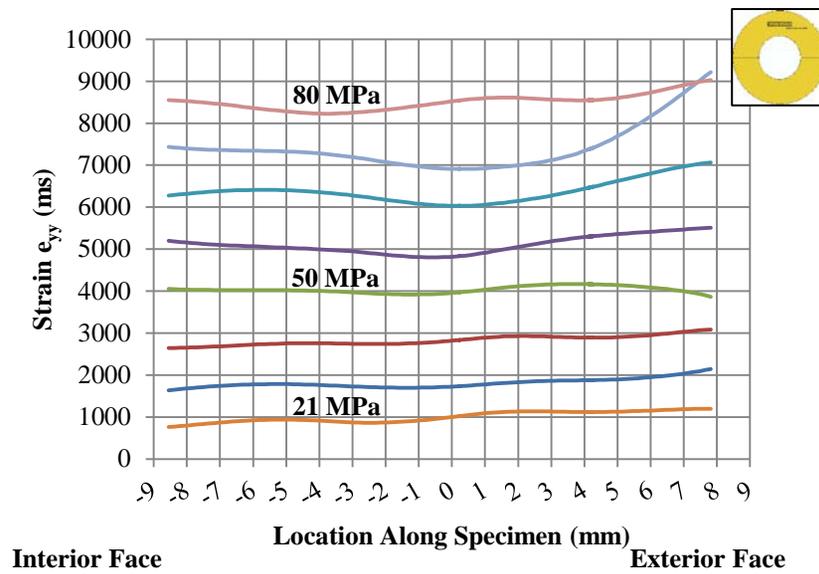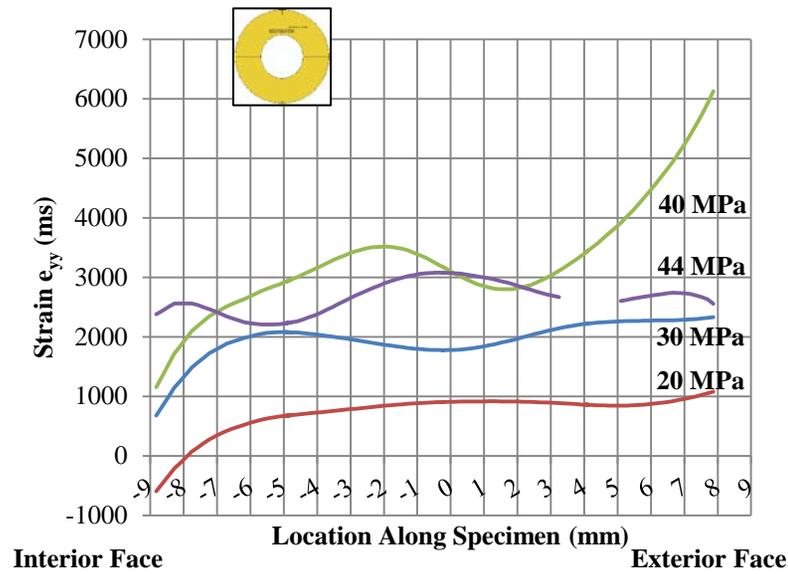
Figure A-21: Specimen TG21-13 (Free): Inner (Upper Left), Middle (Upper Right), Outer (Lower Left), & Radial Manual Values (Lower Right)

231
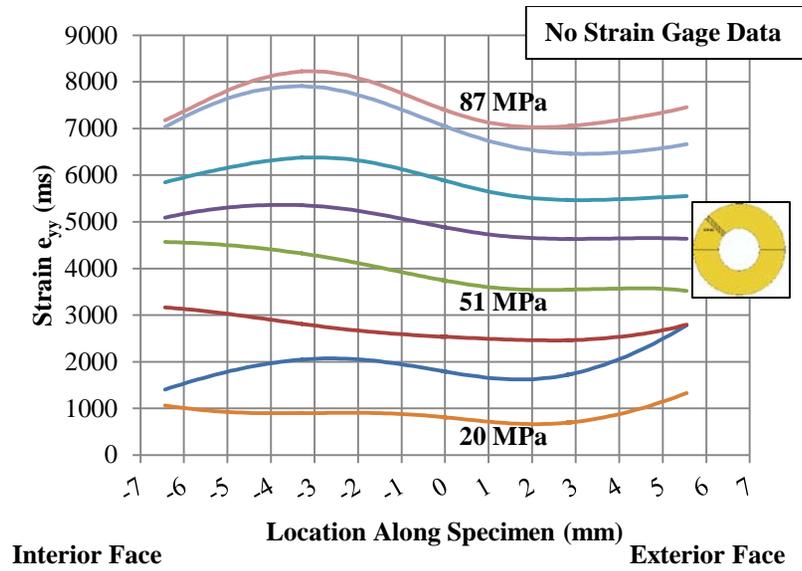
Figure A-22: Specimen TG21-13 (Free): Radial Trial 2 Values
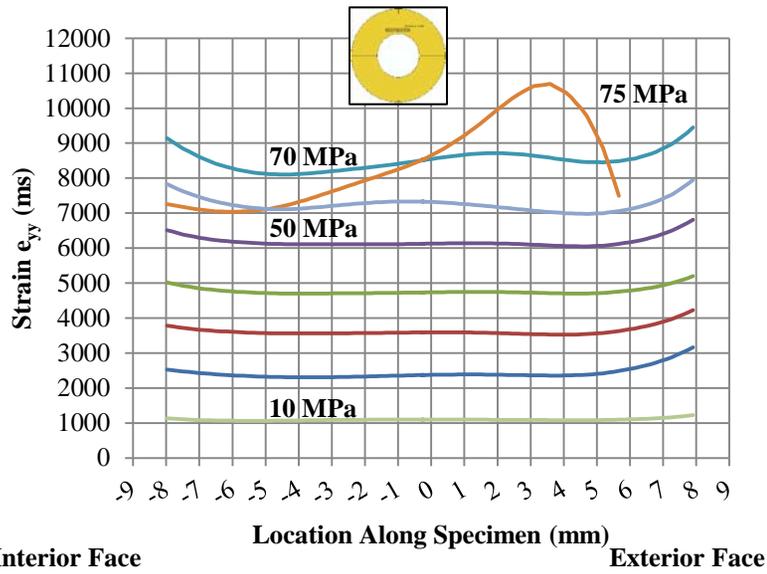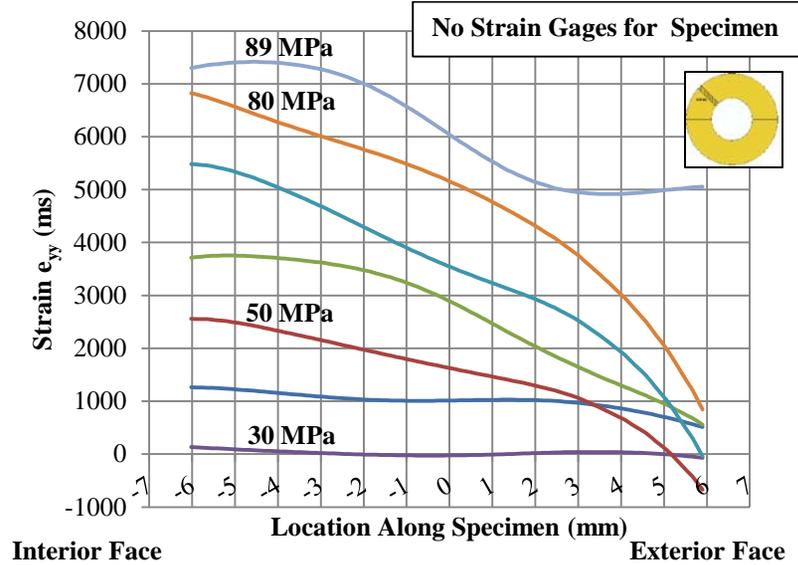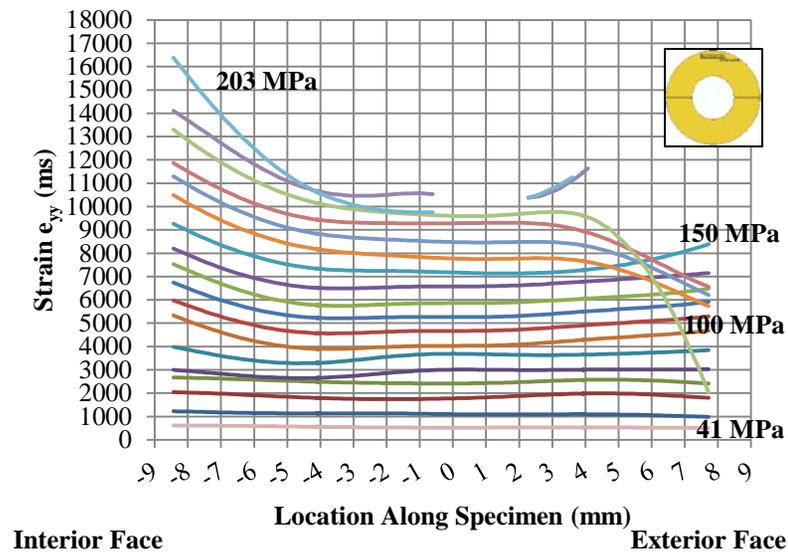
Figure A-23: Specimen TG21-13 (Fixed): Inner (Upper Left), Middle (Upper Right), Outer (Lower Left), & Radial (Lower Right)

233
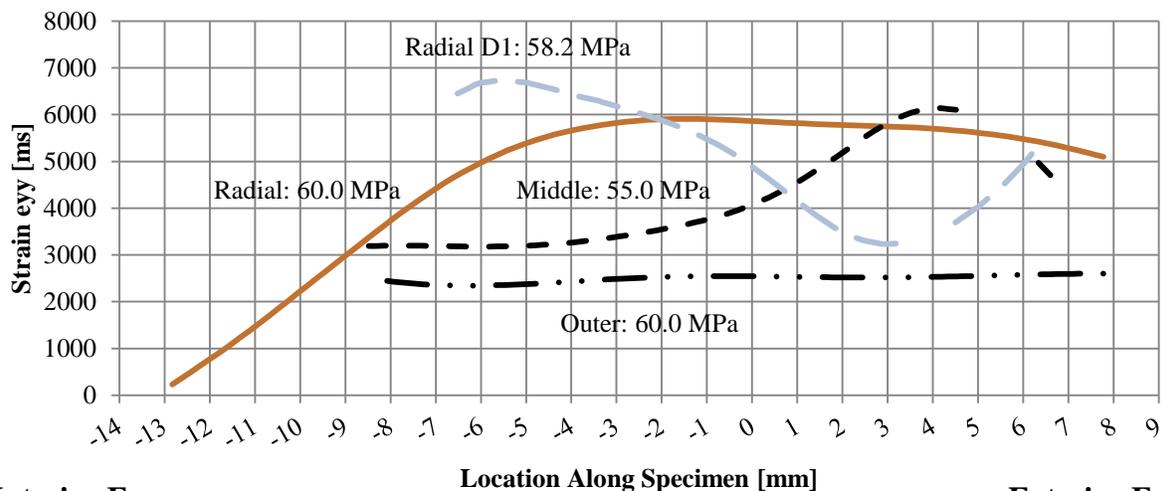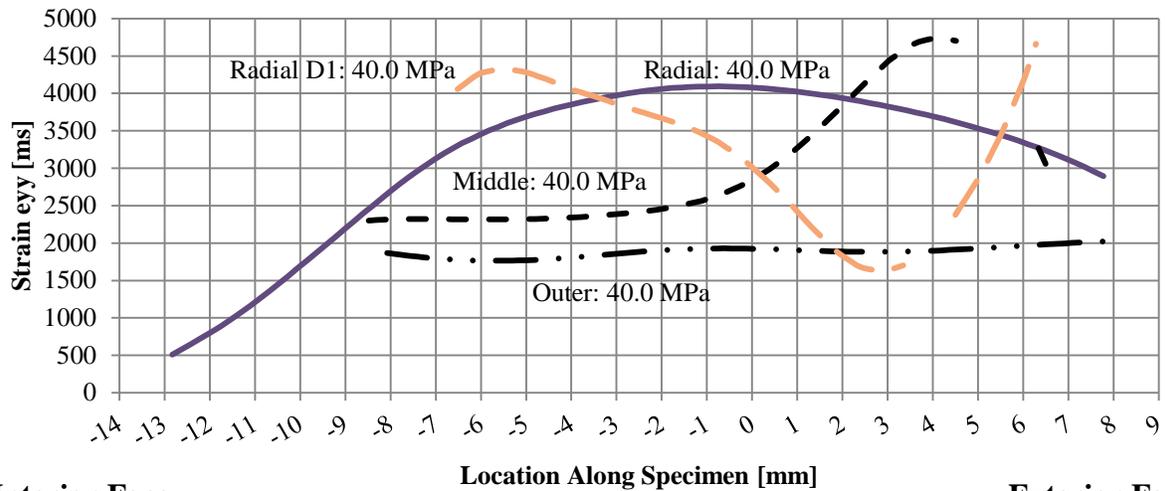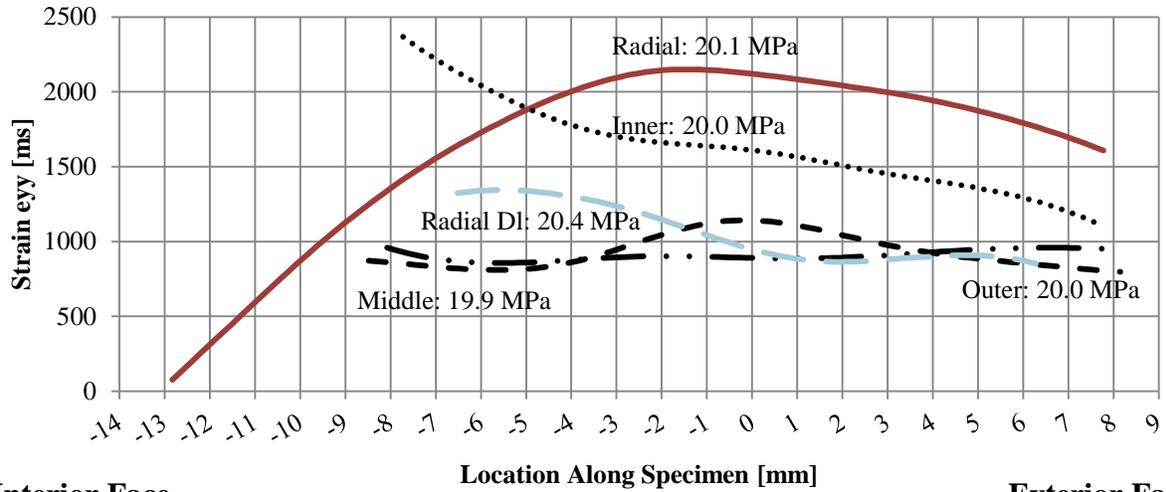
Figure 1: TG1-1 Free Specimens

234
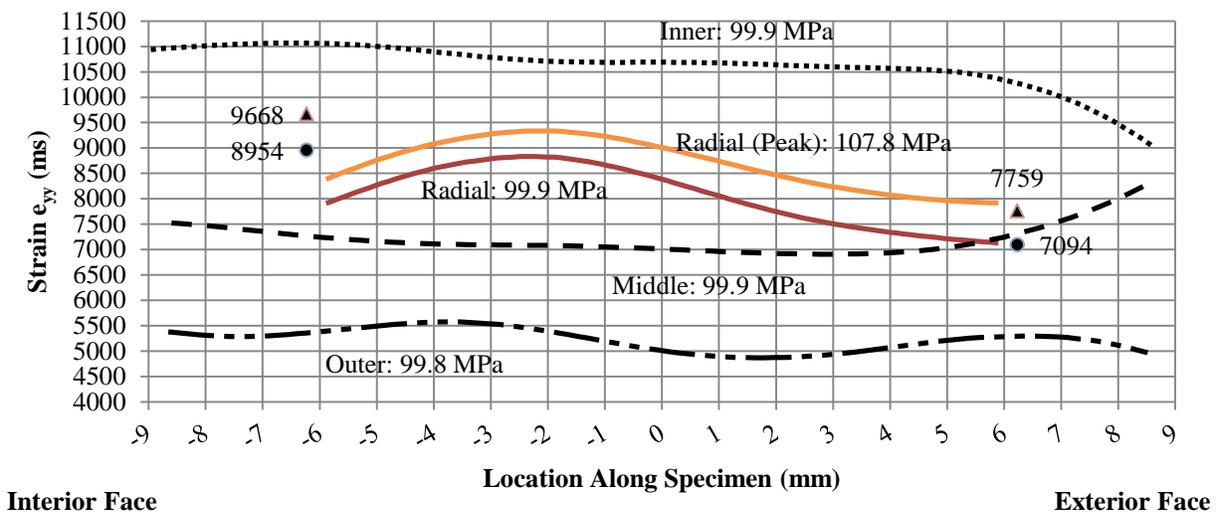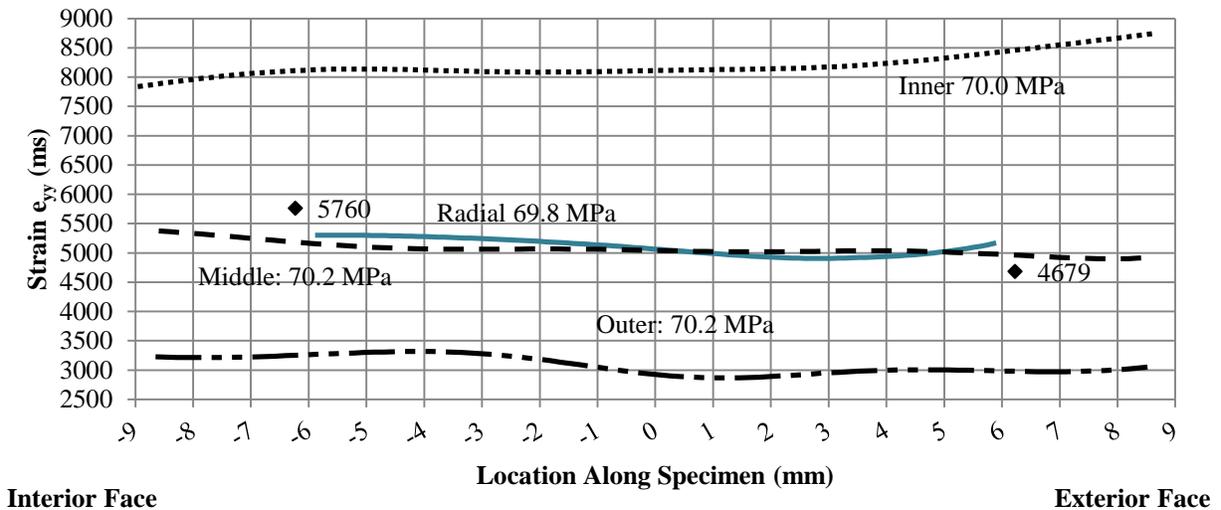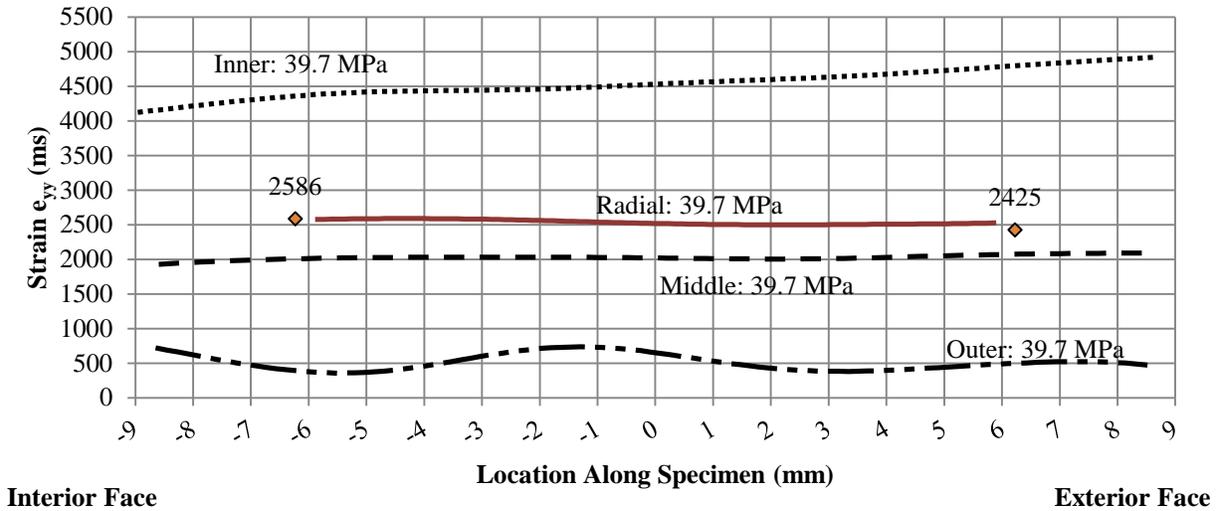
Figure A-24: TG1-5 Free Specimens

235
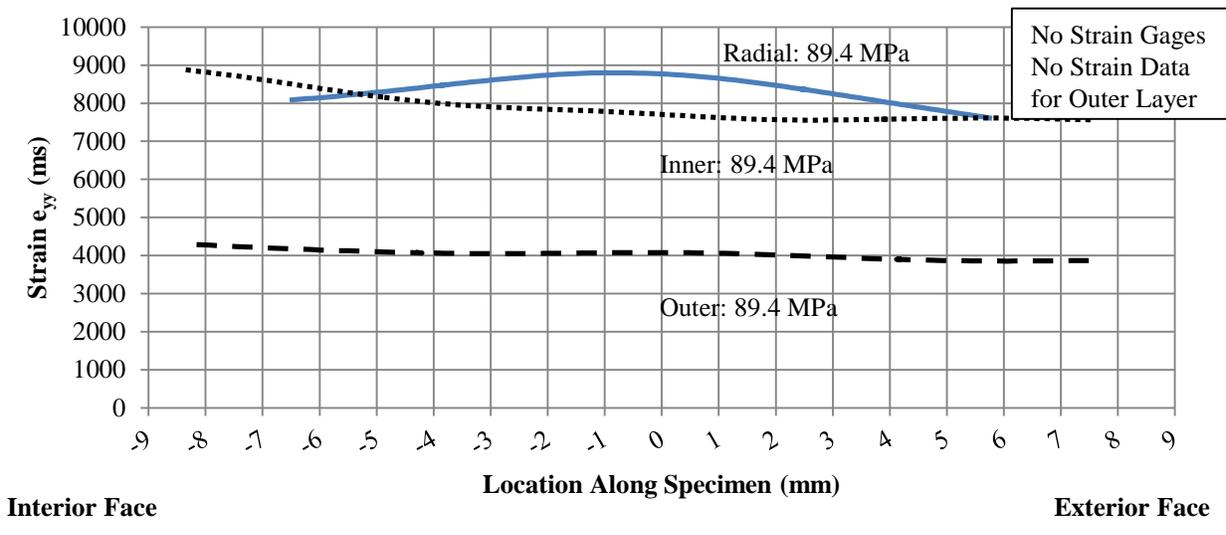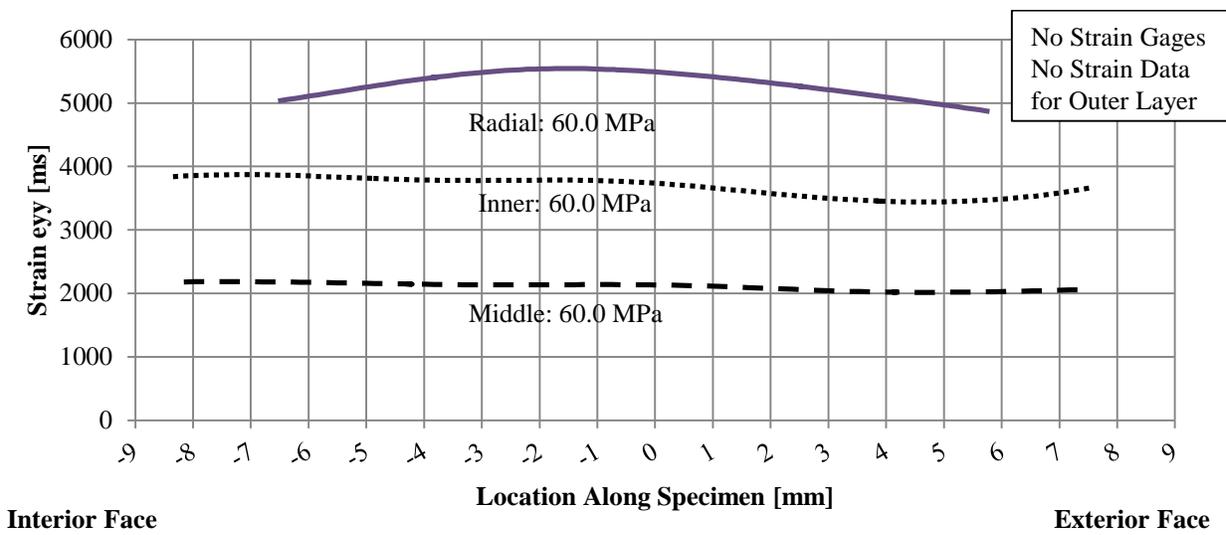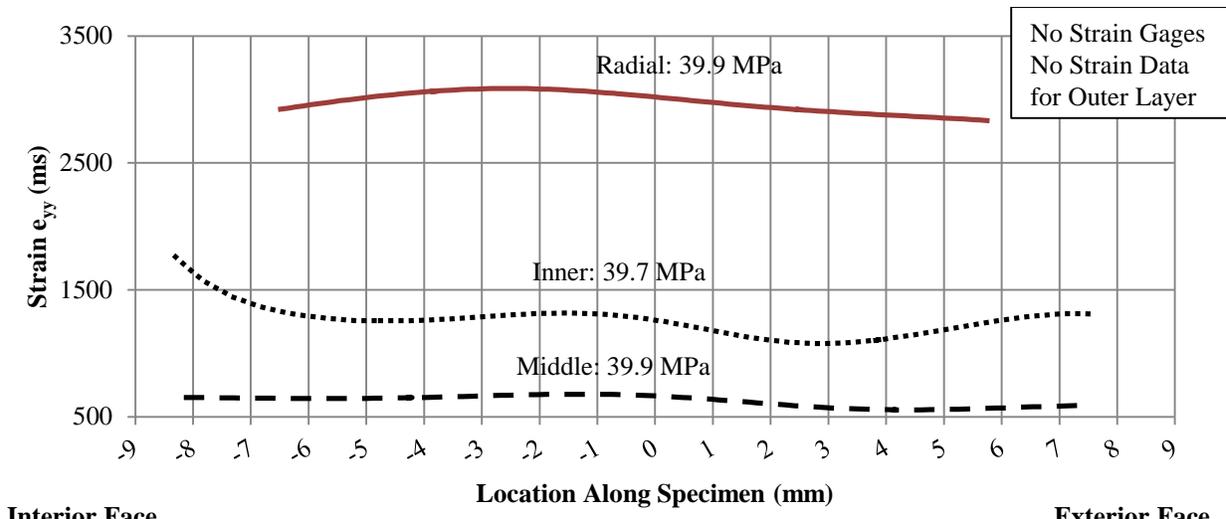
Figure A-25: TG1-5 Fixed Specimens
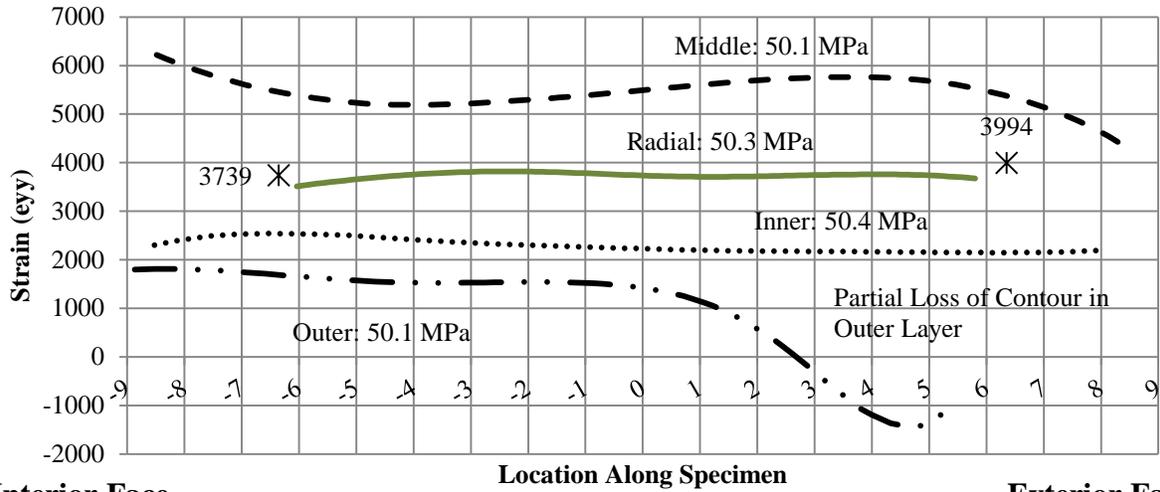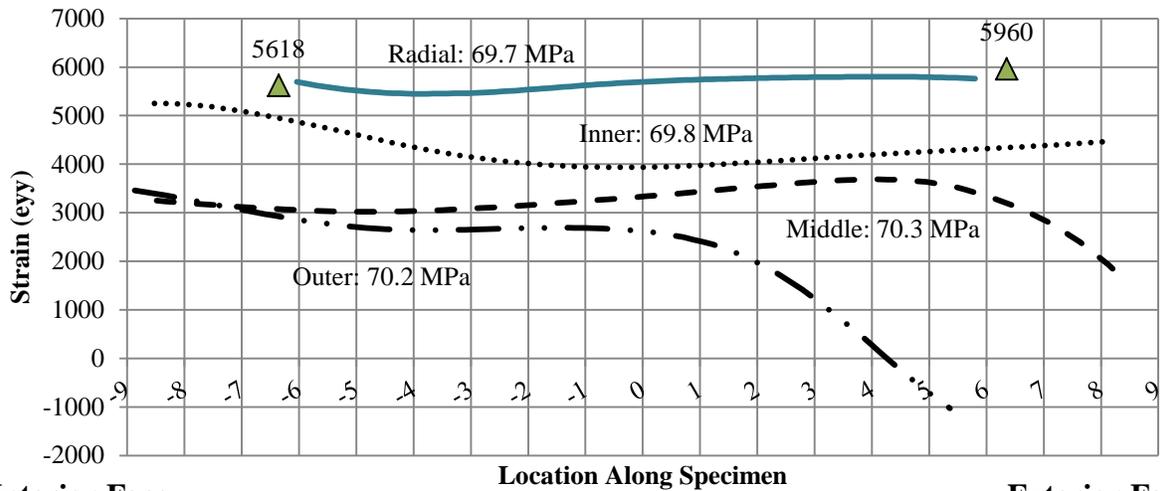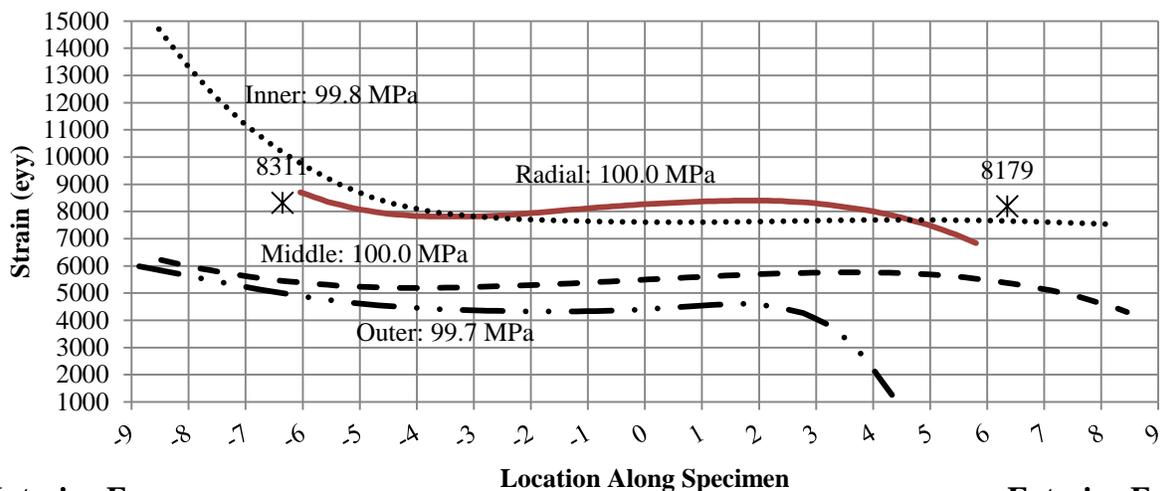
Figure A-26: TG1-6 Free Specimens
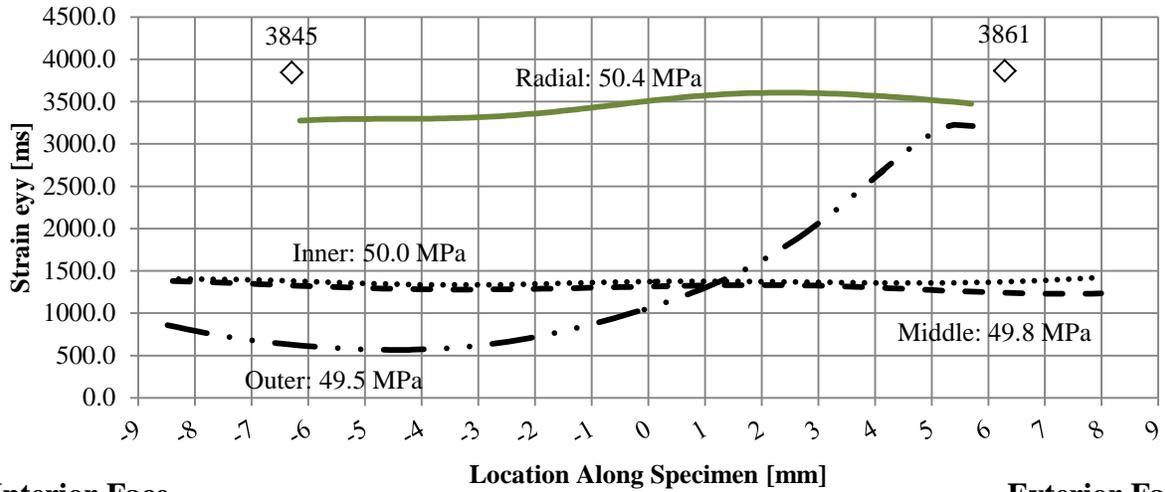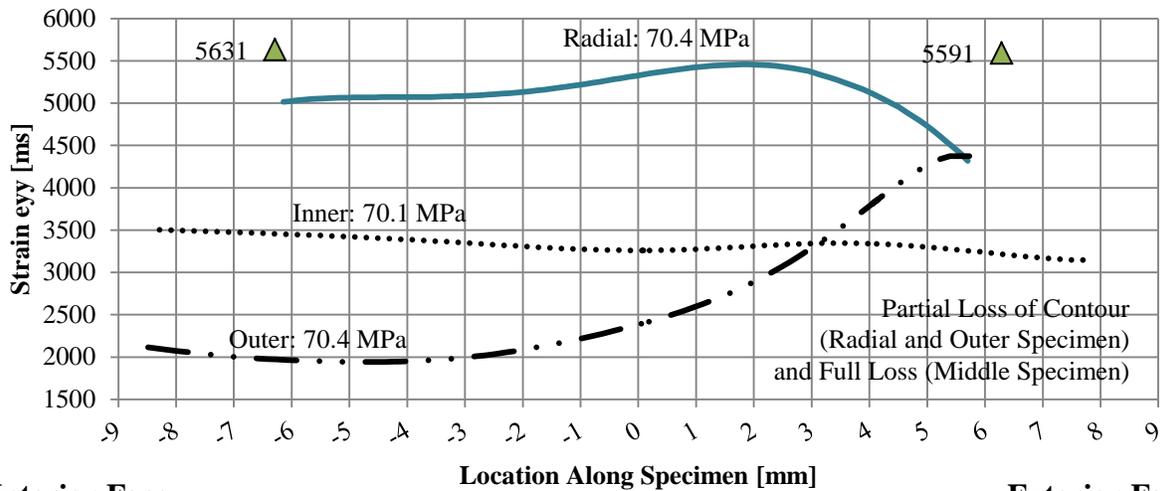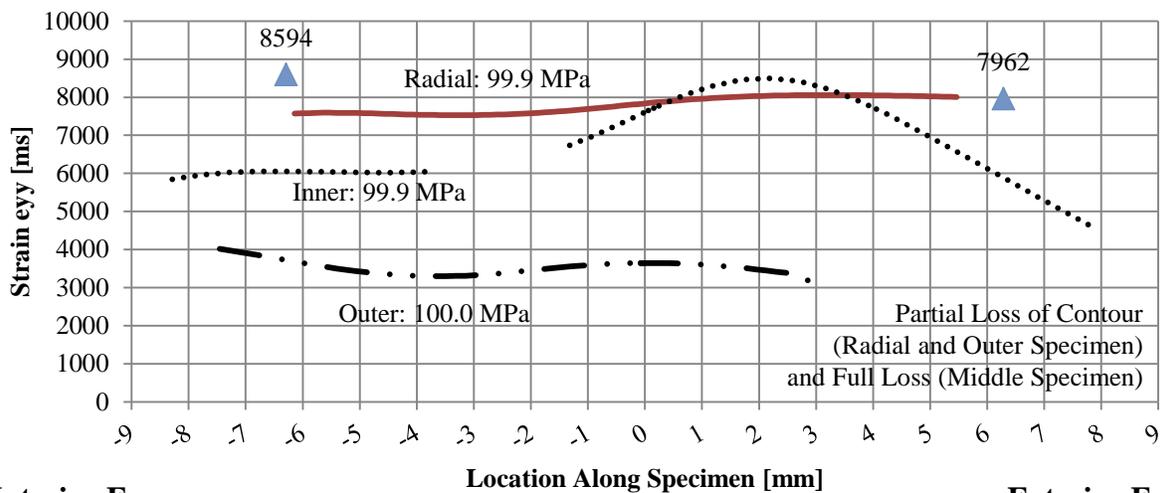
Figure A-27: TG1-6 Fixed Specimens
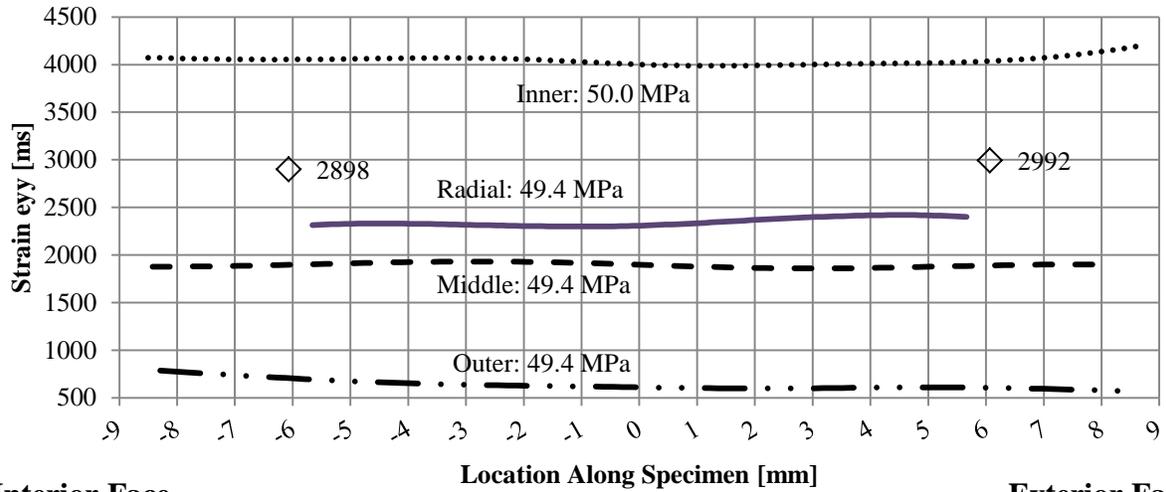
Figure A-28: TG1-7 Free Specimens
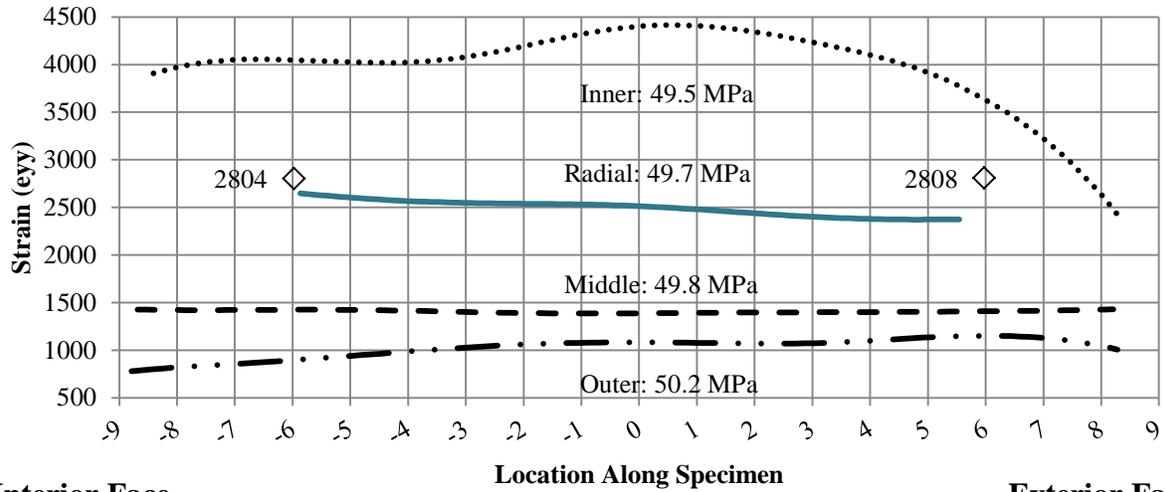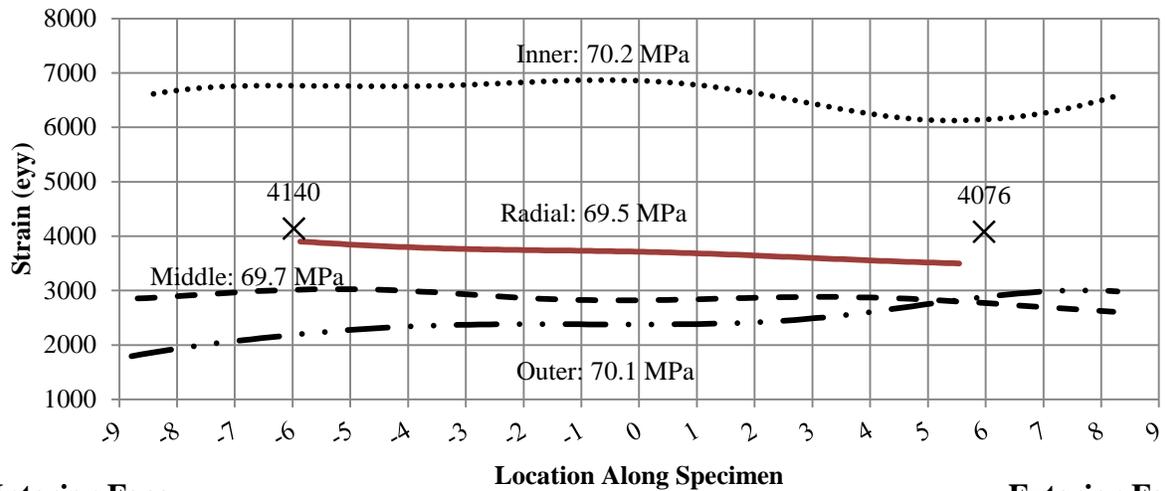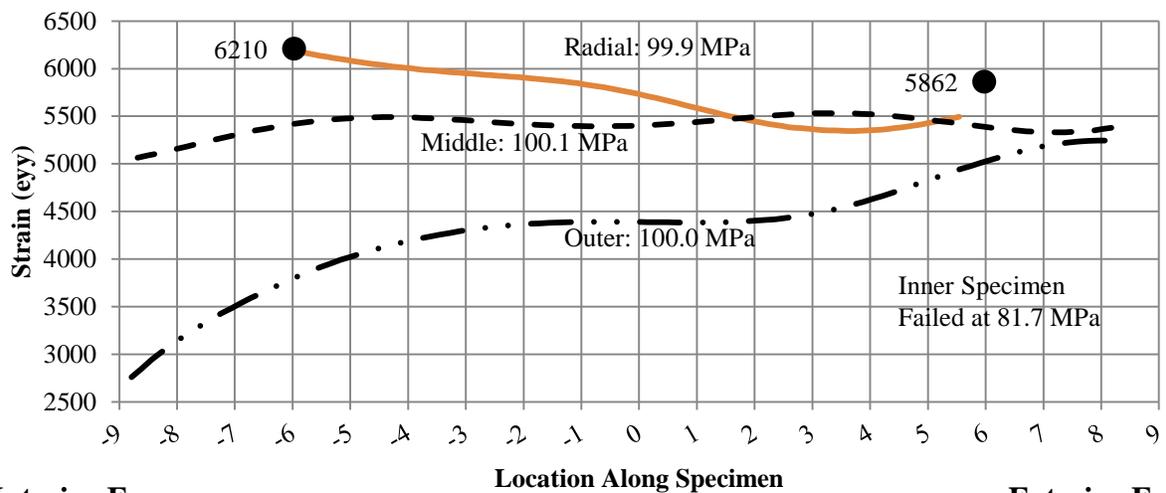
**Figure A-29: TG1-7 Fixed Specimens**
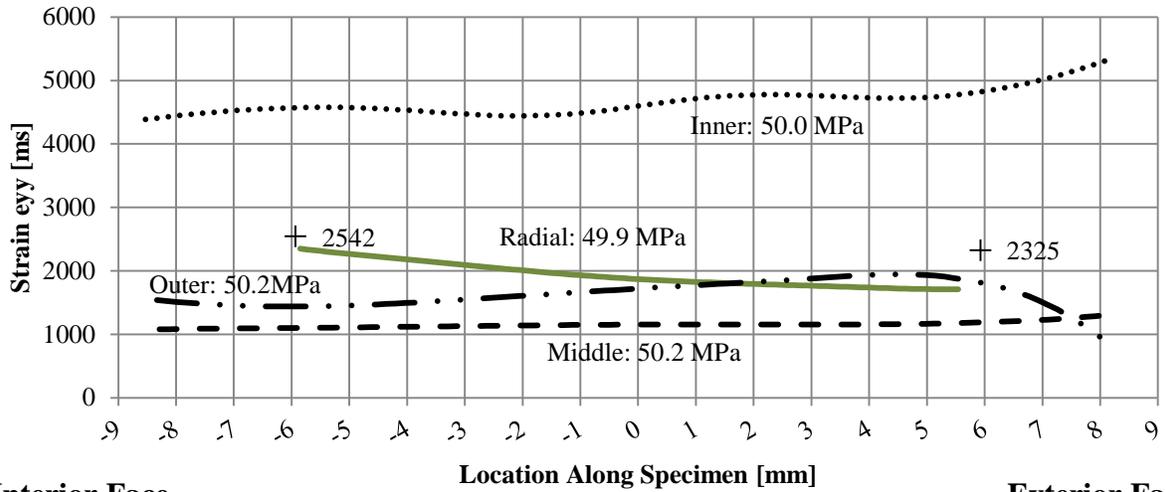
Interior Face
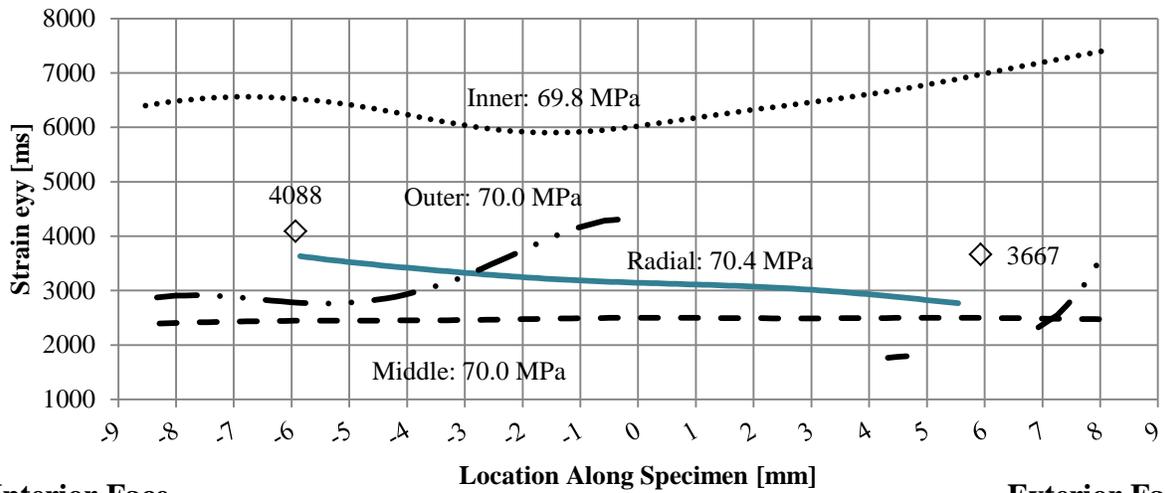
Exterior Face

Interior Face
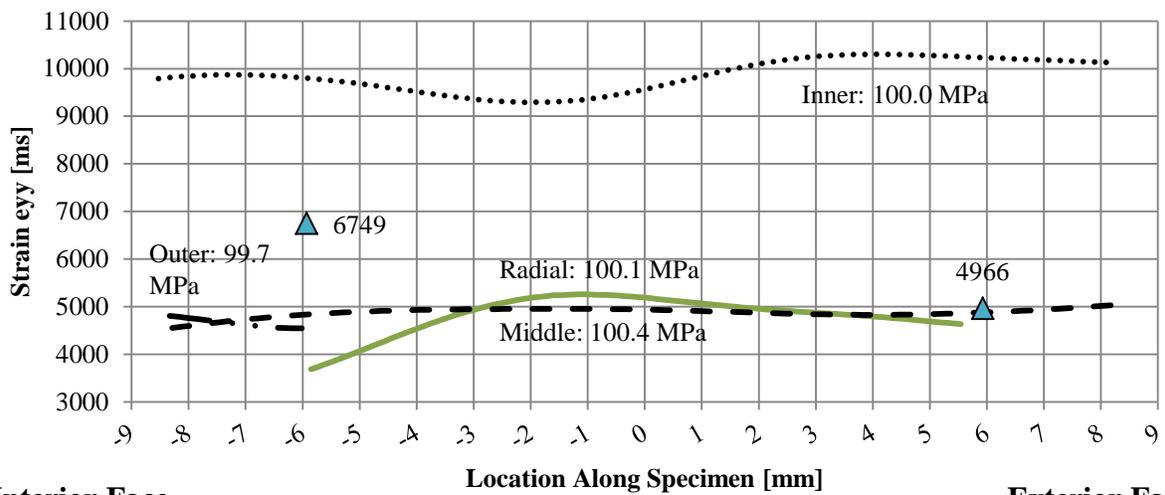
Exterior Face

Interior Face

Exterior Face

Figure A-30: TG 1-8 Free Specimens
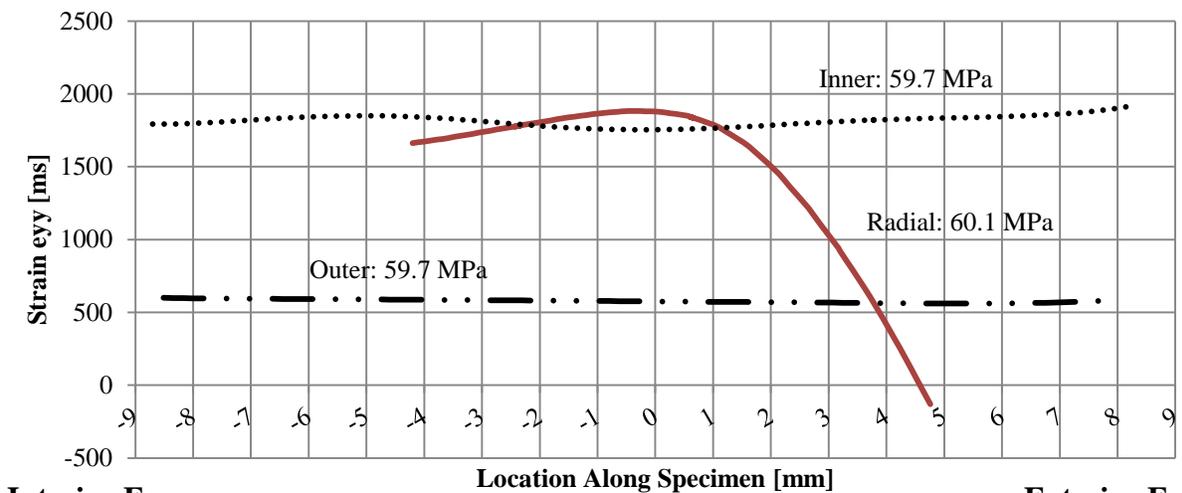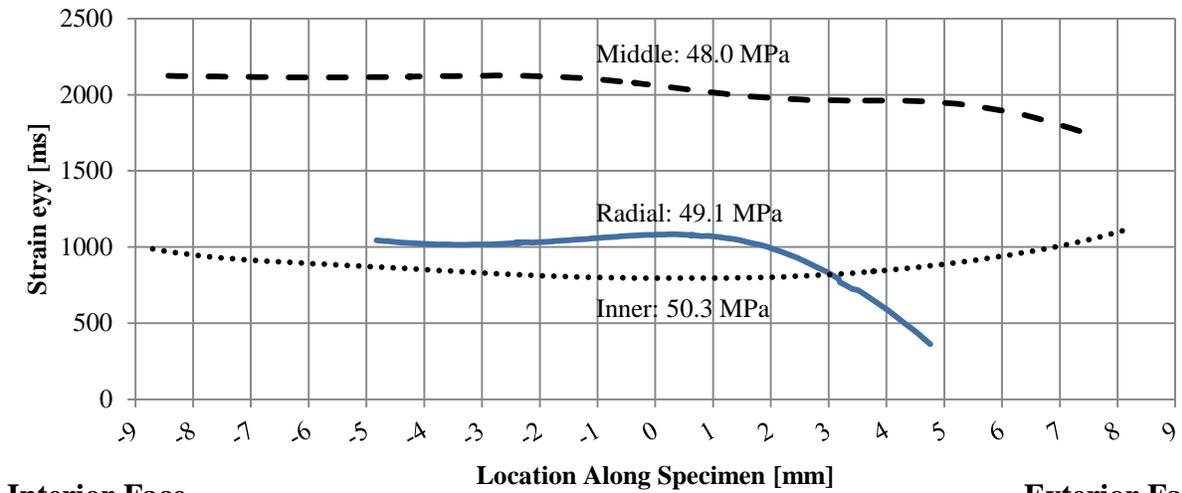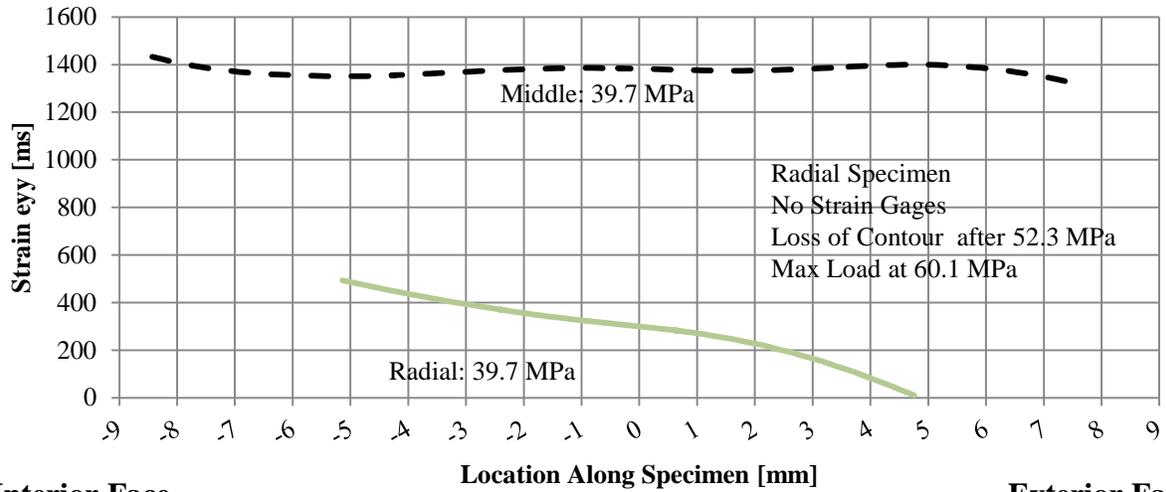
Figure A-31: TG1-8 Fixed Specimen
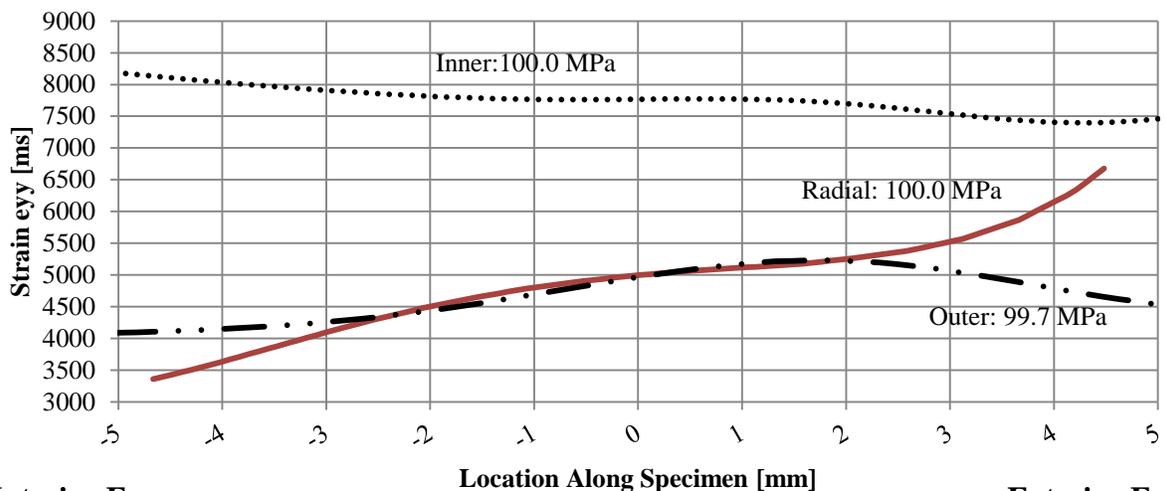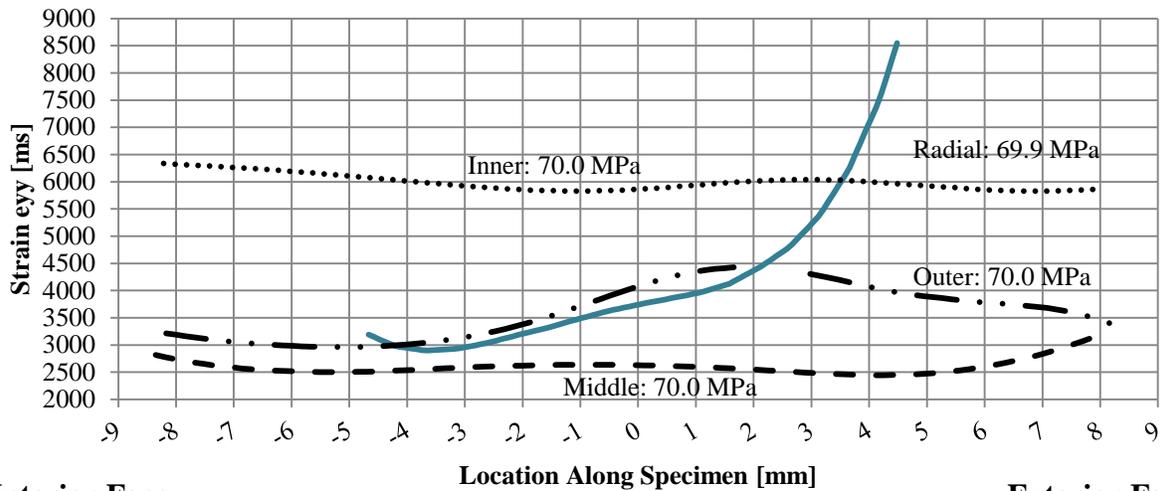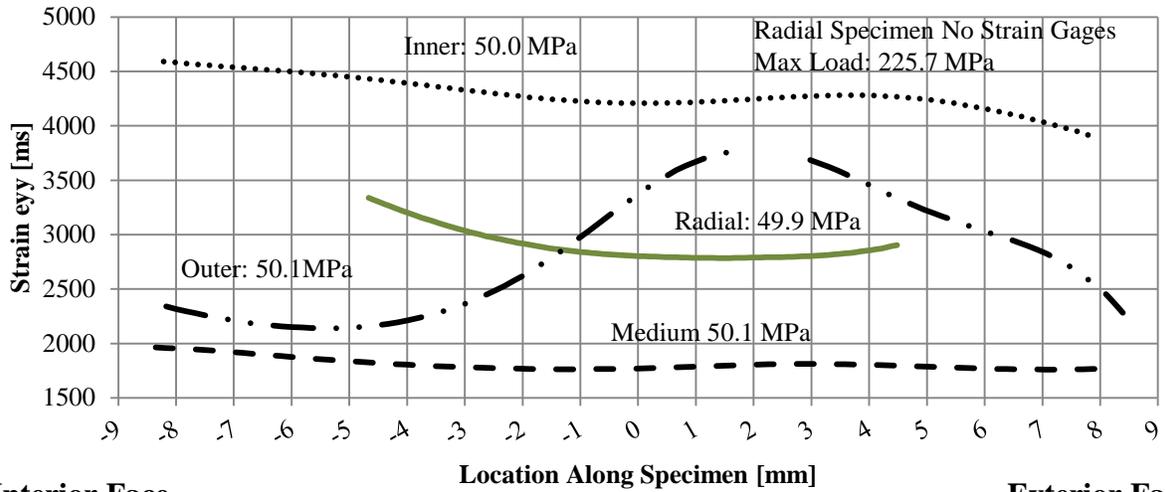
Figure A-32: TG1-9 Free Specimens

243

Figure A-33: TG1-9 Fixed Specimens
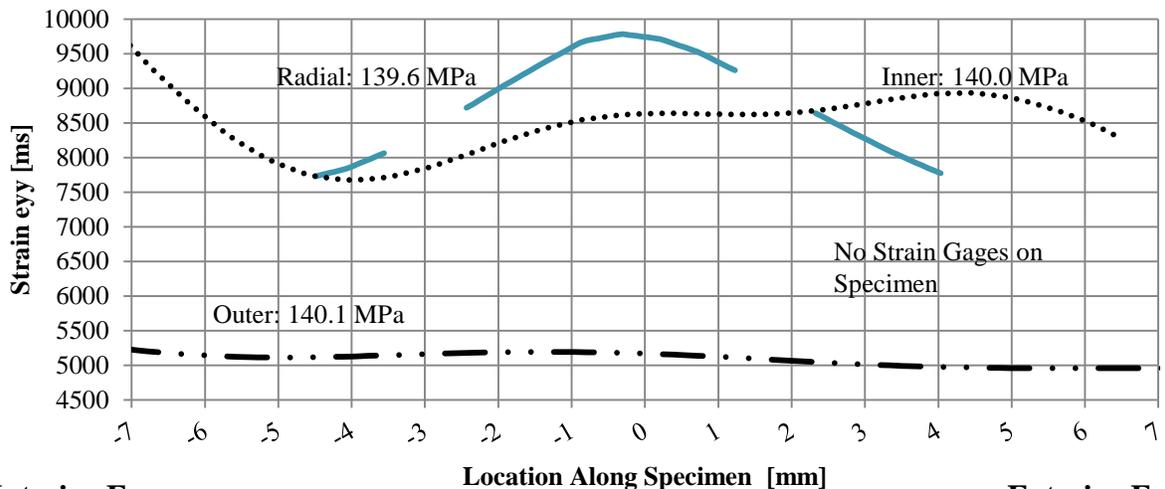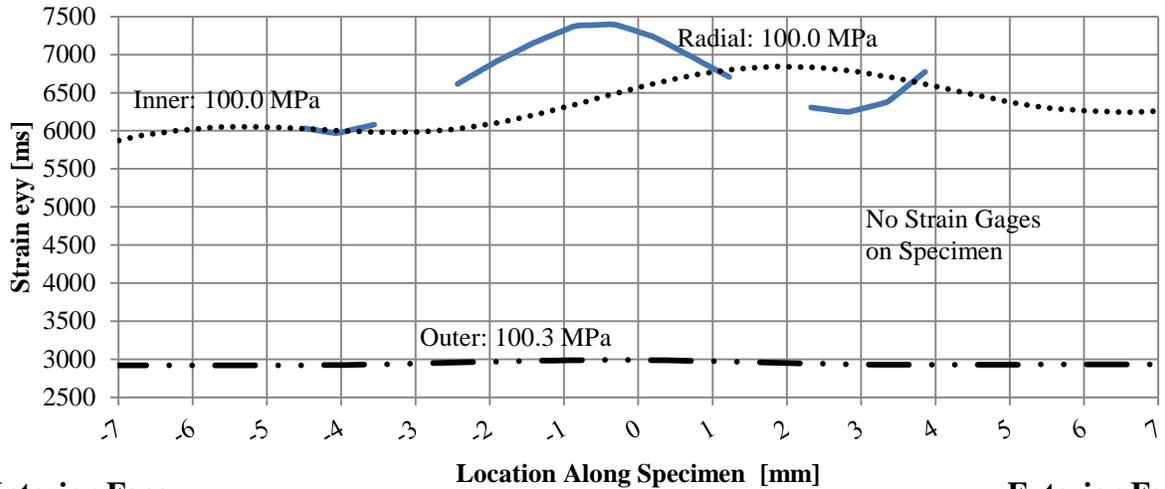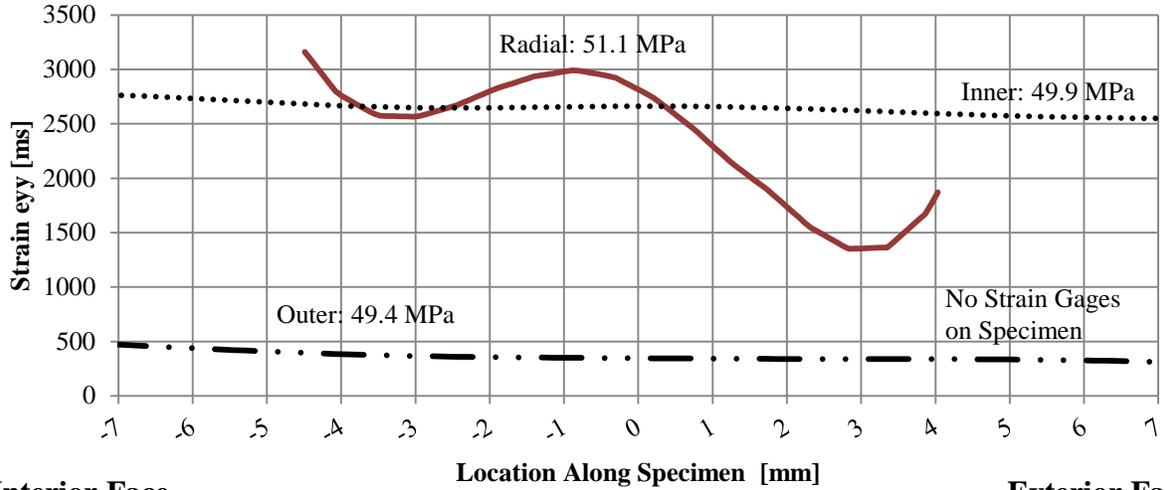
**Figure A-34: TG1-10 Free Specimens**

Figure A-35: TG1-10 Fixed Specimens

**Figure A-36: TG1-11 Free Specimens**
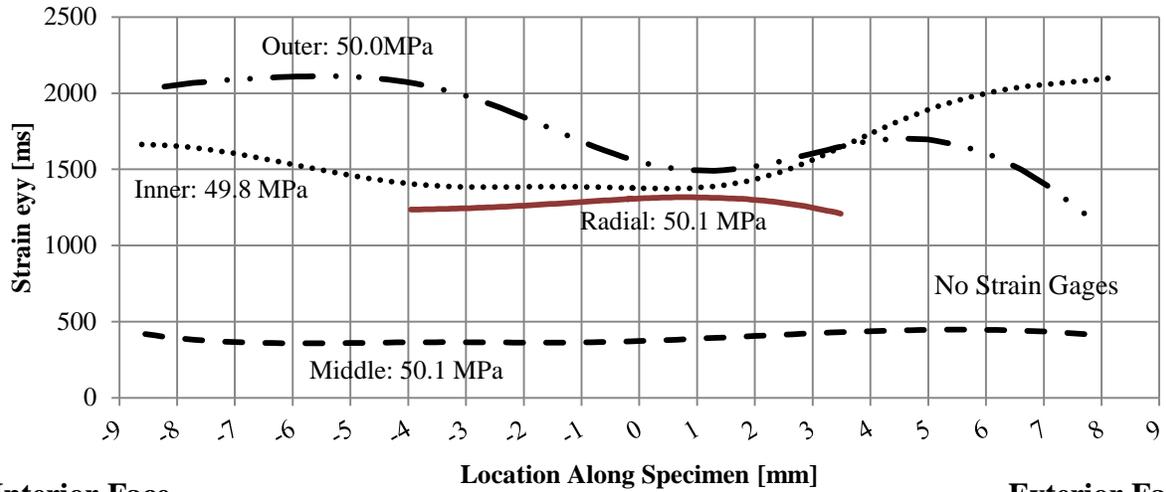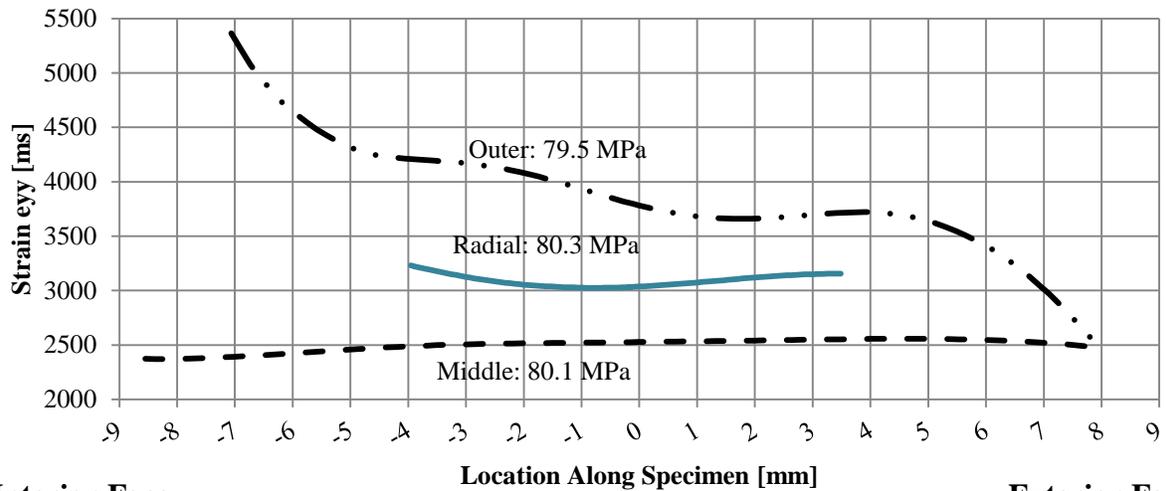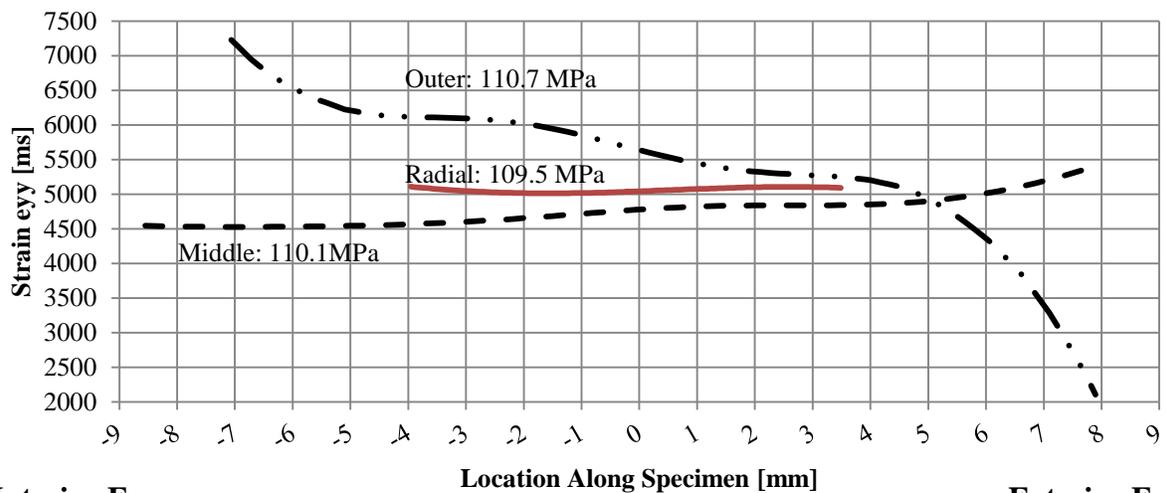
Figure A-37: TG1-11 Fixed Specimens
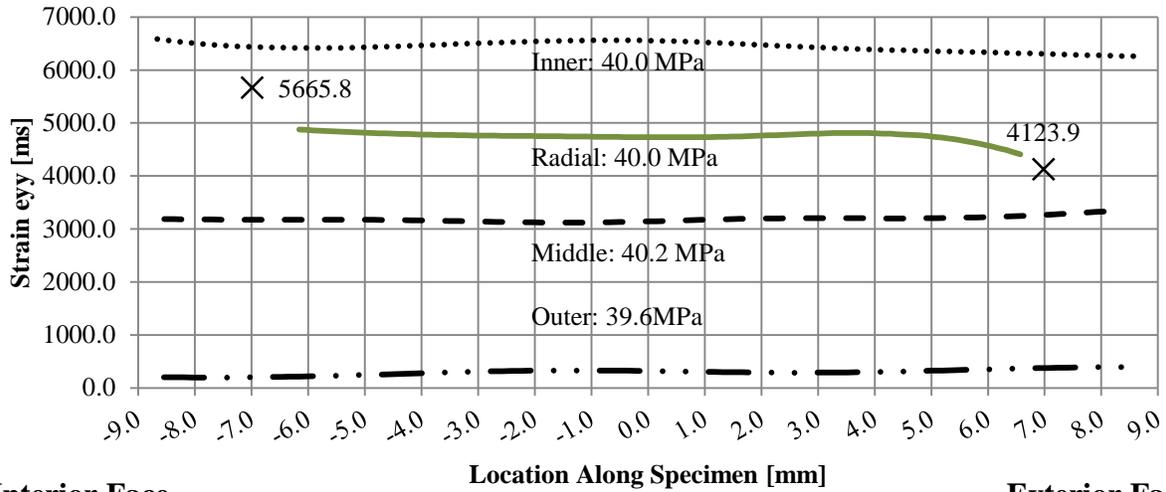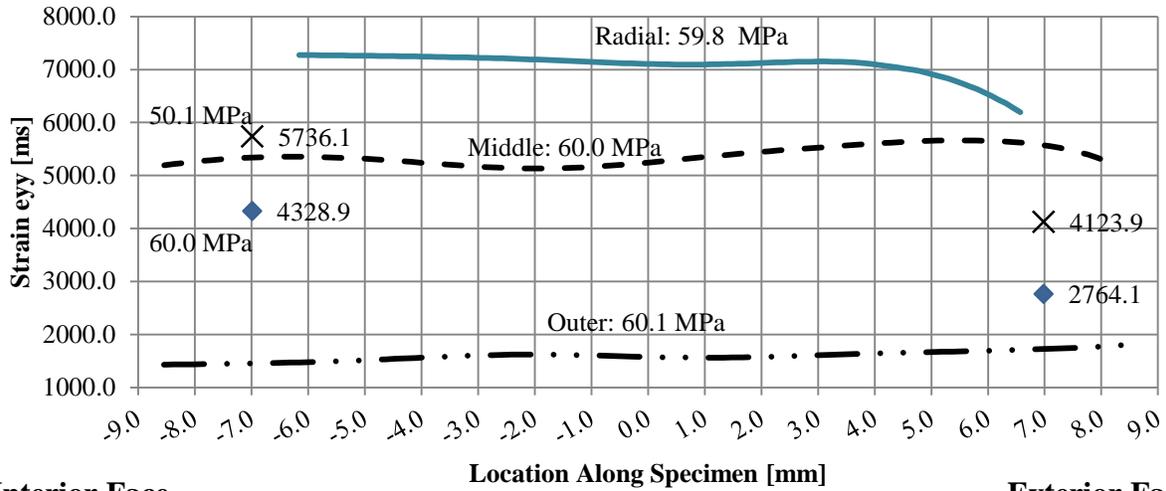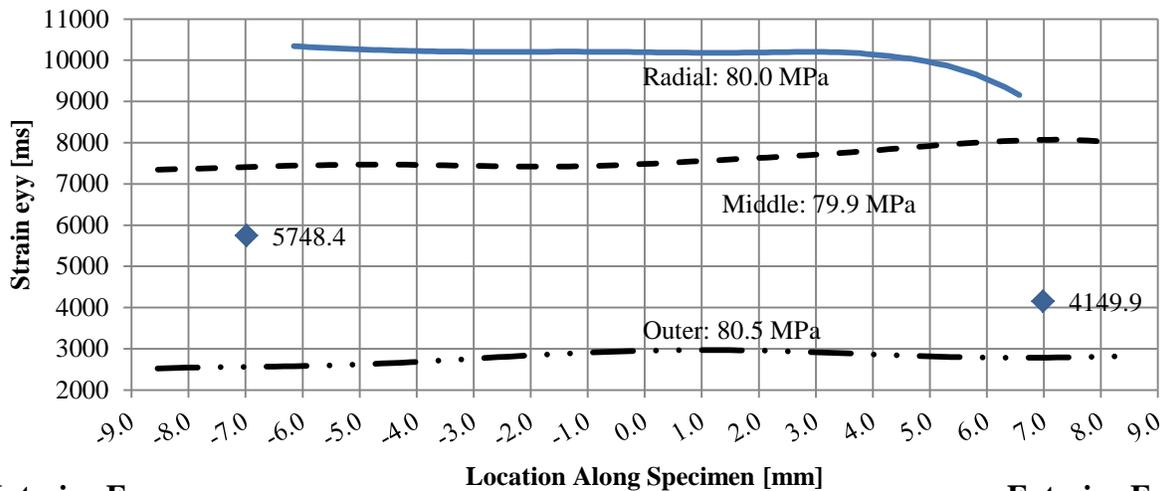
Figure A-38: TG21-11 Free Specimens
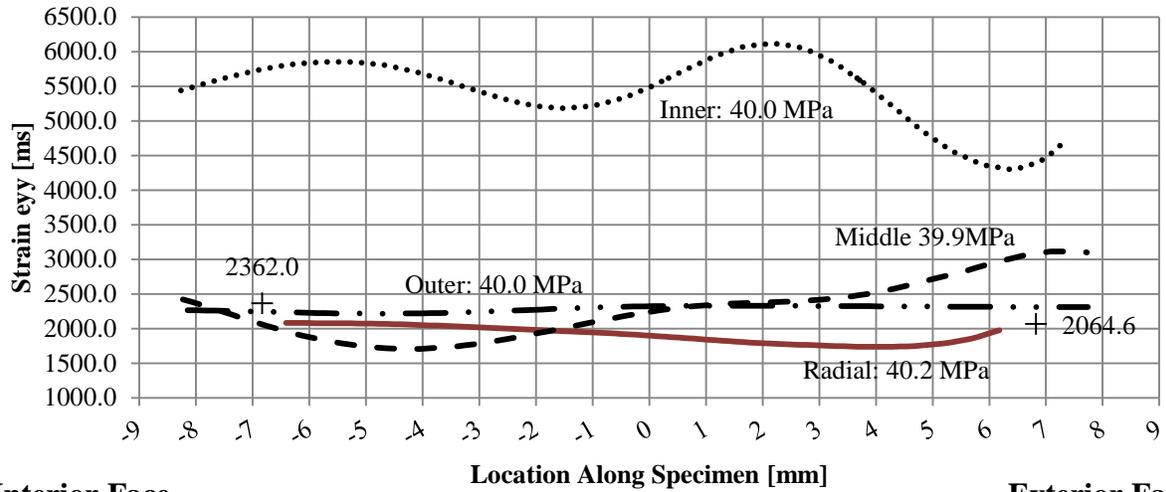
249
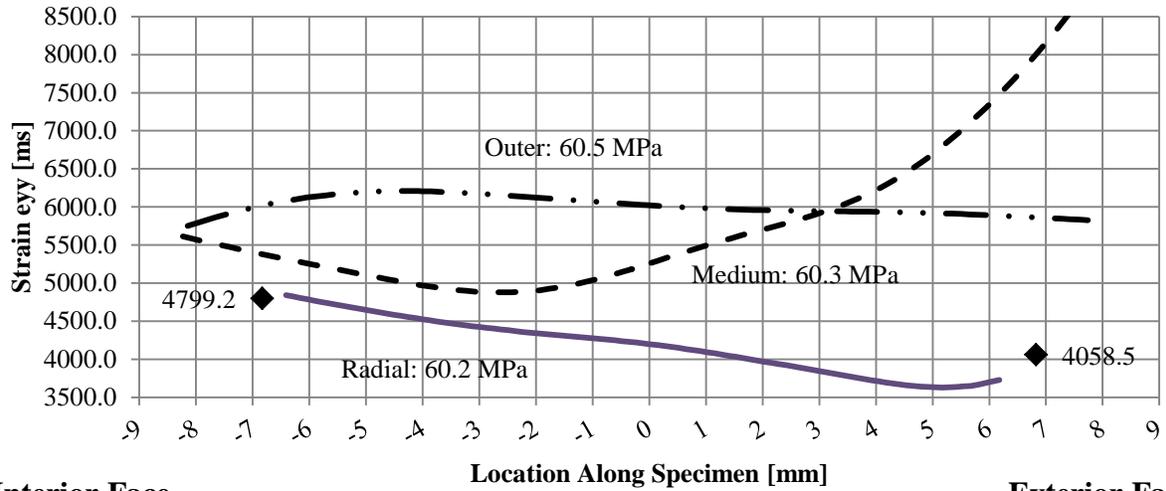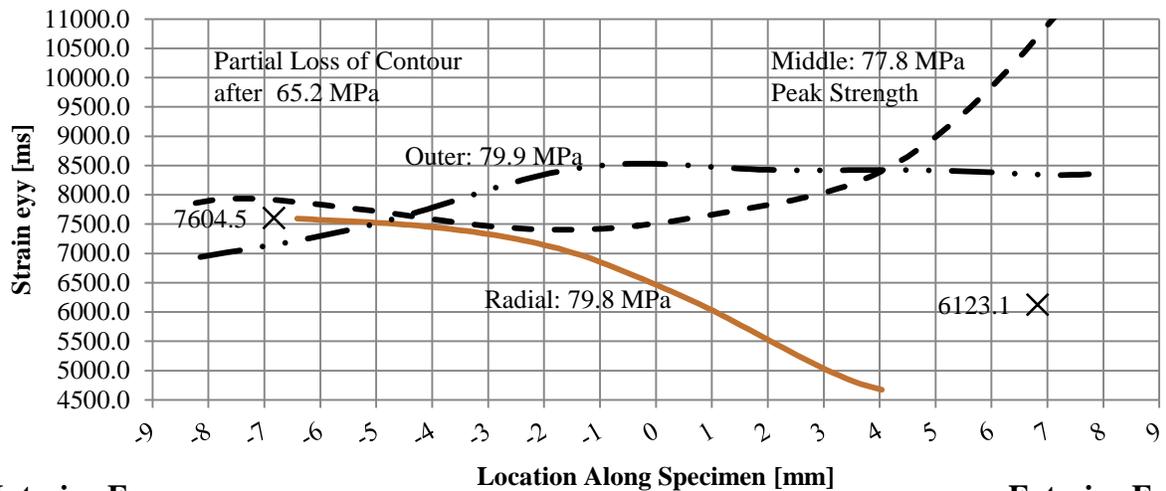
Figure A-39: TG21-11 Fixed Specimens
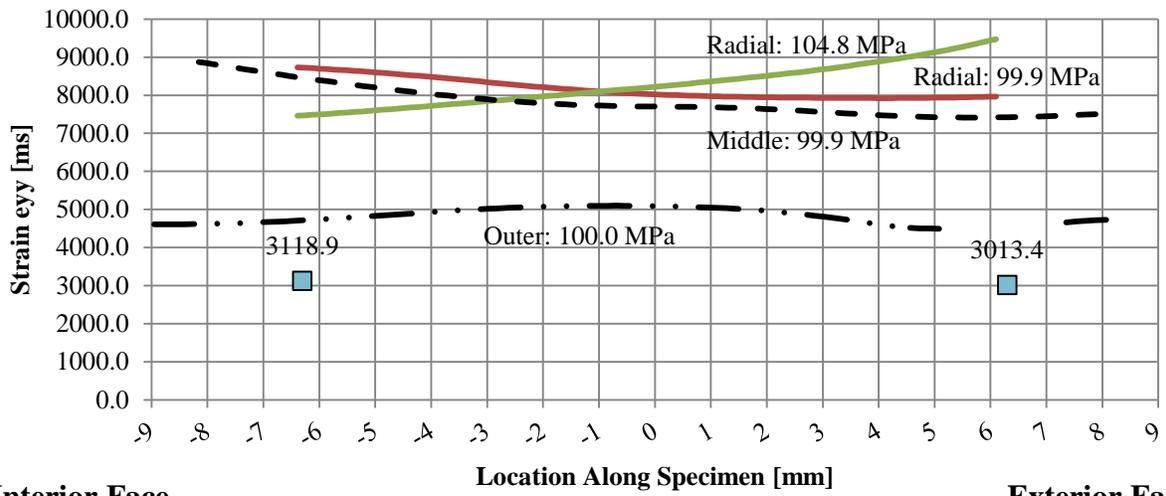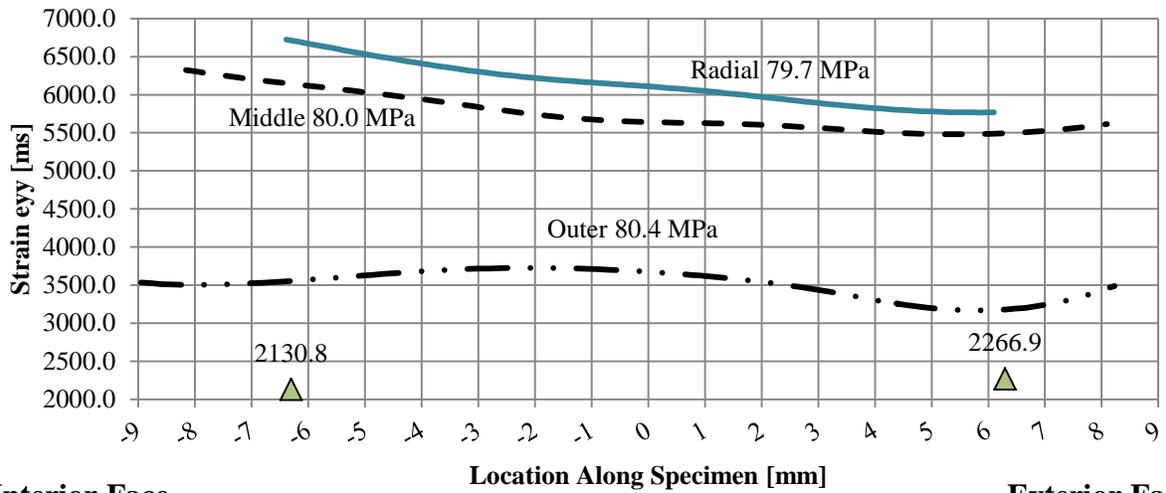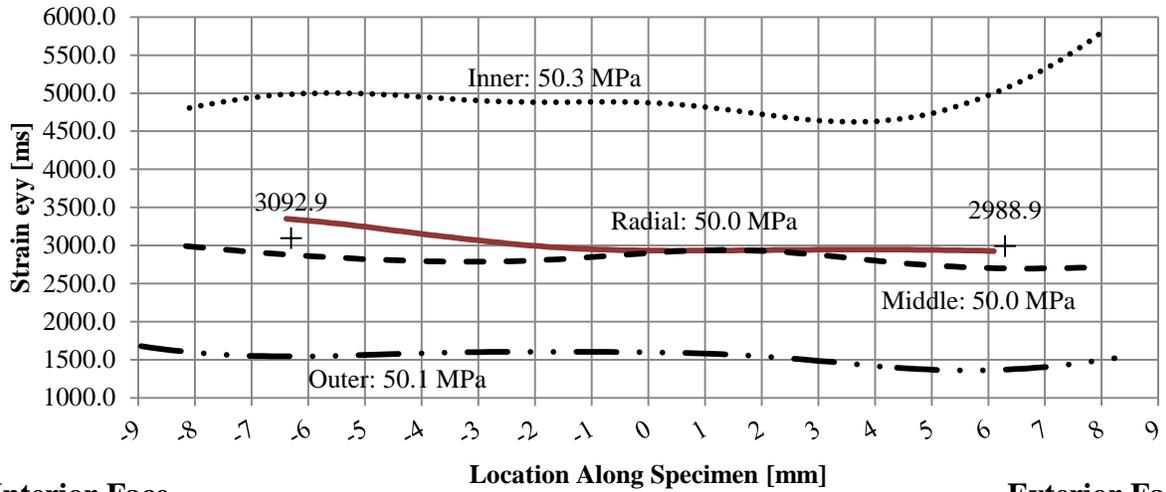
Figure A-40: TG21-12 Free Specimen
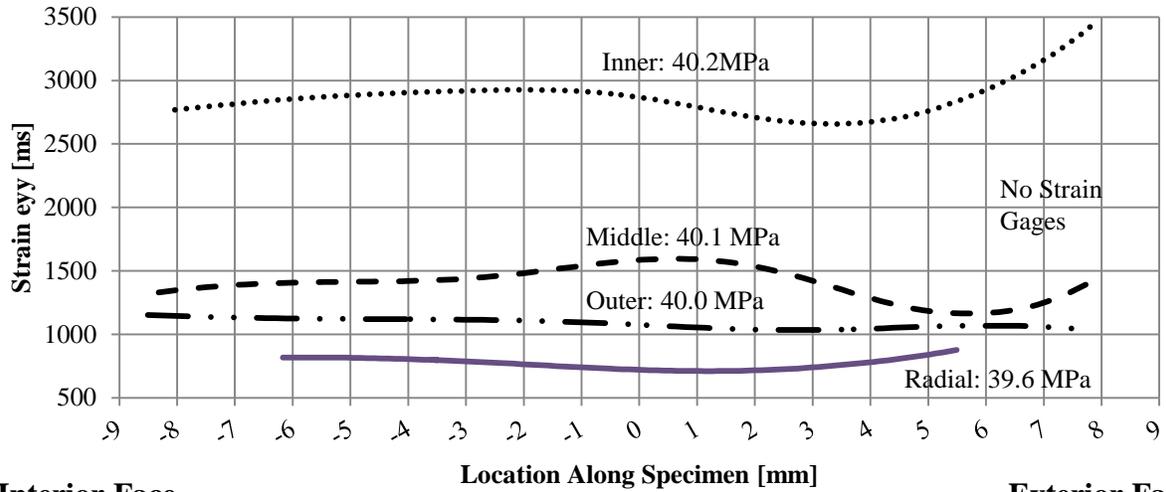
251

Interior Face (under first plot)   **Exterior Face**

Interior Face (under second plot)   **Exterior Face**
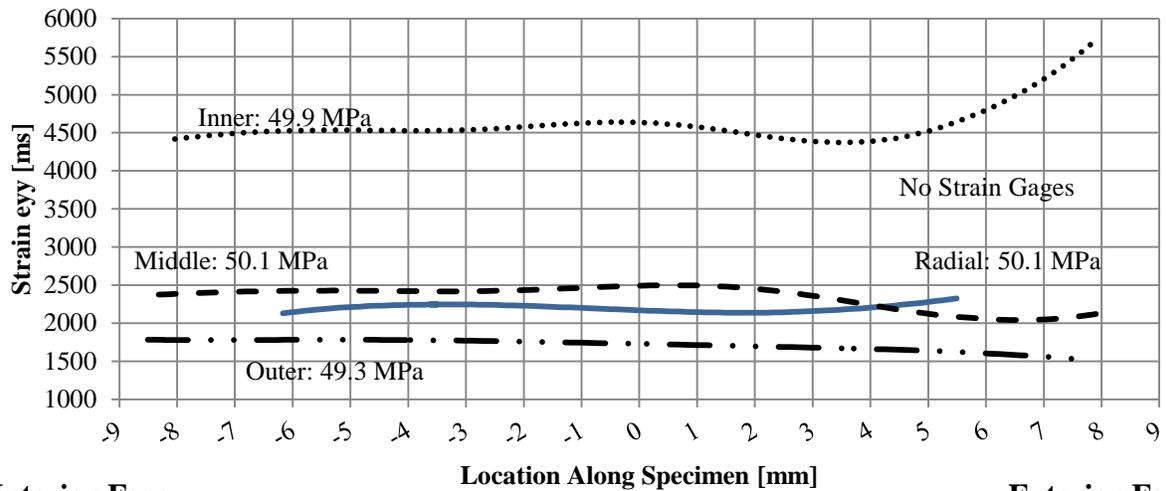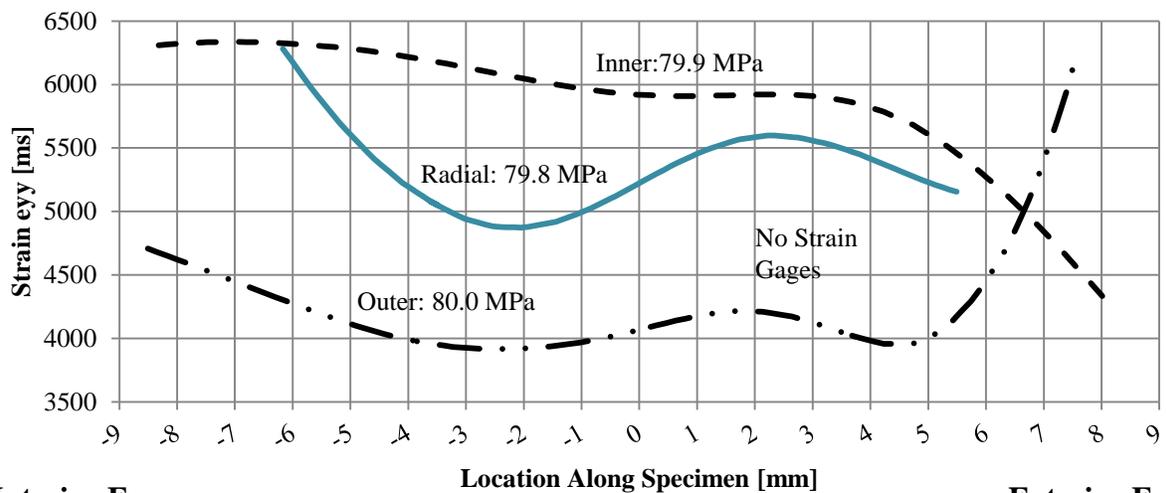
Interior Face (under third plot)   **Exterior Face**

**Figure A-41: TG21-12 Fixed Specimens**

252
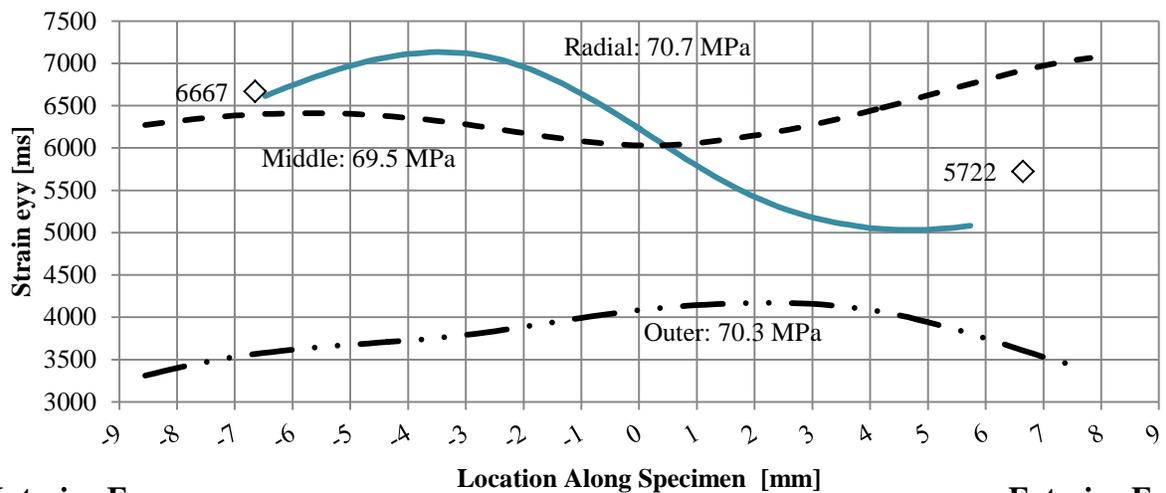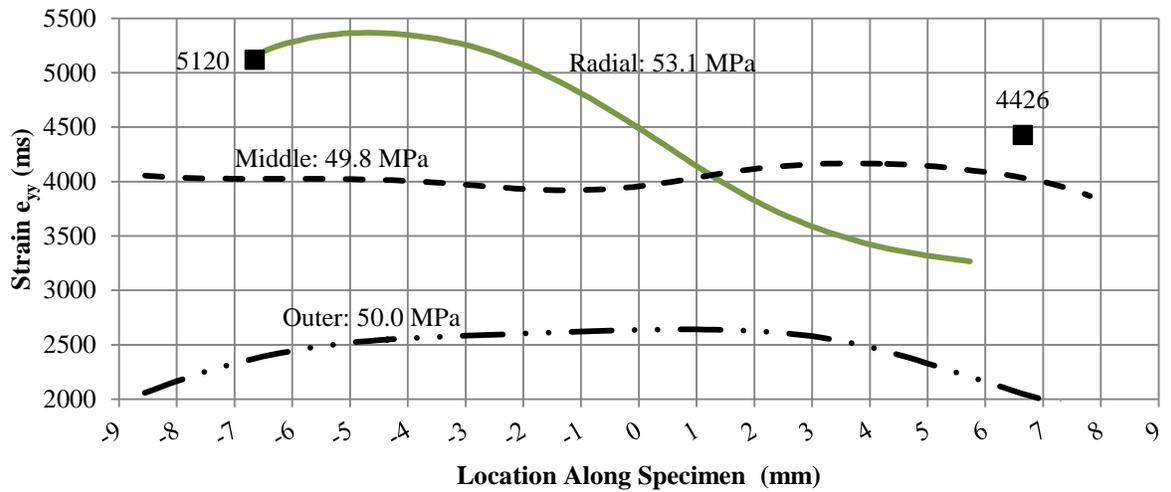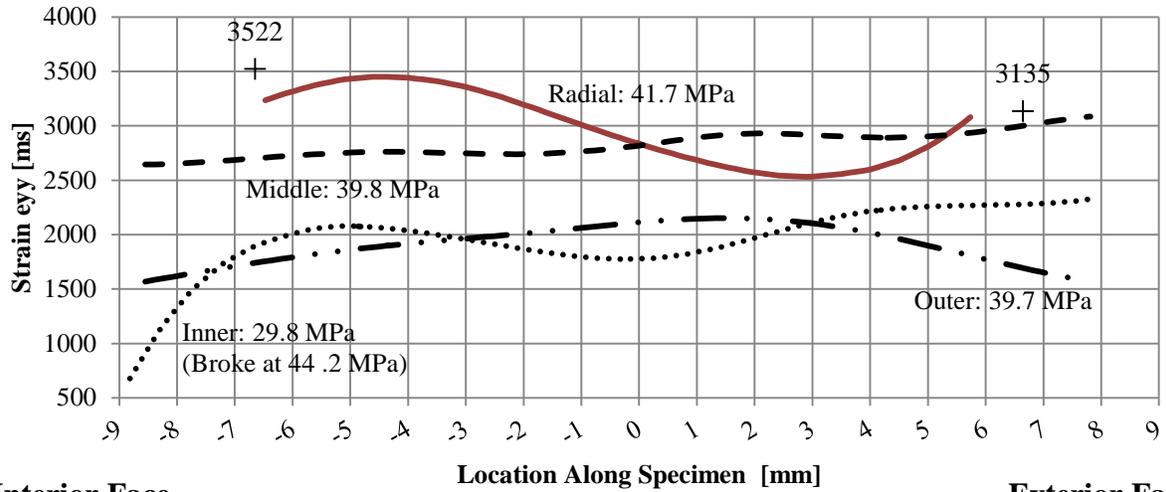
Figure A- 42: TG21-13 Free Specimens
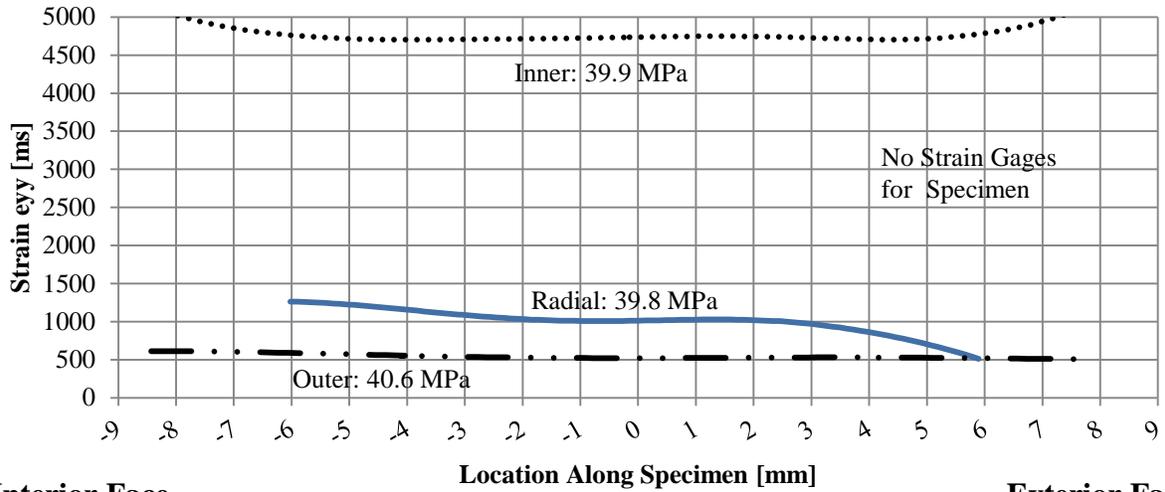
Interior Face
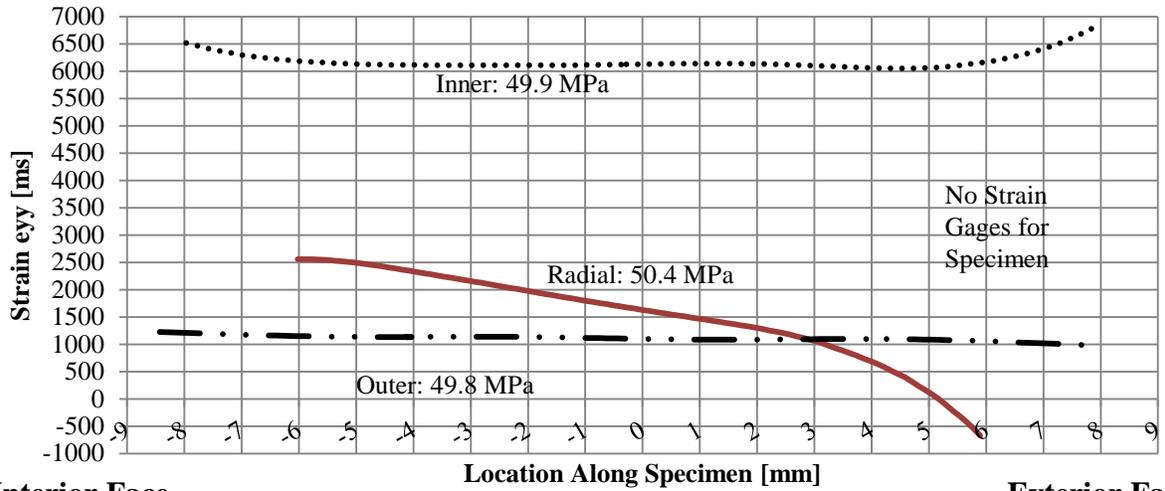
Exterior Face

Interior Face
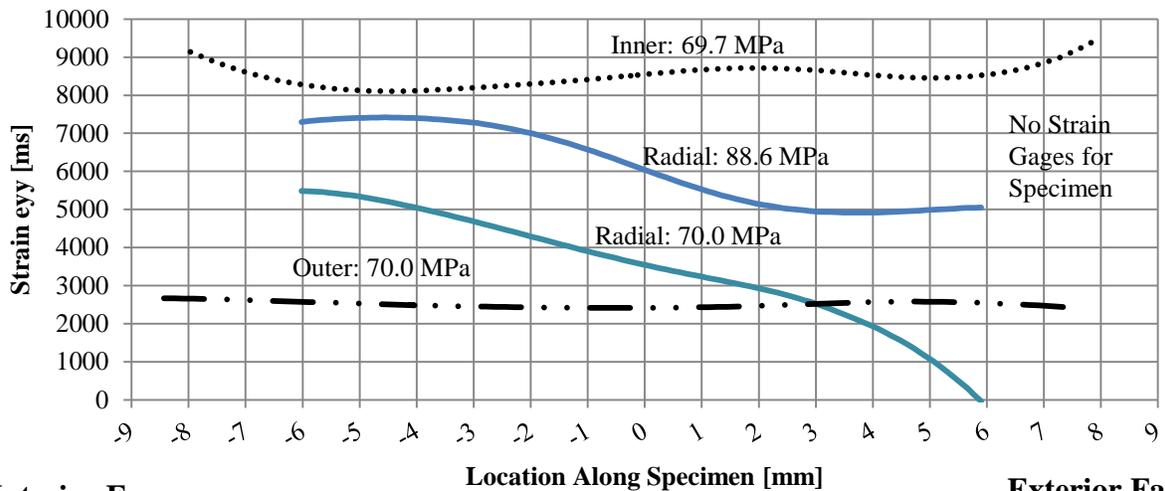
Exterior Face

Interior Face

Exterior Face

Figure A-43: TG21-13 Fixed Specimens

254
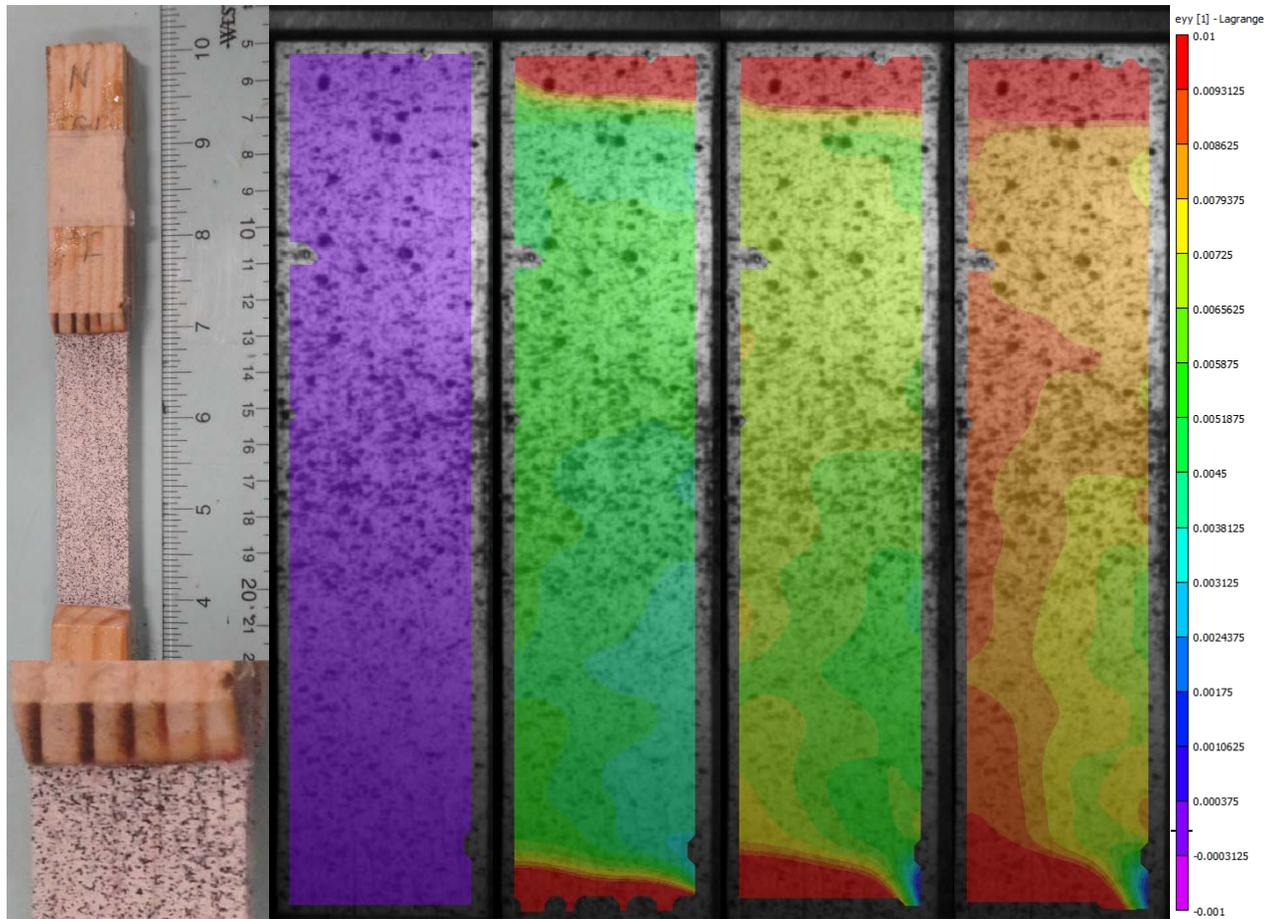
**Figure A-44: Contour Banding in Radial Free Specimen TG21-12**
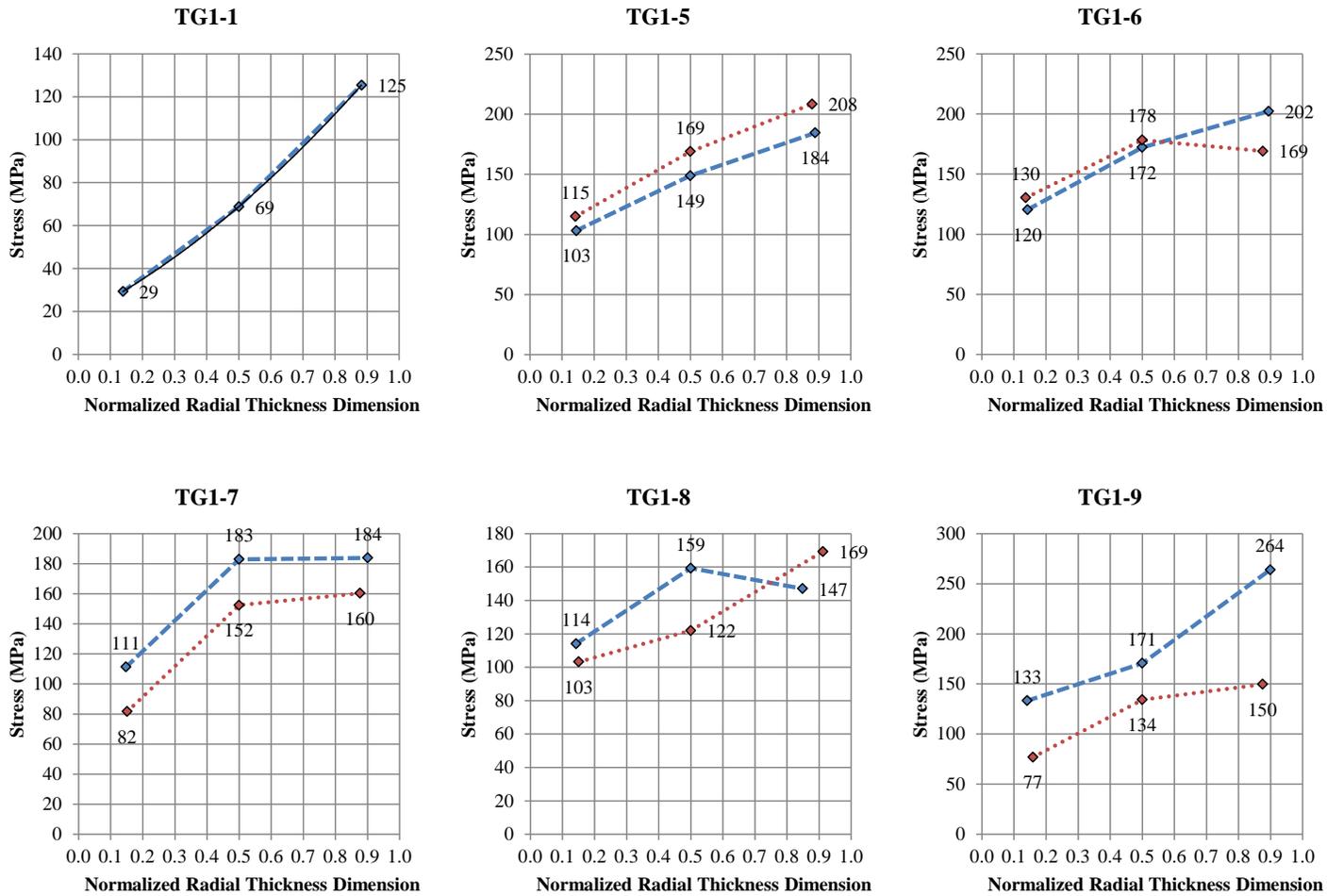
**Figure A-45: Stress versus wall thickness location**
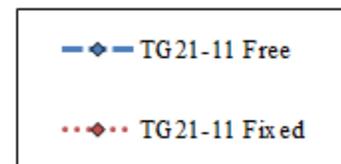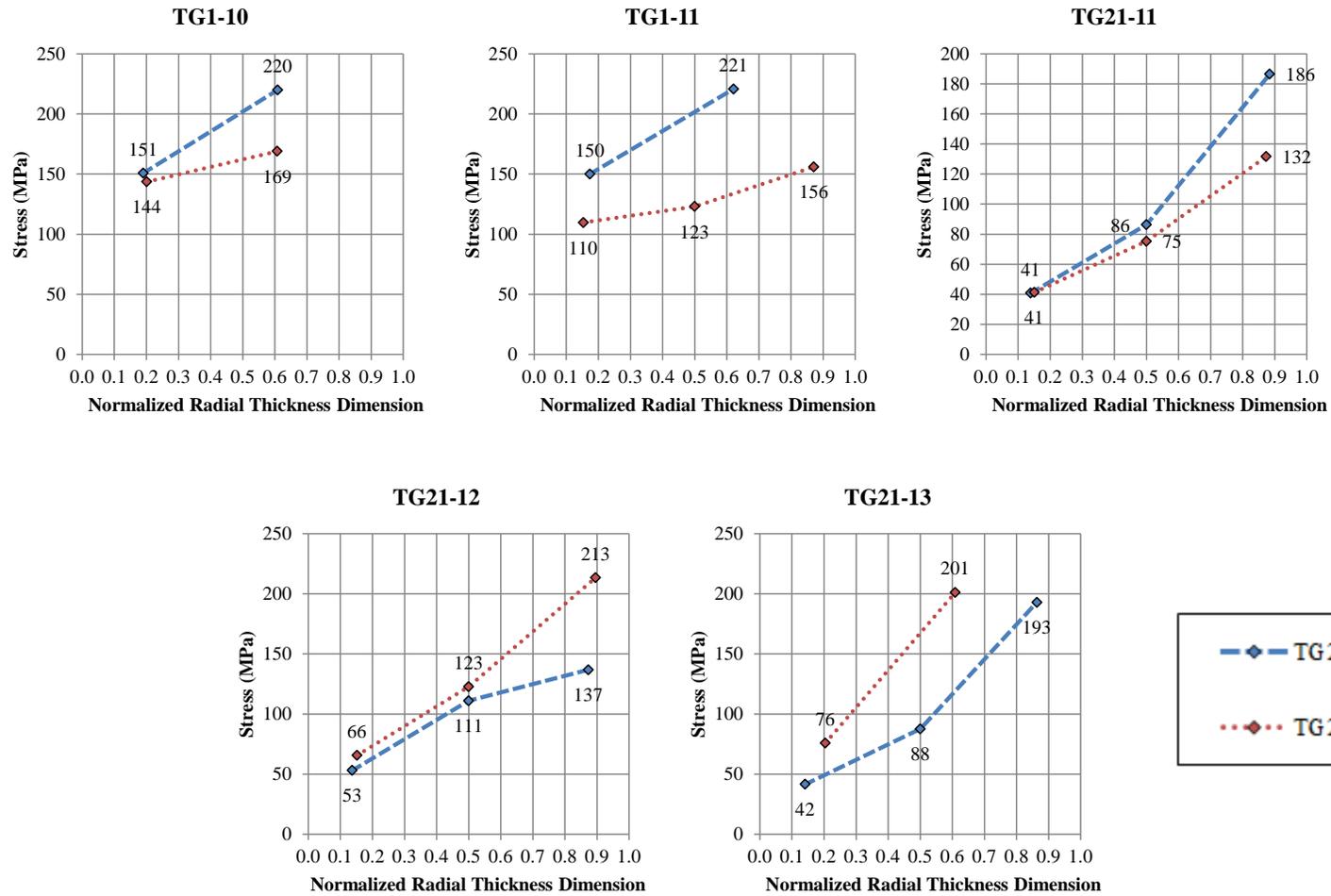
Figure A-46: Stress versus wall thickness location (cont.)

257

CITED REFERENCES

Achá Navarro, E. H., (2011). Bamboo: High Tech Material for Concrete Reinforcement. Doctoral Thesis, *Pontifícia Universidade Católica do Rio de Janeiro*, June 2011, 138 pp.

Adhikary, N., (2008). An experiment with a locally constructed bouccherie treatment plant in Nepal. *Modern Bamboo Structures*, Xiao, Y., Inoue, M., and Paudel S.K., eds., London, UK, pp. 103-110.

Ahmad M. and Kamke F.A., (2005). Analysis of Calcutta bamboo for structural composite materials: physical and mechanical properties. *Wood Science and Technology*, **39**, pp. 448-459.

Aktas, C.B. and Bilec, M.M. (2012). Impact of Lifetime on U.S. residential building LCA Results. *The International Journal of Life Cycle Assessment*, **17**(3), pp. 337-349.

Albermani, F., Goh, G.Y., and Chan, S.L., (2007). Lightweight bamboo double layer grid system. *Engineering Structures*, **29**, pp.1499-1506.

Amada, S., Ichikawa, T., Munekata, T., Nagase, Y., and Shimizu, H., (1997). Fiber texture and mechanical graded structure of bamboo, *Composites: Part B*, **28B**, pp. 13-20.

Amada, S., Munekata, T., Nagase, Y., Ichikawa, Y., Kirigai A., and Zhifei, Y., (1996). The Mechanical Structures of Bamboo in Viewpoint of Functionally Gradient and Composite Materials, *Journal of Composite Materials*, **30**(7), pp. 800-819.

Amada S. and Untao, S., (2001). Fracture properties of bamboo, *Composites: Part B*, **32**, pp. 451-459.

American Forest and Paper and Association and American Wood Council, (2005). *National design specification (NDS) for wood construction and supplement*. AF & PA, Washington, D.C.

American Institute of Steel Construction, (2011). *Steel Construction Manual*. 14th ed. AISC, Chicago, IL.

Arce-Villalobos, O.A., (1993). Fundamentals of the design of bamboo structures. Master's Thesis, *Eindhoven University of Technology*, Netherlands, September 1993, 167 pp.

ASTM International, (1978). ASTM D2733-70: *Method for Interlaminar Shear Strength of Structural Reinforced Plastics at Elevated Temperatures*, West Conshohocken, PA: ASTM International

ASTM International, (2008). ASTM D3039-08: *Standard Test Method for Tensile Properties of Polymer Matrix Composite Materials*, West Conshohocken, PA: ASTM International

ASTM International, (2009). *ASTM D143-09: Standard Test Methods for Small Clear Specimens of Timber*, West Conshohocken, PA: ASTM International

ASTM International, (2010). Structural Bamboo. *ASTM Standardization News*. November/December, pp. 50.

ASTM International, (2011). ASTM E8-11: *Standard Test Methods for Tension Testing of Metallic Materials*, West Conshohocken, PA: ASTM International

Athaus, H., Werner, F., Stettler, C., and Dinkel, F., Basel, C., (2007). *Ecoinvent report No. 21: Life Cycle Inventories of Renewable Materials*, Swiss Centre for Life Cycle Inventories, Dübendorf, Switzerland, December 2007, 127 pp.

Banik, R., (1995). INBAR *Technical Report No. 06: A Manual for Vegetative Propagation of Bamboos*, International Network for Bamboo and Rattan, Beijing, China, 66 pp.

Breyer, D.E., Fridley, K.J., Cobeen, K.E., and Pollock, D.G., (2007). *Design of Wood Structures: ASD/LRFD*. 6th ed. McGraw-Hill, New York, NY.

Brink, F.E. and Rush, P.J., (1966). *Bamboo Reinforced Concrete Construction*. U.S. Naval Civil Engineering Laboratory, Port Hueneme, CA.

Brown, K., Eells, P., Nites, M., Pagliassotti, M., Stein, A., and Zimmerman, C., (2012). *Design of a Rapidly Deplyable Bamboo Gridshell Structure.* International Research Experience for Students Report (unpublished), University of Pittsburgh, 45 pp.

Bureau of Indian Standards, (2005). *National Building Code of India: Part 6 Structural Design Section 3: Timber and Bamboo: 3B Bamboo.*

Burgers, J.W. 1935. Mechanical considerations - model systems - phenomenological theories of relaxation and of viscosity. *First Report on Viscosity and Plasticity*, Nordemann Publishing Company, New York, NY.

Chapman, G.P., (1996). *The Biology of Grasses*, CAB International, Wallingford.

Chapman, G.P. and Peat, W.E., (1992). *An introduction to the grasses (including bamboos and cereals)*, CAB International, Wallingford.

Choi, M., Kwon, A., Lawit O., Macready, P., Ringel, C., and Zettl, J., (2011). *Comparative Life Cycle Analysis for Portal Frame Construction.* International Research Experience for Students Report (unpublished), University of Pittsburgh, 26 pp.

Clark, L.G. and Pohl, R.W., (1996). *Agnes Chase's First Book of Grasses: The Structure of Grasses Explained for Beginners*, 4th ed., Smithsonian Institution Press, Washington.

Correal, L. and Lopez, L., (2008). Mechanical Properties of Colombian glue laminated bamboo. *Modern Bamboo Structures*, Xiao, Y., Inoue, M., and Paudel S.K., eds., London, UK, pp. 121-127.

CORRIM (Consortium for Research on Renewable Industrial Materials), (2011). *Research, Life Cycle Inventory and Life Cycle Assessment.* CORRIM, <http://www.corrim.org/research/lci_lca.asp>, (December 12, 2011).

Cox F.B. and Geymayer H.G., (1969). *Expedient reinforcement for concrete for use in S.E. Asia. Report 1-Preliminary Tests of Bamboo.* Monograph. (as reported by Arce-Villalobos 1993).

Crow, J.M., (2008). The concrete conundrum. *Chemistry World*, **5**(3) pp. 62-66.

Cruz, M.L.S., (2002). Caracterização fisica e mecânica de colmos inteiros do bambu da espécie phyllostachys aurea: comportamento à flambagem (in Portuguese). Master's Thesis, *Pontifícia Universidade Católica do Rio de Janeiro*, August 2002, 122 pp.

De Flander, K. and Rovers, R., (2009). One laminated bamboo-frame house per hectare per year. *Construction and Building Materials*, 23, pp. 210-218.

Dickson, M., (2002). Engineering buildings for a small planet: Towards construction without depletion. *The Structural Engineer*, **80**(3), pp. 35-43.

Duff, C.H., 1941. Bamboo and its structural used. *The Engineering Society of China*, session 1940-41, paper #ICE. 1. Institution of Civil Engineers of Shanghai, pp. 1-27. (as reported by Arce-Villalobos 1993)

Ecoinvent Unit Processes Database (Ecoinvent). <www.ecoinvent.org/database/>

Ghavami, K., (1988). Application of bamboo as a low-cost construction material. *Proceedings of International Bamboo Workshop*, Cochin, India, pp. 270-279.

Ghavami, K., (2005). Bamboo as reinforcement in structural concrete elements. *Cement and Concrete Composites*, **27**, pp. 637-649.

Ghavami, K., (2008). Bamboo: Low cost and energy saving construction materials. *Modern Bamboo Structures*, Xiao, Y., Inoue, M., and Paudel S.K., eds., London, UK, pp. 5-21.

Ghavami, K., and Moreira, L.E., (2002). Buckling behaviour of compression elements in bamboo space structure. *Spaces Structures 5.* Parke, G.A.R. and Disney, P. Disney, eds., Thomas Telford Ltd., London, pp. 133-144.

Ghavami, K., Rodriques, C.S., and Paciornik, S., (2003). Bamboo: Functionally Graded Composite Material. *Asian Journal of Civil Engineering (Building and Housing)*, 4(1), pp. 1-10.

Government of the Republic of Haiti, (2010). *Action Plan for National Recovery and Development of Haiti: Immediate key initiatives for the future.*

González, G. and Gutiérrez, J., (2005). Structural performance of bamboo 'bahareque' walls under cyclic load. *Journal of Bamboo and Rattan*, **4**(4), pp. 353-368.

Grewal, J.K., (2009). Bamboo as a Structural Material. Bachelors Thesis, *University of Southampton*, April 2009. 50pp.

Grosser, D. and Liese, W., (1971). On the Anatomy of Asian Bamboos, with Special Reference to their Vascular Bundles. *Wood Science and Technology*, **5**, pp. 290-312.

Guan, M.J. and Zhu, E.C., (2008). Flexural properties of bamboo sliver laminated lumber under different hygrothermal conditions. *Modern Bamboo Structures*, Xiao, Y., Inoue, M., and Paudel S.K., eds., London, UK, pp. 151-157.

Gupta, S., Sudhakar, P., Korde, C., and Agrawal, A., (2008). Experimental verification of bamboo-concrete composite column with ferro-cement bond. *Modern Bamboo Structures*, Xiao, Y., Inoue, M., and Paudel S.K., eds., London, UK, pp. 253-258.

Gutiérrez, J., (2004). Notes on the Seismic Adequacy of Vernacular Buildings. *13th World Conference on Earthquake Engineering*, August 2004, Vancouver, Canada.

Harries, K.A., Petrou, M.F., and Brooks, G., (2000). Structural Characterization of Built-Up Timber Columns. *Journal of Structural Engineering*, **6**(2), pp. 58-65.

Harries, K.A., Sharma, B., and Richard M.J., (2012). Structural Use of Full Culm Bamboo: The Path to Standardisation. *International Journal of Architecture, Engineering and Construction*, **1**(2), June 2012, pp. 1-10.

ICC-ES (International Code Council Evaluation Service), (2013). *Evaluation Service Report 1636: Structural Bamboo Poles*. ICC-ES.

IDEMAT Database. <www.idemat.nl>

INBAR (International Network of Bamboo and Rattan), (1999). *An International Model Building Code for Bamboo*, Janssen, J.A., ed., INBAR, Beijing.

Inglês, L., (2012). Personal interview, June 2012.

Inoue, M., Tanaka, K., Tagawa, Y., Nakahara, M., Goto, Y., Imabayashi, M., and Uchiyama, U., (2008). Application of bamboo connector to timber structure – Introduction of construction and dismantlement of Japanese government pavilion Nagakute in Expo 2005 Aichi, Japan. *Modern Bamboo Structures*, Xiao, Y., Inoue, M., and Paudel S.K., eds., London, UK, pp. 191-199.

ISO (International Organization for Standardization), (2004a). *International Standard ISO 22156:2004 (E), Bamboo – Structural Design*. Geneva, Switzerland: ISO.

ISO (International Organization for Standardization), (2004b). *International Standard ISO 22157-1:2004 (E), Bamboo – Determination of Physical and Mechanical Properties – Part I: Requirements*. Geneva, Switzerland: ISO.

ISO (International Organization for Standardization), (2004c). *International Standard ISO 22157- 2:2004 (E), Bamboo – Determination of Physical and Mechanical Properties – Part II: Laboratory Manual*. Geneva, Switzerland: ISO.

ISO (International Organization for Standardization), (2006), *ISO 14040: Environmental management – Life cycle assessment- Principles and framework.* Geneva, Switzerland: ISO.

Iyer, S., (2002). Guideline for Building Bamboo-Reinforced Masonry in Earthquake-Prone Areas in India. Masters of Building Science Thesis, *University of Southern California*, May 2002. 80pp.

Janssen, J., (1981). Bamboo in Building Structures. Doctoral Thesis. *Eindhoven University of Technology*, Netherlands.

Janssen, J.J.A., (2000). *Designing and Building with Bamboo: INBAR Technical Report 20*. International Network for Bamboo and Rattan, Beijing, China, 211pp.

Jayanetti, D.L. and Follett, P.R., (2008). Bamboo in construction. *Modern Bamboo Structures*, Xiao, Y., Inoue, M., and Paudel S.K., eds., London, UK, pp. 23-32.

Johnson, L.R., Lippke, B., Marshall, J.D., and Comnick, J., (2005). Life-Cycle Impacts of Forest Resource Activities in the Pacific Northwest and Southeast United States. *Wood and Fiber Science*, **37**(CORRIM Special Issue), pp. 30-46.

Kaushik, H.B., Dasgupta, K., Sahoo, D.R., and Kharel, G., (2006a). *Reconnaissance Report: Sikkim Earthquake of 14 February 2006.* National Information Center of Earthquake Engineering, Indian Institute of Technology Kanpur, April 2006. 13pp.

Kaushik, H.B., Dasgupta, K., Sahoo, D.R., and Kharel, G., (2006b). Performance of Structures during the Sikkim Earthquake of 14 February 2006. *Current Science*, **91**(4), pp. 449-455.

Klarreich, K., (2010). Haiti earthquake diary: The quest for temporary housing. *The Christian Science Monitor*.

Laroque, P., (2007). Design of a Low Cost Bamboo Footbridge. Master's Thesis, *Massachusetts Institute of Technology (MIT)*, June 2007, 87 pp.

Li, H. and Shen S., (2011). The mechanical properties of bamboo and vascular bundles. *Journal of Materials Research*, **26**(21), pp. 2749-2756.

Li, X.B., Shupe, T.F., Peter, G.F., Hse, C.Y., and Eberhardt, T.L., (2007). Chemical Changes with Maturation of the Bamboo Species *Phyllostachys Pubescens*. *Journal of Tropical Forest Science*, **19**(1), pp. 6-12.

Li, Y.S., Shan, W., and Liu, R., (2008). Experimental study of mechanical behavior of bamboo-steel composite floor slabs. *Modern Bamboo Structures*, Xiao, Y., Inoue, M., and Paudel S.K., eds., London, UK, pp. 275-284.

Liese, W., (1987). Research on Bamboo. *Wood Science and Technology*, **21**, pp. 189-209.

Liese, W. and Weiner, G., (1996). Ageing of bamboo culms. A review. *Wood Science and Technology*, **30**, pp. 77-89.

Lobovikov, M., Paudel, S., Piazza, M., Ren, H., and Wu, J., (2007). *World Bamboo Resources: A Thematic Study Prepared in the Framework of the Global Forest Resources Assessment 2005*. Rome, Italy: Food and Agriculture Organization (FAO) of the United Nations.

Lobovikov, M., Schoene, D., and Yping, L., (2012). Bamboo in climate change and rural livelihoods. *Mitigation and Adaptation Strategies for Global Change*, **17**, pp. 261-276.

Low, I.M., Che, Z.Y., and Latella, B.A., (2006), Mapping the structure, composition and mechanical properties of bamboo. *Journal of Materials Research*, **21**(8), pp. 1969-1976.

McLaughlin, E.C., (1979). A note on the strength of Jamaica grown bamboo. *Wood and Fiber Science*, **11**(2), pp. 86-91. (as reported by Arce-Villalobos 1993).

Milota, M. R., West, C. D., and Hartley, I.D., (2005). Gate-To-Gate Life-Cycle Inventory of Softwood Lumber Production. *Wood and Fiber Science*, **37**(CORRIM Special Issue), pp. 47-57.

Mitch, D., (2009). Splitting Capacity Characterization of Bamboo Culms. University of Pittsburgh Honors College Thesis, *University of Pittsburgh*, March 2009. 88pp.

Mitch, D., (2010). Structural Behavior of Grouted-Bar Bamboo Column Bases. Master's Thesis, *University of Pittsburgh*, July 2010. 99pp.

Mitch, D., Harries, K.A., and Sharma, B., (2010). Characterization of Splitting Behavior of Bamboo Culms, *ASCE Journal of Materials in Civil Engineering*, **22**(11), pp. 1195-1199.

Moreira, L.E., (1991) Desenvolvimento de estruturas treliçadas espaciais de bamboo (in Portuguese). Doctoral Thesis, *Pontifícia Universidade Católica do Rio de Janeiro*.

Moreira L.E. and Ghavami, K., (2009). Bamboo Space Structure. *Proceedings of the 11th International Conference on Non-conventional Materials and Technologies (NOCMAT 2009)*, September 2009, Bath, UK, 8 pp.

Mori, T., Umemura, K., and Norimoto, M., (2008). Manufacture of drift pins and boards made from bamboo fiber for timber structures. *Modern Bamboo Structures*, Xiao, Y., Inoue, M., and Paudel S.K., eds., London, UK, pp. 129-137.

Murty, C.V.R. and Sheth, A. (editors), (2012). *The M_w 6.9 Sikkim-Nepal Border Earthquake of September 18, 2011*. EERI Special Earthquake Report, February 2012, 14 pp.

Obataya, E., Kitin, P., and Yamauchi, H., (2007). Bending characteristics of bamboo (Phyllostachys pubescens) with respect to its fiber-foam composite structure. *Wood Science and Technology*, **41**, pp. 385-400.

Oneil, E.E., Johnson, L.R., Lippke, B.R., McCarter, J.B., McDill, M.E., Roth, P.A., and Finley, J.C., (2010). Life-Cycle Impacts of Inland Northwest and Northeast/North Central Forest Resources. *Wood and Fiber Science*, **42**(CORRIM Special Issue), pp. 29-51.

Ota, M., (1950). Studies on the properties of bamboo stem (part 10). On the relation between the tensile strength parallel to the grain and the moisture content of split bamboo. *Bulletin Kyushu University of Forestry*, **32**, pp. 155-164. (as reported by Arce-Villalobos 1993)

Paudel, S.K., (2008). Engineered bamboo as a building material. *Modern Bamboo Structures*, Xiao, Y., Inoue, M., and Paudel S.K., eds., London, UK, pp. 33-40.

Powell, A.E., (2006). The Widening Gulf. *Civil Engineering Magazine*. American Society of Civil Engineers, **76**(8), pp. 56-61.

Puettmann, M.E., Bergman, R., Hubbard, S., Johnson, L., Lippke, B., Oneil, E., and Wagner, F. G., (2010a). Cradle-to-gate life-cycle inventory of US wood products production: CORRIM phase I and phase II products. *Wood and Fiber Science*, **42**(CORRIM Special Issue), pp. 15-28.

Puettman, M.E., Wagner, F.G., and Johnson, L., (2010b). Life Cycle Inventory of softwood lumber from the Inland Northwest. *Wood and Fiber Science*, **42**, pp.52-66.

Richard, M. J. and Harries K.A., (2012). "Experimental Buckling Capacity of Multiple-Culm Bamboo Columns." *Key Engineering Materials*; **517**, pp. 51-62.

Rittironk, S. and Elnieiri, M., (2008). Investigating laminated bamboo lumber as an alternate to wood lumber in residential construction in the United States. *Modern Bamboo Structures*, Xiao, Y., Inoue, M., and Paudel S.K., eds., London, UK, pp. 83-96.

Robertson, A, (1925). The Strength of Struts. *ICE Selected Engineering Papers*, **1**(28).

Rowell, K. and Jackson, L., (2010). The Haiti Co-Laboratory Project. *ASTM Standardization News*, ASTM International, Nov/Dec 2010, pp. 32-35.

Shao Z., Fang, C., and Tian G., (2009). Mode I interlaminar fracture property of moso bamboo (*Phyllostachys pubescens*). *Wood Science and Technology*, 43, pp. 527-536.

Sharma, B., (2010). Seismic Performance of Bamboo Structures. Doctoral Dissertation, *University of Pittsburgh*, 201 pp.

Silva, E.C.N., Walters, M.C., and Paulino, G.H., (2006). Modeling Bamboo as a Functionally Graded Material: Lessons for the Analysis of Affordable Materials. *Journal of Material Science*, **42**, pp. 6991-7004.

Smith I., Landis, E., and Gong, M., (2003). *Fracture and Fatigue in Wood*. John Wiley and Sons Ltd., West Sussex, UK.

Solomon, C., (1994). Cement. *1994 Mineral Yearbook*, United States Geological Survey (USGS), pp. 1-20.

Southern Pine Association, (2006). *Southern Pine for Structural Components*. S. P. Association. Kenner, LA.

Southwell, E. V., (1932). On the Analysis of Experimental Observations in Problems of Elastic Stability. *Proceedings of Royal Society of London*, 135, pp. 601-616.

Spoer P., (1982). The Use of Bamboo in Space Trusses. Master's Thesis, *Technical University of Denmark*. (as reported by Arce-Villalobos 1993)

Sudhakar, P., Gupta, S., Bhalla, S., Kordke, C., and Satya, S., (2008). Conceptual development of bamboo concrete composite structure in a typical Tribal Belt, India. *Modern Bamboo Structures*, Xiao, Y., Inoue, M., and Paudel S.K., eds., London, UK, pp. 65-73.

Tan, T., Rahbar, N., Allameh, S.M., Kwofie, S., Dissmore, D., Ghavami, K., and Soboyejo, W.O., (2011). Mechanical properties of functionally graded hierarchical bamboo structures. *Acta Biomaterialia*, **7**, pp. 3796-3803.

United Nations, (2004). *Tents: A guide to the use and logistics of family tents in humanitarian relief*. Office for the Coordination of Humanitarian Relief.

United Nations Human Settlements Programme (UN-HABITAT), (2011a). *Affordable Land and Housing in Latin America and the Caribbean*.

United Nations Human Settlements Programme (UN-HABITAT), (2011b). *Affordable Land and Housing in Asia*.

United Nations Human Settlements Programme (UN-HABITAT), (2011c). *Affordable Land and Housing in Africa*.

United Nations Human Settlements Programme (UN-HABITAT), (2011d). *Affordable Land and Housing in Europe and North American*.

United Nations Universal Declaration of Human Rights (UN-UDHR), (1948).

United States Environmental Protection Agency (US-EPA). Tool for the Reduction and Assessment of Chemical and Other Environmental Impacts (TRACI), TRACI 2 version 3.01, <www.epa.gov/nrmrl/std/traci/traci.html>

United States Geological Survey (USGS), (2012). *Cement Statistics and Information*. <http://minerals.usgs.gov/minerals/pubs/commodity/cement/index.html#myb> (January 2013)

United States Geological Survey (USGS), (2012). *Iron and Steel Statistics.* <http://minerals.usgs.gov/ds/2005/140/ironsteel.pdf > (May 2013)

United States Life Cycle Inventory (USLCI) Database. <www.nrel.gov/lci/>

Vaessen, M.J. and Janssen, J.A., (1997). Analysis of the critical length of culms of bamboo in four-point bending tests, *HERON*, 42(2), pp.113-124.

van der Lugt P., van den Dobbelsteen, A.A.J.F., and Janssen, J.J.A., (2006). An environmental, economic and practical assessment of bamboo as a building material for supporting structures *Construction and Building Materials*, **20**(9), pp. 648-656.

van der Lugt, P., Vogtländer, J., and Brezet, H., (2009). *INBAR Technical Report No. 30: Bamboo, a Sustainable Solution for Western Europe Design Cases, LCAs and Land-Use*. International Network for Bamboo and Rattan (INBAR), Beijing, China.

van der Lugt, P., Vogtländer, J.G., van der Vegte, and Brezet, J.C., (2012). Life Cycle Assessment and Carbon Sequestration; the Environmental Impact of Industrial Bamboo Products, *IXth World Bamboo Congress*, April 2012, Belgium, pp. 73-85.

van Oss H. G., (2012). Cement. *2010 Minerals Yearbook*, United States Geological Survey (USGS), pp. 16.1-16.37.

Vengala, J., Jagadeesh, H.N., and Pandey C.N., (2008). Development of bamboo structure in India. *Modern Bamboo Structures*, Xiao, Y., Inoue, M., and Paudel S.K., eds., London, UK, pp. 51-63.

Villalobos, G., Linero, D.L., and Muñoz, J.D., (2011). A statistical model of fracture for a 2D hexagonal mesh: The Cell Network Model of Fracture for the bamboo Guadua angustifolia. *Computer Physics Communications*, **182**, pp. 188-191.

Vogtländer, J.G., (2001). The model of the Eco-costs/Value Ratio, a new LCA based decision support tool. Doctoral thesis, *Delft University of Technology*, Delft, Netherlands.

Vogtländer, J., van der Lugt, P., and Brezet, H., (2010). The sustainability of bamboo products for local and Western European applications. LCAs and land-use. *Journal of Cleaner Production*, **18**, pp. 1260-1269.

Wessex Resins and Adhesives Limited, (2003). *Resorcinol Resin*. <http://www.wessex-resins.com> (November 22, 2011).

Wilson, J., (2010). Life-Cycle Inventory of Formaldehyde-Based Resins Used in Wood Composites In Terms of Resources, Emission, Energy and Carbon. *Wood and Fiber Science*, **42**(CORRIM Special Issue), pp. 125-143.

World Resource Institute, (2009). *State of the World's Forests*. <http://www.wri.org/map/state-worlds-forests> (January 2013).

World Steel Association, (2012). *Annual crude steel production archive*. <http://www.worldsteel.org/statistics/statistics-archive/annual-steel-archive.html> (January 2013).

World Steel Association, (2012). *World Crude Steel Production – Summary*. <http://www.worldsteel.org/dms/internetDocumentList/press-release-downloads/2012/2012-statistics-table/document/2012%20statistics%20table.pdf> (May 2013)

Xiao, Y., Shan, B., Chen, G., Zhou, Q., and She L.Y., (2008). Development of a new type of Glulam – Glubam. *Modern Bamboo Structures*, Xiao, Y., Inoue, M., and Paudel S.K., eds., London, UK, pp. 41-47.

Xiao, Y., Zhou, Q., and Shan, B., (2010). Design and Construction of Modern Bamboo Bridges. *Journal of Bridge Engineering*, **15**(5), pp.533-541.

Yu, C., Lange, J., and Mastrangelo, G., (2010). Lessons Learnt from Natural Disasters – Shelters and the Built Environment. *Indoor and Built Environment*, **19**(3), pp. 307-310.

Yu W.K., Chung K.F., and Chan S.L., (2003). Column buckling of structural bamboo. *Engineering Structures*, **25**, pp. 755-768.

Yu W.K., Chung K.F., and Chan S.L., (2005). Axial buckling of bamboo columns in bamboo scaffolds. *Engineering Structures*, **27**, pp. 61-73.

Zeng, Q.Y., Li, S.H., and Bao, X.R., (1992). Effect of bamboo nodal on mechanical properties of bamboo wood. *Scientia Silvae Sinicae*, **28**(3), pp. 247-252 (in Chinese: as reported by Shao et al. (2009)).

Zhao, J., Ma, S., Liu, H., and Ren, H., (2011). Experimental investigation of the mixed-mode crack expanding in bamboo. Advanced Materials Research, **146-147**, pp1285-1288.

Zhou, G.M. and Jiang, P.K., (2004). Density, storage and spatial distribution of carbon in *Phyllostachys pubescens* forest. *Scientia Silvae Sinicae*, **6**, pp 20-24. (in Chinese with English summary; reported by van der Lugt (2012)).